Pressure and Temperature Effects on the Enzymatic Conversion of Biopolymers

vorgelegt von
Dipl.-Ing.
Roman Buckow

von der Fakultät III – Prozesswissenschaften
der Technischen Universität Berlin
zur Erlangung des akademischen Grades

Doktor der Ingenieurwissenschaften
- Dr.-Ing. -
genehmigte Dissertation

Promotionsausschuss:
Vorsitzender: Prof. Dr. Ulf Stahl
1. Berichter: Prof. Dr. Dietrich Knorr
2. Berichter: Prof. Dr. Marc Hendrickx

Tag der wissenschaftlichen Aussprache: 24. Oktober 2006

Berlin 2006
D-83

ACKNOWLEDGMENTS

This thesis is based on experimental work at the Berlin University of Technology, Department of Food Process Engineering and Food Biotechnology from 2002 to 2006. Numerous people have given advice, encouragement and support to my work. First and foremost, my sincere gratitude goes to Prof. Dr. Dietrich Knorr for giving me academic guidance and inspiration as well as support, resources and funds throughout the course of this work. I would like to acknowledge Prof. Dr. Marc Hendrickx for critical corrections and for and taking his time to come to Berlin to be an examiner for my thesis. My gratitude is also to Prof. Dr. Ulf Stahl for being the chairman of the evaluation committee.

Special thanks go to Dr. Volker Heinz for his scientific advice, for giving impulses, ideas and for the fruitful discussions since my first days working with high hydrostatic pressure.

To all present and former colleagues of the Department I am thankful for providing a very comfortable atmosphere. A particular thanks to the technical assistants Irene, Stefan, Gabi, Gisi and Bunny. My former office mate Edwin and Adriano as well as Stefan, Alex, Ulrike, Gabriel and Cornelius I want to thank for encouragements, helpful discussions and assistance. Thanks to the diploma students Assita, Diane and Filip for your support and your activities!

I would like to thank for financial support from the German Ministry of Economics and Technology, the Science Support Agency of the German Brewers Association and the German Ministry for Education and Research.

Very special thanks to my parents and to Antje for their love, support and sacrifice during my study!

CONTENT

LIST OF ABBREVIATIONS

p	pressure [MPa]
T	temperature [°C; K]
V	volume [m^3]
V_R	reaction volume [$cm^3\ mol^{-1}$]
a_w	water activity
ΔG	Gibbs free energy [J mol^{-1}]
R	universal gas constant [8.314 J mol^{-1} K^{-1}]
k	rate constant [min^{-1}]
K	rate constant of equilibrium
C	concentration [mg/mL]
β	coefficient of compressibility [Pa^{-1}]
v	specific volume [$m^3\ kg^{-1}$]
η	viscosity [Pa s]
ρ	density [kg m^3]
S	entropy [J K^{-1} mol^{-1}]
U	inner energy [Jmol^{-1}]
w	volumetric work [J]
q	specific heat quantity [J kg^{-1}]
H	enthalpy [J mol^{-1}]
G	free enthalpy [Jmol^{-1}]
c_p	specific heat capacity [J $kg^{-1}K^{-1}$]
α	coefficient of thermal expansion [Pa^{-1}]
γ	coefficient of activity
ε	dielectric constant
K_A	thermodynamic equilibrium constant
E_A	activation energy [J mol^{-1}]
$\Delta V^{\#}$	activation volume
a_D	degree of denaturation
t	time [min]
A	enzyme activity [U/mL]
A_0	initial enzyme activity [U/mL]
D	decimal reduction time [min]
k’	specific rate constant
k_{inact}	inactivation rate constant [min^{-1}]
k_{conv}	conversion rate constant [min^{-1}]
K_{gel}	gelatinization rate constant [min^{-1}]
n	reaction order
r^2	coefficient of regression
z	resistance constant [MPa; °C]
S	Substrate
P	product
E	enzyme
ES	enzyme-substrate complex

v	initial rate [min^{-1}]
V_{max}	maximum rate [min^{-1}]
K_m	Michaelis-Menten constant [mg mL^{-1}]
AMY1	α-amylase isoenzyme 1
AMY2	α-amylase isoenzyme 2
BASI	barley α-amylase subtilisin inhibitor
ACES	N-(2-Acetamido)-2-aminoethanesulfonic acid
GA1	glucoamylase isoenzyme 1
GA2	glucoamylase isoenzyme 2
PrP	prion-related protein
PrP^{C}	'normal' (cellular) form of PrP
PrP^{Sc}	'infectious' (scrapie) form of PrP
DSC	differential scanning calorimetry
FTIR	Fourier transform infra red spectroscopy
HPLC	high performance liquid chromatography

LIST OF TABLES

LIST OF FIGURES

ABSTRACT

The impact of high hydrostatic pressure and temperature on the gelatinization of maize starch granules and on the stability and catalytic activity of α- and β-amylase from barley malt, β-glucanase from barley malt and *Bacillus subtilis* as well as glucoamylase from *Aspergillus niger* was investigated.

The thermal and combined pressure-temperature inactivation experiments were performed at temperatures of 30-95°C and pressures up to 1400 MPa in different model systems. The isobaric/isothermal kinetics of studied enzymes indicated deviations from simple first-order kinetics in the pT domain investigated and, therefore, were described by using a n^{th}-order reaction model. An order of 1.4 (β-amylase), 1.6 (β-glucanase from barley malt), 1.8 (β-glucanase from *B.subtilis*) and 2.1 (α-amylase) was found to be the minimum of the cumulative standard error of fit and was used for the determination of the inactivation rate constants for all p-T conditions tested. The inactivation kinetics of glucoamylase showed a clear biphasic character due to the existence of two isoenzymes and could be described by a two-fractional-model using first-order kinetics. The change in inactivation rate constants k in response to pressure and temperature were successfully described by using thermodynamically based polynomial equations.

Glucoamylase isofraction GA1 appeared to be the most piezo-tolerant enzyme in this study, preserving its activity up to 1200 MPa at temperatures below 60°C. β-amylase looses 95% of its activity when pressurized at 620 MPa and 30 °C for 30 min. At 40°C α-amylase (in the presence of Ca^{2+} ions) was inactivated by 95% at 720 MPa, GA2 at 810 MPa and β-glucanase lost 95% of its initial activity at approximately 900 MPa (barley malt) and 1100 MPa (*B.subtilis*) after 30 min. Nevertheless, the enzymes investigated showed a significant stabilization against thermal induced denaturation at approximately 200 (α- and β-amylase), 400 (β-glucanase from barley malt and GA2), 500 (β-glucanase from *B.subtilis*) and 600 MPa (GA1), respectively.

Mathematic models describing the effect of pressure and temperature on enzyme inactivation were then used to correct the apparent enzymatic substrate conversion from the simultaneously occurring enzyme inactivation. This procedure allowed an isolated inspection of the effect of pressure and temperature on the conversion rate constant over a wide range of pressure-temperature combinations.

β-glucanase from *B.subtilis* showed significant higher catalytic activity at elevated pressures and temperatures. However, this was not found for the other enzymes where the catalytic reactions were reduced at increased pressures but strongly enhanced by raising the temperature. For the overall reaction of substrate conversion and simultaneously occurring

enzyme inactivation specific pressure-temperature-time combinations were found to give a maximum in substrate conversion. Individual maxima were found at 165 MPa and 66°C (α-amylase), 106 MPa and 60°C (β-amylase), 220 MPa and 55°C (β-glucanase from barley malt), 270 MPa and 80°C (glucoamylase in the presence of maize starch), 307 MPa and 63°C (β-glucanase from *B.subtilis*) and 318 MPa and 84°C (glucoamylase in the presence of maltose monohydrate) after 30 min exposure time. Compared to the maximal rate at ambient pressure theses optimal p-T conditions provide an acceleration of enzymatic catalysis of 20-400%.

The loss in birefringence has been used as an indicator of maize starch granule gelatinization in response to pT combinations in the range 0.1-650 MPa and 30-75°C. The granule gelatinization at ambient pressure as well as under high pressure followed a reaction order of 1.65. Using a sigmoidal secondary model with the melting temperature (T_m) as reference point, the rate constant is given as a function of pressure and temperature. The rate of birefringence loss was found to be temperature dependent, only, unless the pressure is exceeding 300 MPa. At those pressures, the isorate lines are bended to the left, indicating that starch gelatinization is occurring at lower temperatures. At 30°C, complete gelatinization of maize starch was found after a treatment at 650 MPa for 30 min.

Finally it was shown that the saccarification of native maize starch granules by glucoamylase was approximately 2.5 fold higher at optimal pT conditions compared to optimal conditions at ambient pressure. Due to the higher thermo-stability of glucoamylase under high pressure conditions the process temperature could be increased to a level where the inert starch granules convert into an enzymatic digestible substrate within extremely short times.

Furthermore, it was proven that the enzymatic conversion of barley malt can be accelerated by increasing the pressure and temperature which reduces the process time by 25%.

ZUSAMMENFASSUNG

Untersucht wurde der Einfluss von hydrostatischem Hochdruck und Temperatur auf den Abbau von Maisstärkekörnern sowie die Stabilität und katalytische Aktivität von α- und β-Amylase aus Gerstenmalz, β-Glucanase aus Gerstenmalz und *Bacillus subtilis* als auch Glucoamylase aus *Aspergillus niger*.

Kinetische Untersuchungen zur Enzymdeaktivierung wurden bei verschiedenen Druck-Temperatur-Kombinationen im Bereich 30-95°C und Drücken bis zu 1400 MPa in verschiedenen Modellsystemen durchgeführt. Innerhalb des untersuchten Druck-Temperatur Bereichs zeigten die Deaktivierungskinetiken der untersuchten Enzyme unter isobaren und isothermen Bedingungen eine Abweichung zur einfachen Reaktion erster Ordnung und wurden daher mit einem Reaktionsmodel n-ter Ordnung beschrieben. Die Analyse der Deaktivierungskurven im untersuchten Temperatur- und Druckbereich mittels verschiedener kinetischer Modelle ergab, dass eine Beschreibung der gefundenen Kurven am besten mit der Reaktionsordnung n = 1,4 (β-Amylase), 1,6 (β-Glucanase aus Gerstenmalz), 1,8 (β-Glucanase aus *B.subtilis*) und 2,1 (α-Amylase) beschrieben erfolgen konnte. Nach Festlegung der Reaktionsordnung konnte nun die Geschwindigkeitskonstante der Deaktivierung k als alleiniger druck- und temperaturabhängiger Parameter ermittelt werden. Die Deaktivierungskurven von Glucoamylase zeigten einen klaren biphasischen Verlauf, was mit der Existenz zweier Enzymisoformen erklärt werden konnte. Die Kinetiken erster Ordnung wurden daher mit einem Zwei-Fraktions-Modell beschrieben. Schließlich konnten die gefundenen Abhängigkeiten der Deaktivierungsgeschwindigkeitskonstanten von Druck und Temperatur erfolgreich mit einem thermodynamisch basierten Polynom-Modell beschrieben werden.

Im Rahmen dieser Arbeit zeigte die Isoform GA1 der Glucoamylase mit Abstand die größe Toleranz gegenüber hohem hydrostatischen Druck. Ein Aktivitätsverlust konnte selbst nach einer Behandlung bei 1200 MPa und Temperaturen unter 60°C nicht festgestellt werden. β-Amylase verlor 95% ihrer Aktivität nach einer 30 minütigen Behandlung bei 620 MPa und 30°C. Bei 40°C wurde α-Amylase (in Anwesenheit von Ca^{2+} Ionen) bei 720 MPa, GA2 bei 810 MPa und β-Glucanase bei etwa 900 MPa (Gerstenmalz) und 1100 MPa (*B.subtilis*) nach 30 Minuten zu 95% deaktiviert. Gleichwohl zeigten die untersuchten Enzyme eine signifikante Stabilisierung gegenüber thermisch-induzierter Denaturierung bei 200 (α- and β-Amylase), 400 (β-Glucanase aus Gerstenmalz), 500 (β-Glucanase aus *B.subtilis*) bzw. 600 MPa (Glucoamylase).

Die mathematischen Modelle zur Beschreibung der Enzymdeaktivierung bei verschieden Druck-Temperaturkombinationen wurden anschließend benutzt, um den gefundenen enzymatischen Substratumsatz von der eventuell überlagerten Enzymdeaktivierung zu

korrigieren. Diese Prozedur erlaubt nun die isolierte Betrachtung des Einflusses von Druck und Temperatur auf den Substratumsatz.

β-Glucanase aus *B.subtilis* zeigte eine deutlich erhöhte katalytische Aktivität bei erhöhtem Druck und Temperatur. Alle anderen Enzyme zeigten eine reduzierte katalytische Aktivität bei erhöhtem Druck, aber eine stark erhöhte Aktivität mit einer Erhöhung der Temperatur. Für die Gesamtreaktion des Substratumsatzes mit gleichzeitig stattfindender Enzymdeaktivierung konnten spezifische Druck-Temperatur-Zeit-Kombinationen ermittelt werden, die ein Maximum an Substratumsatz liefern. Die jeweiligen Optima lagen dabei bei 165 MPa und 66°C (α-Amylase), 106 MPa und 60°C (β-Amylase), 220 MPa und 55°C (β-Glucanase aus Gerstenmalz), 270 MPa und 80°C (Glucoamylase in Anwesenheit von Maisstärke), 307 MPa und 63°C (β-Glucanase aus *B.subtilis*) und 318 MPa und 84°C (Glucoamylase in Anwesenheit von Maltosemonohydrat) nach einer Prozesszeit von 30 Minuten. Im Vergleich zum maximalen Substratumsatz bei Umgebungsdruck konnte bei optimalen Druck-Temperatur-Bedingungen etwa 20% (β-Amylase) bis zu 400% (β-Glucanase aus *B.subtilis*) mehr Substrat umgesetzt werde.

Der Verlust der Doppelbrechung von polarisiertem Licht wurde als Indikator zur Beschreibung irreversibler Quellungs- und Verkleisterungsvorgänge in Maisstärkekörnern verwendet. Stärkequellung wurde in einem Druckbereich von 0.1-650 MPa und Temperatur von 30-75°C bestimmt. Die Quellung der Stärkekörner verlief mit einer Reaktionsordung von 1,65 sowohl unter Umgebungsdruck als auch unter Hochdruckbedingungen. Die Geschwindigkeitskonstante konnte anschießend als Funktion von Druck und Temperatur mit einem sigmoidalen Modell beschrieben werden, wobei die Schmelztemperatur der Stärkekörner als Referenzpunkt benutzt wurde. Es zeigte sich, dass die Geschwindigkeit der Stärkeverkleisterung ausschließlich abhängig von der Temperatur war, solange der Druck 300 MPa nicht überstieg. Bei höheren Drücken verlagerte sich der Punkt der Stärkeverkleisterung hin zu niedrigen Temperaturen. Bei 30°C wurde eine komplette Verkleisterung der Maisstärke nach einer Behandlung bei 650 MPa für 30 Minuten festgestellt.

Abschließend konnte gezeigt werden, dass im Vergleich zu optimalen Bedingungen bei Umgebungsdruck die Verzuckerung von nativer Maisstärke durch Glucoamylase durch eine Druck- und Temperaturerhöhung um das 2,5 fache beschleunigt werden kann. Ebenfalls konnte bewiesen werden, dass die enzymatische Verzuckerung von Gerstenmalz durch eine Druckbeaufschlagung bei gleichzeitiger Temperaturerhöhung beschleunigt und die Prozesszeit damit um ein Viertel reduziert werden kann.

1. INTRODUCTION

High pressure processing (HPP) of foods has been suggested as an alternative to conventional thermal preservation processes due to its ability to inactivate micro-organisms and enzymes while the quality attributes, such as color, flavor and the nutritional value, remain unchanged (Knorr and Heinz 2001; Tauscher 1995; Torres and Velazquez 2005). For the last 15 years, the use of HPP has been explored extensively in the food industry and at present 92 industrial installations exists from 35 to 360 litres with an annual production volume of more than 120,000 tons (Tonello, C., personal communication). 56 companies worldwide already decided to apply high pressure treatment in their production, in most of the cases for food safety reasons or to extent the shelf-life. Typically, pressures up to 600 MPa and treatment times from a few seconds to several minutes are used to kill bacteria. However, high hydrostatic pressure constitutes an efficient physical tool to modify food biopolymers, such as proteins or starches and there are first commercial examples which make use of high pressure technology for the modification of food properties or functionality. E.g. oysters are treated at 300 MPa for preshucking which strongly increases the consumer convenience (Anonymus 2006). In Japan, rice is pressurized at 400 MPa and 60°C to enhance the flavour and to reduce the allergenic potential of this ready-to-eat rice product (Kishi, Y., personal communication).

Chemical transformations under high pressure can be irreversible or reversible, depending on involved substances, environmental conditions, and the combination of pressure, temperature, and exposure time. High-pressure treatment effects on foods are highly dependent on the primary effects of pressure and temperature on the relevant thermodynamic and transport properties of food systems which in general are density, viscosity, thermal conductivity, compressibility, heat capacity, diffusivity, phase transition properties (e.g. melting point), solubility, etc. Pressure as a fundamental state variable drastically influences the values of those properties.

Amylolytic enzymes, especially those from bacterial and fungal origin, are widely applied for the industrial production of spirits and glucose syrups from starch. α- and β-amylase and β-glucanase from barley malt have major importance for the preparation process of alcoholic beverages, such as beer and whisky.

Enzymatic starch liquefaction and saccharification is one of the most important applications of enzymes in food industry. However, the rate of enzymatic starch conversion is often limited by the thermo-sensibility of the enzymes used.

It is known that hydrostatic pressure has a strong effect on the activity and substrate specificity of enzymes (Knorr et al. 2006; Masson et al. 2004; Mozhaev et al. 1996b), in particular a protection against thermal denaturation of proteins has been reported frequently (Cheftel 1992; Heremans 1982; Ludikhuyze et al. 2003). This response to variations in pressure and temperature may possibly be exploited for industrial processes by operating enzymatic reactors at optimized conditions.

The main objective of this basic study was the identification of specific pressure-temperature conditions that are appropriate to maximize the conversion reactions of α- and β-amylase from barley malt, β-glucanase from barley malt, β-glucanase from *Bacillus subtilis* and glucoamylase from *Aspergillus niger*. Kinetic measurements of enzyme stability and specific conversions of different substrates were performed separately in different pressure-temperature-domains. In addition, the impact of pressure and temperature on gelatinization kinetics of maize starch was assessed by microscopic inspections of the granule's loss in birefringence.

2. BACKGROUND AND LITERATURE REVIEW

2.1 Enzyme principles

2.1.1 Introduction

An enzyme can be defined as a biological molecule that catalyzes a chemical reaction. Usually, enzymes are globular proteins and posses the functional characteristics of globular proteins of binding one or more substrate molecules. However, recently it was found that some RNA molecules also have catalytic activity, and to differentiate them from protein enzymes, they are referred to as RNA enzymes or ribozymes (Tucker 1995).

The first clear recognition of an enzymatically catalysed reaction was described by Persoz and Payen in 1833 who recognized that barley malt contains a substance that is able to convert starch to sugar. This substance was called diastase, which is now recognized as the malt α-amylase.

Enzymes are biocatalysts that usually show high affinity to a specific substrate and that only act under specific conditions (temperature, pH, a_w). The substrate molecules are bond in a hydrophobic cleft known as the active site and even small structural changes in this active site can result in a complete loss of enzyme activity (Tsou 1986). Enzymes are essential for living cells since they accelerate chemical reactions which would occur too slowly, or would lead to different products without enzymes under the conditions dominating in organisms. Despite the increased reaction rate the equilibrium of the reaction is usually not shifted since the forward and backward reaction is accelerated by the same factor. However, hydrolases catalyse reactions involving water as a reactant. Since enzymes usually act in an aqueous environment the concentration of water can be assumed as constant. The concentration of water as a reactant is significantly higher as the concentration of the emerging products and therefore, hydrolysed reactions always proceed towards the cleavage of the substrate (Zech and Domagk 1986).

As a true catalyst, an enzyme remain unaltered at the end of the reaction which implies that it has the ability to specifically bind to the reaction partner without changing its individual nature. However, this does not preclude that an enzyme is altered during the reaction but that such an alteration or “intermediate complex” is reversible. Thus, enzymes are like any catalyst and are not consumed in chemical reactions nor do they alter the equilibrium of a reaction.

Enzymes are named according to the reaction they catalyze. Typically the suffix -ase is added to the name of the substrate or the type of reaction. The International Union of Biochemistry and Molecular Biology (Biochemistry 1992) has developed a nomenclature for

enzymes, the EC numbers; where each enzyme is classified by a sequence of four numbers, preceded by "EC". Not all enzymes have been named in this manner, however, to ease the confusion surrounding enzyme nomenclature, a classification system has been developed based on the type of reaction the enzyme catalyzes. The first number broadly classifies the enzyme based on its mechanism:

Tab. 2.1: The international top-level classification of enzymes

EC No.	Class	Type of reaction catalyzed
1	Oxidoreductases	catalyze oxidation/reduction reactions by transfer of electrons
2	Transferases	group transfer reactions
3	Hydrolases	catalyze the hydrolysis of various bonds
4	Lyases	cleave various bonds by means other than hydrolysis and oxidation
5	Isomerases	catalyze isomerization changes within a single molecule
6	Ligases	formation of covalent bonds between two molecules by condensation reactions coupled to ATP cleavage

2.1.2 Structure of enzymes

The activity of an enzyme is determined by its three-dimensional structure. As any protein, enzymes consist of a polypeptide backbone of defined amino acid sequence, which folds in a particular fashion. The shape into which a protein naturally folds is known as its native state. Each type of protein/enzyme differs in its sequence and number of the different L-α-amino acids which fold the protein/enzyme into a unique three-dimensional structures. Individual protein chains may sometimes group together to form a complex. The two ends of a polypeptide chain are chemically different: the end which is terminated by the free amino group is the amino terminus (also known as the N-terminal domain), and that carrying the free carboxyl group is the carboxyl terminus (also known as the C-terminal domain). The amino acid sequence of a protein is always presented in the N to C direction, reading from left to right.

Usually protein's structure is classified into four distinct aspects. The *primary structure* (Fig. 2.1) refers to the linear number and order of the amino acids present and is held together by covalent peptide bonds, which are made during the process of translation (nucleophilic acyl substitution). The array of amino acids in the protein confers typical conformational forms which constitute the *secondary structures* of a protein (Fig. 2.2). In general proteins fold into two broad classes of structure termed, globular proteins or fibrous proteins. Enzymes belong to the class of

globular proteins which are compactly folded and coiled, whereas, fibrous proteins are more filamentous. The α-helix is a common secondary structure found in globular proteins. The formation of the α-helix is spontaneous and is stabilized by hydrogen bonds between amide nitrogens and carbonyl carbons of the peptide bonds. The orientation of H-bonding produces a helical coiling of the peptide backbone in a way that the side-chains lie on the exterior of the helix and perpendicular to its axis. There are 3.6 amino acid residues per turn of the helix. In contrast to an α-helix, β-sheets are composed of two or more different regions of stretches of at least 5-10 amino acids. The folding and alignment of stretches of the polypeptide backbone aside one another to form β-sheets is stabilized by hydrogen bonds as well. However, the bonding residues are present in contiguously opposed stretches of the polypetide backbone. It is said that β-sheets are pleated and are either parallel peptide (chains proceed in the same direction) or antiparallel. The t*ertiary structure* is referred to the overall three-dimensional shape of a single protein. It describes the spatial relationship of different *secondary structures* to one another and how these *secondary structures* themselves fold into the three-dimensional form of the protein. The *tertiary structure* also describes the relationship and interaction of different domains to one another within a protein. Those interactions of different domains are usually governed by hydrogen bonding, hydrophobic interactions, electrostatic interactions and van der Waals forces. The structure formed by the union of more than one protein molecule is known as quaternary structure. Many proteins contain different polypeptide chains (usually called protein subunits) which are associated by the same non-covalent forces that stabilize the tertiary structures of proteins. Those proteins with more than one polypetide chains are called oligomeric proteins.

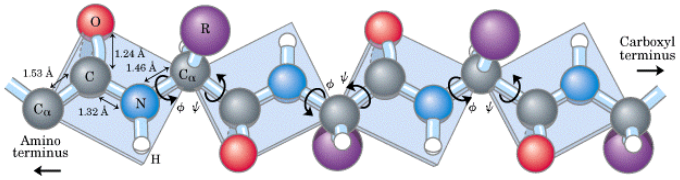

Fig. 2.1: The primary structure a protein is a chain of amino acids.

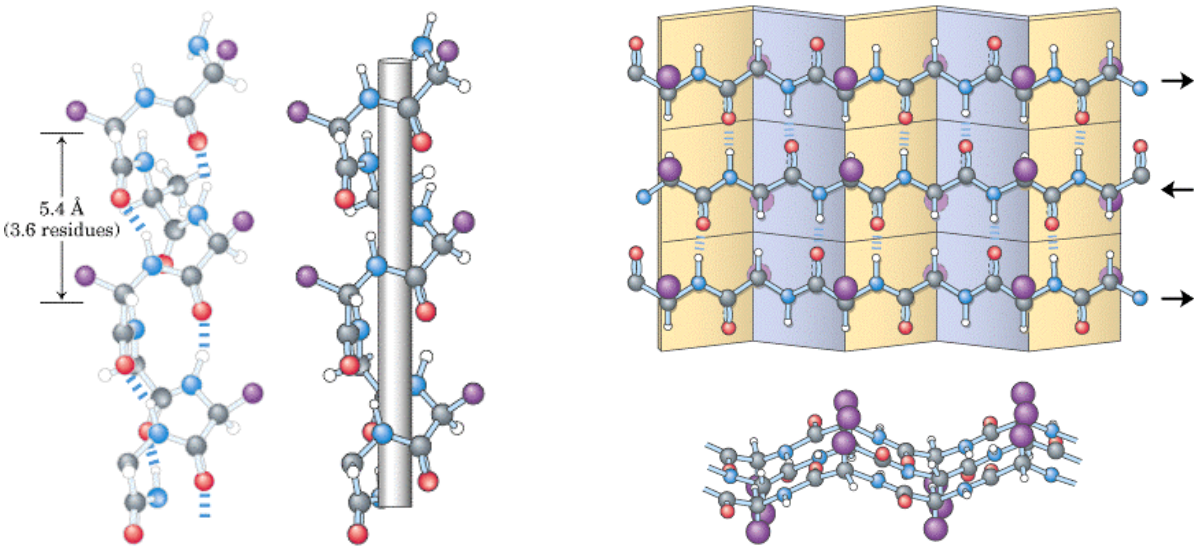

Fig. 2.2: *Left:* Protein α-helix in atomic detail. The protein's N- and C-terminal domains are at the top and bottom of the figure, respectively. *Right:* Top view and side view of an antiparallel β-sheet structure with H-bonding between the protein strands. The coloured spheres in both figures refer to the particular chemical element as follows: Carbon (gray), hydrogen (white), oxygen (red), nitrogen (blue), R group (purple).

Enzymes usually shift between several similar structures in performing of their biological function. Within the scope of these functional rearrangements, the tertiary or quaternary structures (Fig. 2.3) are usually referred to as conformations, and the transition between the native conformations are termed conformational changes.

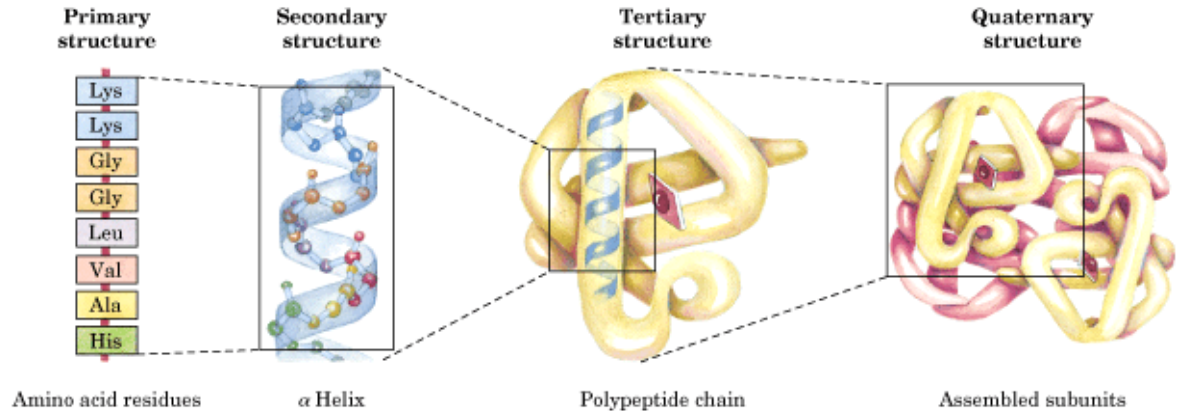

Fig. 2.3: The primary, secondary, tertiary and quaternary structure of proteins.

Naturally, enzymes have a small region of around 10 amino acids where binding of the substrate and then the reaction occurs. These binding sites are known as the active sites. Some enzymes also contain sites that bind cofactors, which directly participate in the catalytic event

and thus are required for enzymatic activity. A cofactor may be an organic molecule (also called coenzyme), or an inorganic metal ion. Those enzymes that require a cofactor are called apoenzymes whereas an apoenzyme together with its cofactor it is called a holoenzyme. The cofactor may be either covalently or loosely bound to the enzyme. If covalently connected, the cofactor is referred to as a prosthetic group. Some enzymes may also have binding sites for small molecules, which are often products or substrates of the reaction which is catalyzed. This binding can increase or decrease the enzyme's activity depending on the molecule and enzyme.

2.1.3 Enzyme mechanisms

Like all chemical reactions, enzyme-catalysed reactions must obey the laws of thermodynamics. Usually a barrier prevents complex molecules from spontaneously degrading and hence, this existing energy barrier has to be overcome for a reaction to occur. In particular, the reaction can only proceed if there is a net loss of free energy, i.e. the Gibbs free energy ΔG is negative. This free energy is dependent on the equilibrium constants of the reaction and the relative concentration of the reaction partners. The ΔG value can therefore be calculated for any reaction using Eqn.2.1:

$$\Delta G = \Delta G^0 + RT \ln \frac{[\text{Reactants}]}{[\text{Products}]} \qquad \textbf{(2.1)}$$

whereas R is the gas constant and T is the temperature. ΔG^0 refers to the standard free energy change of the reaction under ideal conditions and is dependent on the equilibrium rate constants:

$$\Delta G^0 = -RT \ln K \qquad \textbf{(2.2)}$$

Since the most energetically favourable state for any system is when ΔG = 0, the ratio of products to substrates that gives ΔG = 0 is the most stable state, thus reactions will tend to this equilibrium. In terms of thermodynamics, the effect of temperature on the ΔG of a reaction is not an important factor. However, in terms of reaction rate the temperature is a key parameter. Although the free energy ΔG is negative for most chemical reactions as a whole, often there is an intermediate state involved that actually has a higher ΔG than the original reactants. Thus, any molecule must first become sufficiently energized to overcome this energy barrier. The additional needed energy (called activation energy) could be provided by heat but excessive and prolonged temperature is often the unfavourable for a living cell or in food processing. The alternative is to lower the activation energy level through the use of a catalyst and therefore, the use of enzymes is preferred. After an enzyme binds to its substrate, one or more mechanisms of

catalysis lower the energy of the reaction's transition state, by providing an alternative chemical pathway for the reaction.

Another aspect of enzyme catalysed reaction is that of specificity. The exact mechanism by which enzymes act as catalysts is unknown but it was suggested by Emil Fischer in the 1890s that this was because the enzyme had a particular shape into which the substrate(s) fit exactly. In this simplest form which often referred to as "the lock and key" model, indicates that a particular domain (the active side) on the surface of the enzyme is structured to have a precise complementary fit to the substrate. However, nowadays modification of the "lock and key" model are favoured. Enzymes have rather flexible structures and the active site of an enzyme can be modified as the substrate interacts with the enzyme. The initial interaction between enzyme and substrate is relatively weak, but that these weak interactions rapidly induce conformational changes in the enzyme that strengthen binding.

Enzyme activity is affected by various parameters such as enzyme and substrate concentration, pH, temperature, pressure, ionic strength and moisture, the presence or absence of inhibitors or cofactors. Another parameter influencing enzyme activity is the addition of organic solvents, salts polyols or urea of which many of these additives stabilize enzymes in solutions (Bertroft et al. 1984; Guiavarc'h et al. 2003; Ludikhuyze et al. 1997; Weemaes et al. 1997).

2.1.4 Enzyme kinetics

It is often assumed that enzyme catalysed reactions are directly proportional to enzyme concentration. However, this is only true when the substrate level exceeds the enzyme level and even then there are often exceptions. Nevertheless, the rate of an enzyme catalyzed reactions is obviously dependent on substrate concentration. However, it is apparent that the relationship between the reaction's rate v and the concentration of substrate [S] will not be linear. Due to the mechanism of enzyme-substrate interaction in which the enzyme forms an one-to-one stoichiometric complex with its substrate and it is only this complex that can break down to give the product P. Hence, as the concentration of substrate increases the enzyme becomes saturated and thus the activity will tend towards a maximum. It is expected that the initial rate of an unimolecular reaction is proportional at low [S] and approaches a maximum V_{max} at larger [S]. At the maximum rate V_{max} of the enzyme, all enzyme active sites are saturated with substrate, and the concentration of enzyme-substrate complex ES equals the concentration of enzyme.

It is possible to derive mathematical equations to model the relationship between v and [S]. Michaelis and Menten proposed a quantitative theory of enzyme kinetics in 1913, which is

referred to as Michaelis-Menten kinetics (Michaelis and Menten 1913). In the simplest case of an enzyme catalyzed reaction a single substrate is converted into a product as shown in Eqn. 2.3:

$$E + S \underset{k_{-1}}{\overset{k_1}{\rightleftharpoons}} ES \xrightarrow{k_2} E + P \qquad \textbf{(2.3)}$$

where *E* = free enzyme, *ES* = enzyme-substrate complex, and k_1, k_{-1} and k_2 are the rate constants for the formation of *ES*, release of *S* or release of *P*, respectively. The time-dependent variation of the individual reactants is expressed in the following differential equations:

$$\frac{d[S]}{dt} = -k_1[E][S] + k_{-1}[ES] \qquad \textbf{(2.4)}$$

$$\frac{d[E]}{dt} = -k_1[E][S] + (k_{-1} + k_2)[ES] \qquad \textbf{(2.5)}$$

$$\frac{d[ES]}{dt} = -k_1[E][S] - (k_{-1} + k_2)[ES] \qquad \textbf{(2.6)}$$

$$\frac{d[P]}{dt} = -k_2[ES] = v \qquad \textbf{(2.7)}$$

The turnover rate *v* is defined as the increase in product, which is directly proportional to the concentration of the enzyme-substrate complex ES, according to Eqn. 2.7. To solve the differential equations (Eqn. 2.4-2.7) the time dependent concentration changes must be known which is hardly to realize, especially for [*E*] and [*ES*]. The following assumptions can to be made: 1) The concentration of substrate must be larger than of the enzyme; 2) The concentration of P must be effectively zero such that there is no reverse reaction; 3) The rate constant for the release of product k_2 must be the limiting rate for the reaction as a whole and [*E*] and [*ES*] are essentially in equilibrium.

In general, these assumptions are true. Substrate is almost always in large excess, initial rate ensure [*P*] to be approximately zero and the catalytic step (k_2) is usually rate limiting. In the quasi-equilibrium state (steady state) where the [*ES*] complex remains nearly constant the time-dependent concentrations changes of [*E*] and [*ES*] can be assumed to be zero, hence equations 2.5 and 2.6 simplifies to:

$$k_1[E][S] = (k_{-1} + k_2)[ES] \qquad \textbf{(2.8)}$$

and by substituting [*E*] according to the principle of mass conservation the total enzyme in the reaction $[E]_0$ must be equal to the sum of [*E*] and [*ES*], thus $[E]_0 = [E] + [ES]$ and term:

$$[ES] = \frac{k_1[E]_0[S]}{k_1[S] + k_{-1} + k_2} \qquad \textbf{(2.9)}$$

evolves, which is entered into Eqn 2.7 in order to obtain a relationship between turnover rate and substrate amount:

$$v = \frac{\mathrm{d}[\mathrm{P}]}{\mathrm{d}t} = -k_2\,[\mathrm{ES}] = \frac{k_2\,[\mathrm{E}]_0\,[\mathrm{S}]}{\frac{k_{-1}+k_2}{k_1}+[\mathrm{S}]} \qquad \textbf{(2.10)}$$

Since k_1, and k_2 are constant, $(k_{-1}+k_2)/k_1$ is also constant and is referred to as the *Michaelis constant* K_m. Also $k_2\,[E]_0$ represents the maximum possible rate of reaction and is usually written as V_{max}. Substituting the new terms K_m and V_{max} in Eqn. 2.10 we arrive at the conventional *Michaelis-Menten* equation (2.11):

$$v = \frac{V_{\max}[\mathrm{S}]}{K_m + [\mathrm{S}]} \qquad \textbf{(2.11)}$$

This equation was presented in 1925 by Briggs and Haldane, who derived numerous kinetic equations that are still widely used today (Briggs and Haldane 1925). The *Michaelis-Menten* equation (Eqn. 2.11) provides a good working model of unimolecular enzyme reactions. However, this equation still does not allow easy determination of the two key kinetic parameters K_m and V_{max}. Nevertheless, it is possible to rearrange Eqn. 2.11 to give a variety of linear plots. The most used rearrangement is that described by *Lineweaver* and *Burk* in 1934. This rearrangement takes reciprocals of both sides of Eqn 2.11 to give:

$$\frac{1}{v} = \frac{1}{V_{\max}} + \frac{K_m}{V_{\max}[\mathrm{S}]} \qquad \textbf{(2.12)}$$

A plot of $1/v$ against $1/[ES]$ gives a straight line with the intercepts on the y axis equal to $1/V_{max}$ the intercept on the x axis equal to $-1/K_m$ and the slope equal to V_{max}/K_m. Thus, such type of plot allows easy determination of both V_{max} and K_m. K_m usually describes the substrate concentration that is required for an enzyme to reach one-half its maximum rate. This can easily be seen from Eqn 2.11 when $[S]$ is substituted by K_m which gives:

$$v = \frac{V_{\max}}{2} \qquad \textbf{(2.13)}$$

The *Lineweaver-Burk*-plot is the most frequently used method to determine the K_m and V_{max} values, but has the essential disadvantage of the uneven distribution of data. However, the *Hanes* plot provides a good alternative because here the error limits are only slightly distorted. The corresponding equation derives from multiplication of the reciprocal *Michelis-Menten* equation (2.11) by $[S]$:

$$\frac{[\mathrm{S}]}{v} = \frac{[\mathrm{S}]}{V_{\max}} + \frac{K_m}{V_{\max}} \qquad \textbf{(2.14)}$$

In the *Hanes* plot [*S*]/*v* is plotted versus [*S*]. The gradient of the straight line is $1/V_{max}$, intersection with the abscissa is $-K_m$ and with the ordinate K_m/V_{max}.

Each enzyme has a characteristic K_m for a given substrate and this can show how tight the binding of the substrate is to the enzyme. In practical terms, a low K_m value indicates that the ES complex is held together very tightly and hence, that the enzyme works efficiently (i.e. with a high *v*) at low substrate levels and vice versa at high substrate levels. The efficiency of an enzyme can be expressed in terms of k_2/K_m. This is also called the specificity constant and incorporates the rate constants for all steps in the reaction. Because the specificity constant reflects both affinity and catalytic ability, it is useful for comparing different enzymes against each other, or the same enzyme with different substrates. The theoretical maximum for the specificity constant is called the diffusion limit and is about 10^8 to 10^9 M^{-1} s^{-1}. At this point, every collision of an enzyme with its substrate will result in the conversion reaction and the rate of product formation is just limited by the rate of diffusion.

2.1.5 Enzyme inhibition

Enzyme inhibition is defined as the negative effect on enzyme activity by ligands (inhibitors) specifically binding to defined catalytic or regulatory centres (Bissinger 2002). Enzyme activity can be inhibited in various ways but often enzymes tend to exhibit product inhibitions. Competitive inhibition is the easiest to comprehend, usually occurring when an inhibitor (often very similar to the substrate molecules) binds to the active site and prevent binding of the substrate. Thus, high levels of substrate can compete out the inhibitory effect and V_{max} is essentially unaltered although K_m is increased. Uncompetitive inhibition arises when an inhibitor binds to the enzyme at a location other than the active site but once the complex is formed it physically block the normal active site and thus inactivates the enzyme. In other instances, the binding of the inhibitor is believed to change the shape of the enzyme molecule, thereby deforming its active site and preventing it from reacting with its substrate. This latter type of uncompetitive inhibition is called allosteric inhibition; the place where the inhibitor binds to the enzyme is called the allosteric site.

A reduction of the reaction rate can be caused also by other factors such as pH, temperature, ionic strength or polarity of the solvent. Usually such influences occur unspecifically due to changes of the enzyme structure, interactions with charges groups or disturbance of the hydrate shell. However, such effects are not considered as enzyme inhibition.

2.1.6 Effect of temperature on enzyme stability

The structure of a native, catalytically active enzyme, and thus of a protein, is stabilized by a balance sensitive balance of disulfide bonds and various non covalent forces such as hydrogen bonds and hydrophobic, electrostatic and van der Waals interactions. Upon heating, all these forces are weakened particularly due to molecular fluctuations and the protein molecule denatures or unfolds. The amino-acid residues that form the active center of an enzyme are brought together only in the native structure of the molecule and unfolding results in disassembling of this domain and thus, in enzyme inactivation. However, it should be emphasized that inactivation of an enzyme not necessarily include complete irreversible changes of the protein's structure since even partial conformational changes can result in an inactivation of the enzyme's active center.

Usually, denaturation reactions are not strong enough to break the peptide bonds, and hence, the primary structure remains the same after a denaturation process. However, the cleavage of covalent bonds can occur at very high temperatures (e.g. >100°C) and can be brought about by inter- and intra-molecular thiol-disulfphide interchanges, deamidation of asparagine or glutamine residues, oxidation of cysteine sulfhydryl groups or oxidation of the tryptophan indole ring (Ahern and Klibanov 1985; Klibanov 1983; Mozhaev et al. 1988; Tomazic and Klibanov 1988).

In general, denaturation of enzymes occurs because the interactions responsible for the secondary structure (hydrogen bonds to amides) and the tertiary structure are disrupted. The most common observation in the denaturation process is the precipitation or coagulation of the protein. This is often due to the exposure of hydrophobic regions of the protein molecule to the aqueous solution. Since this is thermodynamically unfavourable the hydrophobic spots of unfolded molecules start to interact with each other which results in protein aggregation. However, in highly diluted enzyme solutions a monomolecular process is predominant where the unfolded molecules intermolecularly refold into thermodynamically stable structures. Usually, enzymes are only active in their native conformation and therefore, these incorrect structures are catalytically inactive. After cooling these incorrect structures remain since a high energy barrier prevents spontaneous refolding to the native structure. Nevertheless, there are some studies that report on recovery of enzymes, especially of peroxidases, after thermal inactivation has occurred (Guyer and Holmquist 1954; Ladero et al. 2005; Machado and Saraiva 2002). The often observed biphasic patterns of inactivation kinetics in these studies led to the assumption of an intermediate showing enzyme activity.

Denaturation also disrupts the normal α-helix and β-sheets in a protein and uncoils it into a random shape. However, β-sheets are generally more stable towards temperature than α-helix structures and hence, enzymes that contain large amounts of β-sheets structures tend to exhibit

higher temperature stability than enzymes rich in α-helix structures (Fabian et al. 1993; Scheraga et al. 1962).

The disintegration of the enzyme's tertiary structure results from counteracting exothermic interactions, such as hydrogen bonds and van der Waals interactions, and endothermic hydrophobic interactions. Hydrophobic interactions are of great importance for the stability of the protein molecule and are stabilized up to 60°C (Scheraga et al. 1962). Higher temperatures lead to a destabilization of the hydrophobic domains due to the gradual breakdown of water structures. The quaternary structure of enzymes is maintained by non-covalent interactions and therefore, thermal processing also results in dissociation of oligomeric proteins (Mozhaev and Martinek 1982).

2.1.7 α-amylase

α-amylase (α-1,4 glucan glucanohydrolase EC. 3.2.1.1) catalyzes the hydrolysis of 1,4-α-D-glucosidic linkages in polysaccharides containing three or more 1,4-α-linked D-glucose units in a random manner. Starch is degraded down to low molecular weight dextrins limited by α-1,6 bonds in a way that α-amylase is unable to hydrolyse. α-amylase, especially from bacterial and fungal origin, is widely used for the industrial production of alcohol and glucose syrups from starch(Van der Maarel et al. 2002). α- and β-amylase from barley have major importance for the preparation process of alcoholic beverages, such as beer and whisky.

All known wild α-amylases belong to a group of metalloenzymes that contain a conserved calcium ion. Calcium is therefore required to retain the structural integrity of the enzyme (Vallee et al. 1959). Removal of calcium from the enzyme results in changes of the secondary and tertiary structure (Bush et al. 1989) and to a decrease in thermostability (Nielsen et al. 2003; Saboury and Karbassi 2000; Violet and Meunier 1989) and enzymatic activity (Bozonnet et al. 2003; MacGregor et al. 2001; Rodenburg et al. 1994).

Barley α-amylase contains two isozyme families, AMY1 and AMY2, which are involved in starch mobilization during germination of the seeds and an endogenous inhibitor BASI (barley α-amylase/subtilisin inhibitor) which presumably protects the seed from rapid hydrolysis and exogenous proteases (MacGregor 1987; MacGregor 1988; Vallee et al. 1998). Both groups of isoenzymes differ in their isoelectric points (pIs) which range from 4.7-5.2 (AMY1) to 5.9-6.1 (AMY2) (Ajandouz et al. 1992). Furthermore, each family covers several components resulting from post-translational modifications and different gene expression (Ajandouz et al. 1992; Jones and Jacobsen 1991; Svensson et al. 1987). AMY2, which represents 80-98% of the total α-amylase, is the major isoenzyme in green malt and, in contrast to AMY1, is largely unaffected during kilning (Jones and Jacobsen 1991; MacGregor 1987; Tibbot et al. 2002). Both isoforms

possess 80% homology in their sequence identity (Rogers 1985)but show several differences in physico-chemical properties, such as calcium ion affinity (Bertroft et al. 1984; Bush et al. 1989), thermo- and pH stability (Bertroft et al. 1984; Jones and Jacobsen 1991; Rodenburg et al. 1994) and their activity on starch granules and soluble substrates(Kadziola et al. 1994). In addition, the endogenous inhibitor BASI is highly specific for AMY2, but does not inhibit the AMY1 isoform (Rodenburg et al. 1994; Vallee et al. 1998). The crystal structure and sequences of barley α-amylase isoenzymes and BASI has been determined in the last decade (Kadziola et al. 1994; Kadziola et al. 1998; Robert et al. 2002; Vallee et al. 1998) and are reviewed in a number of papers (MacGregor et al. 2001; Nielsen et al. 2004; Søgaard et al. 1993; Svensson 1994).

Fig. 2.4: Stereographic cartoon of the molecular structure of barley α-amylase, isoenzymes AMY2. Arrows indicate β-sheets, wound ribbons indicate α-helices and balls show the three calcium binding sides. The C domain, on the left side, is organized as a 5-stranded anti-parallel β-sheet. Drawn after Kadziola et al. (1994).

Since the rate of an enzymatic conversion reaction is limited by the thermo-sensitivity of the enzyme some α-amylases became a target for protein engineering using site directed mutagenesis coupled with analysis of the substrate binding domain (Christensen et al. 2002; Juge et al. 1996; Nielsen and Borchert 2000; Svensson 1994; Svensson et al. 1999).

Weemaes and co-workers (Weemaes et al. 1996) compared the thermo- and pressure-stability of three different α-amylases from *Bacillus species* in Tris-buffer (pH 8.6). The authors assumed a correlation between thermal and pressure stability, since, compared to α-amylase from *B. subtilis* and *B. amyloliquefaciens*, α-amylase from *B. licheniformis* showed by far the highest resistance when exposed to high pressures and/or temperature. Inactivation kinetics of α-amylase from *B. subtilis* in Tris buffer were further investigated by Ludikhuyze et al. (Ludikhuyze et al. 1997) over a broad pressure and temperature range. The authors developed

a thermodynamically based model indicating the possible synergistic and antagonistic effects of pressure and temperature on the inactivation of the enzyme. Raabe et al. (Raabe and Knorr 1996) detected a retarded enzymatic hydrolysis of starch by *B. amyloliquefaciens* α-amylase under pressure up to 400 MPa and 25°C which was not primarily due to irreversible inactivation of the enzyme. Matsumoto et al. (Matsumoto et al. 1997) found evidence that hydrostatic pressure up to 300 MPa induced changes in product composition accompanying the hydrolysis of maltooligosaccharides by porcine pancreatic α-amylase.

2.1.8 β-amylase

β-amylase (α-1,4-glucan maltohydrolase; EC 3.2.1.2) hydrolyzes the α–1,4-glucosidic linkages of starch so as to remove successive maltose units from the non-reducing ends of the chains. Barley β-amylase is highly heterogeneous and the number of isoenzymes appears to vary with the barley variety and technique used (MacGregor 1991). Three endosperm-specific β amylase alleles, Bmy1-Sd1, Bmy1-Sd2L and Bmy1-Sd2H, have been identified in cultivated barley. The corresponding enzymes are referred to as Sd1, Sd2L and Sd2H, respectively (Eglinton et al. 1998). These allelic forms of barley β-amylase have been found to be closely related to variation in β-amylase expression, differences in thermo-stability (Eglinton et al. 1998; Ma et al. 2001) and kinetic properties (Ma et al. 2000).

The structural features of β-amylase have, however, been clarified only recently. A comparison of the primary structures has shown that the higher plant β-amylases have amino acid sequences of more than 60% similarity, but that the similarities between plant and micro organism β-amylases are about 30% (Svensson 1988). Further details about the sequences and properties of barley β-amylase has been first published by Kreis et al. (Kreis et al. 1987) and Yoshigi et al. (Yoshigi et al. 1995).

β-amylase is synthesised during the development of the grain and is present in a bond and a free form (MacGregor et al. 1971). The free form is easily extracted in water or salt solutions whereas the bound form is probably linked to other proteins through disulfide bonds and is insoluble in aqueous saline solutions (Evans et al. 1997).

Fig. 2.5: Stereographic cartoon of the molecular structure of a thermostable sevenfold mutant of the free form of barley β-amylase. Arrows indicate β-sheets and wound ribbons indicate α-helices. Drawn after Mikami et al. (Mikami et al. 1999).

In the mature grain equal amounts of bound and free β-amylase are present (Grime and Briggs 1995; MacGregor et al. 1971) but the hydrolytic activity of the bound enzyme is retarded presumably due to steric hindrance of the active side (Sopanen and Laurière 1989). However, after germination a significant proportion of the enzyme undergoes proteolytic modification by cystein endopeptidase resulting in the release and activation of the bound amylase fraction (Guerin et al. 1992; Sopanen and Laurière 1989).

As with most reactions, the rate of the enzymatic conversion reaction can be increased by raising the temperature up to the critical temperature where the protein inactivates. β-amylase from barley malt is less thermostable than α-amylase and a considerable amount of β-amylase activity is lost during kilning. β-amylase is inactivated in the same temperature range as starch is gelatinized and thus the enzyme is usually very close to its upper limit under mashing conditions. Therefore, also this β-amylase was sequenced and cloned to improve its substrate-binding affinity and thermostability (Ma et al. 2001; Mikami et al. 1999; Yoshigi et al. 1995; Yoshigi et al. 1994). In contrast to α-amylase from barley, β-amylase activity is supported by a higher pH level of 5.7-6.2 (Ma et al. 2001; Mikami et al. 1999; Yoshigi et al. 1995; Yoshigi et al. 1994).

It was shown that pressurization of barley flour slurries caused an increase in the action of barley α- and β-amylases above 300 MPa presumably due to gelatinization of the starch (Gomes et al. 1998). Raabe and Knorr (Raabe and Knorr 1996) found that enzymatic hydrolysis of starch by α-amylase from *Baciullus amyloliquefaciens* was retarded under pressures up to 400 MPa and 25°C which was not primarily due to irreversible inactivation of the enzyme. Pressure-induced perturbation of sweet potato β-amylase has been studied by Tanaka et al.

(Tanaka et al. 2001). One subunit of this enzyme contains six cysteine residues which are not reactive to a specific sulfhydryl reagent due to steric hindrance. High pressure enhanced the reactivity of one of the cysteine residues and it was assumed that local conformational changes this effect. However, since pressure impacts both on enzymes and substrate, the mechanism of action is still not fully understood.

2.1.9 Glucoamylase

Glucoamylase (1,4-α-D-glucan glucohydrolase, EC 3.2.1.3) is a multidomain exo-glycosidase that catalyses the hydrolysis of α–1,4 and α–1,6 glucosidic linkages of starch and related polysaccharides to release β–D-Glucose from the non-reducing ends. Glucoamylase from Aspergillus niger occurs naturally in two monomeric, glucosylated isozyme forms, glucoamylase 1 (GA1) and glucoamylase 2 (GA2) having different length and structure of amino acid residues (Christensen et al. 1999; Svensson et al. 1986; Svensson et al. 1982). Unlike GA2, GA1 features a starch binding domain which is connected to the catalytic domain via a 70-aminoacids- long highly O-glycosylated linker (Juge et al. 2002; Svensson et al. 1983). The presence of this starch binding domain of GA1 from Aspergillus niger increases the activity towards hydrated starch of this GA isoform by around 100- fold (Svensson et al. 1982) and results in an enzyme with the ability to digest granular starches (Christensen et al. 2002; Christensen et al. 1999; Southall et al. 1999). GA1 from *A.niger* possess a high homology with glucoamylase from Aspergillus awamori (Aleshin et al. 1994) and shares the starch binding domain with a number of amylolytic enzymes of the glycoside hydrolase families (Svensson et al. 1989). Reports on further structural properties can be found elsewhere (Fogarty and Benson 1983; Frandsen et al. 2000; Reilly 1999; Sauer et al. 2000; Sorimachi et al. 1997).

Due to its low production costs fungal glucoamylase is widely used for the industrial production of spirits and glucose syrups from starch. Large production scales and low profit margins of these products facilitate the development of optimized processes with accelerated enzymatic conversion of the substrate. Since glucoamylase cleaves the α–1,4 linkages about 500 times faster than the α–1,6 linkages (Frandsen et al. 1995; Hiromi et al. 1966) and thus, adversely affects the yield in industrial saccharification of starch, the enzyme became a target for protein engineering using site directed mutagenesis (Christensen et al. 2002; Sierks and Svensson 1996) coupled with analysis of the substrate binding domain (Christensen et al. 2002; Christensen et al. 1996; Hiromi et al. 1983).

It has also been reported that increased enzymatic reaction rates are produced by conformational changes of the protein, by alterations enzyme-substrate interactions, or by the impact on a particular rate-limiting step of the overall reaction. For instance, starch granules

show an increased susceptibility to hydrolysis by amylolytic enzymes once it has been gelatinized by pressurization. Takahashi et al. (Takahashi et al. 1994) showed that the bindability and digestibility of raw maize starch with glucoamylase is markedly enhanced when the starch was pressurized with more than 400 MPa. Selmi et al. (Selmi et al. 2000) reported that, compared with thermally gelatinized wheat starch, the equilibrium yield of glucose production by glucoamylase was significantly improved when using high pressure treated wheat starch. Such response to variations in pressure and temperature can possibly be exploited for industrial applications by operating enzymatic reactors at optimized p-T conditions.

Fig. 2.6: Schematic cartoon of the molecular structure of glucoamylase GA2 from Aspergillus awamori. Arrows indicate β-sheets and wound ribbons indicate α-helices. Circles and sticks represent the atoms of the glycosyl chains. Drawn after Aleshin et al. (Aleshin et al. 1994).

2.1.10 β-glucanase

β-glucans are polymers consisting of 1,3–1,4-mixed linked β-D-glucose units located in the cell walls of the endosperm of grains. Such β-glucans may be depolymerised by 1,3-1,4-β-glucanases (malt β-glucanase, 1,3–1,4-β-D-glucan 4-glucanohydrolase, EC 3.2.1.73), 1,3-β-glucanases (glucan endo-1,3-β-D-glucosidase, EC 3.2.1.39) and 1,4-β-glucanases (cellulase, EC 3.2.1.4) from barley. Several isoforms of these enzymes have been characterized recently suggesting that two isoenzymes of 1,3-1,4-β-glucanase are particularly responsible for the degradation of barley β-glucans (Doan and Fincher 1992; Hrmova and Fincher 1993; Slakeski and Fincher 1992; Woodward and Fincher 1982a; Woodward and Fincher 1982b; Yamashita et al. 1985). The overall structure and the active site of barley 1,3-1,4-β-glucanase, isoenzymes EII

have been described by Verghese et al. (Verghese et al. 1994). The active side is located in a cleft at the bottom of the barrel defined by the C-terminal ends of the parallel intra-barrel β-strands. Further reports on structural properties and specificities can be found elsewhere (Hoj and Fincher 1995; Müller et al. 1998; Verghese et al. 1994).

β-glucanase activity in malt is crucial for the brewing process due to its potential to affect the beer filtration (Home et al. 1993; Narziss 1993). Reduced filterability of mash and beer has often been attributed to large β-glucans which tend to increase the viscosity of beer by forming inter-molecular hydrogen bonds between sequences of β-1,4 linkages (Narziss 1993; Stewart et al. 1998). Particularly in the gel form as well as turbidity complex and in conjunction with other high-molecular ingredients, e.g. high-molecular proteins and arabinoxylans (Li et al. 2005; Stewart et al. 1998), β–glucans impedes the beer filterability by blocking the pores of the kieselghur.

Barley β-glucanases are synthesized during germination but are damaged during malting. During mashing β-glucanase activity is rapidly lost at temperatures above 50°C but solubilization of β-glucans from intact cell walls continues continues (Home et al. 1993; Home et al. 1999; Narziss 1993). This might be attributed to the presence of highly thermoresistant enzymes in barley malt like carboxypeptidase (Bamforth et al. 1979). Thus, the break down of β-glucans during mashing is usually undesirable. Improvements in malt quality or the use of low starting temperatures during mashing have been considered for this problem. However, breweries have moved away from extremely long mashing cycles, because of economic reasons and due to disadvantages in beer quality.

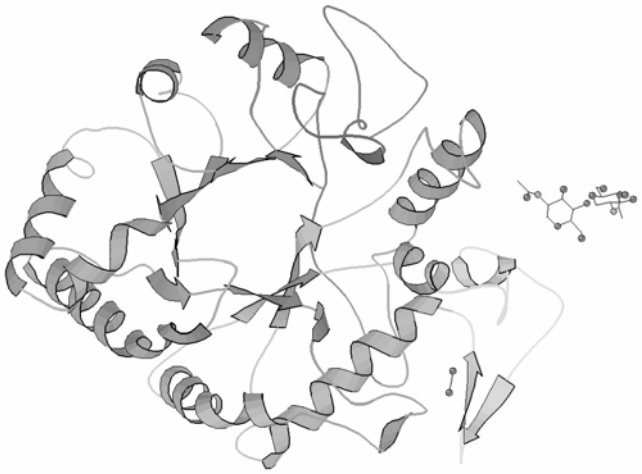

Fig. 2.7: Stereographic cartoon of the molecular structure of barley 1,3-1,4-β-glucanase, isoenzymes EII. Arrows indicate β-sheets and wound ribbons indicate α-helices. Circles and sticks represent the carbohydrate attached to the catalytic side. Drawn after Müller et al. (1998).

β-glucanase from *Bacillus subtilis* (lichenase, cellulase, Endo-1,4-β-D-glucanase, 1,4-(1,3;1,4)-beta-D-glucan 4-glucanohydrolase, EC 3.2.1.4) is known since several decades and

has been characterized in several papers (Aa 1994; Au and Chan 1987; Moscatelli et al. 1961; Rickes et al. 1962; Robson and Chambliss 1989). There has been considerable research interest in cellulases due to their ability to convert agriculture waste material into useful products such as ethanol for use as fuels and/or chemical feedstocks. Cellulose is often found in close association with other polysaccarides, such as hemicellulose or lignin, which makes a bioconversion difficult.

2.2 Starch principles

2.2.1 Introduction

Starch is an essential part in human and animal nutrition. It occurs in a variety of botanical sources including potato, wheat and maize and has been found to play an important role in food manufacturing processes due to their considerable effect on textural properties of food products. For instance, starch (in particular maize starch) is utilised as gelling agents for thickening sauces, desserts and puddings and is also used in the manufacture of adhesives, paper, and textiles.

Photosynthetic plants convert light energy into chemical energy which is stored in a highly condensed manner as amylose and amylopectin in the starch granules. Whereas amylose is a comparably small linear macromolecule with an average molecular weight of 250 kDa (Tegge 2004), amylopectin as the major constituent is one of the largest natural macromolecules with a molecular weight of 10^7 – 10^9 Da and arranged in double helix configuration (Gallant et al. 1992).

Generally, starch is found in plant tubers and seed endosperm in form of granules and is referred to as native when in this particular granular state. Native starches vary widely in size, structure and composition depending on the botanical sources. The granules can be e.g. spherical, oval, polygonal, and lenticular in shape with a diameter of 2 to 175 µm (Tegge 2004). Depending on their origin, starches have typical properties that are attributed to the size, shape, composition, and crystallinity of the granules (Belitz et al. 2004).

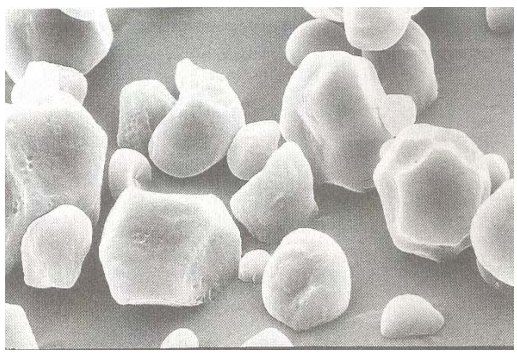

Fig. 2.8: Electron microscopic picture of maize starch (Tegge 2004).

2.2.2 Chemical structure

Amylose and amylopectin are inherently incompatible molecules forming starch granules at a ratio of normally 1:4 to 1:5. Amylose is constituted by glucose monomer units joined to one another head-to-tail with α-1,4 linkages with the ring oxygen atoms all on the same side. Amylopectin differs from amylose in that branching occurs with about one residue in every twenty or so is also linked with an α-1,6 linkage forming the branch-points. The relative proportions of amylose to amylopectin and α-1,6-branch-points both depend on the origin of the starch, e.g. amylomaizes contain over 50% amylose whereas waxy maize starch has almost none (~3%) (Singh et al. 2003).

Amylose is predominantly linear and generally tends to wind up into a rather stiff left-handed single helix or form even stiffer parallel-stranded double helices packed in a parallel fashion of 40–70 glucose units (Imberty et al. 1988; Leloup et al. 1992). In the helix each turn is formed by six glucose units (Zobel 1988) which itself are able to form a complex with an iodine molecule (Tegge 2004). The internal cavity of this helical structure has hydrophobic properties, which can be used by hydrophobic groups of ligands to lie within the helix (Godet et al. 1993). Such van der Waals forces may create absorbent sites directed towards the outside of the helix and together with the intramolecular hydrogen bonding are considered to be responsible for the stability of the amylose molecule (Tako and Hizukuri 2002). Amylose is able to associate with amylopectin by the establishment of thermally stable intermolecular hydrogen bonds (Tako and Hizukuri 2002).

Due to the branch points the overall structure of amylopectin is not that of a linear polysaccharide chain but forms a coiled molecule most suitable for storage in starch grains (Fig. 2.9 A). In amylopectin there are usually slightly more outer unbranched chains (called A-chains) than inner branched chains (called B-chains) (Fig. 2.9 B). A-chains are short, free of side chains and linked to the amylopectin molecule by its reducing end. The longer B-chains bear side chains (A- and B-chains) and can be divided into dense, crystalline regions and less dense, amorphous regions without side chains (Fig. 2.9 C). Parallel A- and B-chains in the same cluster form left-handed double helices originating from branch points with six glucose molecules per turn. There is only one chain (called C-chain) containing the single reducing group (Tegge 2004).

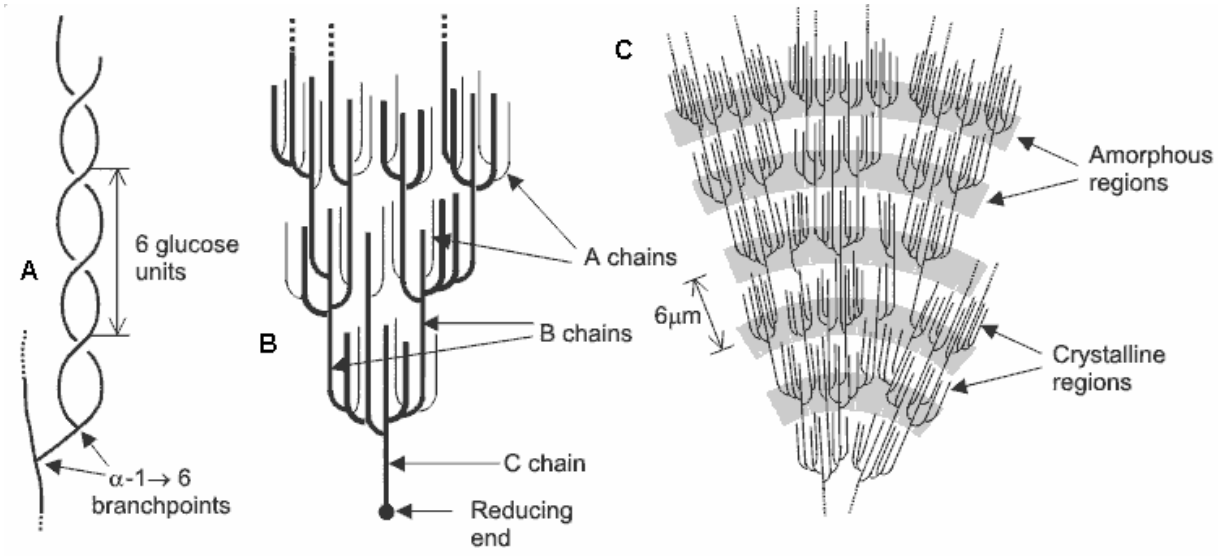

Fig. 2.9: The molecular structure of amylopectine. A: The likely double helix structure taken up by neighboring chains; B: Composition of an amylopectine molecule with A-, B- and C- chains; C: the organization of the amorphous and crystalline regions of the structure generating the concentric layers that contribute to the growth rings (Chaplin 2006).

Several investigations have been carried out to establish the level of organization within the starch granules. Techniques used vary from X-ray diffraction experiments to atomic force microscopy (AFM), transmission electron microscopy (TEM) (Waigh et al. 1999; Waigh et al. 1997). The conventional model of starch is that it is formed from three regions, crystalline and amorphous lamellae, which together form the crystalline growth rings, and amorphous growth rings, as shown in Fig. 2.10. It has been suggested that the length of chain participating in the crystalline domains is comparable to the short chain fraction of amylopectin (French 1984). Hence, the crystalline layers consist of ordered regions composed of double helices formed by the short chains of amylopectin, most of which are further ordered into crystalline structures known as the crystalline lamellae. The amorphous regions of the semi-crystalline layers and the amorphous layers are composed of amylose and non-ordered amylopectin branches (Waigh et al. 1997). The glucose monomers in amylopectin are oriented radially in the starch granule with the non-reducing ends of the chains towards the granule surface (Fig. 2.10). As the radius increases so does the number of branches required to fill up the space, with the consequent formation of concentric regions of alternating amorphous and crystalline structure.

The point of initiation of the granule is called the hilum. It is located near the center of elliptical granules or positioned on the axis of symmetry in pear-shaped granules. So far there are just a few details known on its exact organization and composition but it is usually considered to be less well organized than the rest of the granule (French 1984).

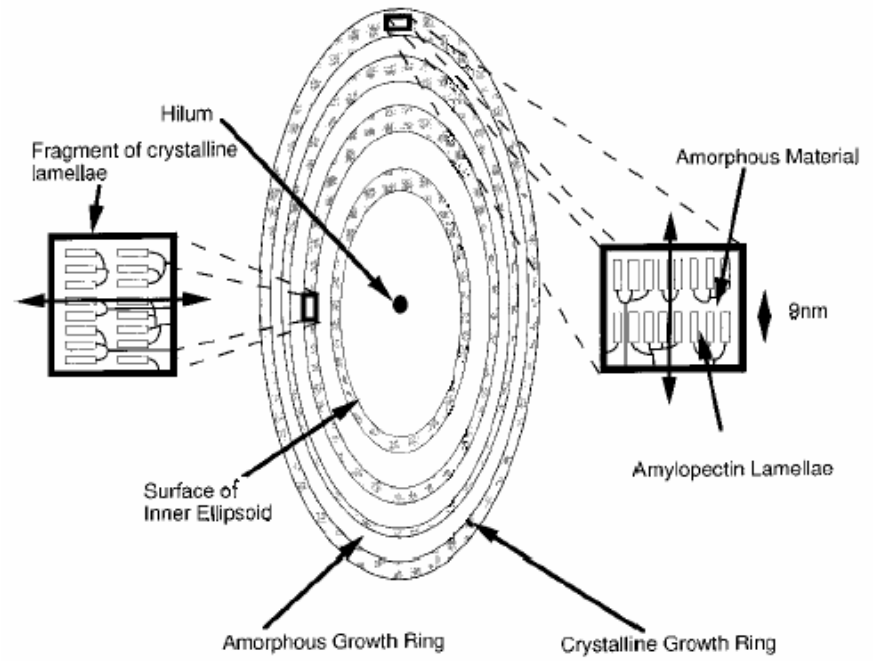

Fig. 2.10: Schematic view of the structure of a starch granule, with alternating amorphous and semi-crystalline zones constituting the growth rings with the orientation of amylopectin double helices in the crystalline lamellae (not to scale) (Waigh et al. 1997).

Fig. 2.11 illustrates the internal architecture of a starch granule. In native starch granules the extent of crystallinity is between 15-45% (Zobel 1988). Special breedings allow unusually high or low contents of amylose like in amylomaize (70%) or in waxy maize (less than 1 %) (Oates 1997). The crystalline regions are predominantly located in the hard (120-400 nm thick) layers of the granule and are composed of stacks of crystalline lamellae which form the backbone of the starch granule. The crystalline lamellae consists of the ordered double helical amylopectin side chain clusters and are alternated with amorphous lamellae consisting of the amylopectin branching regions. Crystalline and amorphous lamellae of the amylopectin are organized into larger, ellipsoid ultrastructures, the so-called blocklets (see Fig. 2.11). The blocklets range in diameter from around 20 to 500nm depending on the botanical source and location in the granule (Gallant et al. 1992). The soft shells of a starch granule are made of smaller blocklets which have a diameter of approximately 20-50 nm, the harder shells consist of larger blocklets ranging in diameter from around 50-500 nm. In the semi-crystalline shells amylopectin is therefore still predominantly in the double helical form, although its crystallinity is reduced possibly due to increased interaction with amylose. However, recently Tang et al. (Tang et al. 2006) described the existence of so called defective blocklet in which lower branching molecules (that are disadvantage to crystallize) are installed in blocklet ultrastructure.

The amorphous fraction (lower branching or non-branching molecules) around each blocklet in the hard as well as in the soft shells is believed to be responsible for the strength and flexibility of the system. The amorphous fraction can absorb and release the free water of the raw starch granules. The surface pores and interior channels as seen in Fig. 2.11 are believed to be naturally occurring features of the starch granule structure, with the pores being the external openings of the interior channels. The radial channels within starch granules are predominantly composed of semi-crystalline or amorphous material and have a diameter of 0.07-0.1 μm (Fannon et al. 1992).

The exact location and organisation of amylose in relation to the blocklet organisation in starch granules is not yet known. It can be hypothesized that a locally higher concentration of amylose (particularly short chains) may be present in the amorphous channels between the blocklets and during gelatinization, amylose is able to exit the granule through these channels. Consideration of the ratio of amylopectin to amylose in starch granules and the overall crystallinity of starch granules (15 to 45 %) leads to the conclusion that amorphous amylopectin is certainly also present in the amorphous regions of the starch granule.

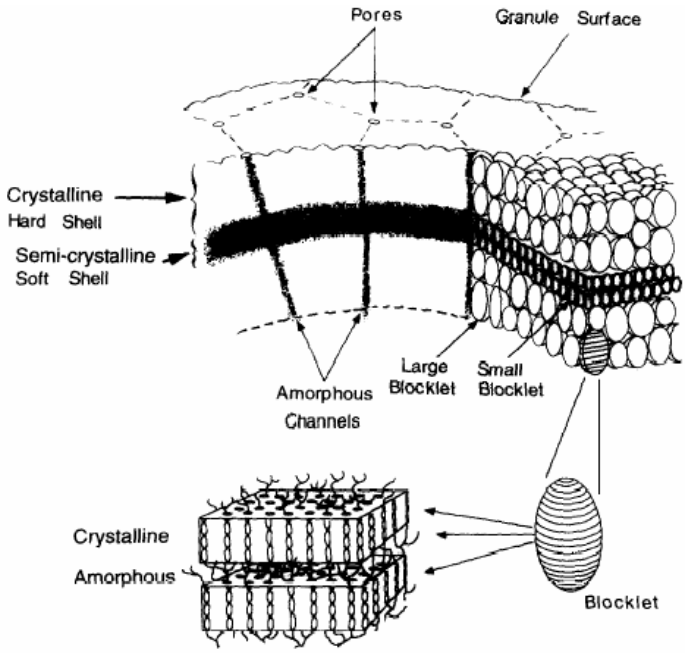

Fig. 2.11: The structure of starch blockets in association with amorphous radial channel and the amorphous crystalline lamella of a single blocket (Gallant et al. 1997).

The stability and functionality of starch is determined by highly ordered structural components: Crystalline and amorphous lamellae which form the crystalline growth ring and amorphous growth rings which alternate in a spacial distance ranging from 120 to 400 nm (Parker and Ring

2001). The crystallinity is classified as A-type or B-type dependent on the configuration of the unit cell of the double helix of the polysaccharides (Fig. 2.12) for which atomic models have been developed and extensively reviewed (Gidley and Bociek 1985).The A-type crystals are dense and consists of starch chains in a staggered monoclinic lattice, while the B-type hexagonal crystals have a large void in which up to 36 water molecules can be accommodated (Imberty et al. 1988; Imberty and Pérez 1988; Parker and Ring 2001; Perera et al. 1997). The unbroken chain lengths of type A crystals is about 23-29 glucose units, whereas type B, has a slightly longer unbroken chain lengths of about 30-44 glucose units. The relative number of associated water molecules per glucose unit is 2/3 and 3 for A-type and B-type, respectively (Gallant et al. 1992; Parker and Ring 2001). Cereal starches (rice, corn, waxy corn, wheat etc.), in most of the cases, show the A-pattern. The B-polymorph is found in banana, some tubers such as potato and high amylose cereal starches. The largest granules can reach a length of the longer semi-axis of up to 100μm in the case of potato starch (Blanshard 1987). There is also a type C structure, which is a combination of types A and B and is found in tropical plants and legume starches as from peas and beans. Furthermore, Hizukuri (Hizukuri 1986) demonstrated that the connecting B chains were more abundant in potato starch. He proposed that they are probably characteristic for starches with the B crystal pattern, since such starches have higher amounts of the B2-B4 chain fractions. This observation fits with the observation of Gallant et al. (Gallant et al. 1997) that, in general, the blocklet size is larger in starches with the B crystal pattern.

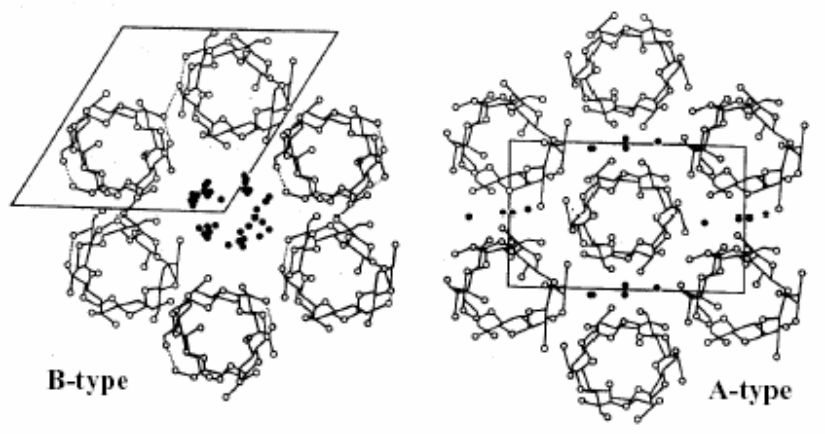

Fig. 2.12: Alignment of double helices in A- and B-type crystals of starches (Blanshard 1987).

2.2.3 Starch gelatinization

In the presence of water and at high temperatures the intermolecular bonds of starch molecules are broken down allowing the hydrogen bonding sites (the hydroxyl hydrogen and oxygen) to engage more water. The disruption of this structure is usually referred to as gelatinization. This process is essential in all kinds of industrial and culinary utilization of starch and is characterized by a loss in crystallinity and birefringence, by a solubilization of amylose and by an irreversible swelling of the granules (Parker and Ring 2001; Waigh et al. 2000; Waigh et al. 1997). The transition entails a loss of structural order in which the starch double helices disappear (Cooke and Gidley 1992). Nevertheless, the hydration of starch is not restricted to gelatinized granules.

The gelatinization process occurs in two steps (Svensson and Eliasson 1995): Initially, the amorphous regions of the granule are hydrated accompanied by a minor reduction in crystallinity. After the swelling of the amorphous domains, the growth ring structure of the granule starts to disintegrate and the crystalline regions undergo melting simultaneously with a progressively increasing hydration (Oates 1997). The penetration of water increases the random character in the general structure and decreases the size and the number of the crystalline region. The crystal regions do not allow water to penetrate into the interior of the starch granule. However, when heat is applied this region will be diffused, and the chains start to pull out from each other.

One of the more recent models proposed that upon separation of the amylopectin double helices from their lamellar crystallites, a true helix–coil transition occurs. In their crystalline smectic arrangement (Waigh et al. 1999; Waigh 1998), the amylopectin side chains intertwined in the double-helices strongly interact with not only their helical duplex partners, but with neighbouring chains in other helices. It is therefore necessary that the double helices dissociate side by side to allow the unwinding transition, since it is otherwise geometrically impossible in the strongly interacting lamellar environment (Waigh et al. 2000). It is predicted that the helix–coil unwinding in amylopectin double helices occurs from the loose ends, and not at the hairpin due to entropic effects (Waigh et al. 2000). The Zimm and Bragg (Zimm and Bragg 1959) model suggested that thermodynamic transition of starch granules is inversely proportional to the double helix length. The rotation of the links of the flexible spacer attached to the amylopectin double helix could affect the rate of gelatinization, i.e., long spacers in A-type starches could encourage rapid dissociation due to their increased flexibility (Buleon and Tran 1990). The longer amylopectin helices in B-type isomorphs (Zimm and Bragg 1959) stabilize an intermediate nematic phase due to their increased aspect ratio compared to A-type starches where the intermediate phase is isotropic (Fig. 2.13). It is therefore assumed that in the initial stage of gelatinization the amylopectin double helices of A-type starches (e.g. wheat)

dissociated from their crystallites and slowly dissociate side-by-side. As temperature is increased the helix coil transition happens as an immediate consequence (Fig. 2.13 right). Due to the helical stability in the B-type starches (e.g. potato), the B-isomorphs undergo an additional smectic-nematic-isotropic transition until helix unwinding starts (Fig. 2.13 left).

Increasing particle size and re-association of solubilized amylose are producing an increase in viscosity and gel formation. A gradual loss of birefringence occurs, and the low molecular weight components such as fats and ions are leached out into the water medium (Greenwood 1997). During this process, the secondary bonds that maintain the granule structure are broken and the micellar network is pulled apart.

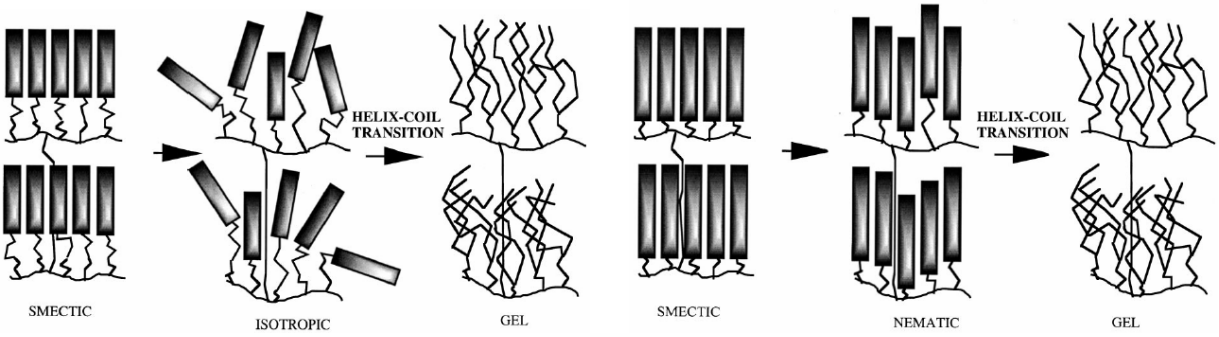

Fig. 2.13: The predicted two stage process involved in gelatinization of A-type (left) and B.type (right) starches (Waigh et al. 2000).

2.2.4 Enzymatic starch conversion

Enzymatic degradation of starch is widely used for the production of many products in food industry (e.g. beer, glucose syrup etc.). Gelatinization by heat is very often a pre-requisite for increasing the yield of the reaction and to run the process efficiently.

Native starches are generally insoluble in water at room temperature. Starch granules are quite resistant to penetration by water and therefore also by hydrolytic enzymes due to the formation of hydrogen bonds within the same molecule and with other neighboring molecules. However, degradation of native starch macromolecules takes place – at least in part and at a much lower rate – during pancreatic or microbial α-amylolysis. The starch granule is enzymatically attacked at the surface (exocorrosion) or via special susceptibility domains or randomly scattered irregular surface cavities (endocorrosion). In the latter case (e.g. maize or rice) those pits are increasingly eroded until canals through the growth ring structure of the granule are formed. For waxy maize starch this perforation is superimposed by a tangential attack on the amorphous part of the granule's shell structure (Gallant et al. 1992).

Complete starch degradation by amylolytic enzymes is largely dependent on the thermal stability of the enzymes and on the availability of substrate. α-amylase is able to partially

hydrolyze native starch (Sun and Henson 1991), however, the rate is much slower than for the degradation of solubilized starch (Slack and Wainwright 1980). β-amylase has no ability to hydrolize native starch granules but shows significant hydrolysis of gelatinized starch (Sun and Henson 1991). Hence, solubilization or gelatinization is a prerequisite of starch hydrolysis. MacGregor et al. (MacGregor et al. 2002) found that the pasting temperatures of the starches raised with the content of amylose. However, starches with an amylose content of ca. 25% had the lowest gelatinization temperature and were readily soluble in water at 48-60°C and were susceptible to enzymatic degradation. Efficient hydrolysis of gelatinized starch during mashing is considered to result from the combined action of α-amylase, β-amylase and limit dextrinase (MacGregor et al. 1999).

Tab. 2.2 presents the most important enzymes for industrial hydrolysis of starch. Commercial α-amylases are usually isolated from bacterial sources (e.g. *Bacillus spp*.). They often have a high thermostability which is important during the initial phase of starch conversion. Here, high temperatures are required to gelatinize the starch. Often calcium ions are required for enzyme activity and stability, and reactions are generally performed at neutral pH. α-amylases randomly attack only the α-1,4 bonds of the large polymer particles which drastically reduces the viscosity of gelatinized starch solution, resulting in a process called liquefaction (Fig. 2.14). The final stage of starch depolymerization is characterized by the formation of mono-, di-, and tri-saccharides due to the action of glucoamylases and/or β-amylases. This process is called saccharification because of the formation of saccharides. Most hydrolytic enzymes are specific for α-1,4-glucosidic links (Fig. 2.14). Debranching enzymes such as pullanase act specifically on the α-1,6-glucosidic links in polysaccharides and are often used in conjunction with other amylolytic enzymes to increase the degree of dextrinization. The joint hydrolysis of pullanase and glucoamylase produces high glucose syrups, whereas pullanase with fungal α-amylase increases the yield of fermentable maltose and maltotriose.

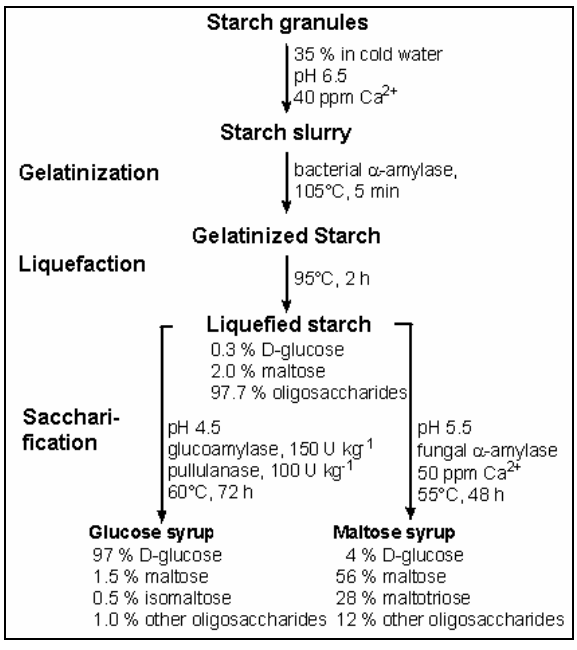

Fig. 2.14: Typical conditions for enzymatic starch conversion in industry.

Tab. 2.2: Enzymes used in starch hydrolysis.

Enzyme	Origin	Action
α-amylase	*B. amyloliquefaciens*	Cleaves α-1,4-oligosaccharide links to give α-dextrins and predominantly maltose (G2), G3, G6 and G7 oligosaccharides
	B. licheniformis	Cleaves α-1,4-oligosaccharide links to give α-dextrins and predominantly maltose, G3, G4 and G5 oligosaccharides
	Aspergillus oryzae, A. niger	Cleaves α-1,4 oligosaccharide links to give α-dextrins and predominantly maltose and G3 oligosaccharides
	B. subtilis (*amylosaccharitícus*)	Cleaves α-1,4-oligosaccharide links to give α-dextrins with maltose, G3, G4 and up to 50% (w/w) glucose
β-amylase	Barley malt	Only α-1,4-links are cleaved from the non-reducing ends, to give limit dextrins and β-maltose
Glucoamylase	*A. niger*	α-1,4 and α-1,6-links are cleaved, from the non-reducing ends, to give β-glucose
Pullulanase	*B. acidopullulyticus*	Cleaves the α-1,6-links to give straight-chain maltodextrins

2.3 High hydrostatic pressure

2.3.1 Introduction

The first important report of the application of high hydrostatic pressure to food preservation was published by Hite in June of 1899 (Hite 1899). Hite showed that the shelf-life of milk could be extended by about 4 days after pressure treatment at 600 MPa for one hour at room temperature. In 1914 Bridgman (Bridgman 1914) coagulated egg albumin under pressure. Surprisingly, it took some time for the next remarkable contributions of pressure on biological material and the food industry had to wait until the late eighties to attract the attention of researchers.

Hydrostatic pressure may be generated by the addition of free energy, e.g. heating at constant volume or mechanical volume reduction. It is now technically feasible to reach pressures up to several gigapascals and to keep it constant for a comparably long time in specially designed vessels made from highly alloyed steel.

A major task of high pressure application in food industry is the extension of shelf-life or the elimination of microbial pathogens since the viability of vegetative micro-organisms is affected by inducing structural changes at the cell membrane or by the inactivation of enzyme systems which are responsible for the control of the metabolic actions (Knorr and Heinz 2001). At

pressures higher than 400 MPa a significant inactivation of vegetative bacteria, yeast or virus is observed even at ambient temperatures within treatment times of several minutes (Chen et al. 2005; Hashizume et al. 1995; Solomon and Hoover 2004). By increasing the pressure to 800-900 MPa (at present the technical limit of industrial high pressure equipment) most inactivation reaction are strongly accelerated. At those conditions and in combination with temperatures higher than 80°C even bacterial spores are irreversibly inactivated (Heinz and Knorr 2002).

2.3.2 Thermodynamics of high hydrostatic pressure

Thermodynamic properties and phase equilibrium of any system as well as transport properties have to be considered in their functional relationship with temperature and pressure. Also the equilibrium concentrations of chemical reactions are related to these quantities.

Pressure primarily affects the volume of a one-phase system. The amount of contraction is governed by the compressibility β, which is dependent on the intermolecular forces acting within the substance. Compression results in decreasing the average intermolecular distance and reducing rotational and translational motion. Compressibility as an intrinsic physical property of the material is defined by Equation 2.15 (Bridgman 1912) and exhibits a high variability ranging from gases (order of magnitude 10^{-5}-10^{-6} Pa^{-1}) to liquids (10^{-6}-10^{-10} Pa^{-1}) to solids (10^{-10}-10^{-12} Pa^{-1}).

$$\beta \equiv -\frac{1}{v}\left(\frac{\partial v}{\partial p}\right)_T = -\frac{1}{\rho}\left(\frac{\partial \rho}{\partial p}\right)_T \qquad \textbf{(2.15)}$$

with the specific volume v, pressure p, the absolute temperature T and viscosity ρ.

The compressibility of liquids decreases with pressure, since the initial free volume has largely disappeared, and the repulsive potential of molecules is stronger than the attractive under high pressures. On the other hand, compressibility of most liquids increases with temperature due to the increase of the internuclear distances (increase in free volume) by thermal expansion. Water is an exception because its isothermal compressibility β decreases with temperature passing through a minimum around 46°C (see also Fig. 2.17).

Pressure is generally expressed as the change of inner energy U at constant entropy S. For a closed hydrostatic system the first law of thermodynamics describes the change of inner energy U as the sum of changes in volumetric work and absorbed and/or dissipated heat quantity:

$$dU = dw + dq \qquad \textbf{(2.16)}$$

Expressing heat in terms of temperature and entropy we achieve an equation which is convenient for situations involving variations in internal energy U, with changes in volume V and entropy S:

$$dU = -pdV + TdS \quad \textbf{(2.17)}$$

From this equation it is possible to define a new characteristic function enthalpy H which is a good tool to solve problems involving heat quantities, such as heat capacities, latent heat, and heats of reactions, when pressure is the variable being controlled.

$$H \equiv U + pV \quad \textbf{(2.18)}$$

which, after integration gives:

$$dH = Vdp + TdS \quad \textbf{(2.19)}$$

Similarly relationships can be derived for the Helmholz and Gibbs function of free energy G which is the fundamental equation for a system where pressure and temperature are the independent variables.

$$A \equiv U - TS \quad \textbf{(2.20)}$$

$$dA = -SdT - pdV \quad \textbf{(2.21)}$$

$$G \equiv H - TS \quad \textbf{(2.22)}$$

$$dG = Vdp - \Delta ST \quad \textbf{(2.23)}$$

As the enthalpy function H, U, A, and G are actual functions of S, V, T and p, their differentials are exact differentials. Therefore, the same condition can be applied to obtain the Maxwell's relations, shown below.

$dU = -pdV + TdS$ gives $\left(\frac{\partial T}{\partial V}\right)_S = -\left(\frac{\partial p}{\partial S}\right)_V$ **(2.24)**

$dH = Vdp + TdS$ gives $\left(\frac{\partial T}{\partial p}\right)_S = -\left(\frac{\partial V}{\partial S}\right)_p$ **(2.25)**

$dA = -SdT - pdV$ gives $\left(\frac{\partial S}{\partial V}\right)_T = -\left(\frac{\partial p}{\partial T}\right)_V$ **(2.26)**

$dG = Vdp - \Delta ST$ gives $\left(\frac{\partial S}{\partial p}\right)_T = -\left(\frac{\partial V}{\partial T}\right)_p$ **(2.27)**

These equations do not refer to a process but express relations that hold at any equilibrium state of a hydrostatic system.

Based on the previous statements and relations, for instance, if the enthalpy function H is known as a function of p and T for a system, all the other thermodynamic properties of the system can be calculated by differentiation. Upon compression of a liquid, heat is evolved due to the work of compression against repulsive intermolecular forces. Once a substance experiences a positive thermal expansion, this temperature rise increases the volume and affects the value of compressibility. To calculate the dependence of the isobaric heat capacity one can write:

$$dH = \left(\frac{\partial H}{\partial T}\right)_p dT + \left(\frac{\partial H}{\partial p}\right)_T dp \qquad \textbf{(2.28)}$$

The first partial derivative of the right-hand side is the isobaric heat capacity, whereas the second partial derivative deserves extra attention. Solving the Gibbs function (2.22) for the enthalpy term with respect to pressure at constant temperature becomes:

$$\left(\frac{\partial H}{\partial p}\right)_T = \left(\frac{\partial G}{\partial p}\right)_T + T\left(\frac{\partial S}{\partial p}\right)_T \qquad \textbf{(2.29)}$$

Solving the Gibbs function at constant pressure and constant temperature yields the following relationship for a closed system:

$$\left(\frac{\partial G}{\partial p}\right)_T = V \qquad \textbf{(2.30)}$$

$$\left(\frac{\partial G}{\partial T}\right)_p = -S \qquad \textbf{(2.31)}$$

If taking the second derivatives of Eqn. 2.30 and Eqn. 2.31 with respect to temperature and pressure, and combine it with Eqn 2.29 using the cross partial differentiation rule, one gets:

$$\left(\frac{\partial H}{\partial p}\right)_T = V - T\left(\frac{\partial V}{\partial T}\right)_p \qquad \textbf{(2.32)}$$

Introducing the definition of isobaric heat capacity and Eqn. 2.32 into Eqn. 2.28 will yield the following term:

$$dH = c_p dT + \left[V - T\left(\frac{\partial V}{\partial T}\right)_p\right] dp \qquad \textbf{(2.33)}$$

which, after integration, gives the final format of the pressure dependence of the isobaric heat capacity c_p:

$$\left(\frac{\partial c_p}{\partial p}\right)_T = -T\left(\frac{\partial^2 V}{\partial T^2}\right)_p \qquad \textbf{(2.34)}$$

However, for the calculation of occurring adiabatic heating of a closed system from a given starting temperature, it is usually sufficient to have knowledge of the compressibility β of the system and its isobaric heat capacity c_p and the coefficient of thermal expansion α. This temperature rise is accompanied by a dissipation of heat within and through the pressure vessel, which is dependent on the rate of compression, vessel size, initial and boundary conditions, and heat transfer parameters. According to the first fundamental theorem of thermodynamics and for a constant pressure, c_p is usually defined as:

$$c_p \equiv \left(\frac{\partial H}{\partial T}\right)_p \qquad \textbf{(2.35)}$$

Similar to Eqn. 2.15, the coefficient of thermal expansion can be defined as (Bridgman 1912):

$$\alpha \equiv \frac{1}{V}\left(\frac{\partial V}{\partial T}\right)_p = -\frac{1}{\rho}\left(\frac{\partial \rho}{\partial T}\right)_p \qquad \textbf{(2.36)}$$

If α is known as a function of pressure and temperature, it is possible to calculate the volume expansion and/or volume contraction as a result of temperature change. The resulting pressure can then be determined by basic thermodynamic relationships.

Combining the pressure dependence of the isobaric heat capacity (Eqn. 2.34) with Eqn. 2.36 yields:

$$\left(\frac{\partial c_p}{\partial p}\right)_T = -T\left(\frac{\partial^2 V}{\partial T^2}\right)_p = -\frac{T}{\rho}\left[\alpha^2 + \left(\frac{\partial \alpha}{\partial T}\right)_p\right] \qquad \textbf{(2.37)}$$

The change of isobaric thermal expansion coefficient α with pressure is the complement of the change of isothermal coefficient of compressibility β with respect to temperature (Eqn. 2.15) which gives Eqn. 2.38:

$$\left(\frac{\partial \alpha}{\partial p}\right)_T = \left(\frac{\partial \beta}{\partial T}\right)_p \qquad \textbf{(2.38)}$$

The complex variation of the pressure dependence of isobaric heat capacity is not easily interpreted in terms of physical changes in the liquid, where specific interactions may occur depending on the nature of the liquid. Thermal expansion of liquids usually decreases with pressure. Water below 40°C is, once again, an exception showing a very anomalous behavior in the pressure range from atmospheric to 1 GPa (Bridgman 1931).

Nevertheless, another expression for the adiabatic heating of a system can also be obtained by making use of the second law of thermodynamic, which derives a relation for enthalpy, entropy and temperature:

$$\left(\frac{\partial H}{\partial T}\right)_p = T\left(\frac{\partial S}{\partial T}\right)_p \qquad \textbf{(2.39)}$$

Combining Eqn. 2.39 with the basic equations for the compressibility of a system (Eqn 2.15) and specific heat capacity at constant pressure (Eqn. 2.35) derives a general expression for the temperature increase upon compression in adiabatic-isentropic-situations:

$$\left(\frac{\partial T}{\partial p}\right)_S = \frac{\beta T}{c_p \rho} \qquad \textbf{(2.40)}$$

In case of a phase transition is occurring in a one-component-system, the derived relationships of temperature change during compression and vice versa are only valid in a very limited range. If the two states of a system are in equilibrium during the phase transition, then the molar free enthalpies G_1 and G_2 of a substance are equal in both phases. This is described by the fundamental equation of Gibbs 2.23. However, the Clausius-Clapeyron relation, in thermodynamics, is a way of characterizing the phase transition between two states of matter, such as solid and liquid. On a pressure-temperature (p-T) diagram, the line separating the two phases is known as the coexistence. The Clausius-Clapeyron relation (Eqn. 2.41) gives the slope of this curve and provides a relation of the temperature dependence of the melting pressure.

$$\frac{dp}{dT} = \frac{\Delta H}{T\Delta V} \qquad \textbf{(2.41)}$$

For many simple organic or inorganic reactions the pressure and temperature dependence of the equilibrium constant is known and in some situations also the impact on the kinetics is predictable (in: (Van Eldik et al. 1989)). A quantitative expression is given by the van't Hoff equation (2.42) which relates the pressure dependence of the equilibrium constant K which is defined by the law of mass with the volume difference ΔV^* of products and reactants. The unit of the reaction volume is [cm^3/mol)]. R is the universal gas constant (R=8.314 J/K mol).

$$\left(\frac{\partial \ln K}{\partial p}\right) = -\frac{\Delta V^*}{RT} \qquad \textbf{(2.42)}$$

ΔV^* is useful for the estimating impact of pressure on the chemical equilibrium. A negative reaction volume indicates that product formation is favored by increasing pressure. For examples dissociation reactions often show a negative ΔV^* (water: -22.2 cm^3mol^{-1}; phosphate buffer: -16.3 cm^3mol^{-1}). However, some buffer systems are rather stable with pressure and have a slightly positive ΔV^* (TRIS: +1.0 cm^3mol^{-1}; imidazol: +1.8 cm^3mol^{-1}). Other reactions, such as hydrogen bond formation, hydrophobic interactions or van der Waals forces are expected to show a shift of the equilibrium to the product side at elevated pressures (Boonyaratanakornkit et al. 2002; Hei and Clark 1994; Tauscher 1995).

The rate of chemical reactions under pressure is dependent of the molecules and the reaction mechanism under consideration. Similar to the Arrhenius equation which quantifies the dependence of reaction rate from the temperature level at which the reactants are kept, a relationship has been derived from the transition-state theory (Eyring 1935) which relates the rate constant k with pressure:

$$\left(\frac{\partial \ln k}{\partial p}\right) = -\frac{\Delta V^{\#}}{RT} \qquad \textbf{(2.43)}$$

In Eqn.2.2 $\Delta V^{\#}$ with the unit [cm^3mol^{-1}] denotes the activation volume of the reaction. A negative $\Delta V^{\#}$ produces an increased reaction rate k whereas positive $\Delta V^{\#}$ indicates that the reaction is retarded. Examples of accelerated reactions can be found among polymerizations, cycloadditions, and solvolytic reactions (Tauscher 1995).

For complex chemical structures like proteins or polysaccharides the available information on ΔV^{*} and $\Delta V^{\#}$ is still limited. Moreover, the effects are by far more difficult to categorize especially when the reactants are exposed to combined pressure-temperature conditions.

2.3.3 Effect of pressure on water

The physical properties of water under pressure exert a profound influence on foods treated with high hydrostatic pressure, since water represents the major component of most food systems itself and is typically used as the pressure transmitting liquid. In this context, the liquid state of water is most significant, since a phase transition to the solid state would have profound effects on the food matrix. However, there are special high pressure applications which use the possibility to have a instantaneous phase transition in the food by increasing the pressure at low temperatures.

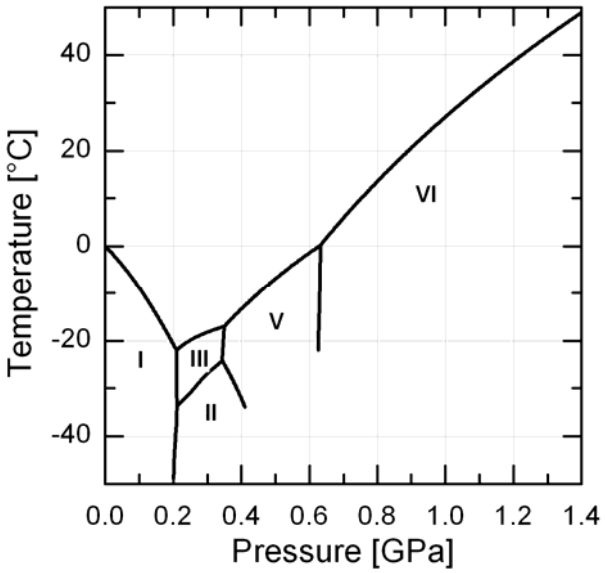

Fig. 2.15: Phase diagram of water, after Bridgman (Bridgman 1912)

The phase diagram of water as a function of temperature and pressure delimits distinct crystalline ice forms and has been determined first by Bridgman (Bridgman 1912). Fig. 2.15

presents the phase transition lines of water and its different ice modifications according to Bridgman.

Besides the liquid state and the ice modification I at ordinary ambient pressure, water exhibits a range of solid phases, and all of these are referred to as forms of 'ice'. Ice possesses 12 different crystal structures, plus two amorphous states. Ice I represents a specialty since only this ice modification shows a positive volume change ΔV at the transition from the liquid to the solid state. Besides the depression in the freezing point, a reduction in the enthalpy of crystallization can also be observed ranging from 334 kJ/kg (at atmospheric pressure) to 193 kJ/kg (at 210 MPa). The crystallization of higher ice modifications, like ice III or ice V, features even smaller enthalpies, and also the volume change ΔV is smaller than the phase transition solid-liquid at ambient pressure.

The properties of water under high pressure conditions vary and are largely a function of the pressure range (Cavaille and Combes 1996). The particular properties are observed for pressures below 200 MPa. However, at higher pressures water loses its particular characteristics and acts like a normal hydrogen bonded liquid. Based on a number of detailed studies the *International Association for the Properties of Water and Steam* (IAPWS) has published a number of formulations of the main thermodynamic properties of water in dependence on pressure and temperature. Fig. 2.16-2.18 show the pressure dependence of the volume V, the heat capacity c_p, the density ρ, the dielectric constant ε, the thermal expansion coefficient α, and the isothermal compressibility β, deviated from the regular laws determined in the range of 0-100°C. The volume contraction of water is approximately 10% at 400 MPa and 17% at 800 MPa (Fig. 2.16). The isothermal lines remain in about the same distance as at ambient pressure. With regard to this change in volume it is not surprising that the density of water is increased by the same factor as the volume is decreased (Fig. 2.16). The heat capacity shows a strong decrease when increasing the pressure up to 400 MPa but features only a small change at higher pressures (Fig. 2.17). Similar to the compressibility, the isothermal heat capacity of water is an exception because its decreases with temperature passing through a minimum around 46°C. The dielectric constant ε has importance in the calculation of ionic reactions and shows noticeable changes with pressure and temperature (Fig. 2.17). The thermal expansion coefficient α and the coefficient of compressibility β are most important in the calculation of adiabatic heating as a result of compression. β shows an extensive decrease with pressure at all temperatures (0-80°C). Whereas α is increase of with pressure at low temperatures (e.g. at 20°C), a decrease with pressure can be observed at higher temperatures (e.g. at 80°C).

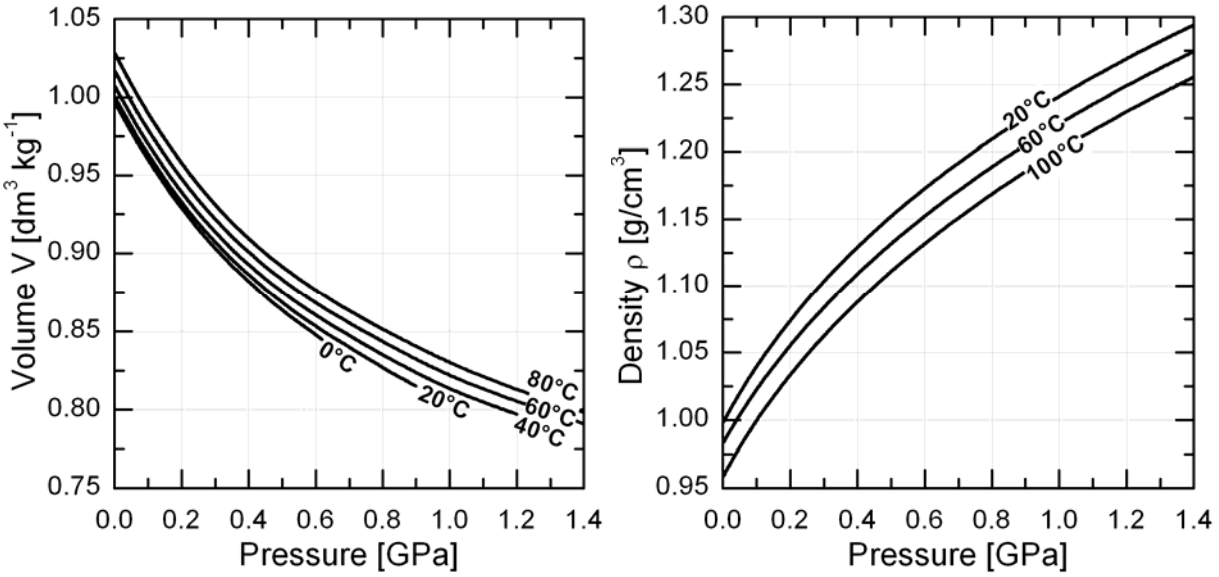

Fig. 2.16: Isothermal lines for the specific volume V (left) and the density ρ (right) of water as a function of pressure.

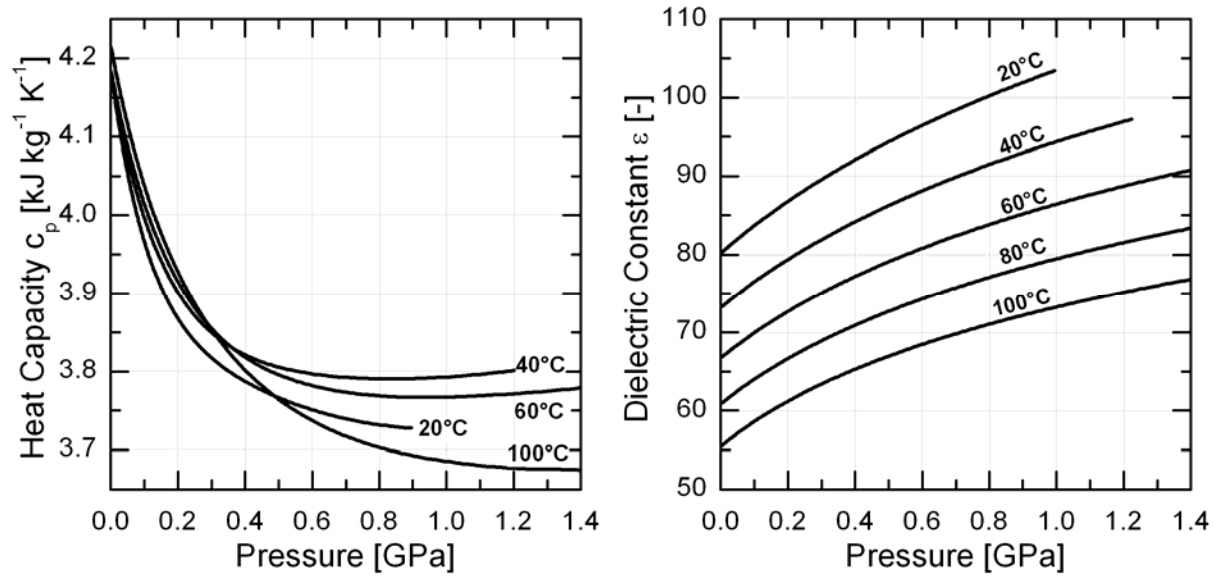

Fig. 2.17: Isothermal lines for the heat capacity c_p (left) and the dielectric constant ε (right) of water as a function of pressure.

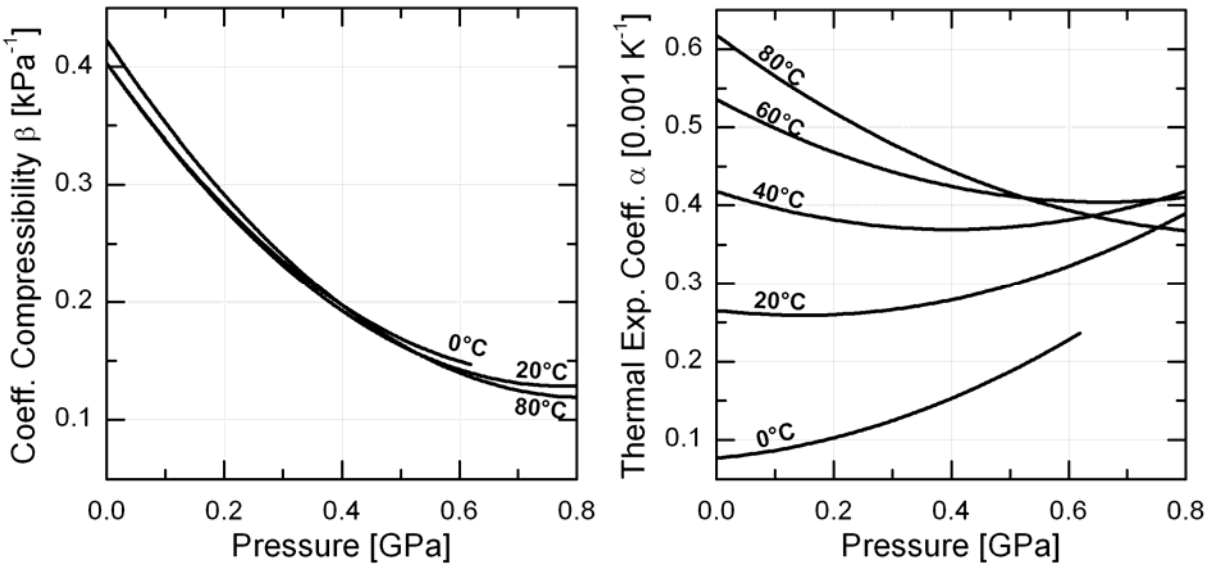

Fig. 2.18: Isothermal lines for the coefficient of compressibility β (left) and the thermal expansion coefficient α (right) of water as a function of pressure.

Fig. 2.19 presents the change of temperature during adiabatic compression of water up to 1400 MPa. At low starting temperatures the increase in temperature due to compression is significantly lower (approx. 2 K / 100 MPa) than at higher starting temperatures (up to 5 K / 100 MPa at T>80°C). After compression in a high pressure vessel, water is warmed to a value of temperature which depends on the geometry of the system and on the required time for the compression phase. Since adiabatic heating is reversible, the temperature will drop immediately during pressure release and the water returns to its initial temperature, or even to a lower value. Higher compression rates result in a higher absolute value of temperature which follows the pressure build-up. Since momentum transport in liquids and solids happens practically without delay, each volume element of a pressurized product is characterized by the same pressure level and, in adiabatic situations, by the same temperature. This effect can be used to achieve a sterilizing end-temperature within a short time and to immediately cool the product after the desired temperature holding time. Hence, coupling pressure and temperature can result in a new approach to food sterilization with a significant improvement in product quality.

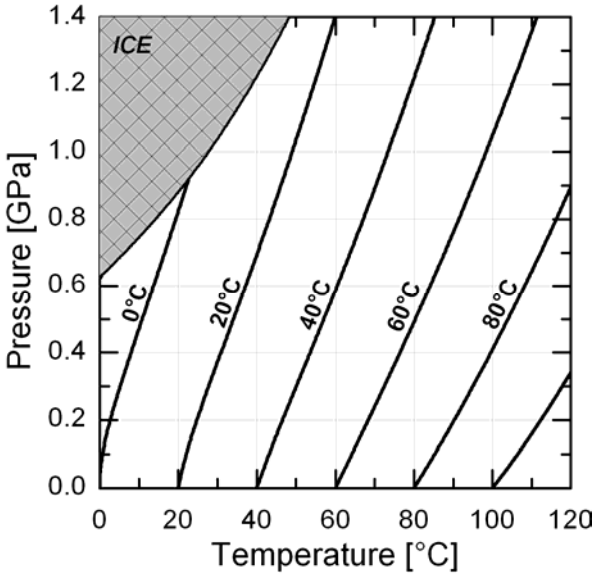

Fig. 2.19: Isolines of adiabatic heating of water due to compression as a function of pressure and temperature. Isolines were calculated according to Eqn. 2.15 and Ardia et al. (Ardia 2004).

2.3.4 Effect of pressure on the pH of aqueous systems

The activity of hydrogen ions in buffer solutions varies with pressure and temperature. The pH value for different pressure temperature combinations can be derived from thermodynamic equations which incorporate the pressure dependence of the dielectric permittivity, the density, the volume change and the equilibrium constant. According to Kitamura and Itoh (Kitamura and Itoh 1987) some buffers, such as Tris, Imidazole or ACES buffer, show high piezo-stability with a maximum pH-difference between 0.1 and 1000 MPa of +0.5 units. In contrast, phosphate buffer us known to be very piezo-labile showing a shift in pH 0.1 and 1000 MPa of -2.5 units (Mathys et al. 2005). However, such calculations present only isothermal pressure dependencies of the pH. Since the compression of water up to 1000 MPa produces a temperature increase of approximately 38 K, it is useful to implement the known temperature dependence of the specific buffer solution (Goldberg et al. 2002).

The pH-value in buffer solutions varies with pressure due to their activity coefficients and equilibrium constants changing. A good approximation of the activity coefficients in aqueous solutions can be estimated by the limiting Debye-Hueckel law (Debye and Hueckel 1923) in Eqn. 2.44:

$$\lg \gamma_i = -1.825 \cdot 10^6 \cdot z_i \cdot \sqrt{\frac{I \cdot \rho}{\varepsilon^3 \cdot T^3}} \qquad \textbf{(2.44)}$$

with the activity coefficients γ_i and the number of elementary charges z_i of the ion i, the ion strength I, the density ρ, the dielectric permittivity ε and the temperature T.

Hamann (Hamann 1982) found a relationship between the thermodynamic equilibrium constant K_A and high pressure up to 1000 MPa (Eqn. 2.45):

$$\ln\left(K_A(p)\right) = \ln(K_A) - \frac{pV_R}{RT(1+bp)} \qquad \textbf{(2.45)}$$

where p is the pressure, V_R is the reaction volume at atmospheric pressure, R is the gas constant and b = $9.2*10^{-4}$ MPa^{-1}.

With $K_A(p)$ it is possible to obtain the pressure dependence of the pK_A-value, respectively (Eqn. 2.46):

$$pK_A(p) = -0.4343 \cdot \ln(K_A(p)) \qquad \textbf{(2.46)}$$

According to the law of mass action the pH under pressure pH(p) is given by Eqn. 2.47. This relationship holds remarkably true for most equilibria up to 1000 MPa (Hamann 1982).

$$pH(p) = pK_A(p) + \lg\left(\frac{\gamma_A}{\gamma_{HA}}\right) + \lg(pH - pK_A) \qquad \textbf{(2.47)}$$

The p-T-diagrams in Fig. 2.20 of water and 10 mM ACES buffer show different changes of the pH under pressure and temperature.

These temperature dependencies can be very high and could compensate the advantages from the isothermal pressure dependence as well. In any case, a proper selection of the buffer has to be adjusted with the applied p-T-parameters to achieve a low change of the pH under pressure.

The change of the pH under high pressure plays a major role in sensitive reactions e.g. inactivation of enzymes and micro-organisms. Applying the above models, these sensitive reactions can be better anticipated in planning experimental designs.

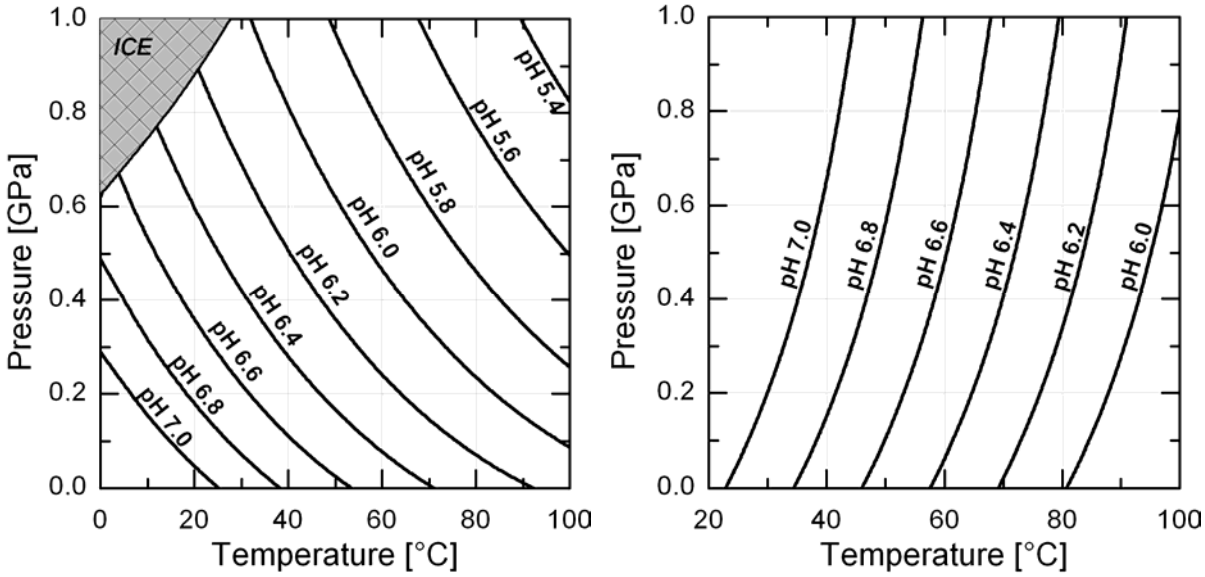

Fig. 2.20: The change of pH of water (left) according to Marshall and Frank (Marshall and Franck 1081) and 10 mM ACES buffer (right) with pressure and temperature (Kitamura and Itoh 1987; Mathys et al. 2005). Isolines indicate those pT conditions that results in a constant pH value (calculated for pH 7.0 at 25°C).

2.3.5 Effect of pressure on proteins

Biopolymers, such as starches and proteins, show changes of their native structure under high hydrostatic pressure analogous to the changes occurring at high temperatures. The effect of pressure on proteins and enzymes is related to reversible or irreversible changes of the native structure (Cheftel 1992; Heremans 1982).

Although denaturation of proteins is induced either by heat, chemicals or high pressure the residual molecular structure can vary significantly. Temperature and/or chemical induced protein denaturation often unfold the complete protein irreversibly because of covalent bond breaking and/or aggregation of the molecule. In contrast, high pressure can leave parts of the molecule unchanged, indicating that the denaturation mechanisms are substantially different.

A proposed mechanism of high pressure induced denaturation of proteins is shown in Fig. 2.21. In aqueous solution pressure affects mainly the tertiary and quaternary structure of proteins. Oligomeric enzymes have been found to dissociate into individual subunits even at about 150-200 MPa (Balny and Masson 1993; Barbosa-Cánovas et al. 1997; Knudsen et al. 2004) (see Fig. 2.21). Imperfect packaging of atoms at the subunit interface together with the disruption of hydrophobic and/or electrostatic interactions in the subunit area might account for the volume changes involved (Mozhaev et al. 1994; Penniston 1971). The disturbance of the tertiary structure, which is predominately stabilized by hydrophobic and electrostatic interaction,

usually takes place at pressures beyond 150-200 MPa (Balny and Masson 1993; Barbosa-Cánovas et al. 1997; Cheftel 1992).

Covalent bonds are rarely affected by high pressure and even α-helix or β-sheet structures appear to be almost incompressible (Balny and Masson 1993; Heremans and Smeller 1998). Since solvent water has to be considered as an integral part of dissolved proteins and enzymes, the hydration patterns of side chains strongly influences the structural and dynamical properties of enzymes and their catalytic reactions (Smolin and Winter 2004; Smolin and Winter 2006; Teeter 1991). In contrast to temperature which destabilizes the protein molecule by transferring non-polar hydrocarbons from the hydrophobic core towards the water, pressure denaturation is initiated by forcing water into the interior of the protein matrix. Water penetration into the protein as a prerequisite of pressure unfolding has been suggested by many researchers (Nash and Jonas 1997; Zhang et al. 1995). A loss of contact between groups in the non-polar domains is causing the unfolding of parts of the molecule. Hence, the stability of a protein under high pressure conditions is largely affected by its conformational flexibility to compensate losses of non-covalent bonds due to relocation of water molecules (Boonyaratanakornkit et al. 2002; Priev et al. 1996; Smeller 2002). As a result of water penetration into the protein interior, pressure is likely to lead to conformational transitions resulting in unfolding (Saad-Nehme et al. 2001).

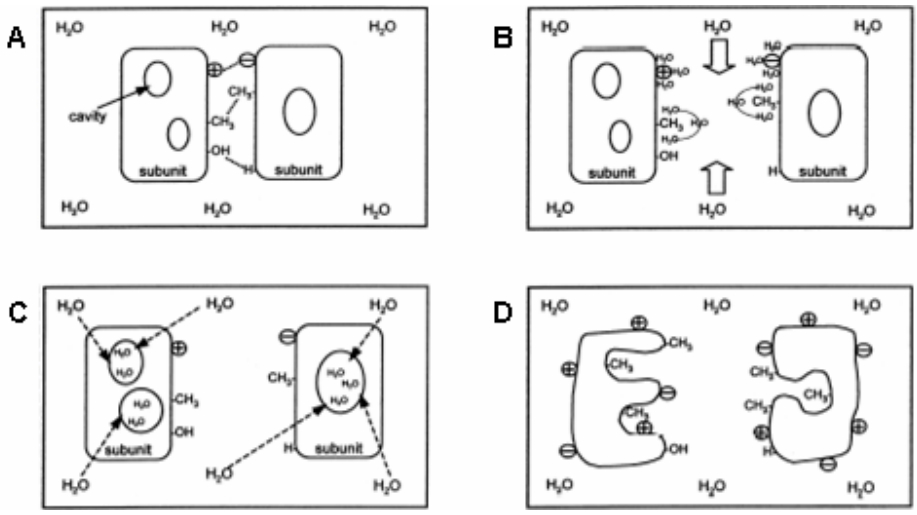

Fig. 2.21: Effect of pressure on molecular interactions in multimeric proteins at various pressure levels. A: Native protein at ambient pressure. B: Dissociation and electrostriction believed to occur at 50-200 MPa. C: Conformational fluctuations and water penetration into the protein interior at approximately 200-1400 MPa. D: Unfolding and disruption of tertiary protein structure at pressures higher 300 MPa. The pressure levels indicating the above molecular effects may vary for different proteins. Adapted and modified from Boonyaratanakornkit et al. (Boonyaratanakornkit et al. 2002).

There are numerous reports indicating an increased thermo-stability of proteins and enzymes under specific pressure conditions (Heremans and Smeller 1998; Kunugi and Tanaka 2002; Ludikhuyze et al. 2002; Northrop 2002; Smeller 2002). High pressure stabilization of proteins takes place when the denatured state is less compressed than the native state. Hence, the volume difference between folded and unfolded proteins will be positive and, since higher pressure stabilizes the smaller volume, the native folded state is favoured. This might happen when at high pressure hydrogen bond formation within the protein is promoted (Jaenicke 1981). Van der Waals forces are presumably favoured by pressure since they tend to maximize the packing density, producing a reduction in volume of the protein (Boonyaratanakornkit et al. 2002; Gross and Jaenicke 1994). Opposing effects of pressure and temperature on hydrophobic interactions and hydrogen bonds formation have been put forward as possible explanations for pressure stabilization of proteins against thermal denaturation (Balny and Masson 1993; Mozhaev et al. 1996b). Hydrogen bonds are almost pressure insensitive (Mozhaev et al. 1996a). However, they might be slightly stabilized or destabilized under pressure depending on the system investigated (Gross and Jaenicke 1994; Van Eldik et al. 1989). Mozhaev et al. (Mozhaev et al. 1996b) hypothesized that at the initial step of thermal inactivation, a protein looses a number of essential water molecules, and this loss may give rise to structural rearrangements. High pressure may hamper this process owing to its favorable effect on hydration of both charged and non-polar groups (Gross and Jaenicke 1994; Mozhaev et al. 1996b).

2.3.5.1 Effect of pressure on enzyme stability

It is known for a long time that high hydrostatic pressure has a strong impact on the activity and stability of enzymes. Nowadays there are a number of studies describing the effect of pressure on selected enzyme systems (see reviews (Balny 1998; Balny and Masson 1993; Knorr et al. 2006; Ludikhuyze et al. 2002; Northrop 2002)). However, reports on high pressure inactivation of enzymes are much less frequent than those of temperature inactivation (Silva and Weber 1993). The pressure stability of enzymes can vary dramatically ranging from pressure sensitive enzymes (<400 MPa) such as phosphohexoseisomerase from bovine milk (Rademacher and Hinrichs 2006) to extreme pressure resistant enzymes (>1GPa) such as peroxidase from horseradish (Smeller and Fidy 2002) or pectin methylesterase from tomatoes (Crelier et al. 2001). However, since there is a structural manifoldness among enzymes catalysing the same reaction it is not appropriate to categorize enzymes with respect to their pressure (and/or thermal) stability. For example pectin methylestrase from banana shows a significant higher pressure stability than pectin methylesterase from orange (Ly-Nguyen et al.

2003; Van den Broeck et al. 2000a) and even isoforms of one enzyme from the same origin can show extreme differences in their physical stability (Buckow et al. 2005b; Rodrigo et al. 2006a).

Similar to the thermal stability, the pressure resistance of enzymes exhibits a significant dependency on environmental conditions such as pH (Riahi and Ramaswamy 2004; Weemaes et al. 1997; Zipp and Kauzmann 1973) and the presence of sugars, salts, or other food additives (Ludikhuyze et al. 1996; Weemaes et al. 1997). The presence of substrate may have protective effects but can also lead to a strong destabilization of an enzyme (Garcia et al. 2002).

If subjected to changes, enzymes can be unfolded or inactivated which destroys the three-dimensional structure of the protein. However, the denaturation of an enzyme by pressure and/or temperature is sometimes reversible (Guyer and Holmquist 1954; Palou et al. 2000). The changes of water properties with increasing pressure, temperature and the presence or absence of solutes reflects changes in the arrangement of water molecules which might explain the baroprotective effects of solutes on proteins under denaturing conditions. Due to the major importance of the hydration water on enzyme flexibility and stability even small changes of its properties due to chemical denaturants or co-solvents can tip the balance from the native to the denatured state. The effect of pH on protein stability is due to the different pK_a values of the various ionizable groups in the folded and denatured state. In consequence, due to locally different changes of the electrostatic contributions to the intermolecular interactions and salvation energy the enzyme's stability shows an optimum at a certain pH value. For instance, Fig. 2.22 shows the change of first-order inactivation rate constant k_{inact} of β-amylase from *Bacillus cereus* observed at 60°C and ambient pressure which is in good accordance to the literature data (Hirata et al. 2004; Nanmori et al. 1983). Highest thermo-stability of the enzyme was found at pH 6.0 in phosphate buffer and pH 6.7 in ACES buffer. This difference might be explained by the significant difference in pH stability at higher temperatures of both buffers (see chapter 2.3.4). Whereas phosphate buffer shows almost no change of pH with temperature the change in ACES buffer is approximately -0.02 units per Kelvin. Hence, at 60°C the difference in pH between phosphate and ACES buffer adds up to 0.7 units (assuming pH adjustment at 25°C) which is exactly the difference of the pH optimum indicated in Fig. 2.22.

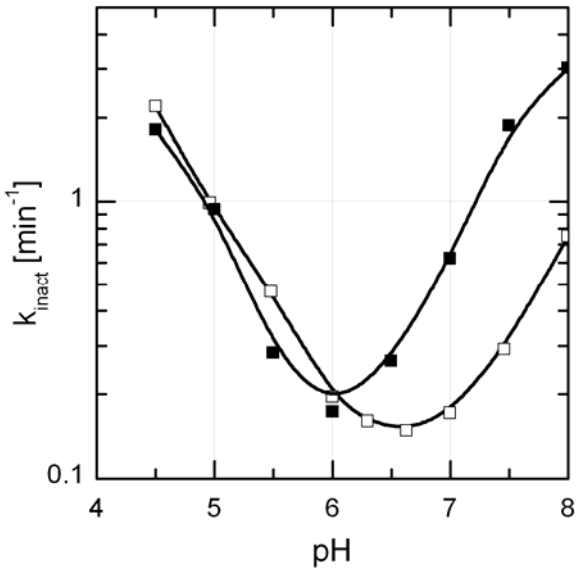

Fig. 2.22: Effect of pH on the inactivation rate constant k_{inact} of β-amylase from *Bacillus cereus* at 60°C. The enzyme was diluted in 50 mM phosphate buffer (■) and in 50 mM ACES buffer (□) respectively. The indicated pH values have been adjusted at 25°C.

2.3.5.2 Effect of pressure on the catalytic activity of enzymes

The over-all effect of pressure on the catalytic activity of an enzyme depends on the sign and magnitude of volume changes accompanying the binding and elementary chemical steps. The functional relationship of the main parameters in enzymatic conversion reactions K_m and k_{conv} with pressure can either be linear or non-linear. It has been reported that enzymatic reactions may be reversibly enhanced (Masson et al. 2004; Mozhaev et al. 1996b) or reduced (Dallet and Legoy 1996; Verlent et al. 2005; Verlent et al. 2004a) by pressure due to changes of the substrate specificity or by alteration of rate limiting molecular structures (Gekko 2002). Pressure might also affect a rate-determining step of an over-all enzyme reaction (Morild 1981) e.g. by changing the substrate (unfolding/gelatinization of polymers). For instance Gomes et al. (Gomes et al. 1998) found an increased action of amylases in flours upon pressure induced starch gelatinization.

Furthermore, there is evidence that pressure changes the specificity of enzymatic action (Makimoto and Taniguchi 1988) and might induce changes in the composition of products (Matsumoto et al. 1997). These phenomena may explain why pressure dependencies of the rate of enzyme reactions usually show concave curves (Masson and Balny 2005; Mozhaev et al. 1996b), maxima (Kunugi et al. 1997; Masson et al. 2004) or even a break (Dallet and Legoy 1996) when plotting $\ln(k_{conv})$ versus pressure.

In Fig. 2.23 the competing reactions of enzymatic catalysis and protein unfolding are presented schematically. Since reaction equilibrium and kinetics of both pathways are affected by temperature and pressure but potentially in a different manner, it is straightforward to find optimum pressure-temperature (p-T) conditions which maximize the catalytic reaction.

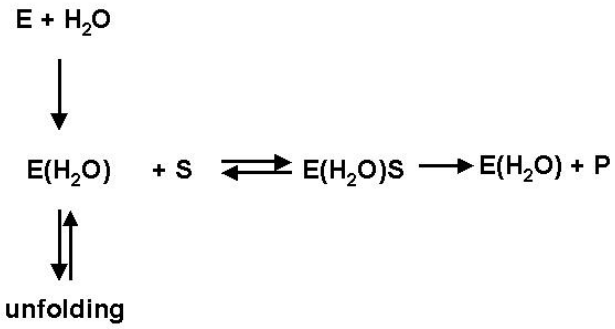

Fig. 2.23: Reaction scheme of enzymatic catalysis, superimposed by enzyme unfolding. E: enzyme; S: substrate; P: product.

So far, there is only very few data available on the effect of pressure and temperature on enzymatic conversion reactions. Polygalacturonase from tomatoes showed a significant deceleration of its catalytic activity when increasing the pressure up to 200 MPa and this decrease is more pronounced at higher temperatures (Verlent et al. 2005; Verlent et al. 2004a). Knorr et al. (Knorr et al. 2006) reported that the activity of several amylases is progressively decreased with pressure but this deceleration of catalytic activity was found to be temperature independent. In contrast, some pectin methylesterases were found to be activated under high pressure conditions. The catalytic activity of tomato pectin methylesterase has been found to be 3-4 fold higher at elevated pressure than at atmospheric pressure (Van den Broeck et al. 2000b; Verlent et al. 2004b). These studies also showed that pressure shifts the temperature of optimal enzyme activity towards higher temperatures. Pressure also proves to be very efficient to stimulate the catalytic activity of pectin methylesterase from pepper (Castro et al. 2006a). The purified enzyme showed a maximum at 200 MPa and 55°C yielding approximately 20% higher activity compared to optimal conditions at ambient pressure (~50°C). Pectin methylesterase activity in shredded carrots was found to be approximately doubled when increasing the pressure from atmospheric to 300-400 MPa at constant temperature (Sila et al. 2007). Finally, Duvetter and co-workers (Duvetter 2006) reported a highly accelerated pectin conversion by fungal pectin methylesterase under elevated pressure/temperature conditions. However, no significant effect of increasing pressure up to 300 MPa and/or temperature on the mode of pectin conversion was detected for all listed pectin methylesterases here.

2.3.5.3 Effect of pressure on prions

There is strong evidence that misfolded prions are the cause of neurodegenerative diseases like BSE or Scrapie. Two forms of the prion-related protein (PrP) with significant structural differences can be present in mammals. The 'normal' PrP^C conformation PrP^C and PrP^{Sc} which is supposed to be the infectious agent of BSE, Creutzfeldt-Jakob disease (CJD), kuru, and Gerstmann-Straussler syndrome. It is known that PrP^C is rich in α-helix structures and susceptible to proteolytic attack, whereas the misfolded PrP^{Sc} protein has a high content of β-sheets, is resistant to enzyme digestion and forms amyloid fibrils (Baskakov et al. 2002; Cohen and Prusiner 1998; Prusiner 1991).

During the last years, high hydrostatic pressure has become an interesting tool to inactivate prions, since it is known to shift the conformational transition of proteins towards the state that occupies a smaller volume, and thus can lead to a partial unfolding of a protein. Hence, several publications on the effects of pressure on prions have recently been published. Zhou et al. (Zhou et al. 2001) reported that the *Saccharomyces cerevisiae* prion protein Ure2 presents a strong structural stability at ambient temperatures even when exposed to pressures up to 600 MPa. However, in the presence of non-denaturating concentrations of guanidinium chloride unfolding was observed already at 200 MPa. Syrian golden hamster prion protein ($SHaPrP_{90-231}$) has been subjected to pressures up to 400 MPa (Alvarez-Martinez et al. 2003). Aggregates of prions which were formed above 60°C or higher at atmospheric pressure could be recoverd into a soluble state. Kuwata et al. (Kuwata et al. 2002) worked with the same prion protein ($SHaPrP_{90-231}$) and found a metastable conformer of PrP^C under various pressure conditions (up to 250 MPa) by using ^{15}N-^{1}H two-dimensional NMR measurements. This metastable conformer was suggested to be the putative precurser PrP* which interacts with PrP^{Sc} before being transformed to the infectious form. In addition, the pressure sensitivity of the cellular form of the hamster prion protein ($SHaPrP_{90-231}$) has been found to reversibly convert into a β-rich intermediate form at 200 MPa (Torrent et al. 2003) and to form pre-amyloid structures with high resistance to digestion by proteinase K at 600 MPa (Torrent et al. 2004). However, the possible infectivity of these pressure induced intermediate forms was not assayed. Reduced digestibility resistance and infectivity of pressure treated scrapie 263K prions were observed by Garcia et al. (Garcia et al. 2004). The misfolded prion form PrP^{Sc} proved to be proteinase K sensitive when pressurized 2 hours at 60°C and 500-1000 MPa and showed increased survival of infected hamsters when pressurized 2 hours at 60°C and 700-1000 MPa. However, in an acidic matrix the inactivation scrapie 263K prions seemed to be slower than in buffer at neutral pH (Heindl et al. 2005). Brown et al. (Brown et al. 2003) attained reduced infectivity of the same scrapie 263K prions by applying short high pressure pulses up to 1200 MPa and 121-137°C. Inactivation of bovine

prions has been achieved by Heinz et al. (Heinz and Kortschack 2002) with pressure-temperature combinations allowing future sterilization processes to include destruction of infectious prion proteins. Folding and aggregation of prions have been reviewed recently (Silva et al. 2006).

However, Nishida et al. (Nishida et al. 2005) found that mice infected with an attenuated Creutzfeldt-Jakob disease agent (SY-CJD) are resistant against superinfection by a more virulent human-derived CJD agent (FU-CJD). Since pathological prion protein PrP^{Sc} has not been found the prion-only concept is challenged. The exposure to high pressure which specifically affects the configuration of proteins might be a suitable tool to get new insights how those diseases are spreading.

2.3.5.4 Effect of pressure on viruses

Viruses regardless of their envelope show a wide range of sensitivities in response to high hydrostatic pressure (Grove et al. 2006). Especially virus with proteinaceous coats like HIV, HAV are very susceptible to pressure and are already inactivated at pressures well below 600 MPa (Calci et al. 2005; Chen et al. 2005; Chen et al. 2004; Gaspari et al. 2002; Isbarn et al. 2007; Kingsley et al. 2002; Tian et al. 2000).

Most of the examined viruses were markedly inactivated at pressures $\leqslant$ 500 MPa as summarized by Grove et al. (Grove et al. 2006). So far, the mechanisms of virus inactivation under pressure are poorly understood and further studies are required to identify those structural components of the virus envelope that represent the most pressure-sensitive targets in pressure-induced inactivation. This pressure sensitivity does not depend on whether a lipid envelope or a protein capsid surrounds these viruses. However, some single stranded, positive-sense RNA viruses such as the tobacco mosaic virus (TMV), the poliovirus-1, coxsackievirus strain B5, and Aichi virus showed a remarkable piezotolerance at 920 MPa and 600 MPa, respectively (Giddings et al. 1929; Kingsley et al. 2004; Wilkinson et al. 2001). Their RNA genomes are small sized with 6.4 kb to 8.3 kb and protected by few structural proteins. The long rod of the plant virus TMV is constructed upon the helical arrangement of the RNA protected by protein subunits. Poliovirus-1, coxsackievirus strain B5, and Aichi virus, all members of the Picornaviridae, are enveloped by a spherical capsid assembled by four or three structural proteins, respectively. But viruses of the genus Enterovirus such as coxsackievirus strains and poliovirus-1 differed widely in their sensitivity to high pressure (Kingsley et al. 2004). Thus, piezotolerance is restricted to some virus strains of a small single stranded RNA genome protected by structural proteins.

2.3.5.5 Effect of pressure on microorganisms

Since Hite's first report in 1899 (Hite 1899) the lethal effect of hydrostatic pressure on microorganisms is now known for more than century and has been the objective of innumerable papers (for reviews see (Cheftel 1995; Farkas and Hoover 2001; Heinz and Knorr 2002; Ludwig et al. 1992; San Martín et al. 2002; Smelt et al. 2002))

It has often been suggested that the mechanisms of pressure induced death and injury of some microorganisms may involve the inactivation of enzymes and/or proteins crucial for life processes (Farkas and Hoover 2001; Hashizume et al. 1995; Perrier Cornet et al. 2004). However, pressurized cell membranes normally show altered permeabilities and is generally believed to be the primary side of pressure damage of vegetative microorganisms (Paul and Morita 1971). This might be the reason why gram negative bacteria usually show higher piezo-tolerance than gram negative bacteria (Cheftel 1995).

Changing pressure stability of mesophylic bacteria and yeasts at low temperatures have been reported frequently (Hashizume et al. 1995; Moussa et al. 2006; Reyns et al. 2000; Sonoike et al. 1992) and might be explained by changes in water compressibility. Since the compressibility of water, and hence, the compressibility of cell cytoplasm is increases with decreasing temperature (Bridgman 1912), the mechanical energy transferred to the microbial cell is increased as well. Assuming microbial cell death is initiated at a certain threshold of mechanical energy transferred into the cellular system, at low temperatures this lethal threshold is achieved at lower pressures than the pressure needed at higher temperatures.

2.3.6 Thermodynamics of protein unfolding

The dynamic behavior of proteins is determined by the free volume which results from the conformation of the molecule. Whereas heating causes an increase in molecular fluctuation and thus in free volume, the effect of high pressure is related to the contraction in volume.

Total atomic volume, void volume and hydration volume contribute to the relative change of the molar volume in response to pressure. In proteins the compressibility is largely reflected by changing spatial positions of secondary and tertiary structure domains.

A number of studies focused on protein denaturation assessed by *in situ* techniques like NMR, FTIR, X-ray scattering, etc. (Lullien-Pellerin and Balny 2002). In aqueous solutions reversible folding/unfolding transitions were observed within a pressure range from two to 1000 MPa. The solvent dependent equilibrium between the folded structure of a protein with hydrophilic core and the unfolded or open structure is affected by pressure.

The pressure and temperature dependence of the reaction rate constant k is often expressed combining the equations of Arrhenius and of Eyring:

$$\ln(k) = \ln(k_0) - \frac{E_a}{R \cdot T} + \left(\frac{-\Delta V^{\#}}{RT} \right) p \qquad \textbf{(2.48)}$$

introducing the activation energy E_a for the temperature dependence and the activation volume $\Delta V^{\#}$ as the characteristic parameter for the pressure dependence of k (Morild 1981); R is the universal gas constant (8.314 J mol^{-1} K^{-1}). However, this model is inappropriate if there is an effect of pressure and/or temperature on E_a and/or $\Delta V^{\#}$ as it is often described for proteins and enzymes (Ludikhuyze et al. 2002; Scharnagl et al. 2005; Smeller 2002).

The most useful models governing the stability of an enzyme subjected to pressure and temperature is based on the transition state theory of Eyring, suggesting that enzyme inactivation is accompanied by the formation of a folding/unfolding transition state which exists in equilibrium with the native enzyme. The free energy difference between these two states can be very small due to the fact that the entropic contribution and the enthalpic contribution to the folding process almost cancel (Nienhaus 2004).

Assuming that there are only two district states of a protein (native and denatured), the Gibbs free energy (ΔG) for the equilibrium process between the native and denatured state can generally be expressed as:

$$\Delta G = G_{denatured} - G_{native} \qquad \textbf{(2.49)}$$

$$\Delta G = -RT \ln K \qquad \textbf{(2.50)}$$

where at a given pressure the equilibrium constant K is dependent on the degree of denaturation a_D:

$$K = \frac{a_D}{1 - a_D} \qquad \textbf{(2.51)}$$

The deviation of the pressure dependence of ΔG is given by the van't Hoff equation (Eqn. 2.42) which can be extended by the following relationship:

$$\left(\frac{\partial \ln K}{\partial p} \right) = -\frac{\Delta V^{*}}{RT} = -\left(\frac{\partial \Delta G}{RT \partial p} \right) \qquad \textbf{(2.52)}$$

In order to asses the effects of pressure and temperature on ΔG Hawley (Hawley 1971) proposed an equation including the coupling ΔV and ΔS via the thermal expansion factor $\Delta\alpha$.

$$d(\Delta G) = \Delta V dp - \Delta S dT \qquad \textbf{(2.53)}$$

Upon integration of this equation from an arbitrarily chosen reference point T_0, p_0 Eqn. 2.53 can be approximated by a series expansion (Smeller 2002). In Eqn. 2.54 such an expansion has been truncated after the second order terms.

$$\Delta G = \frac{\Delta\beta}{2}(p-p_0)^2 + \Delta\alpha(p-p_0)(T-T_0) - \Delta C_P\left[T\left(\ln\frac{T}{T_0}-1\right)+T_0\right] + \Delta V_0(p-p_0)^2 - \Delta S_0(T-T_0)+\Delta G_0 \qquad \textbf{(2.54)}$$

where Δ denotes the change of the corresponding parameter during unfolding. S_0 is the entropy, β is the compressibility factor, C_p the heat capacity. Recently it has been suggested that in the vicinity of the reference point (T_0, p_0) Eqn. 2.54 can be modified using the following second-order approximation (Meersman et al. 2006; Smeller 2002):

$$\Delta G=\Delta G_0+\Delta V_0(p-p_0)-\Delta S_0(T-T_0)+(\Delta\beta/2)(p-p_0)^2 -(\Delta C_p/2T_0)(T-T_0)^2+\Delta\alpha(p-p_0)(T-T_0) \qquad \textbf{(2.55)}$$

From the quadratic approximation of the difference in Gibbs free energy it is evident that the equilibrium condition ($\Delta G = 0$) will appear as an elliptical line in the p-T plane (Zhang et al. 1995). Since the first approaches of Brandts (Brandts et al. 1970) and Hawley (Hawley 1971) such elliptic phase diagrams have been reported for proteins and enzymes, e.g. cytochrome c (Lesch et al. 2002) or staphylococcal nuclease (Lassalle et al. 2000).

However, the addition of higher terms was found to give better fits for a number of enzymes (Indrawati et al. 2002; Ly-Nguyen et al. 2002; Ly-Nguyen et al. 2003; Nunes et al. 2006; Rapeanu et al. 2005; Yamaguchi et al. 1995). This might be necessary when the second derivatives $\Delta\beta$, $\Delta\alpha$ and ΔC_p of the Gibbs free energy difference (ΔG) are temperature and/or pressure dependent (Smeller and Heremans 1997; Yamaguchi et al. 1995). In general there are 4 third degree terms.

$$(\Delta\beta_2/2)(p-p_0)^3\ ;\ (\Delta C_{p2}/2T_0)(T-T_0)^3\ ;\ \Delta\alpha_{2A}(p-p_0)^2(T-T_0);\ \Delta\alpha_{2B}(p-p_0)(T-T_0)^2$$

where the subscript “2” refers to the coefficients of the higher order terms.

Smeller and Heremans (Smeller and Heremans 1997) showed that the main form of the elliptical shape of the transition line remains when adding third order terms to Eqn. 2.55, but the actual shape of the curve is distorted. This distortion becomes obvious at high pressure and/or temperature, where the third order terms become dominant.

However, also Hawley’s approach fails if unfolding is irreversible and it is intended to describe the kinetics of denaturation. Along the equilibrium line ($\Delta G = 0$) the concentrations of the native and unfolded state are constant, but no information is available on the rate of transition. Nevertheless, lines of identical transition rate constants of proteins and enzymes also show an elliptical shape when plotted in a pT diagram and not a linear or just slightly skewed line as it might be expected from Eqn. 2.48.

Contrary to the derivative of Eqn. 2.55, which is based on the assumption that there are p-T conditions where the native and the denatured state are at equilibrium, isorate curves result from the identical reaction barrier between both states at different p-T conditions. Currently, concepts relating kinetics and thermodynamics of protein unfolding are still under discussion (Kaya and Chan 2002), but several empirical equations have been proposed for the mathematical handling of the experimental isorate curves. Eqn.2.56 basically reflects Eqn.2.55 and is useful for the description of elliptically shaped kinetic diagrams of enzymes (Castro et al. 2006b; Guiavarc'h et al. 2005; Ly-Nguyen et al. 2003; Rapeanu et al. 2005) but applies also to microbes (Hashizume et al. 1995; Reyns et al. 2000; Sonoike et al. 1992) and even to bacterial spores (Ardia 2004; Margosch et al. 2006):

$$\ln(k) = A_0 + A_1 p + A_2 T + A_3 p^2 + A_4 T^2 + A_5 pT + \text{higher order terms} \qquad \textbf{(2.56)}$$

2.3.7 Effect of pressure on starch

Similar to proteins, it can be assumed that both temperature and pressure are crucial parameters when changes in polysaccharide structures are intended to be brought about in food processing.

Apart from heating, gelatinization has also been reported to be initiated by high hydrostatic pressures, although the degradation of granules happens in a somehow different manner. The application of up to 400 MPa revealed that pressure has an impact on the gelatinization temperature in the case of wheat and potato starch (Muhr et al. 1982; Thevelein et al. 1981). More recent studies (Douzals et al. 2001; Rubens and Heremans 2000) confirmed these findings for wheat and rice also presenting elaborated pressure-temperature phase transition diagrams for those starches.

Although gelatinization can clearly be detected by DSC, FTIR, or by the loss in birefringence, the viscosity of high pressure treated granule suspensions is usually lower than after heat treatment (Stolt et al. 2001; Stute et al. 1996). Contrary to thermal gelatinization, pressure gelatinized starches starch granules remain intact or just partly disintegrated and the solubilization of amylose is rather poor (Stute et al. 1996). It has been assumed, that the crystalline components are prevented from melting since the amylopectin in the granule is stabilized by the still present amylose (Stolt et al. 2001). This could explain why maize starch is completely decomposed while waxy maize starch (containing almost no amylose) is not. In fact the hydration of the largely amorphous regions of the growth rings is the first step of gelatinization, but surprisingly, at this point there is hardly any water absorbed from the crystalline lamellae (Jacobs et al. 1998). Since it is also know that starch granules can deposit

reversibly about 30% of water it is questionable whether the amorphous regions of the granule play an important role in controlling the rate of gelatinization (Parker and Ring 2001). For heat gelatinization it is more likely that the loss of crystallinity is the rate limiting step which is certainly of importance for pressure induced process, too. Nevertheless, the pressure range in which gelatinization occurs is specific for each starch and is partly dependent on its crystalline structure, e.g. B-type starches are more resistant to pressure than A- and C-type starches (Muhr et al. 1982; Stolt et al. 2001; Stute et al. 1996).

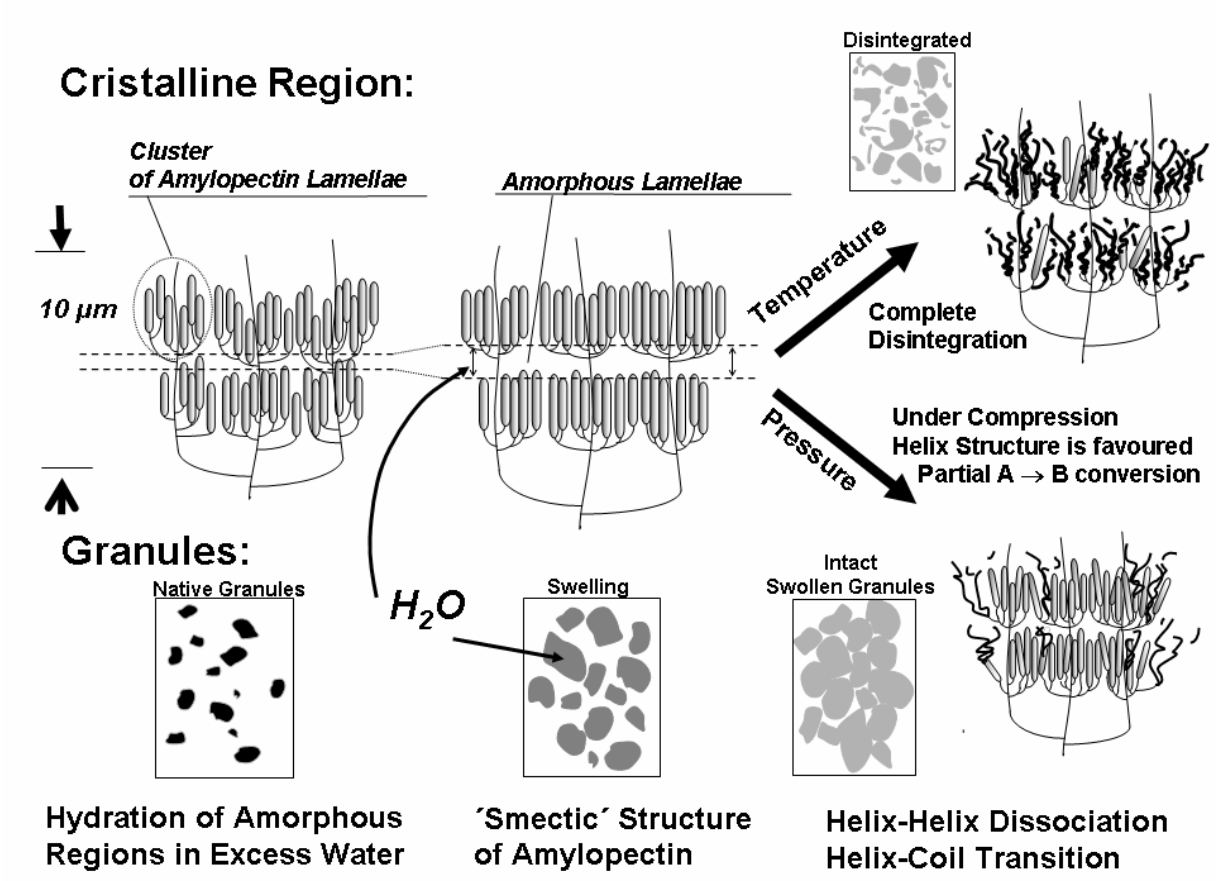

Fig. 2.24: Scheme of starch gelatinization. In excess water, the amorphous growth ring regions are hydrated and in the crystalline domain amorphous lamellae are formed. The granule is swelling. The smectic crystalline structure is decomposed by helix-helix dissociation followed by helix coil transition when the gelatinization temperature is exceeded (Waigh et al. 2000). It is suggested that under pressure the disintegration of the macromolecule is incomplete since the pressure stabilization of hydrogen bonds favors the helix conformation. Even crystalline conversion from A to B-isomorph under pressure has been reported (Katopo et al. 2001).

As already mentioned in chapter 2.2.3, it is suggested that the smectic arrangement of the amylopectin double-helices in the lamellar clusters of the crystalline growth ring regions is

loosened, followed by a helix coil transitions of the macromolecule and eventually the complete loss of granular structure and the formation of stable gels in the case of A-starch (Waigh et al. 2000). Under pressure, the side by side dissociation and helix unwinding might be suppressed because van der Waals and hydrogen bonds are stabilized which should favour the helix structure. Consequently, starch gelatinization is interrupted because the disintegration of the crystalline regions remains incomplete (see Fig. 2.24). For a 690 MPa high pressure treatment at ambient temperature, it has been found that large parts of the crystalline regions are retained (Katopo et al. 2001). Interestingly, A-starches underwent changes in the crystallinity pattern from A to the B-isomorph which obviously is favoured by pressure because of the higher number of associated water molecules stabilizing the helix structure by van der Waals forces.

It has to be discriminated between the methodologies used for detection, but the extent of gelatinization reached depends on pressure level, treatment temperature and processing time (Stolt et al. 2001). For protein unfolding it has already been stated that high pressure can not be seen independently from the temperature at which the treatment is performed. Therefore, the occurrence of intermediate degradation levels of the lamellar crystalline regions of the starch granule can be anticipated which is a possible reason for the significant difference e.g. in viscosity between starch gels formed at different pressure/temperature conditions.

When different pressure/temperature conditions have been identified where the native granule structure is irreversibly lost, a phase transition line can be generated in a p/T-diagram. A compilation of such transition lines is given in Fig. 2.25. For all starches it is evident that the gelatinization temperature is decreasing when the suspension is exposed to higher pressure. This is especially true at lower temperatures. The pressure effect is by far smaller when the treatment temperature is approaching the gelatinization temperature at atmospheric pressure. An increase in gelatinization temperature is rarely found, but it has been reported in an early study (Muhr et al. 1982).

Most curves in Fig. 2.25 have been derived from microscopic inspections of the granule's birefringence. Along those lines the viscosity of the gelatinized suspension is increasing with increasing temperatures. In other words: the structural network for pressure induced gels is much weaker. Incomplete granule degradation with no or only partial melting of the crystalline regions prevents amylose and amylopectin from gel formation as it happens in thermal gelatinization. In contrast, it can be assumed that the hydration of the amorphous domain either in the growth ring structures or in the lamellar structure of the crystalline regions is improved by pressure. The main contribution to increased viscosity of high pressure suspension comes from the irreversibly swollen granules which are reducing the liquid's free volume.

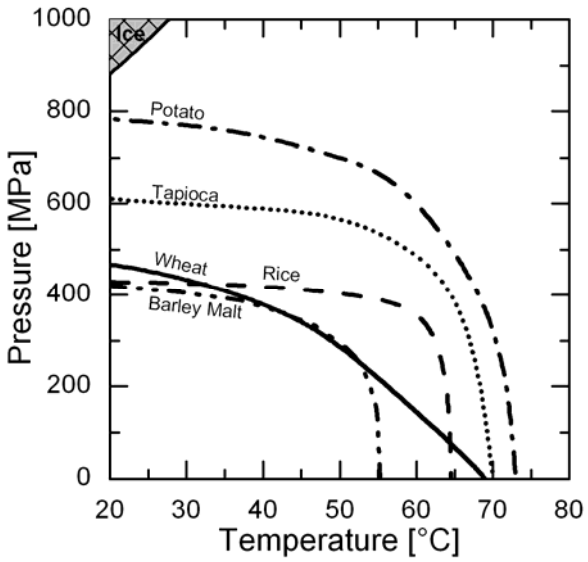

Fig. 2.25: Phase transition lines of starch gelatinization. The lines indicate a 100% loss in birefringence of different starch suspensions (5% w/w): barley malt (-··), rice (--), wheat (—), tapioca (····) and potato (-··-). Isolines are drawn after (Bauer and Knorr 2005; Heinz et al. 2005; Rubens and Heremans 2000; Rumpold 2005).

At present, the knowledge on the mechanistic background of pressure induce starch gelatinization is not complete. p-T diagrams showing the phase transition of starches over a wide range of temperature and pressure are rare. The few data that are available can be modelled by an empirical model with a thermodynamic background. For analyzing the p-T-behaviour of proteins, a two-state transition is assumed which is at equilibrium at the phase transition line (e.g. between native and unfolded). Although starch degradation is an irreversible process, the rate of the overall degradation reaction depends on the processing parameters temperature and pressure. From the phase transition diagrams in Fig 2.23 it can be assumed that there is an interrelation between thermodynamics and kinetics of starch gelatinization - at least on a phenomenological basis. This gives rise to apply the well known Clausius-Clapeyron equation to kinetic data transposed to the p-T domain as shown in Eqn 2.57:

$$\frac{dT}{dp} = T\frac{\Delta V}{\Delta H} \qquad \text{or} \qquad \frac{dT}{dp} = \frac{\Delta V}{\Delta S} \tag{2.57}$$

Since the volume ΔV and the entropy ΔS of the transition are inherently dependent on pressure and temperature, Eqn. 2.57 is better used in a generalized form (Rubens and Heremans 2000):

$$\frac{dT}{dp} = \frac{\Delta V_0 + \Delta\alpha(T - T_0) + \Delta\beta(p - p_0)}{\Delta S - \Delta\alpha(p - p_0) + \Delta C_P(T - T_0)/T_0} \tag{2.58}$$

$\Delta\alpha$ and $\Delta\beta$ denote the thermal expansion and the isothermal compressibility, respectively. ΔC_P indicates the change in heat capacity.

Rubens and Heremans (Rubens and Heremans 2000) have demonstrated the similarity between protein unfolding (of chymotrypsinogen) and rice starch gelatinization by applying the same thermodynamically derived model of Eqn. 2.58. In both cases the molecular stability is based on hydrogen and van der Waals bonds which give rise to the assumption that the transition temperature of starch depends on pressure, also. However, since gelatinization is a multi-stage process the extent and the mechanism of hydration under pressure prior to melting of the crystalline regions seem to be an important factor which is not yet completely understood.

2.4 Inactivation kinetics

2.4.1 Rate constants

Kinetic parameters and models have been developed processes to ensure safety during food preservation. They also provide the tools to compare the impact of different process technologies on reduction of microbial populations. The parameters used to analyze and report the reduction of microbes or enzymes as a function of process parameters include empirical coefficients experimentally determined from inactivation kinetics, as well as constants from expressions based on chemical reaction kinetics.

A general model to describe the reduction of a specific ingredient in a solution as a function of processing time t can be written as:

$$\frac{dC}{dt} = -k_{p,T} \cdot C^n \qquad \textbf{(2.59)}$$

The rate constant $k_{p,T}$ of the reaction is dependent on pressure and temperature but independent from the concentration C. The reaction order n characterizes the dependence of the reaction from the concentration of reactants. In a reaction of order n=0 the rate constant k is independent from C and in a first order reaction (n=1) k is proportional to C. However, in complex reactions, such as occurring in food systems, the reaction order can be negative or can have fractional values also (Kessler 1996).

Under constant extrinsic conditions, the integration of Eqn. 2.59 gives Eqn. 2.60:

$$C_t = \left[C_0^{(1-n)} + (n-1)k_{p,T} \cdot t\right]^{\frac{1}{1-n}} \qquad \textbf{(2.60)}$$

In the case of a first order reaction, integration of Eqn. 2.59 yields an equation which is often used to describe thermal inactivation kinetics of microbes and enzymes:

$$C_t = C_0 \exp\left(-k_{p,T} \cdot t\right) \qquad \textbf{(2.61)}$$

The corresponding model to describing changes in enzyme activity as a function of time is usually written as follows:

$$A = A_0 \exp(-k \cdot t) \quad \textbf{(2.62)}$$

where A is the enzyme activity at time t and A_0 is the initial enzyme activity.

Eqn 2.62 can be logarithmically transformed to give:

$$\ln(A) = \ln(A_0) - k \cdot t \quad \textbf{(2.63)}$$

When the natural logarithm of enzyme activity is plotted versus time, the inactivation rate constant k can be derived by linear regression analysis.

The traditional approach to describing first order reactions is to express the changes in enzyme activity as a function of time by the decimal reduction time (D value) which is expressed in Eqn. 2.64:

$$\log\left(\frac{A}{A_0}\right) = \frac{-t}{D} \quad \textbf{(2.64)}$$

By comparing Eqn. 2.64 and Eqn. 2.64, the relationship between the decimal reduction time and the first-order reaction rate constant is:

$$k = \frac{2.303}{D} \quad \textbf{(2.65)}$$

The primary parameters (D-value or k) would describe the inactivation at a constant and defined temperature and/or pressure. The inherent assumption in the use of these models (and the corresponding parameters) is that the reduction in enzyme activity is described by the first-order reaction model.

However, sometime enzyme inactivation kinetics show a biphasic characteristic where a fast initial inactivation period is followed by a decelerated decay. Such kinetics have been attributed to the occurrence of isoenzymes with different stabilities and both are inactivated according to a first order reaction (Buckow et al. 2005b; Hendrickx et al. 1998). For constant extrinsic and intrinsic conditions and assuming that the inactivation reaction of both isofractions is independent of each other, Eqn 2.66 can be used:

$$A = A_{0S} \exp(-k_S \cdot t) + A_{0I} \exp(-k_I \cdot t) \quad \textbf{(2.66)}$$

where A_{0S} and A_{0I} refers to initial activity of a stable and a labile isofraction, respectively.

Alternative models, such as the fractional conversion model, log-logistic model or Weibull-model, have been suggested to explain non-linear inactivation behaviour, in particular of enzymes, microbes and spores (Anderson et al. 1998; Heinz and Knorr 1996; Hendrickx et al. 1998; Peleg et al. 2005; Rizvi and Tong 1997; Xiong et al. 1999). If there is evidence of a

different reaction model, different parameters need to be identified and used for process development and prediction purposes.

2.4.2 Temperature coefficients

Traditionally, the temperature dependence of inactivation rates has been expressed in terms of the thermal resistance constant (z-value) using the following model:

$$\log\left(\frac{D}{D_{ref}}\right) = -\frac{(T - T_{ref})}{z} \qquad \textbf{(2.67)}$$

The thermal resistance constant z (T) is the temperature increase needed to accomplish a 1-log cycle reduction in the D-value (min). The reference decimal reduction time (D_{ref}) is the magnitude at the reference temperature (T_{ref}) within the range of temperatures used to generate experimental data.

An alternative model for describing the influence of temperature on inactivation rates is the Arrhenius equation (Eqn. 2.68). The model illustrates the influence of temperature on the reaction rate constant (k), as follows:

$$k = k_{ref} \exp\left[\frac{E_a}{R}\left(\frac{1}{T_{ref}} - \frac{1}{T}\right)\right] \qquad \textbf{(2.68)}$$

where E_a is the activation energy (kJ/mol), k is the inactivation rate constant, k_{ref} is the inactivation rate constant at reference temperature (T_{ref}), R is the universal gas constant (8.314 $Jmol^{-1}K^{-1}$) and T is the absolute temperature.

Based on the Arrhenius model (Eqn. 2.68), the slope of ln (k) in contrast to 1/T plot determines the temperature coefficient E_a. The activation energy describes the influence of temperature on the magnitude of the first-order reaction rate constant (k).

2.4.3 Pressure coefficients

Similar to the thermal resistant constant z(T) the pressure dependence of inactivation rate constants can be described by Eqn. 2.69 (Zook et al. 1999):

$$\log\left(\frac{D}{D_{ref}}\right) = -\frac{(p - p_{ref})}{z} \qquad \textbf{(2.69)}$$

with D_{ref} as the decimal reduction time at reference pressure p_{ref}. The z(p) value is defined as the pressure increase required to accomplish a 1-log reduction in the decimal reduction time (D-value). When the decimal logarithm of the D-value is plotted versus pressure at a constant temperature, the z(p) value can be derived from the slope based on linear regression analysis.

As an alternative, the pressure dependence of enzyme inactivation rate constant at a constant temperature can be expressed with the Eyring equation (Eqn. 2.70):

$$k = k_{ref} \exp\left[-\frac{\Delta V^{\#}}{RT}\left(p - p_{ref}\right) \right] \qquad \textbf{(2.70)}$$

Introducing the activation volume $\Delta V^{\#}$ as the characteristic parameter for the pressure dependence of k (Morild 1981). p is the pressure, p_{ref} is the reference pressure, R is the universal gas constant, T the absolute temperature and k_{ref} is the inactivation rate constant at reference pressure.

The magnitude of $\Delta V^{\#}$ increases as the slope of the plot increases. When the rate of microbial inactivation increases significantly with small changes in pressure, the magnitude of $\Delta V^{\#}$ will be larger.

3. MATERIALS & METHODS

3.1 Enzymes

3.1.1 α-amylase

α-amylase (EC 3.2.1.1) from barley malt was purchased in a dried state from Sigma (#A-2771, Sigma, DE). 150 µg of the enzyme powder was dissolved in one mL 0.1M ACES buffer at pH 5.6 (#115226, Merck, DE). In some experiments ACES buffer (0.1 M, pH 5.6) was used which contained 90 mM NaCl and 3.8 mM $CaCl_2$. Here, 100 µg of the enzyme powder was dissolved in one mL buffer. During the experiments for detecting the conversion rates, 20 µg of α-amylase powder was diluted in 0.1 M ACES buffer (pH 5.6) containing 90 mM NaCl and 3.7 mM $CaCl_2$.

3.1.2 β-amylase

β-amylase from barley (EC 3.2.1.2, Sigma, #A-7130) was purchased in a dried state containing 20-80 units/mg protein. In all experiments, 0.1M ACES buffer (Sigma, #A-9758) at a pH of 5.6 was used to avoid a pressure induced decrease during the high pressure treatment. The enzyme was dissolved in ACES buffer at 0.0625 mg/mL.

3.1.3 Glucoamylase

Glucoamylase from *Aspergillus niger* (EC 3.2.1.3, Sigma, #A-7420) was purchased in a dried state containing approximately 30-60 units/mg. One unit is defined as the amount of enzyme that will liberate 1.0 mg of glucose from starch in 3 min at pH 4.5 and 55°C. In all experiments, 0.1M pressure invariant ACES buffer (Sigma, #A-9758) at a pH of 4.5 was used. The enzyme was dissolved in ACES buffer at a concentration of 0.5 mg/mL. According to the manufacture's information, this glucoamylase has a pH optima of 4.5 and is stable in the range of pH 4.0 – 8.0.

3.1.4 β-glucanases

β-glucanase from barley malt (EC 3.2.1.2) was extracted from malt using 0.1 M ACES buffer (Merck, # 1.15226.0250, DE) at pH 5.6. ACES buffer was used to prevent a pressure induced decrease of the pH during the high pressure treatments. The pH was chosen to be similar to that of barley malt mash and wort. The malt used consisted of the barley variety *Prestige* which was harvested in the year 2004 in France. The β-glucanase activity of this malt was found to be 210.4 U/kg. One Unit of enzyme activity equals one micromole of glucose reducing sugar equivalent released per minute at 30°C and pH 4.6.

The malt was ground in an ultra-centrifugal mill (ZM1, Retsch GmbH & Co, DE) using a ring sieve with 2.0 mm holes. Then starch granules were sieved to a particle size of ca. 0.5 mm. 1 g malt flour was added to 8 ml ACES buffer and thoroughly stirred on a vortex mixer. After 15 minutes occasional mixing at room temperature the sample was centrifuged at 1000 g for 10 minutes. The supernatant obtained was tested on its β-glucanase activity using Azo-Barley glucan (Megazyme, # S-ABG100, IR) and was eventually diluted with ACES buffer to give an absorbance of 0.8 (approximately 26.3 mU/ml) at 590 nm.

β-glucanase (EC 3.2.1.2) from *Bacillus subtilis* was purchased from Sigma (#49106) in a dried state and was dissolved in 0.1 M ACES (pH 5.6) 0.04 mg/mL.

3.2 Starches

3.2.1 Maize starch

Commercial maize starch (Bestfoods, Heilbronn, DE) was purchased at a local supermarket. A dry matter of the starch powder of 88.16% was verified in a dry air oven at 105°C during 5 hours. On the basis of dry matter, starch powder consists of 0.29% fat (assayed according to ISO 3947), 0.12% ash content (assayed according to ISO 3593) and 23.3% amylose content, as determined with the amylose/amylopectin assay kit from Megazyme (#K-AMYL, Megazyme, IR).

3.2.2 Barley malt starch

The malt used consisted of the barley variety *Prestige* which was harvested in the summer of 2004 in France. The dry matter of the malt granules was 95.5%.

The malt was ground in an ultra-centrifugal mill (ZM1, Retsch GmbH & Co, DE) using a ring sieve with 2.0 mm holes. Then starch granules were sieved to a particle size of 0.06-0.25 µm which were used in the experiments.

3.3 High pressure apparatuses

3.3.1 High pressure multi-vessel equipment

Most pressurization experiments were performed with a multi-vessel rig described by Arabas et al. (Arabas et al. 1999) elsewhere. The equipment allows pressurization up to 700 MPa in a temperature range of -40 to 140°C by using a low viscous heat and pressure transferring liquid (silicone oil M60.115.05, Novodirect, DK, #85321). Five high-pressure vessels (inner volume: 3 mL) made from beryllium copper alloy are mounted in a thermostate (Huber, DE, #CC 245).

Each vessel is connected by separate pipings and valves with a high-pressure intensifier (Unipress, PL, #U111) allowing for separate decompression. This high pressure equipment is designed to perform kinetic investigations with constant boundary conditions for various pressurization times. The maximum operation pressure (700 MPa) can be reached in less than 30 seconds. The occurring heat of compression (in aqueous media approx. 3°C per 100MPa) has been taken into account by keeping the sample at a lower temperature level prior to pressurization. The timer for measuring the reaction time was started after having reached isobaric and isothermal conditions (typically <30 s after the onset of compression).

3.3.2 High pressure single-vessel equipment

Some high pressure experiments had to be performed on a single vessel high pressure equipment (#U1000, Unipress, PL) due to the high piezo-stability of enzymes at low temperatures (20-50°C). This high pressure apparatus is similar to U111 (see chapter 3.3.1) but uses a manual pump to compress up to 1000 MPa. The vessel was immersed in an oil-bath (#85321, silicone oil M60.115.05, Novodirect, DK) equipped with temperature control (#CC 245, Huber, DE). Pressure transmitting fluid was silicon oil (#85321, Novodirect, DK). Details of the equipment can be found in elsewhere (Schlüter et al. 2004). Comparability of the U1000 equipment with the U111 equipment was proven by reiterating selected kinetics of enzyme inactivation in both machines. No difference reaction rate was detected.

3.3.3 High pressure micro-vessel equipment

Recently, this high pressure micro-vessel unit (Micro-system, Unipress, Warsaw, PL) has been described by Ardia (Ardia 2004) in detail. Briefly, the equipment consists of one pressure vessel (inner volume: 200 µL), placed into a heating-cooling block and connected to a high pressure intensifier through a capillary (inner diameter 0.5 mm). The heating-cooling block, made from copper, allowed quick changes in the temperature of the pressure vessel. Therefore, it was possible to heat the high pressure cell during the compression phase, reproducing the increase of temperature due to adiabatic heating of the sample. This option permitted to realize compression phases under adiabatic conditions, since the gradient of temperature between the sample and the vessel was minimized.

Di-2-ethyl-hexyl sebacate (Sigma-Aldrich Chemie GmbH, Germany) was used as pressure transmitting fluid since it does not undergo a phase transition in the applied pressure-temperature range. For instance, no phase transition was observed at 1400 MPa and 20°C.

Pressure was generated by a step motor (Unipress, PL) driving a piston into an intensifier which permitted a pressure build-up to 1400 MPa in less than 30 seconds. Pressure release was done by moving the piston back which needed the same time than required for compression.

By developing a suitable PC program pressure build-up and release, dwell time and temperature control was performed automatically and allowed optimal processing conditions. Selection of pressure-time profiles, as well as temperature conditions, diagnostic information and data acquisition, were available at the PC interface.

3.4 Enzyme activity assays

3.4.1 α-amylase

The enzyme activity was assayed spectrophotometrically by using non-reducing-end blocked *p*-nitrophenyl maltoheptaoside (BPNPG7) in the presence of excess levels of a thermostabile α-glucosidase (#K-CERA, Megazyme, IR) (McCleary and Sheehan 1987). The enzyme solution and assay solution (5.45 mg BPNPG7 + 12.5 U α-Glucosidase per mL) were pre-incubated at 40°C for 5 min respectively. To 0.1 mL assay solution, 0.1 mL of enzyme solution was added and incubated at 40°C for exactly 10 minutes. After the incubation time the enzymatic reaction was terminated by vigorously mixing the tube content with 1.5 mL tri-sodium phosphate buffer (pH 11.0). The absorbance of the solution and of a reaction blank was measured at 400 nm against distilled water. Blank samples were determined in the same way but tri-sodium phosphate buffer was added to the assay solution before the enzyme. One unit of α-amylase was defined as the amount of enzyme producing one micromole of *p*-nitrophenol from BPNPG7 (in the presence of excess thermostable a-glucosidase) in one minute at 40°C.

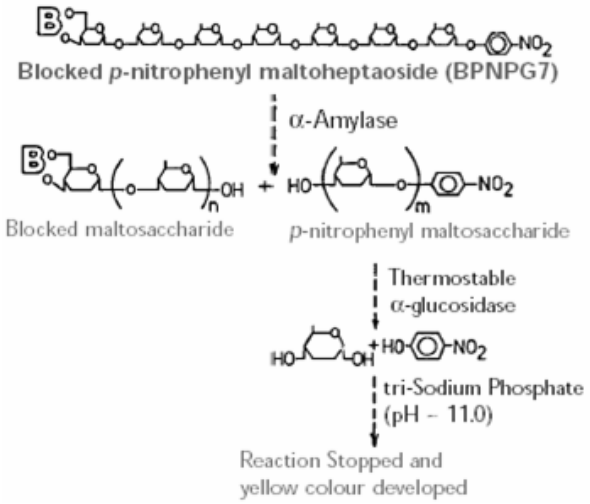

Fig. 3.1: Theoretical basis of the Ceralpha α-amylase assay (**#**K-CERA, Megazyme, IR) procedure.

3.4.2 β-amylases

The enzyme activity was measured spectrophotometrically using a modified method of *Bernfeld* (Stellmach 1986). Here, soluble starch (*Zulkowsky* starch, Merk, Darmstadt, DE, #101257) was used as substrate. 0.5 mL enzyme solution was tempered at 25°C and was mixed with 0.5 ml likewise heated substrate solution (3.33 mg starch/mL acetate buffer (0.1M, pH 4.8)). After 3 min incubation the reaction was stopped by adding 1 ml dinitrosalicylacid solution (1g $(NO_2)_2OHC_6H_2COOH$ in 80 mL distilled H_2O and 20 mL 2n NaOH + 30 g $C_4H_4KNaO_6 \cdot 4\ H_2O$). The mixture was heated for 5 min in a boiling water bath and after cooling down in ice water the solution was diluted with 10 mL distilled H_2O. The absorbance was measure at 490 nm against a blank where distilled H_2O was used instead of enzyme solution. The colour change has been calibrated by maltose-monohydrate and by Eqn.3.1. The specific enzyme activity in units per mg is obtained:

$$\frac{\mu\text{mol maltose}}{3 \cdot w} = \text{units/mg} \qquad \textbf{(3.1)}$$

μmol Maltose = value determined from calibration curve

3 = reaction time [min]

w = weighted enzyme sample in mg/0.5 mL solution used

3.4.3 Glucoamylase

During inactivation experiments, the enzyme activity was measured spectrophotometrically based on a method of McCleary (McCleary et al. 1991) using ρ-Nitrophenyl-β-maltoside plus thermostable β–Glucosidase (#R-AMGR3, Megazyme International Ireland Ltd., Bray, IR) as substrate. 10 mL ρ-Nitrophenyl-β-maltoside (4mM) plus β–Glucosidase (25U/ml) solution was dissolved in 10 mL distilled water. 100 μL enzyme solution was diluted with 900 μL ACES buffer (0.1M, pH 4.5) and pre-equilibrated at 40°C for 5 min. 0.2 mL of pre-heated enzyme solution was pipeted in a makro cuvette, then mixed with 0.2 mL pre-equilibrated substrate solution and incubated at 40°C for exactly 10 min. The reaction was terminated and the colour developed by adding 3.0 mL of 2% Trizma base solution (pH ~ 8.5; Sigma #T-1503). The absorbance was measured at 400 nm against a reagent blank. The reagent blank was prepared by adding 3.0 mL of Trizma base solution (2%) to 0.2 mL of reagent mixture with vigorous stirring, followed by the enzyme solution (0.2 mL) with stirring. The specific enzyme activity in units per mg is obtained by:

$$\text{Activity(U/ml)} = \left(\frac{\Delta A_{410}}{10}\right) \cdot \left(\frac{3.4}{0.2}\right) \cdot \left(\frac{1}{18.1}\right) \cdot \text{Dilution} \qquad \textbf{(3.2)}$$

ΔA_{410} = absorbance (reaction) - absorbance (blank)

10 = incubation time

3.4 = final reaction volume (mL)

0.2 = volume of enzyme assayed (mL)

18.1 = *E*mM *p*-nitrophenol in 2% trizma base (pH ~ 8.5) at 400 nm.

3.4.4 β-glucanases

The activity of β-glucanase was measured spectrophotometrically using a modified method of McCleary and Shameer (McCleary 1986; McCleary and Shameer 1987). Briefly, malt extract and Azo-Barley glucan substrate (Megazyme, # S-ABG100, IR) were pre-incubated at 30°C for 5 min. To 0.5 mL substrate, 0.5 mL aliquot of malt extract was added, vigorously mixed and then incubated at 30°C (β-glucanase from barley malt) and 40°C (β-glucanase from *B.subtilis*) for exactly 10 minutes. The reaction was terminated by adding 3 mL of a precipitant solution (40 g $CH_3COONa.3H_2O$ and 4 g zinc acetate in 200 mL distilled and with HCl adjusted H_2O (pH 5.0) and 800 mL methoxyethanol) and the tube contents stirred vigorously. After 5 min at room temperature, the sample was centrifuged at 1000g for 10 min. The absorbance of the clear supernatant was measured at 590 nm against a reaction blank. The reaction blank was prepared by adding precipitant solution to the Azo-Barley glucan substrate before the addition of malt extract.

3.5 Isothermal and isobaric inactivation kinetics

3.5.1 α-amylases

α-amylase was subjected to isobaric/isothermal conditions in the range of 0.1-800 MPa and 30-75°C. Isothermal treatments of α-amylase at ambient pressure were carried out by immersing glass reaction tubes (#H500, C.A.T. GmbH & Co, DE) containing 0.5 mL of the enzyme solution in a temperature controlled water bath. After preset time intervals, the samples were withdrawn and immediately cooled in ice water. Within 60 minutes of storage on ice the remaining enzyme activity was measured as described. Reactivation of α-amylase was not observed. The initial activity (A_0) was defined as the activity found when heating a sample to target temperature (ca. 45 s) and immediately cooling it in ice water.

α-amylase kinetics for pressure inactivation were derived from close-to isobaric experiments using the residual enzyme activity after treatment. Enzyme solutions were pressurized in the multi-vessel high pressure equipment (see chapter 3.3.1). At low temperatures fast inactivation of α-amylase occurred at pressures exceeding 700 MPa, only. These trails were performed using the high pressure single-vessel equipment (see chapter 3.3.2).

The α-amylase solution was transferred into 1.65 mL flexible ampulles (Cryotubes 375 299, Nunc, DK) and incorporated in the heated pressure vessel. Compression was started when the temperature of the sample reached a level which eventually results in the target temperature after the occuring heat of compression during the coming-up time. Temperature control of the sample was achieved by placing a thermocouple directly inside the tubes. Pressurization rate was standardized at approximately 25 MPa/s to minimize the loss of enzyme activity. The timer for measuring the dwell time was immediately started after having achieved the desired pressure-temperature conditions. The initial activity (A_0) was defined as the activity found immediately after pressure build-up. This was done to exclude the impact of variable pressure-temperature conditions on enzyme inactivation during the compression phase. After pressure release, the samples were stored in ice water for at least 10 min but longest for 60 min before determining the enzyme activity. No reactivation of α-amylase was noticed within 8 hours.

3.5.2 β-amylase

The thermal treatments of β-amylase at ambient pressure were carried out under isothermal conditions. The preheated enzyme samples were filled in glass reaction tubes and heated in a water bath with temperature control. To stop thermal inactivation after preset times, the samples were removed and cooled in ice water immediately. The remaining enzyme activity was measured as described above.

β-amylase kinetics for pressure inactivation were derived from close-to isobaric experiments using the residual enzyme activity after treatment. In contrast to thermal treatments here the initial activity (A_0) was defined as the activity found immediately after pressure build-up. This was done to exclude the variable pressure-temperature conditions during the compression phase.

2 mL sample tubes (Cryotubes 375 299, Nunc, DK) containing enzyme solution were pre-heated in a way that the desired temperature was achieved after adiabatic heating during pressure build-up. Pressure treatments were performed using the high pressure multi-vessel equipment, and were carried out in a range of 100-700 MPa and at process temperatures of 20-70 °C. After pressure release, the samples were stored on ice before determining the enzyme activity.

3.5.3 Glucoamylase

The thermal treatments of glucoamylase at ambient pressure were carried out under isothermal conditions. The enzyme solution was filled in glass reaction tubes and heated in a water bath with temperature control. After heating to target temperature within less than 15 seconds, remaining activity was measured and defined as initial activity (A_0). Kinetic behaviour

was determined by removing samples from the water bath after selected exposure times and immediately cooling them in ice water to stop thermal inactivation immediately. The remaining enzyme activity was measured as described.

Glucoamylase kinetics for pressure inactivation were derived from close-to isobaric experiments using the residual enzyme activity after treatment. Similar to thermal treatments, the initial activity (A_0) was defined as the activity found immediately after pressure build-up. This was done to exclude the variable pressure-temperature conditions during the compression phase. 150 µL containers (RS Components GmbH, Mörfelden-Walldorf, DE,) containing enzyme solution were heated inside the high pressure vessels in a way that the desired temperature was achieved after adiabatic heating during pressure build-up. Pressure treatments were performed using the high pressure micro-vessel equipment (see chapter 3.3.3), and were carried out in a pT range of 100-1400 MPa and 40-95 °C. After pressure release, the samples were stored on ice before determining the enzyme activity.

3.5.4 β-glucanases

Isothermal treatments at ambient pressure were carried out by immersing glass reaction tubes containing the enzyme solution in a temperature controlled water bath. After specified time intervals, the tubes were removed and cooled in ice water immediately. Within 60 minutes of storage on ice the remaining enzyme activity was measured as described above. The initial activity (A_0) was defined as the activity found when heating a sample to target temperature (ca. 45 s) and immediately cooling it in ice water. Thermal inactivation of β-glucanase from barley malt was investigated between 40-65°C. Thermal inactivation kinetics of β-glucanase from *B.subtilis* have been performed at 50-75°C.

Close-to isobaric experiments of β-glucanase in ACES buffer were performed with the high pressure multi-vessel and single-vessel equipment described in chapter 3.3.1 and 3.3.2, respectively. The enzyme solution was transferred into 2 mL sample tubes (Cryotubes 375 299, Nunc, DK) and placed into the pressure vessel which was warmed to target temperature. Temperature control was achieved by placing a thermocouple directly inside the Cryotubes. Compression was started when the temperature of the sample reached a level which eventually results in the target temperature after adiabatic heating during pressure build-up. Pressure build up rate was approximately 20 MPa/s to minimize the loss of enzyme activity. The timer for measuring the dwell time was started after having reached isobaric and isothermal conditions. Similar to thermal treatment, the initial activity (A_0) was defined as the activity found immediately after pressure build-up. This was done to exclude the variable pressure-temperature conditions during the compression phase. Pressure treatments of β-glucanase from barley malt were

performed in a range of 100-900 MPa and at process temperatures of 30-75°C. β-glucanase from *B.subtilis* was treated up to 1000 MPa at 30-75°C After pressure release, the samples were stored in ice water for at least 10 min but longest for 60 min before determining the enzyme activity.

3.6 Isothermal and isobaric conversion kinetics

3.6.1 α-amylase

In-situ measurement of the cleavage of BPNPG7 by α-amylase in different pressure and temperature domains was performed by mixing the enzyme solution (20 µg enzyme/mL ACES buffer) 1:1 with substrate solution on ice. The substrate solution consisted of 5.45 mg BPNPG7 (#O-BNPG4, Megazyme, IR) dissolved in 1 mL 0.1 M ACES buffer (pH 5.6, containing 90 mM NaCl and 3.8 mM $CaCl_2$). At ambient pressure, 0.3 mL of the mixture was transferred into glass reaction tubes (#H500, C.A.T. GmbH & Co, DE) and transferred in a temperature controlled water bath. Samples were kept at different temperatures (30-70°C) for up to 60 min. After different times, the tubes were removed and immediately heated in a boiling water bath for 2 min to stop the enzymatic reaction. The samples were then stored on ice water for 20-60 min. The degree of BPNPG7 hydrolysis was measured by adding 20 µL thermostabile α-glucosidase from *B. stearothermophilus* (#E-TSAGL, Megazyme, IR) to sample solution which was previously tempered at 40°C for 5 min. The mixture was kept at 40°C for exactly 10 minutes. α-glucosidase hydrolyses the *p*-nitrophenyl maltosaccharide fragment to glucose and free *p*-nitrophenol. At the end of the 10 min incubation period, 1.5 mL tri-sodium phosphate buffer (pH 11.0) was added and the absorbance was detected at 400 nm against distilled water. The initial absorbance at time = 0 was defined as the value found of the sample that was heated to target temperature (approximately 45 s) followed by immediately cooking for 2 min.

For the measurement of the catalytic activity of α-amylase under high pressure conditions the cooled enzyme-substrate mixture was transferred into flexible tubes (Cryotubes 375 299, Nunc, DK) and placed immediately into the multi-vessel pressure equipment (see chapter 3.3.1) which was warmed to target temperature. A thermocouple was placed inside the tubes to allow the monitoring of the temperature. Pressure build-up was initialized when the sample reached a temperature level which ensured the desired temperature after compression. Samples were kept at different p-T conditions (100-400 MPa, 30-75°C) for up to 60 minutes. After pressure release, the samples were removed and immediately heated in a boiling water bath for 2 min. Following an incubation period of 10-60 min in ice-water the amount of *p*-nitrophenol was measured as described for the thermal treatments. The initial absorbance at time = 0 was defined as the value

found when decompression was carried out immediately after the target pressure has been reached.

3.6.2 β-amylases

Preheated enzyme (0.0625 mg/mL ACES buffer (0.1M, pH 5.6)) and soluble starch (3.33 mg starch/mL ACES buffer (0.1M, pH 5.6)) solutions were mixed in a ratio 1:1, transferred into a cryotube and then placed directly in the high pressure multi-vessel equipment. To study the substrate conversion of β-amylase under high hydrostatic pressure conditions the starch/enzyme preparation was kept at different p-T conditions for at least 30 minutes treatment time. Product formation was detected every 5 minutes. The initial maltose concentration at time = 0 was defined as the value found when decompression was carried out immediately after the target pressure has been reached. After pressurization 1 mL sample was taken and enzyme activity was stopped by adding 1 ml dinitrosalicylacid solution. The mixture was cooked for 5 min in water, then cooled in ice water and after adding 10 mL distilled H_2O the absorbency was measure at 490 nm against a blank sample. The maltose concentration of the sample was derived from a calibration curve.

At ambient pressure, 1 mL of enzyme-substrate mixture was transferred into glass reaction tubes (#H500, C.A.T. GmbH & Co, DE) and transferred in a temperature controlled water bath. Samples were kept at different temperatures (20-65°C) for up to 60 min. After different times, the tubes were removed enzyme activity was stopped by adding 1 ml dinitrosalicylacid solution. Detection of maltose concentration was performed as described above.

3.6.3 Glucoamylase

Maltose conversion of glucoamylase under high pressure conditions was observed by adding cooled maltose monohydrate solution (Merck, #5912) (10 µg/mL 0.1M ACES buffer, pH 4.5) to cold glucoamylase solution (10 µg/mL 0.1M ACES buffer, pH 4.5) in a ratio 9:1.

At ambient pressure, 1 mL of enzyme-substrate mixture was transferred into glass reaction tubes (#H500, C.A.T. GmbH & Co, DE) and transferred in a temperature controlled water bath. Samples were kept at different temperatures (40-75°C) for up to 45 min. To 1 mL enzyme-substrate solution 3 mL GOD-reagent (pH 7.0) was added which stopped the enzyme activity. GOD-reagent consisted of 3.8 mg Peroxidase (Sigma, # 8125) 400 mg Glucose Oxidase (Sigma, #G6766) and 10 mg o-Dianisidindihydrochlorid (Sigma, #3252) which were diluted in 100 mL Tris-buffer solution (30 g hydroxymethylaminoethane (Serva #37190), 42.5 mL 5M hydrochloric acid and 1 mL chloroform dissolved in 1000 mL distilled water). After 60 min storage at room temperature the absorbency was measure at 420 nm against a blank sample (1mL H_2O plus 3

mL GOD-reagent). The glucose concentration of the sample was derived from a calibration curve.

To investigated conversion rates under high pressure conditions the enzyme-substrate mixture was transferred into cryotubes and placed into the high pressure multi-vessel equipment (described in 3.3.1) which was warmed to target temperature. With a thermocouple placed directly inside the cryotubes the temperature was monitored. Compression was started when the temperature of the sample reached a level which eventually results in the desired temperature after adiabatic heating during pressure build-up.

Substrate conversion of glucoamylase under high hydrostatic pressure conditions was observed at different p-T conditions for at least 30 minutes process time. After pressurization the samples were cooled in ice water for exactly 1 minute.

The initial glucose concentration at time = 0 was defined as the value found when decompression was carried out immediately after the target pressure has been reached.

3.6.4 β-glucanases

Glucan hydrolysis by malt β-glucanase under high pressure conditions was measured by adding cooled Azo-Barley glucan to cold β-glucanase solution (enzyme extract from barley malt was diluted 1:10, β-glucanase from *B.subtilis* solution was diluted 1:50 with 0.1 M ACES buffer pH 5.6) in a ratio 1:1. The solution was transferred into Cryotubes and placed immediately into the high pressure multi-vessel equipment (see 3.3.1) which was warmed to target temperature. A thermocouple placed inside the tube allowed the monitoring of the temperature. Pressure build-up was initialized when the sample reached a temperature level which ensured the desired temperature after compression. Samples were kept at different p-T conditions (100-600 MPa, 30-75°C) for up to 60 minutes dwell time. Substrate conversion was detected every 2-10 minutes. After pressure release and removing the sample, 1 mL of enzyme substrate mixture was immediately added to 3 mL cold precipitant solution to stop the reaction. The sample was vigorously stirred and then kept at room temperature for 5 minutes. After centrifugation at 1000g for 10 min the absorbance of the clear supernatant was measured at 590 nm against distilled water. The initial absorbance at time = 0 was defined as the value found when decompression was carried out immediately after the target pressure has been reached.

At ambient pressure 1 mL of enzyme-substrate mixture was pipetted into centrifuge glass tubes and placed in a water bath with temperature control. After heating to target temperature (approximately 45 s) the first sample was removed and mixed with 3 mL cold precipitant solution. After vigorously mixing and 5 min standing at room temperature the centrifuge tube was centrifuged at 1000g for 10 min. The absorbance of the supernatant was measured at 590 nm

against distilled water. The absorbance measured of this sample corresponds to the initial absorbance at time = 0.

Substrate conversion of β-glucanase at ambient pressure was investigated between 30-65°C.

3.7 Isothermal and isobaric gelatinization kinetics

Maize starch was suspended in distilled water (5% w/w) and filled into 1.65 mL flexible tubes (Cryotubes 375 299, Nunc, DK). Isothermal treatments at ambient pressure were carried out by immersing glass reaction tubes (#H500, C.A.T. GmbH & Co, DE) containing 0.5 mL of the enzyme of the maize starch solution in a temperature controlled water bath. After preset time intervals, the samples were withdrawn and immediately cooled in ice water. Within 30 minutes of storage on ice the number of gelatinized starch granules (N) was analyzed by the loss of optical birefringence of the starch granules using a microscope (Eclipse E400, Nikon, Tokyo, JP) equipped with a polarization analyzer. A minimum of 200 starch granules were counted within a defined area (Thoma chamber). The initial number of gelatinized starch granules (N_0) was defined as the number of granules showing no birefringence found when heating a sample to target temperature (ca. 45 s) followed by immediate cooling in ice water. The degree of starch gelatinization (N/N_0) was determined by the number of granules that lost birefringence divided by the product of the total number of counted starch granules and N_0 All measurements were carried out at least in duplicates. Thermal gelatinization of maize starch was investigated between 45-75°C.

Starch solution were pressurized in the multi-vessel, high pressure equipment (#U111, Unipress, PL) described in chapter 3.3.1. Cooled starch suspension (5% w/w) was transferred into 1.65 mL flexible tubes (Cryotubes 375 299, Nunc, DK) and incorporated in the heated pressure vessel. Compression was started when the temperature of the sample reached a level which eventually results in the target temperature (±1°C) after the occurring heat of compression during the coming-up time. Temperature control of the sample was achieved by placing a thermocouple directly inside the tube. Pressurization rate was standardized at approximately 25 MPa/s to minimize the loss of nativeness of the starch granules. The timer for measuring the dwell time was immediately started upon reaching the desired pressure-temperature conditions. After pressure release, the samples were stored on ice for approximately 30 minutes and were then analyzed as described above. The initial number of gelatinized starch granules (N_0) was defined as the number of gelatinized granules found after pressurizing the sample to target pressure followed by immediate pressure release. Pressure treatments were performed in a range of 50-650 MPa, 30-75 °C and up to 35 minutes dwell time. All measurements were carried out at least in duplicates.

3.8 Effect of pH and ions on the thermo-stability of α- and β-amylase

The thermal stability of α-amylase from barley malt was investigated in responds to pH, sodium chloride and calcium concentration. 0.1 M ACES buffer was adjusted to 4.5, 5.5, 6.5, and 7.5. The concentration of $CaCl_2$ in each buffer was varied from 0 up to 18 mM. The concentration of NaCl was measured in the range 0-160 mM. The enzyme was diluted at a concentration of 100 µg/mL. All the samples were isothermally treated at 60°C for 10 min using glass reaction tubes (#H500, C.A.T. GmbH & Co, DE). After the treatment the samples were stored on ice for approximately 10 min.

The thermal stability of β-amylase from barley malt was investigated in responds to pH and sodium chloride concentration. 0.1 M ACES buffer was adjusted to 4.0, 4.8, 5.6, 6.4, and 7.2. 0.13 mg/mL of β-amylase was dissolved in ACES buffer (0.1M, pH 5.6, containing 3 mM $CaCl_2$). The concentration of NaCl was varied from 0-0.72 M. All the samples were isothermally treated at 55°C for 5 min using glass reaction tubes (#H500, C.A.T. GmbH & Co, DE). After the treatment the samples were cooled on ice for approximately 10 min.

The samples of α- and β-amylase were adjusted to pH 5.5 by adding suitable amounts of NaOH or HCl. The residual enzyme activity was then spectrophotometrically measured as discussed previously with the enzyme kit of Megazyme (#K-CERA, Megazyme, IR). Due to the effect of calcium on the catalytic activity of α-amylase the residual enzyme activity after the heat treatment was expressed as the activity found relatively to the activity before the treatment.

The approximated surface response and corresponding iso-inactivation lines representing the percentage relative to the maximum of residual enzyme activity found were calculated using a statistical program (Table Curve 3D v3 Statistical Package, Systat Software Inc., Richmond, CA, USA).

3.9 Enzymatic starch conversion

3.9.1 Hydrolysis of maize starch by glucoamylase

Hydrolysis of maize by glucoamylase from *A.niger* was performed at 40-80°C and 0.1-600 MPa. Maize starch was heated at 90 min for 5 minutes to gelatinize the starch granules. Enzymatic conversion of maize starch was tested by adding cooled maize starch solution (previously treated at 90°C for 10 min) to cold glucoamylase solution (50 µg/mL 0.1M ACES buffer, pH 4.5) in a ratio 9:1. In order to conclude on the Michaelis-Menten constant of glucoamylase the starch concentration was varied from 0.05 to 3.6 mg/mL. The tests at ambient and at elevated pressures were performed as described in chapter 3.6.3.

3.9.2 Hydrolysis of barley malt starch by α- and β-amylase

Barley malt starch hydrolysis was investigated during high gravity mashing (Narziß 1985; Stewart and Russell 1985). Approximately 55 g of the malt was milled in a Büchler-Miag DLFU disc mill with a gap setting of 1.0 mm. 50 g ground malt was suspended in 200 ml preheated, ion exchanged water containing 150 mg $CaCl_2 \cdot 2H_2O$ and 0.3 ml 0.5 M H_2SO_4 to give a grist:water ratio of 1 : 4. The mashing cup was covered with a drilled lid and was placed in the mashing bath (Bender & Hobein MB 3E). By continuous stirring (100 rpm), the malt was mashed at 60°C for 20 min, 65 °C for 30 min and 72 °C for 30 min. The rate of temperature increase was 1°C/min. Samples have been taken at different stages of the process. Samples were immediately stored on ice and mixed with 0.5 M H_2SO_4 in a ratio 1:1 to terminate enzyme activity. The supernatant was further investigated in HPLC analysis to detect the amount of fermentable sugars.

3.9.3 HPLC analysis

The fermentable sugars (glucose, fructose, maltose and maltotriose) of wort samples were determined using a HPLC Pump 64 system of the Dr. Knauer GmbH (Berlin) with a 20µl manuel Injection No. 81743 and a Knauer differential refractive index detector operating at 40°C. The cation-exchange column used was an Bio-Rad Aminex HPX-87P, calcium form, 300 · 7.8mm. A Bio-Rad Deashing cartridge was used as pre-column. The flow rate with HPLC-grade water was 0.5 mL/min and the column temperature 85°C. Data was collected and handled with Software Knauer EuroChrom for Windows, Basic Edition V3.05.

3.10 Data analysis

The analysis of enzyme inactivation is based on determining the inactivation as a function of time under different pressure-temperature conditions. Previous studies (Buckow et al. 2005a; Heinz et al. 2005) revealed that combined thermal and pressure inactivation of enzymes which have more than one catalytic isoforms can simply be described by a n^{th}-order reaction (Eqn. 2.59), expressing the residual enzyme activity (*A*) as a function of time while pressure and temperature remains constant: similar to:

$$\frac{dA}{dt} = -k_{inact} \cdot A^n \qquad \textbf{(3.3)}$$

The reaction order n in this equation was determined by minimizing the cumulative standard error of fit over a wide range of reaction orders, i.e., averaging the predictive error in all individual kinetics of the complete experimental kinetic data set. k_{inact} is the inactivation rate constant (min^{-1}) which is regressively (Table Curve 2D v4.0 Statistical Package, Systat Software

Inc., Richmond, CA, USA) obtained by fitting n-th order kinetics (Eqn. 3.3) to the residual activity data. This allows an appropriate description of non log-linear inactivation curves.

Analysis of the data set of glucoamylase from *A.niger* inactivation kinetics a two step mechanism was evident. A two fractional model (Eqn. 2.66) was, therefore, suggested to describe the biphasic behaviour of enzyme inactivation with time over all tested p-T-combinations. This is in agreement with the existence of two forms of glucoamylase (GA1 and GA2), behaving differently when subjected to inactivation conditions. It was supposed that the two isoforms responded differently to high hydrostatic pressure. Eqn. 3.4 is basically similar to Eqn. 2.66 where $A1_0$ and $A2_0$ refer to the initial activity of the two isoenzymes of glucoamylase and k1 and k2 are the corresponding inactivation rate constants.

$$A = A1_0 \exp(-k1 \cdot t) + A2_0 \exp(-k2 \cdot t) \qquad \textbf{(3.4)}$$

The applied secondary models were based on a thermodynamic derivation which has been introduced by Hawley (Hawley 1971) and by Morild (Morild 1981) (see chapter 2.3.6). The model expresses protein folding/unfolding transitions by changes in Gibbs free energy. Derived from this thermodynamic model a second order polynomial model, sometimes extended with higher order terms, is useful for the description of elliptically shaped kinetic diagrams as often found for proteins and enzymes (Borda et al. 2004; Heinz et al. 2005; Ludikhuyze et al. 2002; Ly-Nguyen et al. 2003; Rapeanu et al. 2005; Rodrigo et al. 2006b). To simplify the calculation of the p-T dependence of the inactivation rate constant k_{inact} the thermodynamic approach model is used in a reformulated way. Adapted to the kinetics of enzyme inactivation the experimental data of $\ln(k_{inact})$ has regressively been fitted to a full third-order polynomial. After reducing the number of parameters, which was done by eliminating those terms which contributed less than 1% to the total fit standard error, Eqn. 3.5 was obtained:

$$\ln(k_{inact}) = A_0 + A_1 p + A_2 T + A_3\, p^2 + A_4\, T^2 + A_5\, pT + A_6 p^3 + A_7 T^3 + A_8 p^2 T \qquad \textbf{(3.5)}$$

where the parameters A_0, A_1, A_2, A_3, A_4, A_5, A_6, A_7 and A_8 were estimated by regression analysis using pressure in [MPa] and temperature in [°C]. For convenience, the use of reference points was abandoned as in this study no negative pressures nor subzero temperatures have been applied. Those third order terms in Eqn. 3.5 that still did not significantly contributed to the fitting of the model to the experimental data were omitted.

The models describing the effect of pressure and temperature on the conversion rate constant k_{conv} was usually derived empirically by fitting a number of simple equations to the data set with a statistical program (Table Curve 3D v3 Statistical Package, Systat Software Inc., Richmond, CA, USA).

4. RESULTS & DISCUSSION

4.1 Stability and catalytic activity of α-amylase

4.1.1 Effect of ions and pH on α-amylase stability

It is well known that the thermal stability of enzymes is highly dependent on environmental conditions such as pH, salts and other additives. Due to the major importance of the hydration water on enzyme flexibility and stability even small changes of its properties due to chemical denaturants or co-solvents can tip the balance from the native to the denatured state. The effect of pH on protein stability is due to the different pK_a values of the various ionizable groups in the folded and denatured state. In consequence, due to locally different changes of the electrostatic contributions to the intermolecular interactions and solvation energy the enzyme's stability shows an optimum at a specific pH value.

Fig. 4.1 A shows the contour plot of the thermo-stability of α-amylase from barley malt in responds to pH and calcium chloride concentration after 10 min heating at 60°C. The iso-inactivation lines indicate the percentage relative to the maximum of the residual enzyme activity observed at pH 6.1 and 3.8 mM $CaCl_2$. It is evident that at any pH the stability α-amylase is dramatically increased by adding calcium chloride up to an optimum of 3.8 mM. In beer brewing industry high gravity mashing is usually done in the presence of 0.5 mM to 4 mM calcium ions (Bak et al. 2001). Since the concentration of α-amlyase used in this study is approximately twice as high as in high gravity mash, this optimum is in agreement with the industrial practice. It also conforms to the results published by other authors who found increased stability of α-amylase in the presence of one mM $CaCl_2$ (MacGregor 1978) and 10 mM $CaCl_2$ (Bertroft et al. 1984). Further increase of the calcium concentration did not show any positive effect on the enzyme stability, although the catalytic activity considerably varies at these calcium concentrations (Rodenburg et al. 1994). Furthermore, at 60°C α-amylase stability in 0.1 M ACES buffer was only marginally affected by sodium ions up to a concentration of 0.1 M in the range of pH 4.5-7.5 (Fig. 4.1 B). The maximum stability of this commercial enzyme preparation at a pH of 6.1 is higher than reported by other authors which varied from 3.0-5.5 for isoenzyme AMY1 (Bertroft et al. 1984; MacGregor 1978) and 5.0 to 5.7 for AMY2 (Bertroft et al. 1984; Comrie 1967). This might be explained by the use of different buffers showing different temperature dependencies of their equilibrium constants. Although ACES buffer used in this experiments is relatively pressure insensitive (Kitamura and Itoh 1987) it shows a shift in pH of ca. -0.02 units/°C which is higher than the detected shift in pH of high gravity mash of ca. -0.01 units/°C (data not shown). Hence,

due to the stronger pH change of ACES buffer at 60°C the optimal pH for enzyme stability shifted towards higher pH values.

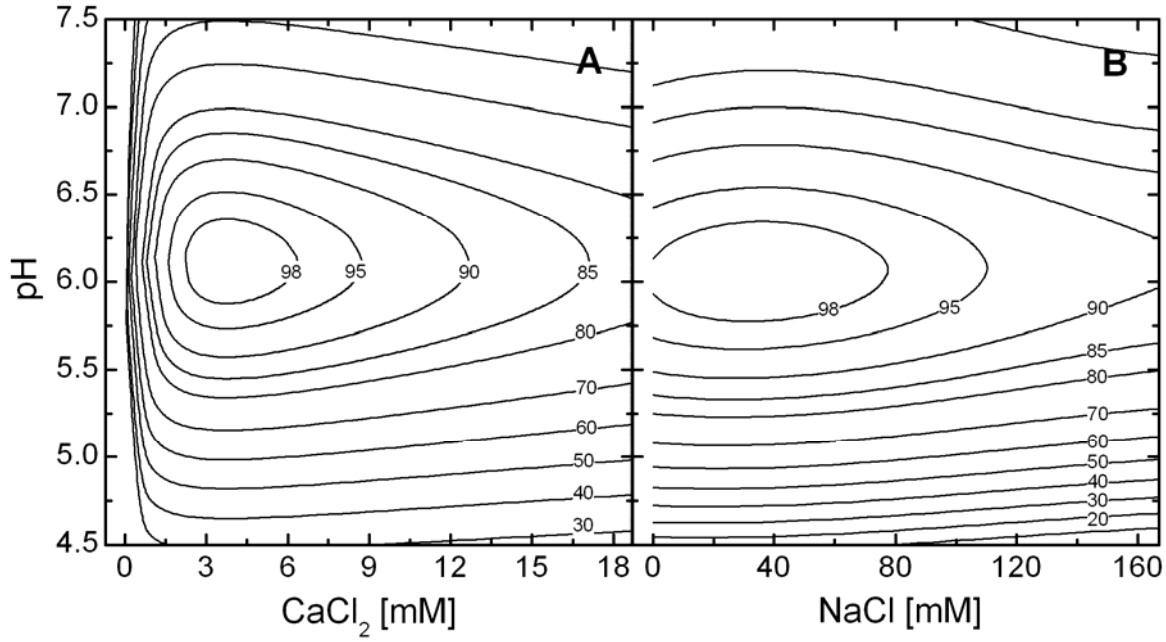

Fig. 4.1: Thermal stability of barley malt α-amylase in dependence of pH and the concentration of calcium chloride (A) and sodium chloride (B). Assay conditions: 0.1 M ACES buffer at various pH (4.5-7.5) containing 0-18 mM $CaCl_2$ (A) and 0-160 mM NaCl (B) respectively, treated for 10 min at 60°C and 0.1 MPa. Iso-inactivation lines indicate the percentage relative to the maximum of residual enzyme activity found at pH 6.1 and 3.8 mM $CaCl_2$ (A) and 38 mM NaCl (B) respectively.

4.1.2 Effect of high pressure-temperature combinations on α-amylase stability

Combined pressure and temperature treatments of α-amylase from barley malt in 0.1 M ACES buffer (pH 5.6) were performed in the range of 20-70°C and 0.1-650 MPa. In the p-T plane the isobaric/isothermal inactivation curves showed deviations from first order kinetics (Fig. 4.2 A). This might be explained by the presence of isoenzyme fractions showing differences in their stability towards pressure and temperature (Bertroft et al. 1984). Fig. 4.2 A shows the pressure inactivation curves of α-amylase from barley malt in 0.1 M ACES buffer (pH 5.6) at 60°C at pressures ranging from 0.1 to 500 MPa. The compression phase with an approximate duration of 20 s already produced a reduction in activity (data not shown) which has been taken into account for the calculation of relative enzyme activities. At 60°C the inactivation curves of α-amylase do not show an increased inactivation rate by increasing the treatment pressure. Whereas at ambient pressure the enzyme lost approximately 90% of its activity, elevated pressures up to 200 MPa conserved approximately 65% of the residual activity after 20 min

treatment time. However, high pressures of more than 400 MPa led to a faster inactivation of α-amlyase than found at ambient pressure.

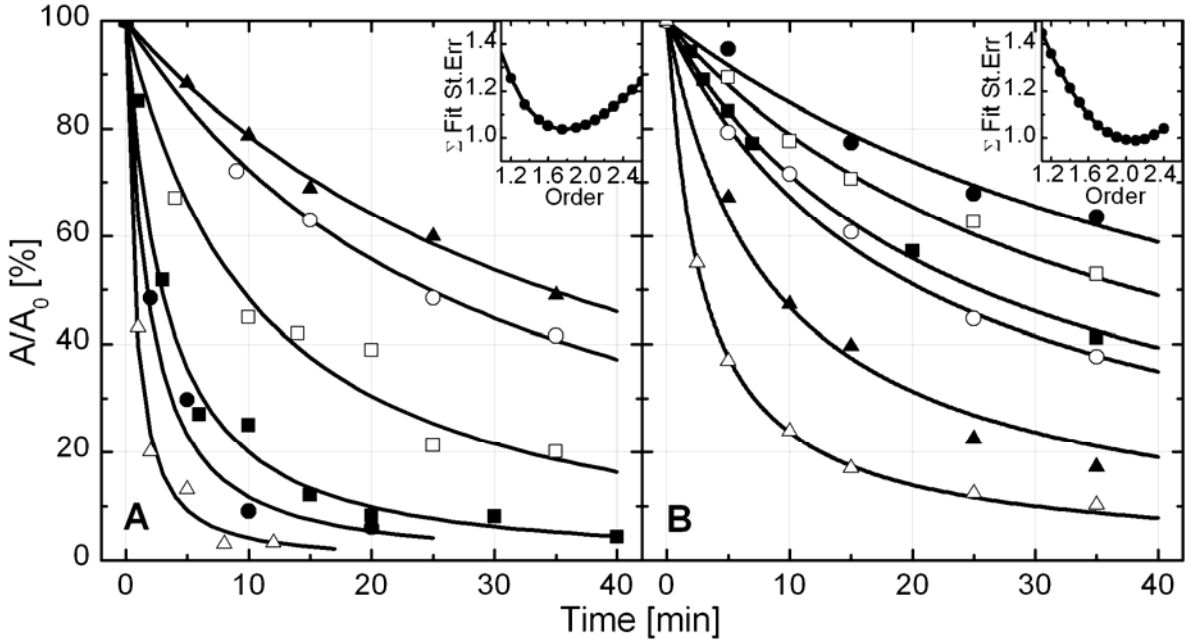

Fig. 4.2: A: 1.75th order inactivation of α-amylase in ACES buffer (pH 5.6; 0.1 M) at 60°C. B: 2.1st order inactivation of α-amylase in ACES buffer (pH 5.6; 0.1 M, containing 90 mM NaCl and 3.6 mM $CaCl_2$) at 65°C. Insets: Dependence of the sum of standard error in the regression analysis of the experimental data on the reaction order used in Eqn. 3.3. The symbols in both figures denote the applied pressures as follows: 0.1 (■); 100 (□); 200 (●); 300 (○); 400 (▲) and 500 (△) MPa.

The influence of the addition of calcium ions on the stability of α-amylase was studied in the range of 30-75°C and 0.1-800 MPa. Again, the enzyme inactivation typically showed strong deviations from simple first-order kinetics at constant temperature and pressure conditions. In Fig. 4.2 B some pressure inactivation kinetics of α-amylase in 0.1 M ACES buffer (containing 3.8 mM $CaCl_2$) at 65°C are presented. It is evident that the addition of calcium ions markedly enhanced the pressure and temperature stability of α-amylase from barley malt. Whereas in the absence of Ca^{2+} ions the enzyme losses approximately 95% of its initial activity within 10 min at 500 MPa and 60°C (Fig. 4.2 A), approximately 25% of its activity is preserved after 10 min at 500 MPa and 65°C by the addition of 3.8 mM $CaCl_2$ (Fig. 4.2 B). It is long been known that α-amylases require a calcium ion to retain the structural integrity and thermo-stability (Vallee et al. 1959; Violet and Meunier 1989). It has been proposed that the mechanism of thermal α-amylases inactivation is a two-stage process. At the initial, reversible dissociation step calcium ions dissociate from the native enzyme which is induced by changes of the enzyme/calcium binding complex and the calcium binding equilibrium. This step is followed by an irreversible

denaturation of the enzyme at high temperatures (Bush et al. 1989; Nielsen et al. 2003; Tanaka and Hoshino 2003). Although direct conclusions on the pressure induced inactivation can not been drawn, it is suggested that a similar mechanism might occur under compression.

Similar to the inactivation behavior of α-amylase in the absence of Ca^{2+} ions, the inactivation rate at 65°C in Fig. 4.2 B did not increase with increasing pressures but showed a pronounced minimum at approximately 200 MPa. Such antagonistic effect of pressure was observed throughout the low pressure / high temperature (> 65°C) range investigated. This phenomenon of pressure induced stabilization of enzymes and other proteins against thermal denaturation has often been encountered in pressure assisted enzyme inactivation (Buckow et al. 2005a; Dalmadi et al. 2006; Ludikhuyze et al. 2002) and is possibly explained by the strengthening of hydrophobic interactions and intramolecular hydrogen bonds formation (Balny and Masson 1993; Mozhaev et al. 1996b). Water molecules also exert a profound influence on protein stability through hydration of the amino acids. At relatively low pressures (<100 MPa) water exchange between the protein interior and bulk solvent is increased due to conformational fluctuations (Tanaka et al. 2000). On the other hand, pressure also increases the density of the first hydration shall at the protein surface which induces highest constrain on lateral chain motions (Mentré and Hoa 2000; Smolin and Winter 2006). Thus, pressure leads to a more compact, rigid protein structure reducing the thermal fluctuations caused by high temperatures. Tauscher (Tauscher 1995) reported that the tertiary and quaternary structure of most proteins is compromised by high pressures up to 200 MPa. Higher pressures may lead to a penetration of water molecules into the protein interior causing an unfolding of the protein molecule (Nash and Jonas 1997; Saad-Nehme et al. 2001; Zhang et al. 1995).

As shown in Fig. 4.2, the isobaric/isothermal kinetics of α-amylase indicated deviations from simple first-order kinetics in the p-T domain investigated and, therefore, were simply described by using a n^{th}-order reaction model (Eqn.3.3). The reaction order n of the enzyme inactivation has been obtained upon minimizing the cumulative standard error while fitting the model equation to the complete experimental kinetic data sets. For α-amylase in 0.1 M ACES buffer (pH 5.6) in the absence of Ca^{2+} ions, an order of 1.75 was determined as the minimum of the error function (see inset Fig. 4.2 A). This order was then used to determine the inactivation rate constants k_{inact} for all p-T combinations tested. In Fig. 4.2 A the lines interpolating the experimental data points of relative residual enzyme activity at 60°C show the fit of 1.75^{th} order kinetics. In Fig. 4.2 B the inactivation kinetics of α-amylase in the presence of Ca^{2+} ions were fitted by using a reaction order of 2.1 which gave the smallest sum of standard error in the regression analysis of the experimental data (see inset Fig. 4.2 B). Hence, this order was used

to calculate the inactivation rate constants k_{inact} for α-amylase in the presence of 3.6 mM calcium chloride.

Fig. 4.3 A is a logarithmic plot of the estimated inactivation rate constants $k1_{inact}$ for α-amylase in the absence of Ca^{2+} ions versus pressure and temperature. It is not surprising that higher temperatures and pressures accelerate the inactivation of the enzyme which, consequently, is resulting in higher rate constants. On the other hand between 20 and 70°C $k1_{inact}$ undergoes a minimum at approximately 200 MPa indicating that the enzyme is markedly stabilized at this pressure. Also the inactivation rate constants $k2_{inact}$ of α-amylase in the presence of Ca^{2+} ions (Fig. 4.3 B) clearly showed a minimum at approximately 200 MPa and an increase by temperature. However, compared to Fig. 4.3 A (α-amylase in the absence of Ca^{2+} ions) the $k2_{inact}$ values for a certain pressure temperature combination are generally reduced indicating higher pressure/temperature stability of the enzyme in the presence of Ca^{2+} ions.

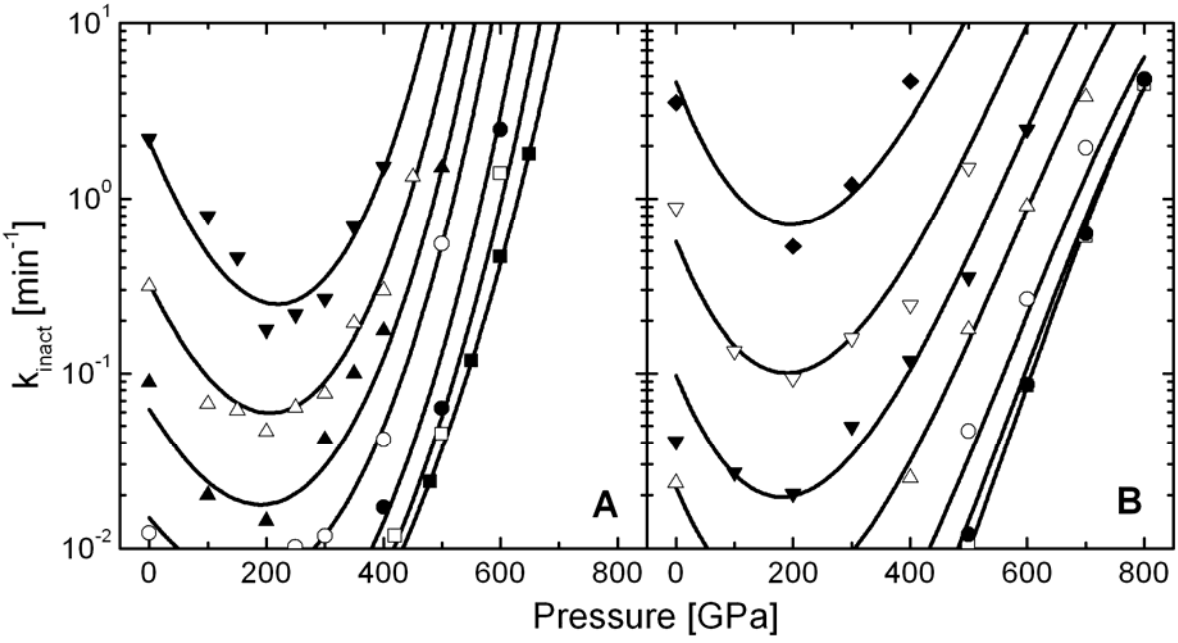

Fig. 4.3: Modelled pressure dependence of the inactivation rate constant k_{inact} of α-amylase in ACES buffer (pH 5.6; 0.1 M) (A) and in ACES buffer containing 90 mM NaCl and 3.8 mM $CaCl_2$ at 20°C (■), 30°C (□), 40°C (●), 50°C (○), 60°C (▲), 65°C (△), 70°C (◆) and 75°C (◇). The rate constants were derived from Eqn. 3.3 and fitted to Eqn. 3.5.

For designing or optimizing a high pressure process it is useful to create a mathematical model describing the pressure-temperature dependence of k_{inact}. Based on the estimated k_{inact} values shown in Fig. 4.3, the change of the inactivation rate constant k_{inact} in response to pressure and temperature was mathematically described by a third order polynomial equation (Eqn. 3.5). All variables in Eqn. 3.5 significantly contributed to the model, except of variable A_8

which contributed less than 1% to the total fit standard error for the data set of α-amylase in the presence of 3.8 mM $CaCl_2$ and hence, the full term (A_8*p^2T) was removed. The model parameters in Tab. 4.1 were estimated by linear regression fitting of Eqn. 3.5 to the inactivation rate constants k_{inact} found in the p-T domains investigated. In both models the correlation coefficient r^2 was > 0.95. Graphically, this fit is shown in Fig. 4.3. The lines are interpolating the results for the change of the rate constant k_{inact} with pressure at constant temperatures.

Tab. 4.1: Estimated model parameters for inactivation of α-amlyase from barley malt based on Eqn. 3.5

Parameter	Estimated parameter values for α-amlyase in the absence of Ca^{2+}ions	Estimated parameter value for α-amlyase in the presence of Ca^{2+} ions
$A_{0:}$	-11.594 ± 3.472	-12.256 ± 2.786
A_1	0.021 ± 0.011	$-9.903*10^{-3} \pm 4.467*10^{-3}$
A_2	0.105 ± 0.199	0.186 ± 0.114
A_3	$-2.212*10^{-5} \pm 3.075*10^{-5}$	$6.240*10^{-5} \pm 0.730*10^{-5}$
A_4	$-6.365*10^{-4} \pm 4.656*10^{-4}$	$-3.637*10^{-3} \pm 2.506*10^{-3}$
A_5	$-6.157*10^{-4} \pm 1.816*10^{-4}$	$-1.397*10^{-4} \pm 0.620*10^{-4}$
A_6	$2.229*10^{-8} \pm 2.183*10^{-8}$	$-3.617*10^{-8} \pm 0.655*10^{-8}$
A_7	$3.000*10^{-5} \pm 3.478*10^{-5}$	$4.819*10^{-5} \pm 1.782*10^{-5}$
A_8	$8.831*10^{-7} \pm 3.139*10^{-7}$	-
	r^2 = 0.959	**r^2 = 0.973**

The functional associations of pressure, temperature and inactivation rate constant k_{inact} are best presented by means of pressure-temperature diagrams, which show those pressure-temperature combinations that will lead to a desired reaction rate constant. For a better comparison of the two models it is useful to replace the inactivation rate constants the n^{th} order reaction (Eqn. 3.3) by the particular model for the pressure-temperature dependence of k_{inact} (Eqn. 3.5). Upon rearrangement the p-T combinations corresponding to a specified reduction of enzyme activity within explicit exposure times can be calculated. The p-T diagram in Fig. 4.4 shows the isorate lines for one log reduction of α-amylase in the absence and in the presence of Ca^{2+} ions occurring after 10, and 30 min treatment time. It is evident from these isolines that calcium increases the temperature and pressure stability of α-amylase from barley by approximately 10°C and/or 120 MPa. Furthermore, it is evident from Fig. 4.4 that in the low pressure region, pressure and temperature act antagonistically on the inactivation rate of the

enzyme, e.g. the thermo stability of the amylase is slightly increased by pressures up to 200 MPa.

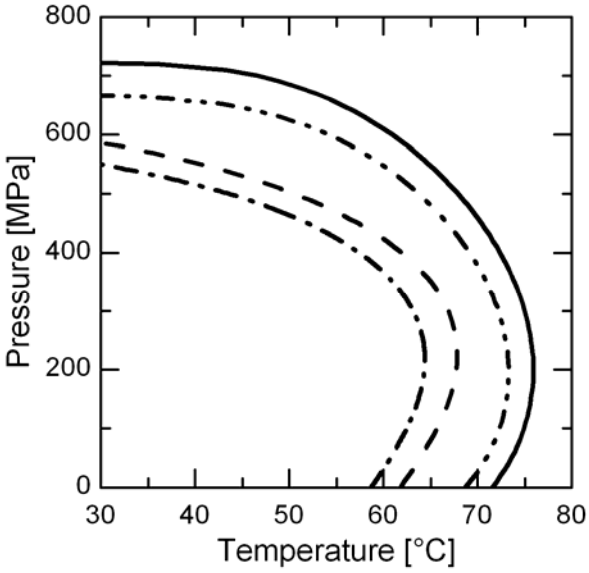

Fig. 4.4: Pressure-temperature isorate diagram for 1 log inactivation of α-amylase in ACES buffer (pH 5.6; 0.1 M) after 10 (**┅**) and 30 (**╍**) minutes and 1 log inactivation of α-amylase after 10 (**┅**) and 30 (—) minutes in ACES buffer (pH 5.6; 0.1 M) containing 90 mM NaCl and 3.8 mM $CaCl_2$.

4.1.3 Catalytic activity of α-amylase at different high pressure-temperature combinations

In-situ experiments of enzymatic substrate conversions were determined under isothermal/isobaric conditions. Fig. 4.5 shows the change of absorbance at 400 nm due to the cleavage BPNPG7 by barley α-amylase in ACES buffer containing 90 mM NaCl and 3.8 mM $CaCl_2$ at different pressures (0.1-400 MPa) and at 65°C. Obviously, at this temperature the substrate conversion is significantly higher at 100 and 200 MPa than at ambient pressure. However, the amount of hydrolyzed substrate after 35 minutes was smaller at 400 MPa than at lower pressures. To understand the effect of pressure and temperature on the catalytic activity of α-amylase, the substrate conversion and the simultaneously occurring enzyme inactivation has to be taken into account. Methodologically, this has been done by correcting the apparent rate of *in-situ* BPNPG7 cleavage with the previously described model of enzyme inactivation. Assuming no effect of the substrate on enzyme stability, the kinetics of product P formation can be formulated as follows:

$$\frac{d[P]}{dt} = k_{conv} \cdot [E]$$
$$\frac{d[E]}{dt} = -k_{inact} \cdot [E]^{2.1} \qquad \textbf{(4.1)}$$

Since an excess of substrate was used in all experiments the conversion reaction is of order 1.0. The reaction of enzyme inactivation is of order 2.1. These equations have been solved numerically for the conversion rate constant k_{conv} and fitted to the kinetics of BPNPG7 cleavage (Fig. 4.5). The inactivation rate constant k_{inact} (for α-amylase in the presence of Ca^{2+} ions) has to be specified for the particular p-T condition. The enzyme concentration [E] is introduced relative to the initial concentration and has randomly been set to 1. Therefore, the inactivation rate constant $k2_{inact}$ derived from Eqn. 3.5 has to be divided by the initial enzyme concentration (20 mg/mL) used in *in-situ* experiments of substrate conversion.

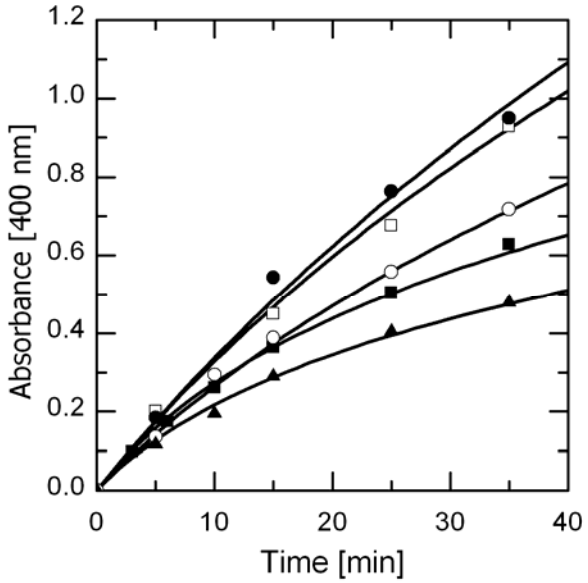

Fig. 4.5: Change of the absorbance at 400 nm due to the hydrolysis of blocked p-nitrophenyl maltoheptaoside (BPNPG7) by barley α-amylase in ACES buffer (pH 5.6; 0.1 M, containing 5.45 mg/mL BPNPG7, 90 mM NaCl and 3.8 mM $CaCl_2$) at 65°C and 0.1 (■), 100 (□), 200 (●), 300 (○) and 400 (▲) MPa.

A logarithmic plot of the corrected rate constant of conversion k_{conv} versus pressure is shown for different temperatures in Fig. 4.6. Evidently, increasing pressure caused a sight deceleration of k_{conv} whereas higher temperatures strongly accelerated the catalytic activity of α-amylase. However, in the pressure range of 0.1-200 MPa only minor reductions of the conversion rate k_{conv} were observed. No evidence was found for an increase of k_{conv} under pressures up to 400 MPa. A reversible reduction of enzymatic reaction rates by pressure has been reported previously by other authors (Buckow et al. 2005b; Colloc'h et al. 2006; Dallet and Legoy 1996)

and were related to changes of the substrate specificity or by alterations of rate limiting molecular structures (Gekko 2002). Pressure might also affect the specificity of enzymatic action (Makimoto and Taniguchi 1988) or even induce changes in the composition of products (Matsumoto et al. 1997). These phenomena may explain why pressure dependencies of the rate of enzyme reactions sometimes show concave curves (Masson and Balny 2005; Mozhaev et al. 1996b), maxima (Kunugi et al. 1997; Masson et al. 2004) or even a break (Dallet and Legoy 1996) when plotting $\ln(k_{conv})$ versus pressure.

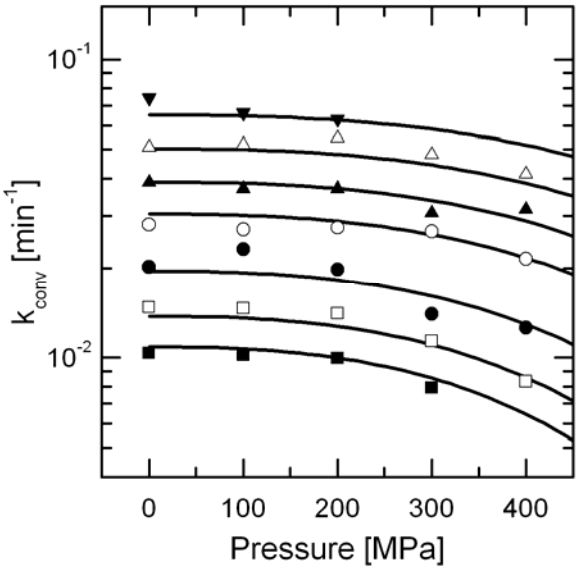

Fig. 4.6: Pressure dependence of the conversion rate constant (k_{conv}) of α-amylase in ACES buffer (pH 5.6; 0.1 M, containing 5.45 mg/mL BPNPG7, 90 mM NaCl and 3.8 mM $CaCl_2$) at 30°C (■), 40°C (□), 50°C (●), 60°C (○), 65°C (▲), 70°C (△) and 75°C (▼). The rate constants were derived from Eqn. 4.1 and fitted to Eqn.4.2.

Empirically, the effect of pressure and temperature on the cleavage of BPNPG7 by α-amylase was derived by fitting a number of simple equations to the data set with a statistical program (Table Curve 3D v3 Statistical Package, Systat Software Inc., Richmond, CA, USA). k_{conv} of α-amylase in responds to pressure and temperature was described by Eqn. 4.2 which sufficiently fitted the data.

$$\ln(k_{conv}) = (A_0 + A_1 \cdot p^{2.5} + A_2 \cdot T^3)^{-1} \qquad \textbf{(4.2)}$$

The regression analysis of the conversion rates of all p-T combination tested gave the best fit ($r^2 = 0.974$) for the following parameter values: $A_0 = -0.173 \pm 0.001$; $A_1 = 4.770*10^{-9} \pm 0.599*10^{-9}$; $A_2 = -2.148*10^{-7} \pm 0.071*10^{-7}$.

Reintegrating the two models for enzyme inactivation and substrate conversion the over-all reaction for BPNPG7 cleavage in response to different p-T combinations can be calculated for a

fixed treatment time. The isolines in Fig. 4.7 denote the percentage of cleaved BPNPG7 by α-amylase relative to the maximum found in the vicinity of 152 MPa and 64°C after 30 min exposure time. At ambient pressure, highest BPNPG7 degradation was found at approximately 59°C. This optimal temperature is slightly lower than proposed by other authors (Bertroft et al. 1984; MacGregor et al. 1999) for α-amylase in starch slurries but might be explained by the use of different buffers and/or stabilizing effects of starch or fibre. At higher temperatures BPNPG7 degradation was smaller which can be related to the promotion of enzyme inactivation. However, an increase in pressure is shifting the optimum of substrate conversion to higher temperatures. Keeping in mind that pressure positively affects the thermo-stability but also impairs the catalytic activity of the α-amylase it is not surprising that at a specific p-T combination a maximum of substrate conversion is produced. After 30 min p-T treatment time cleavage of BPNPG7 could be increased by approximately 25% at optimal pT conditions (152 MPa and 64°C) compared to the local maximum at ambient pressure (59°C).

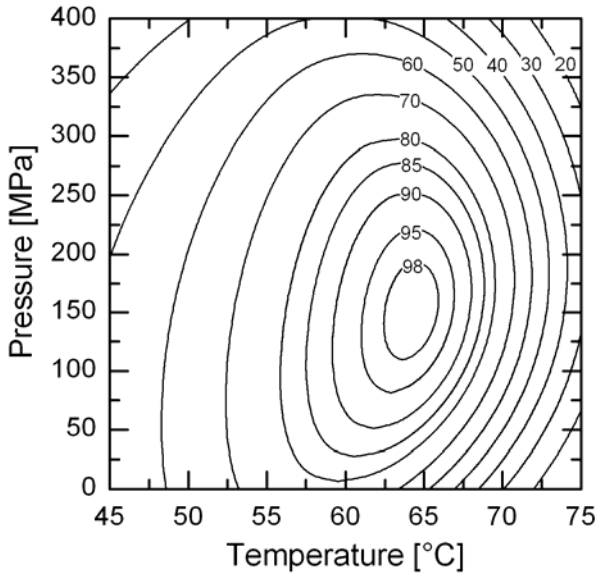

Fig. 4.7: Cleavage of blocked p-nitrophenyl maltoheptaoside (BPNPG7) by α-amylase in ACES buffer (pH 5.6; 0.1 M, containing 5.45 mg/mL BPNPG7, 90 mM NaCl and 3.8 mM $CaCl_2$) at different pressure-temperature combinations after 30 minutes exposure time. Isolines indicate the percentage relative to the maximal break-down of BPNPG7 observed at 152 MPa and 64°C.

In Fig. 4.8 the isorate lines for 35%, 70% and 95% inactivation of α-amylase in the presence of 3.8 mM Ca^{2+} occurring after 30 min treatment time is overlaid by the region of maximal substrate conversion. This region of high BPNPG7 degradation is characterized by an enzyme inactivation of approximately 35% compared to the initial activity which is due to the antagonistic effect of temperature on enzyme stability and catalytic activity. However, exposure to the same temperature at ambient pressure would result in a loss of α-amylase activity of approximately

70%. Although pressure reduces the rate of amylolytic BPNPG7 cleavage, the optimum of the over-all reaction of enzyme inactivation and accelerated enzyme catalysis is evidently shifted towards higher temperatures and pressures.

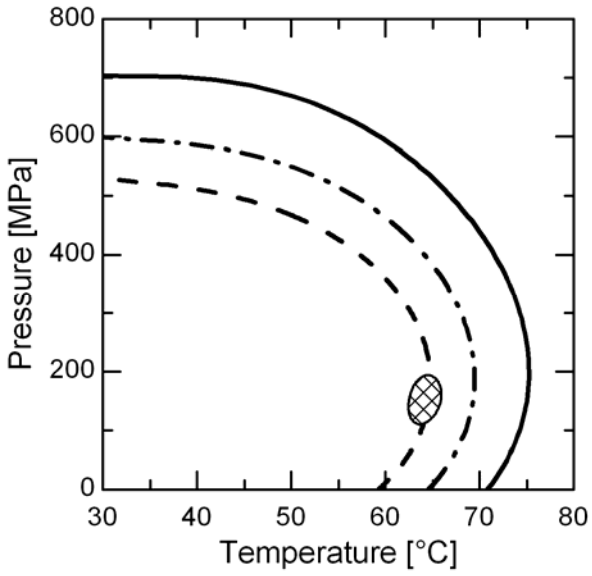

Fig. 4.8: Pressure-temperature isorate diagram of 35% (**--**) 70 % (**·--**) and 95 % (**—**) inactivation of α-amylase (in the presents of 3.8 mM $CaCl_2$) and the region of maximal BPNPG7 cleavage (▩) after 30 minutes exposure time.

4.2 Stability and catalytic activity of β-amylase

4.2.1 Effect of ions and pH on β-amylase stability

Fig. 4.9 presents the contour plot of the thermo-stability of β-amylase from barley malt in responds to different pH and sodium chloride concentration after 5 min heating at 55°C. The iso-inactivation lines indicate the percentage relative to the maximum of the residual enzyme activity observed at pH 6.0 in the absence of NaCl. The stability β-amylase at 60°C was not significantly decreased by adding sodium chloride up to 160 mM but showed high dependence to pH. Proteins are usually known to be sensitive to high ionic strengths due to their effect on the charge of the protein molecule and the distribution of charge on their exterior surfaces. The ionic strength of the solution is also an important parameter affecting enzyme catalytic activity due to the dependence of catalytic reactions on the movement of charged molecules. However, some enzymes, such as pectin methylesterases, are known to show higher stability at increased level of ions present (Guiavarc'h et al. 2005).

Highest thermal stability of β-amylase was found at pH 6.0 which is in agreement with results published by other authors (Hon and Reilly 1979) who found optimal stability of β-amylase in the range of pH 5.0-6.0. The slightly higher thermal maximum stability might be explained by the use of different buffers showing different temperature dependencies of their equilibrium constants.

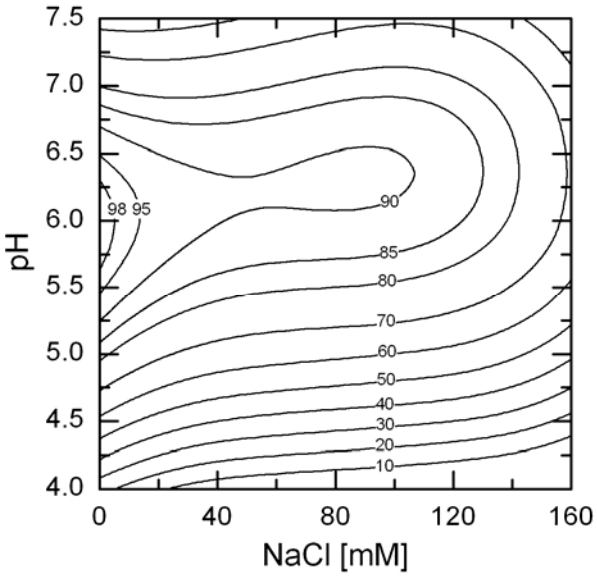

Fig. 4.9: Thermal stability of barley malt β-amylase in dependence of pH and the concentration of sodium chloride. Assay conditions: 0.1 M ACES buffer at various pH (4.0-7.5) containing 0-160 mM NaCl, treated for 10 min at 60°C and 0.1 MPa. Iso-inactivation lines indicate the percentage relative to the maximum of residual enzyme activity found at pH 6.0 and 0 mM NaCl.

4.2.2 Effect of high pressure-temperature combinations on β-amylase stability

Within the p-T domain investigated the inactivation of β-amylase at constant temperature and pressure typically showed deviations from simple first-order kinetics. In Fig. 4.10 A the reduction in enzyme activity measured after the p-T treatment is shown at 65°C for 6 different pressure levels from 0.1 to 500 MPa. The typical compression period with an approximate duration of 30 s followed by an immediate rapid decompression already produced reductions in activity (data not shown). In Fig. 4.10 A this has been taken into account for the calculation of relative enzyme activities. In this representation the inactivation curves showed that at 65°C the reduction is not accelerated by increasing the treatment pressure. Whereas the highest (500 MPa) and the lowest (0.1 MPa) pressure produced a residual activity of less than 20% within 3 min, 200 or 300 MPa stabilized more than 50 % activity even after 20 min, which apparently is in contradiction to Eqn. 2.70. Although the determination of the activity has been carried out after pressure release, the *in-situ* degradation of starch showed a quite similar behaviour. In Fig. 4.10 B the concentration of reducing sugars after 30 min high pressure treatment of enzyme in the

presence of substrate, given as units maltose, is significantly higher at 100, 200 and 300 MPa compared to ambient pressure. For a better understanding of those observations it has to be discriminated between the impact of high pressure and temperature on irreversible protein denaturation and reversible alterations of substrate conversion, respectively. Methodologically, the apparent rate of *in-situ* starch degradation by β-amylase activity has to be corrected by the simultaneously occurring enzyme inactivation. Within a temperature range from 20 to 70°C and up to a maximum treatment pressure of 700 MPa, separate kinetic analyses of enzyme inactivation as well as substrate conversion have been performed. The reaction order n of the enzyme inactivation has been determined by minimizing the cumulative standard error of the fit of Eqn. 3.3 to the complete experimental kinetic data set.

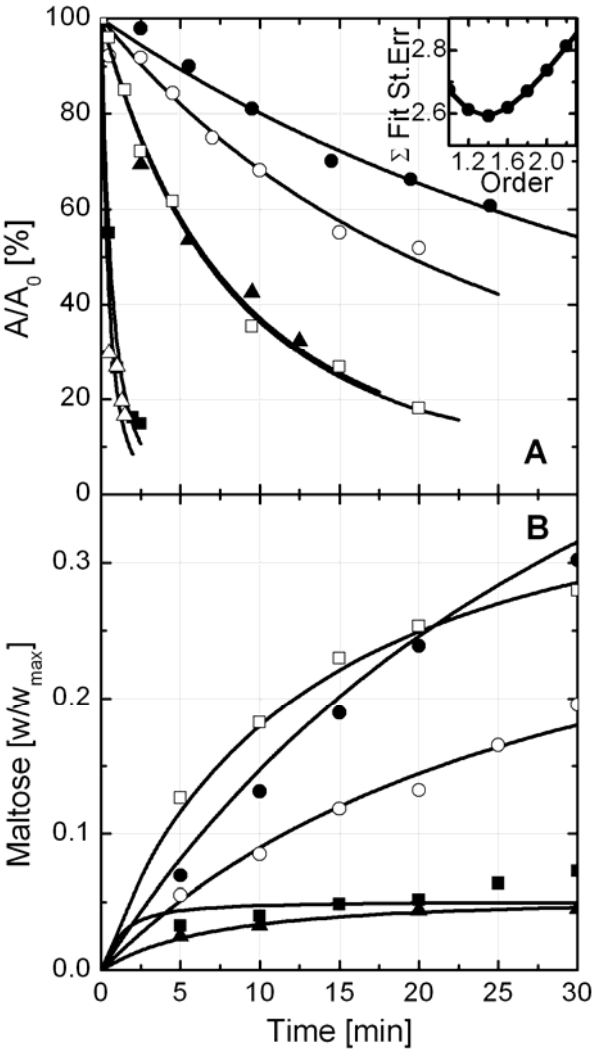

Fig. 4.10: A: 1.4th order pressure inactivation of β-amylase in ACES buffer (pH 5.6; 0.1 M) at 65°C. B: Liberation of maltose monohydrate during the exposure of starch solubilized in water (3.33 mg starch/mL ACES buffer (0.1M, pH 5.6)) to high pressure. The symbols denote the applied pressures as follows: 0.1 (■); 100 (□); 200 (●); 300 (○); 400 (▲) and 500 (△) MPa.

The minimum of the error function derived from regression analysis was found for a reaction order of 1.4 (see inset of Fig. 4.10 A). This reaction order was used for the determination of the rate constants k. The lines interpolating the experimental results of relative enzyme inactivation show the fit of 1.4th order kinetics. The experimental results of all p-T conditions tested are shown in Fig. 4.11. The inactivation rate constants k_{inact} are plotted versus pressure. It is readily seen that between 20 and 70°C k_{inact} is minimized at about 200 MPa.

The experimental results of all p-T conditions tested are shown in Fig. 4.11. The inactivation rate constants k_{inact} are plotted versus pressure. It is readily seen that between 20 and 70°C k_{inact} is minimized at about 200 MPa. This behaviour is not in accordance with Eqn. 2.70 predicting continuity in d(lnk)/dp. Evidently the enzyme

is stabilized against thermal inactivation within a particular pressure range.

A better mathematical modelling was obtained by applying the concept of two-state transition (native – inactivated) based on the ΔG (Eqn.4.3). Adapted to the kinetics of enzyme inactivation the experimental data of ln(k) has regressively been fitted to Eqn. 3.5 eliminating those terms which contributed less than 1% to the total fit standard error. Regression analysis of the inactivation data within the p-T domain investigated yielded the following results shown in Tab. 4.2.

Tab. 4.2: Estimated model parameters for inactivation of β-amlyase based on Eqn. 3.5.

Parameter	Estimated parameter values
$A_{0:}$	-7.73 ± 1.409
A_1	0.00399 ± 0.009
A_2	-0.141 ± 0.057
A_3	$4.398*10^{-5} \pm 2.625*10^{-5}$
A_4	$4.0866*10^{-3} \pm 5.313*10^{-4}$
A_5	$-4.278*10^{-4} \pm 1.16774*10^{-4}$
A_6	$-2.610*10^{-8} \pm 1.763*10^{-8}$
A_7	-
A_8	$5.328*10^{-7} \pm 2.268*10^{-7}$
	$r^2 = 0.965$

Graphically, this is shown in Fig. 4.10 A as lines interpolating the results for the change in rate constant with pressure at constant temperatures.

After replacing k_{inact} by Eqn. 3.5 in the basic equation for the 1.4^{th} order kinetics (Eqn. 3.3) and upon rearrangement, all p-T conditions which produce a specified reduction in enzyme activity within explicit exposure times can be calculated. In Fig. 4.12 this is illustrated for a 95% inactivation occurring after 10, 20, or 30 min high pressure treatment time. In this projection the minimum of the rate constant k_{inact} when plotted versus pressure converts to elliptical shaped curves in the p-T plane, indicating a better stabilization against heat attack at about 220 MPa rather than at ambient pressure.

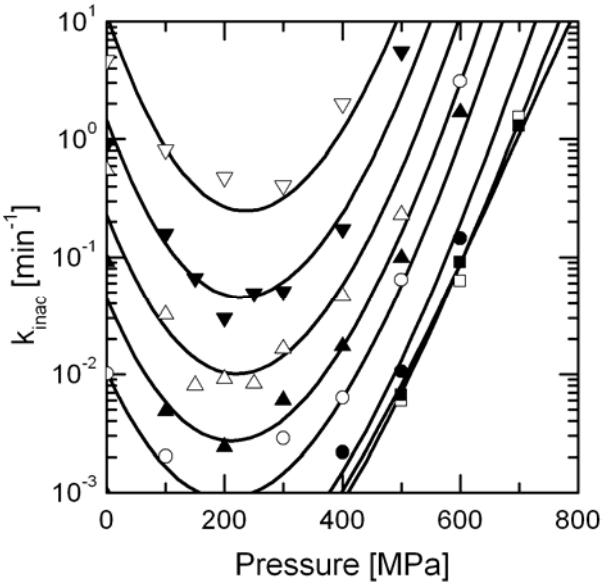

Fig. 4.11: Modelled pressure dependence of the inactivation rate constant (k_{inact}) of β-amylase in ACES buffer (pH 5.6; 0.1 M) at 20°C (■); 30°C (□); 40°C (●); 50°C (○); 55°C (▲); 60°C (△); 65°C (▼) and 70°C (▽).

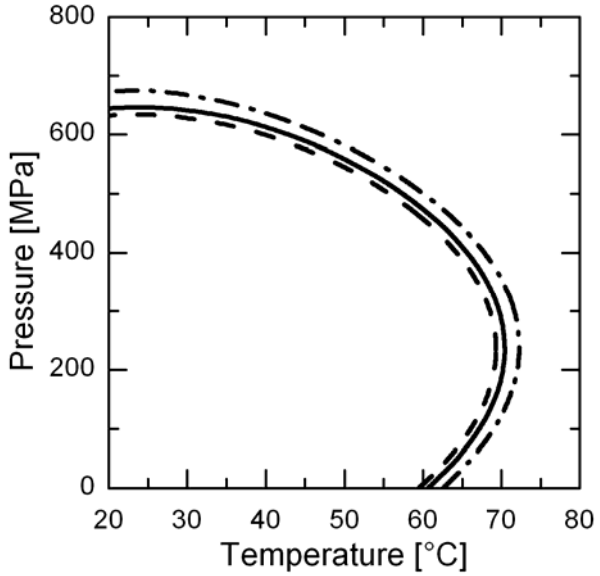

Fig. 4.12: Pressure-temperature isorate diagram for 95 % inactivation of β-amylase after 10 (**-··-**), 20 (**—**) and 30 (**--**) minutes.

4.2.3 Catalytic activity of β-amylase at different high pressure-temperature combinations

The combination of Eqn. 3.3 and Eqn. 3.5 represents a condensed description of the p-T effect on the irreversible inactivation of β-amylase and can serve as a mathematical tool for the

correction of the starch degradation kinetics. Without correction, the pattern of maltose monohydrate release in response to combined p-T treatment is presented in Fig. 4.14 for a 30 min exposure time. The landscape plot has been obtained upon regression analysis of the experimental degradation kinetics of 1% soluble starch dissolved in ACES buffer in the presence of 0.03125 mg/ml β-amylase (like the example in Fig. 4.10 B). Isorates denote the release of reducing sugar units relative to the maximum located at 105 MPa and 60.5°C. At ambient pressure, the conversion rate increases up to 55°C which is in good agreement with results published elsewhere (Yoshigi et al. 1995). At higher temperatures the degradation reaction is impaired as a result of the prevailing effect of enzyme inactivation. With increasing pressure, the temperature relative optimum is shifted to higher temperatures and an absolute maximum of the starch degradation is reached at 60.5°C at a pressure of 105 MPa after 30 minutes.

In order to conclude on the p-T effect on the enzymatic conversion, i.e. on the enzyme-substrate interaction, the starch degradation has to be superimposed by the simultaneously occurring irreversible denaturation of the enzyme. Since an excess substrate concentration was used in all experiments the reaction scheme of Fig. 2.23 simplifies to:

$$E_{INACT} \xleftarrow{k_{inacr}} Starch + E \xrightarrow{k_{conv}} Maltose + E$$

The inactivation and the conversion reaction is of order 1.4 and 1.0, respectively. Hence, the kinetics of the reaction can be formulated similar to Eqn. 4.1:

$$\frac{d[Maltose]}{dt} = k_{conv} \cdot [E]$$
$$\frac{d[E]}{dt} = -k'_{inact} \cdot [E]^{1.4} \qquad \textbf{(4.3)}$$

These equations have been solved numerically for the conversion rate constant k_{konv} and fitted to the kinetics of maltose release in relative units (see Fig. 4.10 B). k'_{inact} denotes the inactivation rate constant which has to be specified for particular p-T conditions. The enzyme concentration [E] is introduced relative to the initial concentration and has arbitrarily been set to 1. Therefore, k_{inact} derived from Eqn. 3.5 has to be divided by the initial enzyme concentration used for the starch degradation experiments:

$$k'_{inact} = k_{inact}(p,T) \frac{1}{0.0625\ mg/mL} \qquad \textbf{(4.4)}$$

This procedure allows the isolation of the p-T effect on the enzyme-substrate interaction from the overall reaction kinetics of the maltose release. In Fig. 4.13 k_{conv} is plotted logarithmically versus pressure. In this representation a linear decrease of the rate constant with increasing pressure is observed throughout the temperature range investigated (20-65°C). Apparently, the conversion reaction is accelerated at higher temperatures. In contrast, high pressure even at

levels below 100 MPa has a retarding effect on the enzymatic hydrolysis of the macromolecule, indicating that steric hindrance of the access to the active centre is increased by pressure treatment. There is no evidence for an activation of the enzyme by pressure. The response of the conversion rate of β-amylase can be described empirically by Eqn.4.5:

$$\ln(k_{conv}) = B_0 + B_1 \cdot p + B_2 \cdot T^2 \qquad \textbf{(4.5)}$$

Regression analysis of the conversion rates yielded the following parameters: B_0 = -6.349 ± 0.105; B_1 = $-4.4*10^{-3}$ ± $3.504*10^{-4}$; B_2 = $7.638*10^{-4}$ ± $0.056*10^{-4}$. In this model the correlation coefficient r^2 was > 0.961.

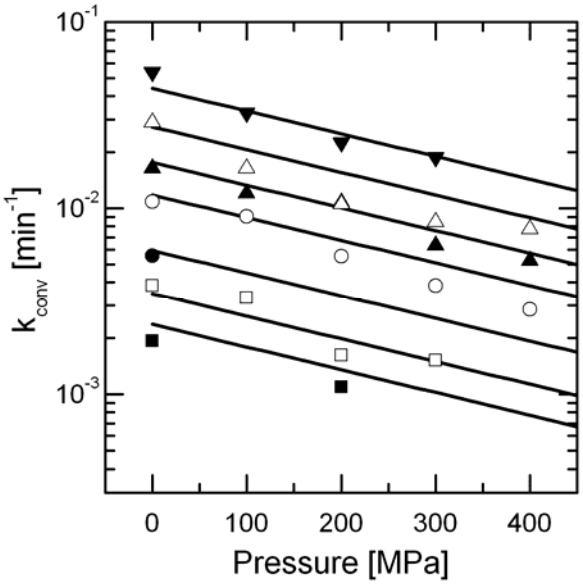

Fig. 4.13: Pressure dependence of the conversion rate constant (k_{conv}) of β-amylase in ACES buffer (pH 5.6; 0.1 M containing 1% soluble starch) at 20°C (■); 30°C (□); 40°C (●); 50°C (○); 55°C (▲); 60°C (△) and 65°C (▼). The rate constants were derived from Eqn.4.3.

In Fig. 4.15 the region of maximum starch degradation is overlaid by the enzyme stability curves for a 30 min exposure to the p-T treatment. Considering the previous finding that the isolated enzymatic conversion is delayed at elevated pressure, it is not surprising that the maximum of the overall reaction of starch degradation does not coincide with the zone where the enzyme stability is highest (right pole of the elliptical lines in Fig. 4.15). Its location after 30 min p-T treatment time is characterized by an already reduced enzyme activity of 50% compared to the initial activity. Exposure to the same temperature at ambient pressure caused a reduction of more than 90%. This observation is in agreement with other reports in literature (Yoshigi et al. 1995). In spite of the retarding effect, high pressure is shifting the balance between heat inactivation and thermal reaction enhancement towards higher temperatures.

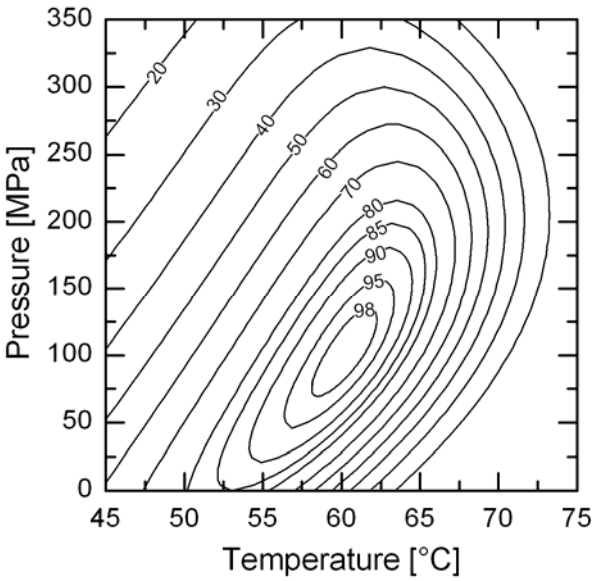

Fig. 4.14: Liberated maltose monohydrate by β-amylase from barley malt versus temperature and pressure after 30 minutes. Isolines denote the percentage relative to the maximum release observed at 105 MPa and 60.5°C.

All experiments on substrate conversion kinetics have been carried out using soluble starch. In real situations this might not always be the case and gelatinization of the starch is needed as a prerequisite of enzyme substrate interaction. Since gelatinization happens at elevated temperatures, it is interesting to investigate the effect of pressure on this reaction.

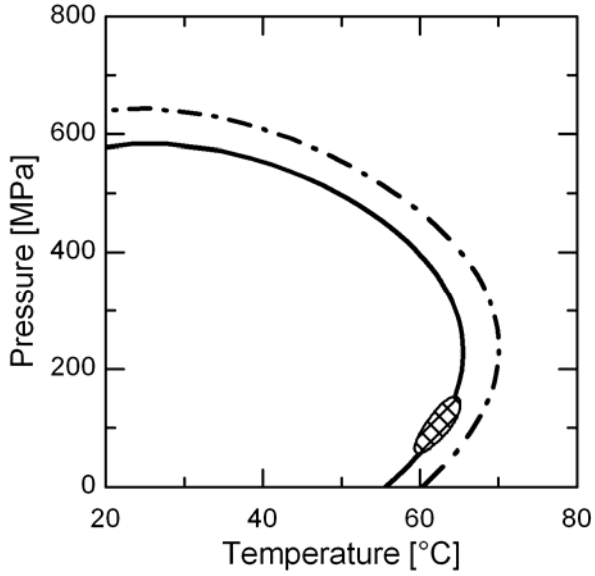

Fig. 4.15: Pressure-temperature isorate diagram of 50 % (**—**) and 90 % (**-··-**) inactivation of β-amylase and the area of high conversion rate (※) after 30 minutes exposure time.

4.3 Stability and catalytic activity of β-glucanases

4.3.1 Effect of high pressure-temperature combinations on the stability of β-glucanase from barley malt

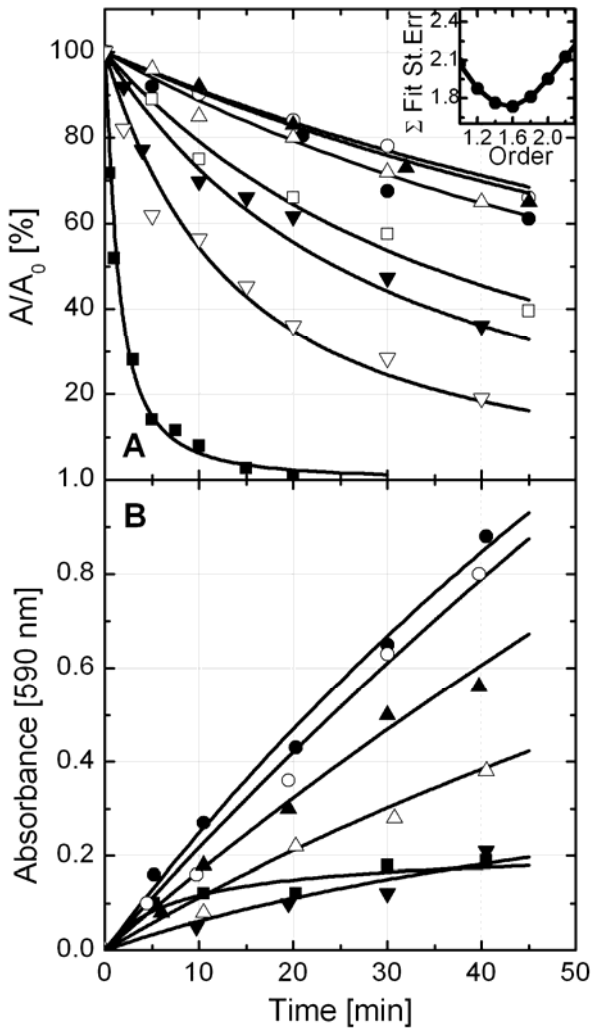

Fig. 4.16: A: 1.6th order pressure inactivation of β-glucanase (barley) in ACES buffer (pH 5.6; 0.1 M) at 55°C. Reaction order was derived from the minimum of the cumulative standard error of the fit of Eqn. 3.3 (see inset in A) B: Time dependent change of absorbance at 590 nm due to the hydrolysis of azo-barley glucan by β-glucanase solubilized in ACES buffer (0.1M, pH 5.6 containing 0.5% Azo-barley glucan). The symbols in both graphs denote the applied pressures as follows: 0.1 (■), 100 (□), 200 (●), 300 (○), 400 (▲), 500 (△), 600 (▼) and 700 (▽) MPa.

Combined pressure and temperature treatments of extracted β-glucanase from barley malt (in 0.1 M ACES buffer, pH 5.6) were conducted in the range between 30-75°C and 0.1-900 MPa. As expected the isobaric/isothermal kinetics of β-glucanase indicated a deviation from simple first-order kinetics in the p-T domain investigated. In Fig. 4.16 A an example for the course of the enzyme inactivation at 55°C and 0.1-700 MPa is presented. It is evident from the kinetics at 55°C (Fig. 4.16 A) that an increase of pressure does not necessarily produce a more rapid inactivation of the enzyme. Whereas at ambient pressure β-glucanase is completely inactivated within 30 min (which is in agreement with other reports (Home et al. 1993; Narziss 1993; Yamashita et al. 1985)), pressures up to 700 MPa resulted in an attenuated loss in enzyme activity. Highest stability of β-glucanase at 55°C was found at 300-400 MPa preserving approximately 65% of initial β-glucanase activity after 45 min.

This antagonistic effect of pressure is often encountered in pressure assisted enzyme inactivation (Hernandez and Cano 1998; Ludikhuyze et al. 2002; Ly-Nguyen et al. 2003) and is possibly explained by the strengthening of interactions and the tendency to hydrate the protein molecules.

A similar behavior was found for the enzymatic conversion of barley β-glucan during *in-situ* experiments in the range of 30-65°C and 0.1-600 MPa. In Fig. 4.16 B, the change of absorbance at 590 nm due to the depolymerization of Azo-barley β-glucan in the presence of β-glucanase (in 0.1 M ACES buffer, pH 5.6; containing 0.5% Azo-barley glucan) at 55°C is shown for 6 different pressure levels from 0.1-600 MPa. At 55°C the hydrolyzation of β-glucan is poor at ambient pressure and at 600 MPa whereas applied pressures between 200-400 MPa resulted in significantly higher degrees of depolymerized β-glucan within 40 minutes.

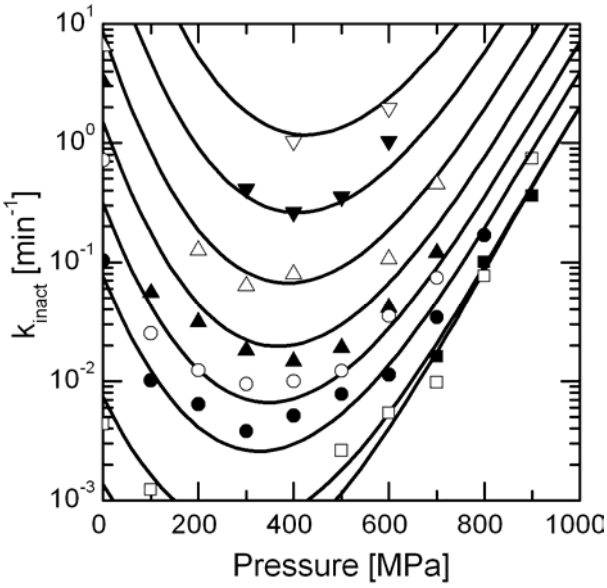

Fig. 4.17: Pressure dependence of the inactivation rate constant (k_{inact}) of β-glucanase (barley) in ACES buffer (pH 5.6; 0.1 M) at 30°C (■), 40°C (□), 50°C (●), 55°C (○), 60°C (▲), 65°C (△), 70°C (▼) and 75°C (▽).

Hence, to assess on the impact of pressure and temperature on the catalytic activity of β-glucanase, enzyme inactivation and substrate conversion have been considered separately.

The reaction order n of the enzyme inactivation has been determined by minimizing the cumulative standard error of the fit of Eqn. 3.3 to the complete experimental kinetic data set.

A reaction order of 1.6 was found to be the minimum of the error function derived from regression analysis (see inset of Fig. 4.16 A). This reaction order was used for the determination of the rate constants k_{inact} for all p-T conditions tested. In Fig. 4.16 A the lines interpolating the experimental results of relative enzyme inactivation at 55°C show the fit of 1.6^{th} order kinetics.
Fig. 4.17 presents the inactivation rate constants k_{inact} plotted against pressure. A minimum of the inactivation rate constants k_{inact} in the tested temperature range was found at 300-400 MPa indicating that β-glucanase inactivation is highly attenuated at this pressure. A further increase of pressure accelerated the enzyme inactivation and hence, increased k_{inact}. This antagonistic

behavior of the inactivation rate constant k_{inact} is not in accordance with the combined Arrhenius and Eyring model (Eqn.2.48), since here the activation volume $\Delta V^{\#}$ as the characteristic parameter for the pressure dependence is obviously affected by pressure itself. Eqn. 3.5 gave a satisfying fit to the data set a of β-glucanase from barley malt using the model parameters in Tab. 4.3. Graphically, this is shown in Fig. 4.17 as lines interpolating the results for the change in rate constant with pressure at constant temperatures.

Tab. 4.3: Estimated model parameters for inactivation of β-glucanase (barley) based on Eqn. 3.5.

Parameter	Estimated parameter values
$A_{0:}$	-7.785 ± 2.793
A_1	$-5.771 \cdot 10^{-3} \pm 0.947 \cdot 10^{-3}$
A_2	$-5.737 \cdot 10^{-2} \pm 1.065 \cdot 10^{-2}$
A_3	$3.364 \cdot 10^{-5} \pm 1.777 \cdot 10^{-5}$
A_4	$3.234 \cdot 10^{-3} \pm 1.029 \cdot 10^{-3}$
A_5	$-3.327 \cdot 10^{-4} \pm 1.467 \cdot 10^{-4}$
A_6	$-1.556 \cdot 10^{-8} \pm 0.748 \cdot 10^{-8}$
A_7	-
A_8	$1.651 \cdot 10^{-7} \pm 2.030 \cdot 10^{-7}$
	$r^2 = 0.951$

Upon exchange of k_{inact} in the basic equation Eqn. 3.3 by the relations of Eqn. 3.5, the specific reduction of β-glucanase activity can be calculated for any p-T process. Fig. 4.18 shows the isorate lines of β-glucanase for 95% inactivation occurring after 10, 20 and 40 min high pressure treatment time. From these isolines it is apparent that the antagonistic behavior of the rate constant k_{inact} with respect to pressure generates elliptic shaped curves in the p-T diagram, indicating a better thermo stability of the enzyme at approximately 400 MPa. At this pressure level β-glucanase can withstand approximately 15°C higher temperatures than at ambient pressure.

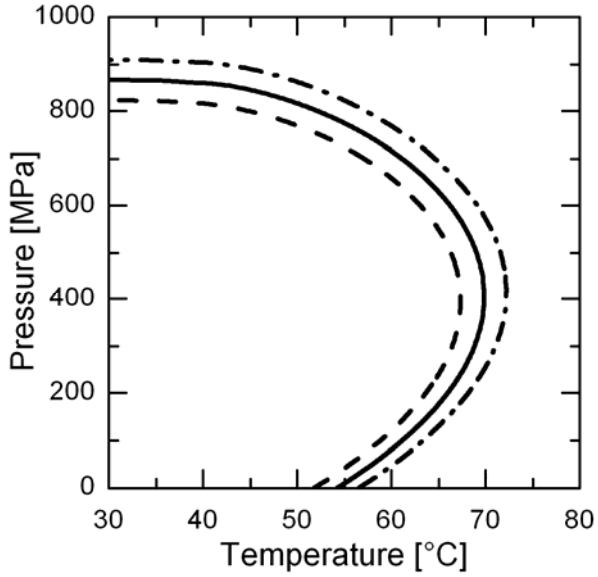

Fig. 4.18: Pressure-temperature isorate diagram for 95 % inactivation of β-glucanase (barley) in ACES buffer (pH 5.6; 0.1 M) after 10 (**┅**), 20 (**—**) and 40 (**╍**) minutes.

4.3.2 Catalytic activity of β-glucanase from barley malt at different high pressure-temperature combinations

The combination of Eqn. 3.3 and Eqn. 3.5 provides a condensed description of the p-T effect on the irreversible inactivation of β-glucanase in ACES buffer (0.1 M, pH 5.6) and was again used to serve as a mathematical tool for the correction of the substrate conversion kinetics.

In order to conclude on the p-T effect on the enzymatic conversion, i.e. on the enzyme-substrate interaction, the substrate conversion found was superimposed by the simultaneously occurring inactivation of the enzyme. An excess of β-glucan was used in all experiments to simplify the mathematic analysis. Assuming no effect of the substrate on enzyme stability, the kinetics of the reaction can be formulated similar to Eqn. 4.1 and Eqn. 4.3 using a reaction order of 1.6 for the enzyme inactivation. The equations have been solved numerically for the conversion rate constant k_{conv} and fitted to the kinetics of β-glucan depolymerization (Fig. 4.16 B). The inactivation rate constant k'_{inact} has to be specified for the particular p-T condition. The enzyme concentration [E] is introduced relative to the initial concentration and has been set to 1. Therefore, the inactivation rate constant k_{inact} derived from Eqn. 3.5 has to be divided by the initial enzyme concentration (1.315 mU/mL) used in *in-situ* experiments of substrate conversion.

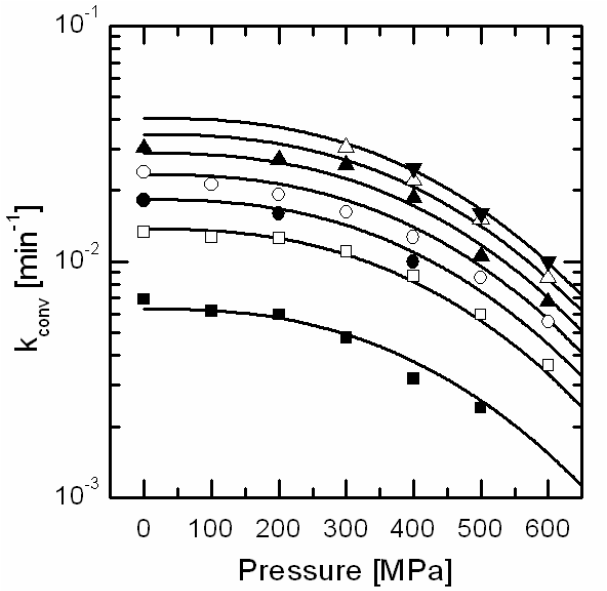

Fig. 4.19: Pressure dependence of the conversion rate constant (k_{conv}) of β-glucanase (barley) in ACES buffer (pH 5.6; 0.1 M containing 0.5% Azo-barley glucan) at 30°C (■), 40°C (□), 45°C (●), 50°C (○), 55°C (▲), 60°C (△) and 65°C (▼). The rate constants were derived from Eqn. 4.6.

In Fig. 4.19 the corrected rate constant of conversion k_{conv} is plotted against pressure in logarithmic scale. Evidently, the conversion reaction is intensely accelerated with higher temperatures. Increasing pressure, on the contrary, implicated a strong deceleration of the catalytic activity of β-glucanase which, with regard to substrate access to the active center of the enzyme, may indicate a detrimental change of the protein structure. However, in the pressure range of 0.1-200 MPa only minor reductions of the conversion rate k_{conv} were observed. No evidence was found that β-glucanase activity is accelerated under high pressure conditions. Empirically, the effect of pressure and temperature on the cleavage of β-glucan by β-glucanase can be described with Eqn. 4.6.

$$\ln(k_{conv}) = (C_0 + C_1 \cdot p^{2.5} + C_2 \cdot T^{-0.5}) \qquad \textbf{(4.6)}$$

Regression analysis of the conversion rates within the p-T domain investigated yielded the following parameters with a r^2 of 0.985: C_0: 0.747 ± 0.140; C_1: $-1.560 \cdot 10^{-7} \pm 0.054 \cdot 10^{-7}$, C_2: -31.831 ± 0.868.

By integration of the two competing reactions (enzyme inactivation and substrate conversion) for a fixed process time, the over-all reaction for β-glucan depolymerization in response to a combined p-T treatment was obtained. In Fig. 4.20 the overall reaction of maltose hydrolysis by glucoamylase in response to combined p-T treatment is presented for a 30 min process. Isolines denote the percentage substrate conversion relative to the maximum which was found in the

vicinity of 217 MPa and 56°C. At ambient pressure, highest degradation of β-glucan was found at approximately 45°C which is in agreement with results published elsewhere(Home et al. 1993; Kettunen et al. 1996; Narziss 1993). At higher temperatures the catalysis is impaired by the dominating effect of enzyme inactivation. With increasing pressure the optimum for the β-glucan degradation is shifting to higher temperatures as a result of the thermo-stabilization of the enzyme. After a 30 min conversion process a maximum is reached in the vicinity of 217 MPa and 56°C providing approximately 65% more degradation of β-glucan compared to the maximum at ambient pressure. Reconsidering the previously found dependency of pressure and temperature on the enzyme inactivation and the catalytic potential of β-glucanase, it is not surprising that at a specific pT combination a maximum of substrate conversion is existent. Its location at an elevated pressure level leads to the conclusion that the positive effect of temperature on the rate of β-glucan conversion is dominating the negative effect caused by the increase of pressure.

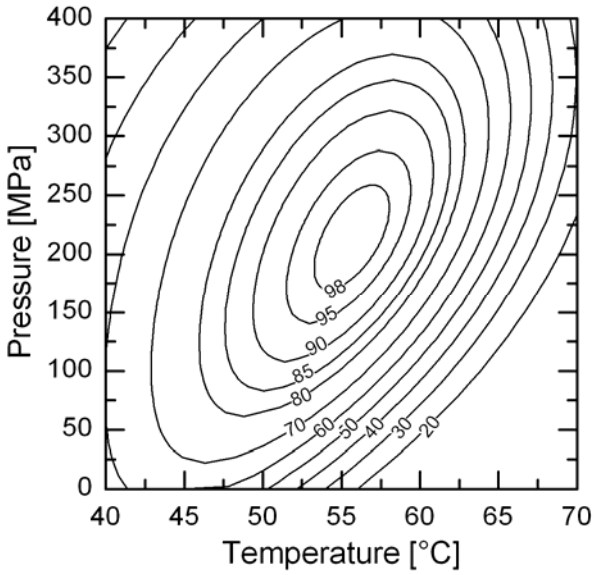

Fig. 4.20: Depolymerised β-glucan by β-glucanase (barley) versus temperature and pressure after 30 minutes. Isolines denote the percentage relative to the maximal degradation observed at 217 MPa and 56°C.

4.3.3 Effect of high pressure-temperature combinations on the stability of β-glucanase from *Bacillus subtilis*

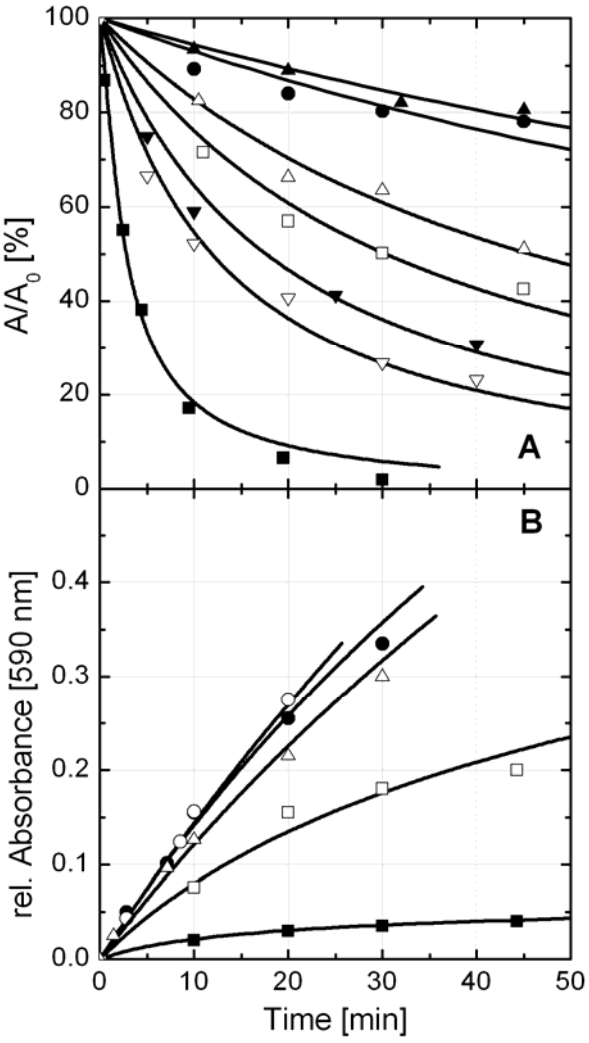

Fig. 4.21: A: 1.8th order pressure inactivation of β-glucanase from *B.subtilis* in ACES buffer (pH 5.6; 0.1 M) at 65°C. B: Time dependent change of relative absorbance at 590 nm due to the hydrolysis of Azo-barley glucan by β-glucanase (*B.subtilis*) solubilized in ACES buffer (0.1M, pH 5.6 containing 0.5% Azo-barley glucan). The symbols in both graphs denote the applied pressures as follows: 0.1 (■), 100 (□), 200 (●), 300 (○), 400 (▲), 500 (△), 600 (▼) and 700 (▽) MPa.

Analog to the investigations of β-glucanase from barley malt, β-glucanase from *B.subtilis* was tested under various pressure-temperature combinations (30-75°C; 0.1-1000 MPa). At isobaric/isothermal conditions the kinetics of this β-glucanase showed strong deviation from simple first-order kinetics as well (Fig. 4.21 A) and therefore, the n^{th} order reaction model (Eqn. 3.3) was used to describe the course of inactivation with time. Exemplarily, Fig. 4.21 A shows some inactivation kinetics found at 65°C. At low temperatures (<50°C) the enzyme showed high pressure stability up to 600 MPa and even at 30°C and 1 GPa was just slowly inactivated by 50% after 45 min (data not shown). However, at 65°C again an antagonistic effect of pressure and temperature was found. Whereas at ambient pressure β-glucanase from *B.subtilis* is inactivated by 90% within 20 min (which agrees with data of Aa et al. (Aa 1994)), pressurization up to 700 MPa led to an attenuated loss in enzyme activity. At 200-400 MPa and 65°C the enzyme looses about 20% of its initial activity within 45 min only.

In Fig. 4.21 B, the change of absorbance at 590 nm (relative to maximal absorbance measured after 24 h incubation of the enzyme at 40°C) due to the depolymerization of Azo-barley β-glucan in the presence of β-glucanase from *B.subtilis* (in 0.1 M ACES buffer, pH 5.6; containing 0.5% Azo-barley glucan) at 65°C is presented. At 65°C and ambient pressure the

rate of β-glucan conversion is slow. However, increasing the pressure up to 500 MPa resulted in significantly higher conversion rates which might be related to increased enzyme stability at these pressures but, as will be shown in the next chapter, also indicates a better substrate affinity and/or higher turnover rates at increased pressure levels.

Analysis of the inactivation kinetics in the pT domains investigated, resulted a good fit of the curves for a reaction order 1.8 used in Eqn. 3.3. Again, the reaction order n of the enzyme inactivation was obtained upon minimizing the cumulative standard error of fit from the complete experimental kinetic data set (data not shown). The lines interpolating the experimental results of relative enzyme inactivation in Fig. 4.21 show the fit of 1.8^{th} order kinetics. Upon fixing the reaction order to 1.8, the inactivation rate constants can be calculated with Eqn. 3.3. Fig. 4.22 shows inactivation rate constants k_{inac} found for all p-T conditions investigated. It is evident that the inactivation rate is significantly decreased by an increase of pressure up to approximately 400 MPa under isothermal conditions. This correlates with a strong stabilization of the enzyme structure against thermal induced denaturation. It is not surprising that under isobaric conditions k_{inac} is highly increased with temperature (Fig. 4.21).

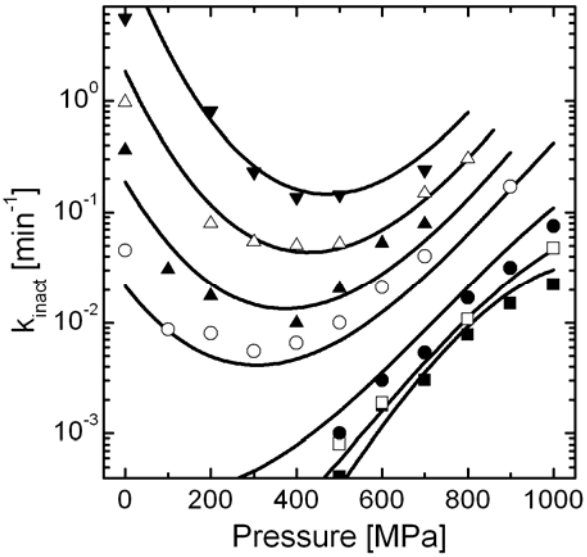

Fig. 4.22: Pressure dependence of the inactivation rate constant (k_{inact}) of β-glucanase (*B.subtilis*) in ACES buffer (pH 5.6; 0.1 M) at 30°C (■), 40°C (□), 50°C (●), 60°C (○), 65°C (▲), 70°C (△), and 75°C (▼).

Similar to other enzymes investigated (see previous chapters), the dependence of k_{inact} of β-glucanase from *B.subtilis* in ACES buffer (0.1 M; pH 5.6) on pressure and temperature was sufficiently described by Eqn. 3.5. Regression analysis resulted in the parameter values

specified in Tab. 4.4 giving the lines of changing inactivation rate constant with pressure at constant temperatures shown in Fig. 4.21.

Tab. 4.4: Estimated model parameters for inactivation of β-glucanase (*B.subtilis*) based on Eqn.3.5.

Parameter	Estimated parameter values
$A_{0:}$	-20.836 ± 7.101
A_1	$3.292*10^{-2} \pm 1.733*10^{-2}$
A_2	0.145 ± 0.089
A_3	$-6.024*10^{-6} \pm 8.102*10^{-6}$
A_4	$2.306*10^{-3} \pm 1.634*10^{-3}$
A_5	$-7.417*10^{-4} \pm 9.117*10^{-4}$
A_6	$-8.037*10^{-9} \pm 6.616*10^{-9}$
A_7	-
A_8	$4.767*10^{-7} \pm 1.139 \cdot 10^{-7}$
	r^2 = 0.931

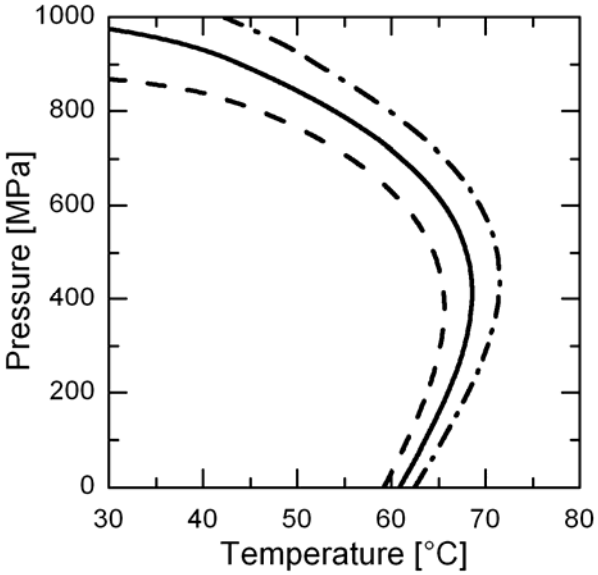

Fig. 4.23: Pressure-temperature isorate diagram for 50 % inactivation of β-glucanase (*B.subtilis*) in ACES buffer (pH 5.6; 0.1 M) after 15 (**--**), 30 (**—**) and 60 (**-·-**) minutes.

Fig. 4.23 shows the pT isorate lines for 50% inactivation of β-glucanase (*B.subtilis*) in ACES buffer (pH 5.6; 0.1 M) occurring after 15, 30 and 60 min treatment time. The lines have been calculated using Eqn. 3.3 with n = 1.8 and replacing k_{inac} by Eqn. 3.5 with parameters shown in

Tab. 4.4. The deceleration of the inactivation rate down to a minimum at approximately 400 MPa (seen Fig. 4.22) leads to elliptical shaped curves in the p-T plane, indicating a stabilization against heat denaturation under high pressure conditions rather than at ambient pressure. Furthermore it is evident from Fig. 2.23 that the enzyme can either inactivated by high temperatures but the same effect can be found when sufficient high pressures at lower temperatures. According to the model suggested, β-glucanase (*B.subtilis*) in ACES buffer (0.1 M, pH 5.6) looses 50 % of its initial activity after 30 min either at 60°C and ambient pressure, 67°C and 400 MPa or 30°C and 970 MPa.

4.3.4 Catalytic activity of β-glucanase from *Bacillus subtilis* at different high pressure-temperature combinations

Isothermal/isobaric kinetics of by β-glucan conversion by β-glucanase from *B.subtilis* have been performed in the range 30-75°C and 0.1-600 MPa. The kinetics presented in Fig. 2.21 B show the change of relative absorbance at 590 nm due to the depolymerization of Azo-barley β-glucan in the presence of β-glucanase from *B.subtilis* (in 0.1 M ACES buffer, pH 5.6; containing 0.5% Azo-barley glucan) found at 65°C and different pressures. It is obvious that at this temperature the rate of substrate conversion k_{conv} is significantly higher at 100-500 MPa than at ambient pressure. However, to conclude on the effect of pressure and temperature on the catalytic activity of β-glucanase from *B.subtilis*, the apparent rate of *in-situ* substrate conversion had to be corrected by the previously suggested of simultaneously occurring enzyme inactivation (Eqn. 3.3 in combination with Eqn. 3.5 using n=1.8 and the parameters from Tab. 4.4). Assuming no effect of the substrate on enzyme stability, the kinetics of product P formation can be formulated similar to Eqn. 4.1 and/or Eqn. 4.3 using a reaction order of 1.8 and 1.0 for the enzyme inactivation and the conversion reaction, respectively.

These equations have been solved numerically for the conversion rate constant k_{konv} and fitted to the kinetics of β-glucan conversion in relative units (Fig. 4.21 B). The enzyme concentration [E] was introduced relative to the initial concentration at time 0 and has been set to 1. Therefore, the inactivation rate constant k_{inact} derived from Eqn. 3.5 has to be divided by the initial enzyme concentration (0.8 µg/mL) used in *in-situ* experiments of substrate conversion.

$$k'_{inact} = k_{inact}(p,T)(0.8\mu g/mL)^{-1} \qquad \textbf{(4.7)}$$

In Fig. 4.24 the corrected k_{conv} is plotted logarithmically versus pressure. Apparently, the conversion reaction is not only accelerated by higher temperatures but also shows a strong increase with pressure. Increasing the pressure at isothermal conditions up to 300 MPa increases the rate of Azo-barley-glucan degradation by this β-glucanase up to 400%. Similar effects of pressure on the catalytic rate of different pectin methylesterases have been reported

recently (Castro et al. 2006a; Duvetter 2006; Sila et al. 2007). According to the principle of Le Chatelier, any phenomenon accompanied by a decrease in volume at constant temperature is favoured under high pressure conditions. Solvation of the charged groups due to pectin deesterification, is accompanied by volume reduction resulting from electrostriction, i.e., the compact alignment of water dipoles owing to the coulombic field of the charged groups (Balny and Masson 1993; Mozhaev et al. 1994). Similar effects may also account for the increased Azo-barley-glucan depolymerization rate under elevated pressure conditions. However, since β-glucanase from barley malt did not show increased catalytic activity on Azo-barley-glucan (see chapter 4.3.2), other effects of pressure have to be taken into account. Pressure may alter the structure of β-glucanase from *B.subtilis* in a way that substrate binding to the active centre and/or substrate affinity is improved.

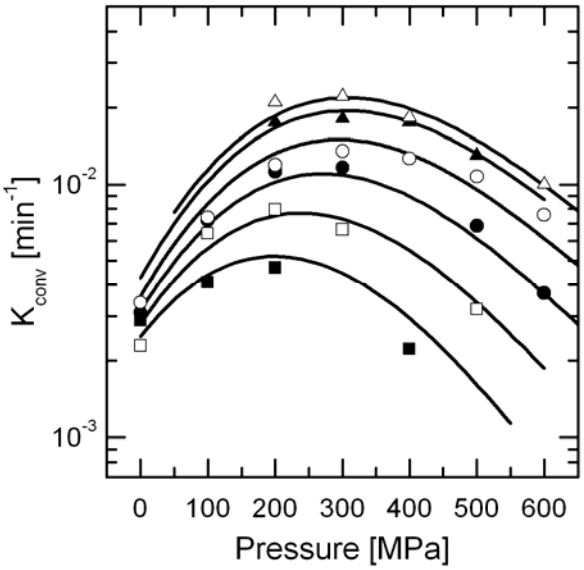

Fig. 4.24: Pressure dependence of the conversion rate constant (k_{conv}) of β-glucanase (*B.subtilis*) in ACES buffer (pH 5.6; 0.1 M containing 0.5% Azo-barley glucan) at 30°C (■), 40°C (□), 50°C (●), 60°C (○), 70°C (▲), and 75°C (△). The rate constants were derived from Eqn.4.7.

As can be seen in Fig. 4.24, the conversion rate constant k_{conv} of β-glucanase (*B.subtilis*) increases with pressure up to a maximum at approximately 300 MPa and decreases at high pressure again. Because of this behaviour the mathematic description of the pressure and temperature effects on k_{conv} yielded inadequate fits to simple equations and therefore, the response of the conversion rate on pressure and temperature was empirically described with Eqn. 4.8.

$$\ln(k_{conv}) = D_0 + D_1 p + D_2 T + D_3 p^2 + D_4 T^2 + D_5 pT + D_6 p^3 + D_7 T^3 + D_8 pT^2 \qquad \textbf{(4.8)}$$

The parameters were estimated by regression analysis of the conversion rates within the p-T domain investigated (30-75°C; 0.1-1000 MPa):

D_0: -4.262 ± 0.613; D_1: $2.184 \cdot 10^{-3} \pm 1.405 \cdot 10^{-3}$, D_2: 0.028 ± 0.042; D_3: $-2.313 \cdot 10^{-5} \pm 2.500 \cdot 10^{-5}$; D_4: $-4.052 \cdot 10^{-4} \pm 9.292 \cdot 10^{-4}$, D_5: $2.363 \cdot 10^{-4} \pm 0.5114 \cdot 10^{-4}$; D_6: $1.136 \cdot 10^{-8} \pm 0.213 \cdot 10^{-8}$, D_7: $3.26407 \cdot 10^{-6} \pm 6.626 \cdot 10^{-6}$ and D_8: $-1.582 \cdot 10^{-6} \pm 4.941 \cdot 10^{-6}$; $r^2 = 0.956$.

Reintegration of the two models for enzyme inactivation and substrate conversion the over-all reaction for glucan degradation in the presence of β-glucanase (*B.subtilis*) at different p-T combinations can be calculated for a fixed treatment time. Fig. 4.25 shows the conversion of Azo-barley-glucan in responds to pressure and temperature after 30 min exposure time. The isolines denote the percentage of hydrolized Azo-barley-glucan relative to the maximum found in the vicinity of 307 MPa and 63°C. At ambient pressure, highest glucan conversion was found at approximately 52°C. At higher temperatures enzymatic conversion of β-glucans was slower which can be related to the promotion of enzyme inactivation. However, at ambient pressure the increase of catalytic activity of β-glucanase (*B.subtilis*) was rather small at all temperatures tested (30-65°C). An increase in pressure slightly shifts the optimum of substrate conversion to higher temperatures. Keeping in mind that pressure positively affects the thermo-stability and increases the catalytic activity of β-glucanase up to an optimum at approximately 300 MPa it is not surprising that at a specific p-T combination a maximum of substrate conversion is produced. Optimal pT conditions (307 MPa and 63°C) increased the substrate conversion of β-glucanase from *B.subtilis* by more than 400 % compared to the local maximum at ambient pressure (53°C) after 30 min p-T exposure time.

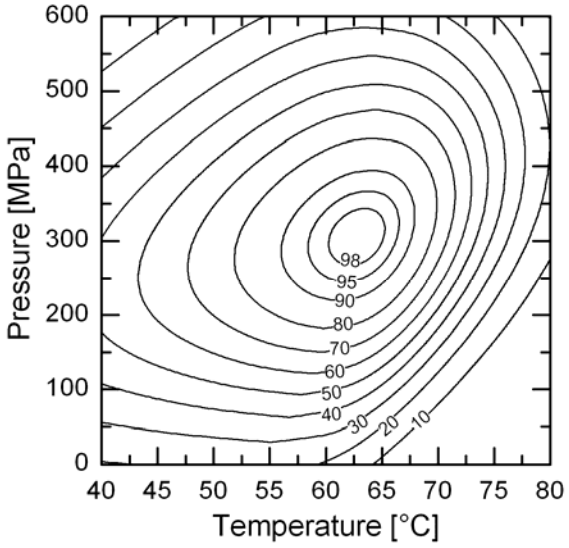

Fig. 4.25: Depolymerised β-glucan by β-glucanase (*B.subtilis*) versus temperature and pressure after 30 minutes. Isolines denote the percentage relative to the maximal β-glucan degradation observed at 307 MPa and 63°C.

Bacterial cellulases are of increasing interest to convert plant waste material into fermentable sugars which can be further converted to bioethanol. Therefore it might be interesting from an industrial point of view, to operate β-glucanase from *B.subtilis* under optimal pressure temperature conditions as this shortens the treatment time and hence, may reduces the processing costs.

4.4 Stability and catalytic activity of glucoamylase

4.4.1 Effect of high pressure-temperature combinations on glucoamylase stability

In the p-T range investigated the kinetics of glucoamylase at constant temperature and pressure showed a biphasic character indicated by a break point in most of the kinetic curves (Fig. 4.26 A and B). In particular, enzyme samples that have been pressurized with more than 800 MPa are characterized by an activity reduction of approximately 21 % immediately after pressure build-up but showed reduced reduction rates with continued dwell time. This behaviour could be explained by the formation of intermediate states of the enzyme and/or by the presence of two isoforms of glucoamylase (GA1 and GA2) which respond differently on high pressure and temperature combinations. By analyzing kinetic inactivation curves (Fig. 4.26 A and B) it was assumed that due to the relatively fast initial enzyme inactivation of 21% of the enzyme activity, the proportion of the two isozyme fraction is 21:79. Since GA2 is the smaller molecule and has a less stable structure than GA1 when exposed to thermal denaturation conditions (Christensen et al. 1999), it was assumed that this behaviour holds true under elevated pressure as well. Similar observations have been reported for pectinmethylesterase isofractions (Goodner et al., 1998; Ly-Nguyen et al., 2002). Therefore, the less resistant fraction was related to the GA2 isoform.

In Fig. 4.26 the kinetics of enzyme inactivation measured after the p-T treatment is exemplarily shown for pressure levels from 500 to 1400 MPa at 50°C (A) and pressures from 0.1 to 1200 MPa at 80°C (B). The compression period up to very high pressures with an approximate duration of up to 60 s followed by a rapid decompression already resulted in a reduced activity. This has not been taken into account for the calculation of relative enzyme activities but was integrated into the mathematical model characterizing the p-T dependence of the inactivation rate constant. Due to the instability of GA2 the relative over-all enzyme concentration was decreasing within seconds to a 0.79 level when pressure exceeded 800 MPa. During exposure to pressure the remaining enzyme activity followed a first order behaviour at significantly lower reduction rates.

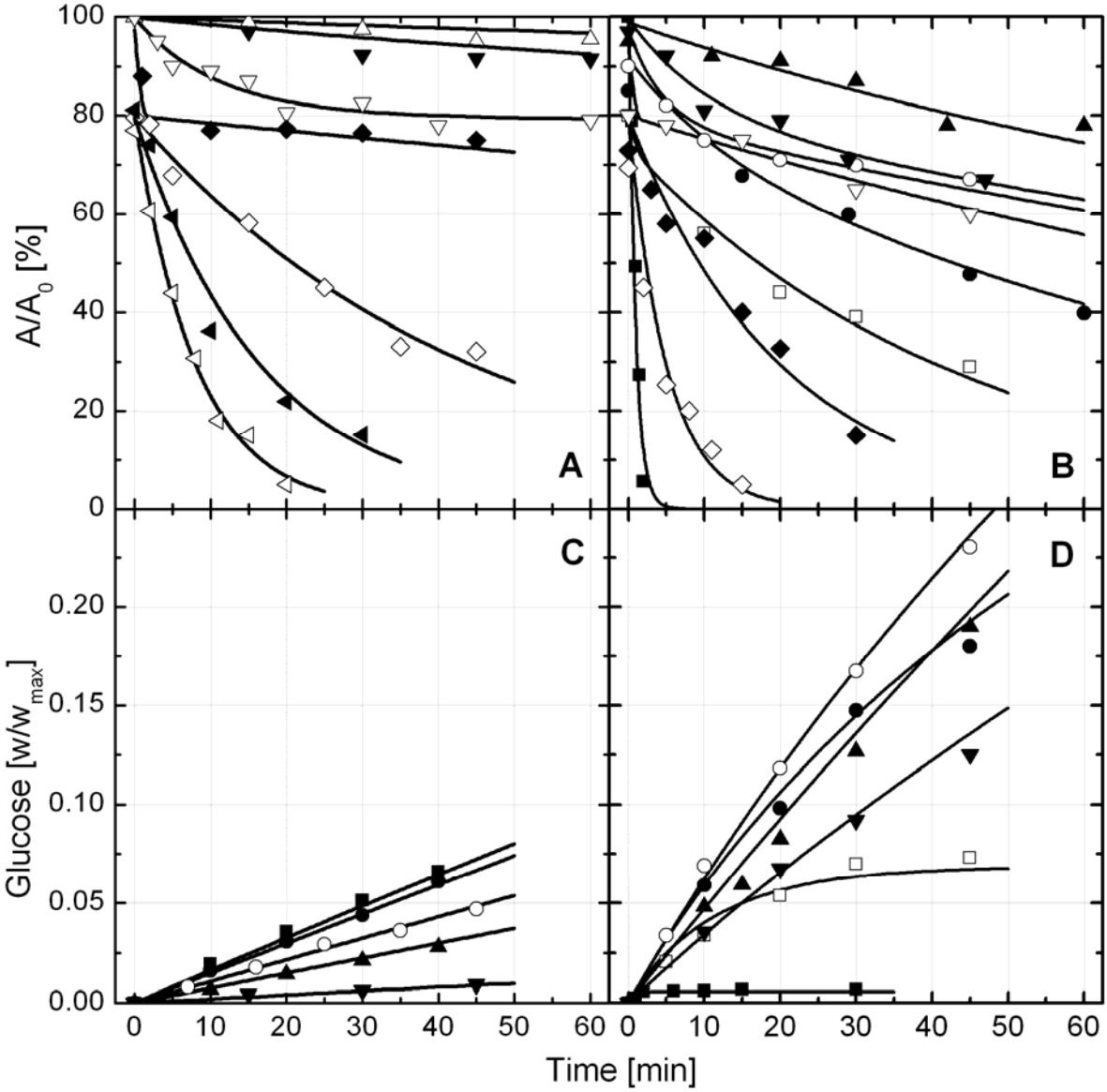

Fig. 4.26: Biphasic pressure inactivation of glucoamylase in ACES buffer (pH 4.5; 0.1 M) at 50°C (A) and 80°C (B), respectively and liberation of glucose during the conversion of maltose monohydrate solution (0.05 g maltose monohydrate/mL ACES buffer (0.1M, pH 4.5)) to high pressure at 50°C (C) and 80°C (D), respectively. The symbols denote the applied pressures as follows: 0.1 (■); 100 (□); 200 (●); 300 (○); 400 (▲), 500 (△), 600 (▼), 800 (▽); 1000 (◆), 1200 (◇), 1300 (◀) and 1400 (◁) MPa.

In Fig. 4.26 the inactivation curves present that at 50°C the residual enzyme activity is accelerated with increasing pressure. At this temperature glucoamylase from *Asperguillus niger* is stable at ambient pressure and only little reduction of activity was measured at 500 and 600 MPa within 60 min. Higher pressure yielded higher inactivation rates but, nevertheless, a residual activity was found even at 1400 MPa and 20 min. As shown in Fig. 4.26 C the *in-situ* hydrolyzation of maltose by glucoamylase is not very high at ambient pressure. At elevated

pressures the rate of glucose release is even lower, indicating a retarding effect of pressure on the catalytic activity of glucoamylase.

However, in contrast to the kinetics at 50°C, at 80°C increasing pressure produced an attenuated activity reduction (Fig. 4.26 (B)). At ambient pressure (0.1 MPa) glucoamylase was completely inactivated within 5 min. Increasing the pressure up to 400 MPa resulted in a considerable stabilization of the enzyme and conserved an activity of 75 % after 60 min. Further increase of pressure produced faster inactivation rates but even at 1200 MPa the residual activity after 5 min was approximately 25 % of the activity before pressurization.

Although the determination of the activity has been carried out after pressure release, the *in-situ* hydrolyzation of maltose showed a similar behaviour. In Fig. 4.26 (D), the concentration of glucose units (concentration is presented relative to the maximum release of glucose by glucoamylase using a substrate solution of 10 µg maltose/mL) within 45 min high pressure treatment of maltose monohydrate in the presence of glucoamylase, is significantly higher at 200, 300 and 400 MPa compared to ambient pressure. This can be explained by simultaneously occurring enzyme inactivation during substrate hydrolysis at 80°C. For a better understanding of the pressure and temperature effect on the catalytic rate of glucoamylase observations it has to be discriminated between the impact of high pressure and temperature on irreversible protein denaturation and reversible alterations of substrate conversion, respectively. Therefore, separated kinetics of enzyme inactivation within a temperature range of 40-95°C and pressures up to 1400 MPa and substrate conversion (T=40-80 °C, p=0.1-600 MPa) have been investigated.

Inactivation kinetics of enzymes describing thermal and/or high pressure processes often follows a first-order behaviour (Hendrickx et al. 1998). Regarding glucoamylase from *Aspergillus niger*, kinetic studies at ambient pressure presented the activity loss to be a first order process (Sasvári and Asboth 1998; Várallyay et al. 1994). Christensen et al. (Christensen et al. 1999) found that the catalytic domain of GA1 and GA2 thermally unfolds irreversibly in an one step process with no observable reversible intermediates, while the starch binding domain unfolds reversibly in the pH range 5.5-7.5. Polakovic and Bryjak (Polakovic and Bryjak 2002) identified a biphasic character of thermal inactivation of glucoamylase from *Aspergillus niger* by conduction of experiments until the almost complete activity loss.

As already mentioned, it was assumed that the initial concentrations of the two isozyme fractions was 0.79 ($A1_0$) and 0.21 ($A2_0$) due to the pronounced biphasic character of the inactivation kinetics (Fig. 4.26). Particular rate constants for GA1 were determined using the first order, two fraction model (Eqn.3.4). The experimental results of all p-T conditions tested for the inactivation rate constants of GA1 and GA2 are presented in Fig. 4.27. For different treatment temperatures, the inactivation rate constants k_{inact} of GA1 and GA2 are plotted versus pressure.

From these figures it is evident that the two isozyme fractions showed slightly different pressure and temperature responses. It is not surprising that both rate constants increase with increasing temperature. However, GA1 is more temperature stable than GA2. At about 400 MPa k_{inact} of GA2 passes trough a minimum whereas k_{inact} of GA1 showed the lowest rates at approximately 500-600 MPa. At this minimum the inactivation reaction is more than 100 times slower (depending on the temperature applied) compared with the inactivation rates at ambient pressure. Further pressure raise led again to an increase of both rate constants. This ellipsoid behaviour, which is not in accordance with the Arrhenius and Eyring model (Eqn.2.48), was interpreted with a pressure induced stabilization of the isozymes against thermal inactivation and can mathematically be described using a polynomial model with linear, quadratic and cross-correlation terms of the independent variables (Eqn.3.5).

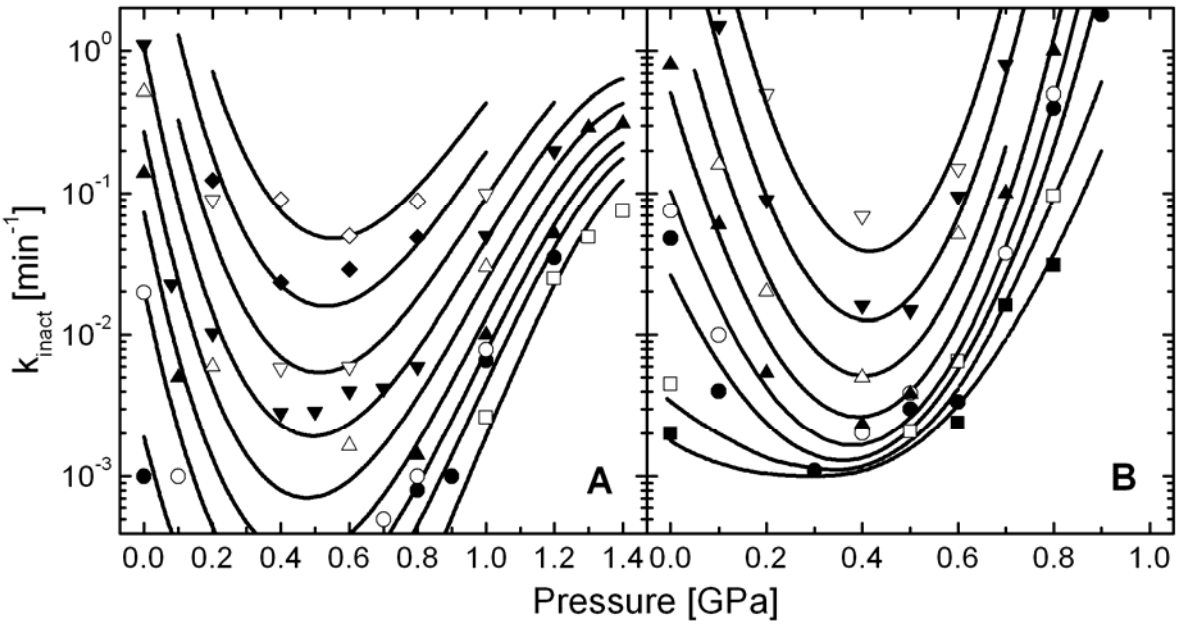

Fig. 4.27: Pressure and temperature dependence of the inactivation rate constant (k_{inact}) of isozyme fraction GA1 (A) and GA2 (B) in ACES buffer (pH 4.5; 0.1 M) at 40°C (■); 50°C (□); 60°C (●); 65°C (○); 70°C (▲); 75°C (△); 80°C (▼), 85°C (▽), 90°C (◆) and 95°C (◇) MPa.

Adapted to the kinetics of enzyme inactivation in response to specific p-T the coefficients (A_0, A_1, A_2, A_3, A_4, A_5, A_6 and A_8) used in Eqn. 3.5 were determined by regression analysis. Within the p-T domain investigated the coefficients shown in Tab. 4.5 were obtained for GA1 and GA2. Graphically, this is shown in Fig. 4.27 as lines interpolating the results for the change in rate constant with pressure at constant temperatures.

Tab. 4.5: Estimated model parameters for inactivation of GA1 and GA2 based on Eqn.3.5.

Parameter	Estimated parameter values for GA1	Estimated parameter value for GA2
$A_{0:}$	-15.882 ± 3.789	-2.210 ± 0.634
A_1	-0.017 ± 0.007	0.044 ± 0.015
A_2	0.123 ± 0.102	-0.296 ± 0.195
A_3	$3.837*10^{-5} \pm 0.865*10^{-5}$	$-4.282*10^{-5} \pm 2.399*10^{-5}$
A_4	$9.587*10^{-4} \pm 6.848*10^{-4}$	$4.555*10^{-3} \pm 1.541*10^{-3}$
A_5	$-1.501*10^{-4} \pm 0.751*10^{-4}$	$-9.990*10^{-4} \pm 2.215*10^{-4}$
A_6	$-1.341*10^{-8} \pm 0.246*10^{-8}$	$3.630*10^{-9} \pm 6.715*10^{-9}$
A_7	-	-
A_8	$9.012*10^{-9} \pm 6.422*10^{-9}$	$1.060*10^{-6} \pm 0.268*10^{-6}$
	$r^2 = 0.963$	**$r^2 = 0.971$**

Upon substituting the inactivation rate constants of GA1 and GA2 ($k1_{inact}$ and $k2_{inact}$) in the basic equation Eqn. 3.4 by the relations of Eqn. 3.5 it was now possible to calculate the specific effect of any kind of pressure cycle on the activity of both isozyme fractions including compression and decompression phase. In addition, all p-T conditions which produce a specified reduction in enzyme activity within explicit dwell times can be derived respectively. Fig. 4.28 shows the isorate lines of GA1 and GA2 for a 50% and 95% inactivation occurring after 30 min high pressure treatment time. It is apparent that the GA1 fraction is much more pressure and temperature stable than GA2. Even 1200 MPa at 50°C reduced the activity of GA1 just by half after 30 min whereas GA2 almost got completely inactivated at 800 MPa and identical temperature-dwell time conditions. However, the minimum of the rate constants k_{inact} when plotted versus pressure generate these tongue-like curves in the p-T diagram, indicating a better stabilization of the proteins against heat at about 400 MPa for GA2 and 550 MPa for GA1 as compared to ambient pressure. Such protection of enzymes against thermal denaturation at specific pressures is not surprising and has been reported frequently (Guiavarc'h et al. 2005; Ludikhuyze et al. 2003; Stoforos et al. 2002).

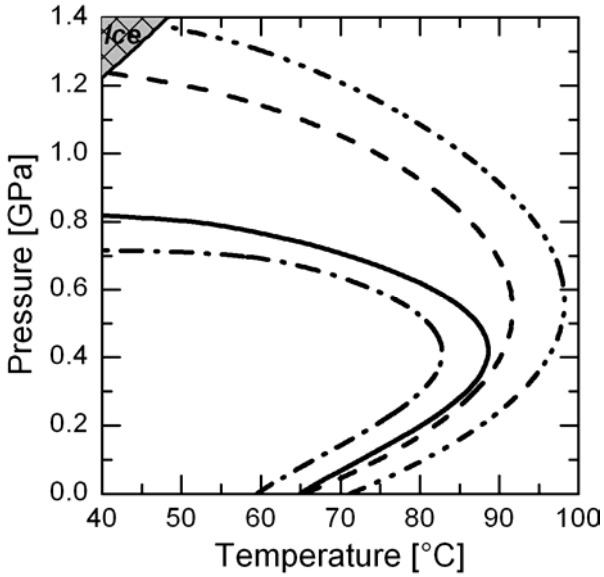

Fig. 4.28: Pressure-temperature isorate diagram for 50% (**-··**) and 95 % (**—**) inactivation of isoenzyme fractions GA2 and 50% (**--**) and 95 % (**-··**) inactivation of GA1 of glucoamylase from *Aspergillus niger* after 30 minutes.

4.4.2 Catalytic activity of glucoamylase at different high pressure-temperature combinations

In order to conclude on the pT effect on the enzymatic conversion, i.e. on the enzyme-substrate interaction, the substrate conversion found has to be superimposed by the simultaneously occurring inactivation of the enzyme. To simplify the mathematic analysis an excess of maltose was used in all experiments resulting in the following reaction scheme:

$$E1_{inact} + E2_{inact} \xleftarrow{k1_{inact} / k2_{inactt}} Maltose + H_2O + E1 + E2 \xrightarrow{k_{conv}} Glucose + E1 + E2$$

The inactivation of both isozyme fractions is of order 1.0. Since an examination of the specific action of GA1 and GA2 on maltose could not be assessed by the methodology used, it was hypothesized that both forms of glucoamylase cleaves maltose monohydrate with similar reaction rates. This is in good agreement with data published from Svensson et al. (Svensson et al. 1982) who found only marginal differences between GA1 and GA2 with respect to the conversion rate of maltose. Interestingly it has been questioned whether glucoamylase forms a stable enzyme substrate complex with maltose (Arica et al. 1998). However, since the objective of this study was to maximize glucose production by variations in pressure and temperature, the formation of possible intermediates E1S and E2S do not need to be considered in the modelling approach.

Assuming no effect of the substrate on enzyme stability, the kinetics of the reaction can be formulated as follows:

$$\frac{d[Glucose]}{dt} = k_{conv} \cdot [E1 + E2]$$
$$\frac{d[E1 + E2]}{dt} = -k1_{inact} \cdot [E1] - k2_{inact} \cdot [E2] \qquad \textbf{(4.9)}$$

These equations have been solved numerically for the conversion rate constant k_{conv} and fitted to the kinetics of glucose release in relative units (Fig. 4.26 C and D). The inactivation rate constants $k1_{inact}$ and $k2_{inact}$ has to be calculated for the particular p-T conditions. The enzyme concentration [E] is introduced relative to the initial concentration and has randomly been set to 1. Therefore, the k_{inact} calculated from Eqn. 3.5 must be divided by the initial enzyme concentration used in the experiments of maltose hydrolysis (10 µg enzyme/mL). With this procedure the isolated inspection of the p-T effect on the enzyme-substrate interaction from the overall reaction kinetics of the glucose release is feasible. In Fig. 4.29 the corrected rate constant of conversion k_{conv} is plotted versus pressure in a logarithmic scale. A strong decrease of the rate constant with increasing pressure can be observed throughout the experimental conditions investigated (40-80°C, 0.1-600 MPa). Evidently, the conversion reaction is intensely accelerated with the increase of temperature. In contrast, pressure leads to a deceleration of the enzymatic hydrolysis of maltose. Presumably steric hindrance of the access to the active centre is increased by pressure treatment. Similar results were found when using dextrines instead of maltose as substrate (data not shown). Pressures up to 200 MPa resulted in only minor reductions of k_{conv}. The response to a p-T process on the conversion rate of glucoamylase can be described empirically by Eqn. 4.10:

$$\ln(k_{conv}) = (E_0 + E_1 p^2 + E_2 T^{1.5})^{-1} \qquad \textbf{(4.10)}$$

Regression analysis of the conversion rates within the p-T domain investigated produced the following parameters (r^2 = 0.987): E_0: -0.109 ± 0.001; E_1: $1.063*10^{-7} \pm 0.032*10^{-7}$, E_2: $-1.340*10^{-4} \pm 0.029*10^{-4}$.

Considering the superposition of different p-T effects on the rate constants of the hydrolytic cleavage and of the previously characterized enzyme inactivation, the occurrence of a maximum of maltose cleavage in the p-T domain can be expected.

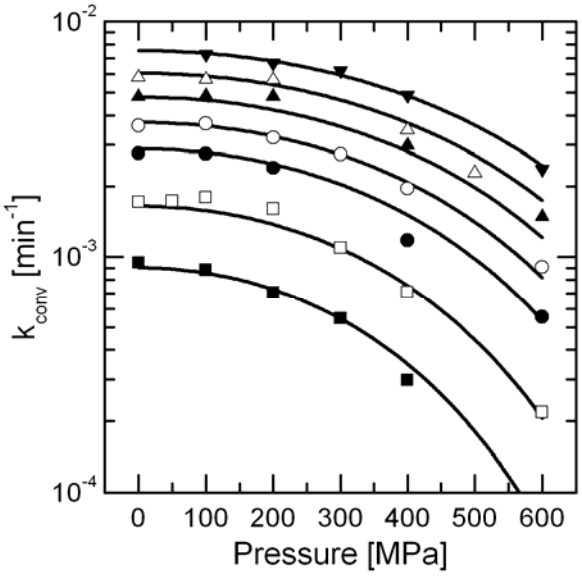

Fig. 4.29: Pressure dependence of the conversion rate constant (k_{conv}) of glucoamylase in ACES buffer (pH 4.5; 0.1 M; containing 0.05 g maltose monohydrate/mL) at 40°C (■); 50°C (□); 60°C (●); 65°C (○); 70°C (▲); 75°C (△) and 80°C (▼).

In Fig. 4.30 the overall reaction of maltose hydrolysis by glucoamylase in response to combined p-T treatment is presented for a 30 min process. The landscape plot has been obtained by integration of the two competing reactions (enzyme inactivation and substrate conversion) for a fixed process time. Isolines denote the percentage release of glucose units relative to the maximum (at 318 MPa and 84°C). At ambient pressure, the conversion rate increases up to approximately 62°C which is in good agreement with results published by (Fogarty and Benson 1983). At higher temperatures the catalytic reaction is impaired as a result of the prevailing effect of enzyme inactivation. At elevated pressures, the course of isolines is shifted to higher temperatures. For a 30 min conversion process an absolute maximum of maltose hydrolysis is located in the vicinity of 84°C and 318 MPa. Here, the yield of glucose is more than twice as high compared to the temperature optimum at ambient pressure (65°C).

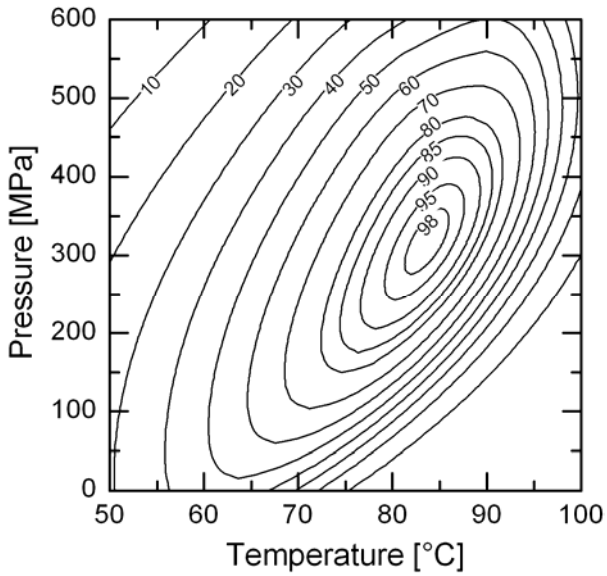

Fig. 4.30: Liberated glucose from hydrolysis of maltose monohydrate by glucoamylase versus temperature and pressure after 30 minutes exposure time. Assay conditions: 0.1 M ACES buffer, pH 4.5, containing 9 µg/mL maltose monohydrate and 50 µg/mL glucoamylase. Isolines denote the percentage relative to the maximum release observed at 318 MPa and 84°C.

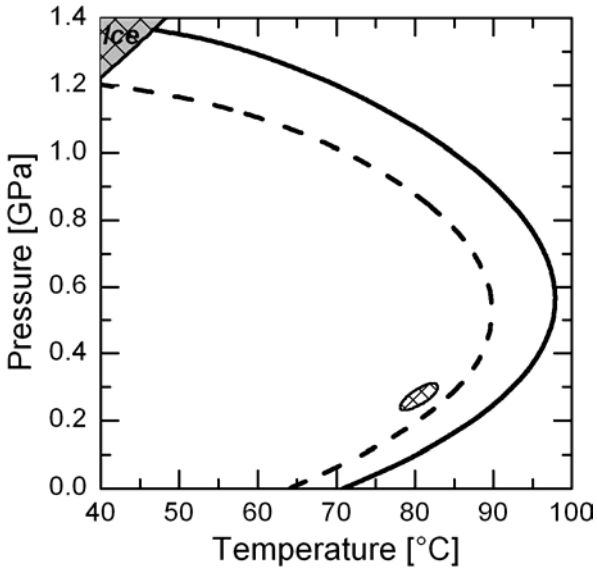

Fig. 4.31: Pressure-temperature isorate diagram of 50 % (**--**) and 95 % (**—**) inactivation of glucoamylase and the area of high conversion rate (※) after 30 minutes exposure time.

Fig. 4.31 represents the isorate lines of accumulated GA1 and GA2 fractions for 50% and 95% inactivation occurring after 30 min dwell time overlaid by the region of maximum maltose hydrolysis. Based on the previous finding that the isolated enzymatic conversion is delayed at

elevated pressure, it is not surprising that the maximum of the overall reaction does not correspond with the area of highest enzyme stability. Its location after 30 min p-T treatment time is characterized by an already reduced enzyme activity of about 50% compared to the initial activity which is due to the different inactivation characteristics of the two isofractions of the enzyme. In spite of the retarding effect, high pressure is obviously shifting the balance between heat inactivation and thermal reaction enhancement towards higher temperatures.

4.4.3 Effect of starch concentration on the catalytic activity of glucoamylase at different high pressure-temperature combinations

The concentration of substrate has an important effect on the catalytic rate of enzymes (see chapter 2.2.4). Therefore, the conversion of maize starch by glucoamylase from *A.niger* was performed at different starch concentrations over a wide range of pressure-temperature combinations (0.1-600 MPa and 30-80°C).

In-situ observation of starch hydrolysis in the presence of glucoamylase showed a reduction in glucose release at low temperatures (<60°C) and elevated pressures (kinetics not shown). However, at higher temperatures starch saccharification to glucose was significantly higher at 200-400 MPa after 35 min compared to ambient pressure. This is similar to what has been found in conversion kinetics of maltose monohydrate by glucoamylase and can be explained by the antagonistic effects of pressure and temperature on enzyme stability and catalytic activity.

Fig. 4.32 and Fig. 4.33 present the *Michaelis-Menten* plot (A) and corresponding *Hanes* plot (B) of glucoamylase from *A.niger* (using gelatinized maize starch as substrate). It is evident from Fig. 4.32 A, that the initial rate *v* of maize starch conversion is significantly increased up to a maximum rate (V_{max}) by an increase of the starch concentration. However, at constant pressure the initial rate *v* of maize starch conversion by glucoamylase is also drastically increased by an increase with temperature (Fig. 4.32 A). This not surprising as it is well known that enzymatic reactions can be accelerated by heat up to a critical temperature when enzyme denaturation becomes dominant. Under conditions that do not lead to an inactivation of glucoamylase (T<60°C; p<800 MPa), pressure was found to progressively reduce the initial rate *v* of enzymatic starch conversion (Fig. 4.33 (A)).

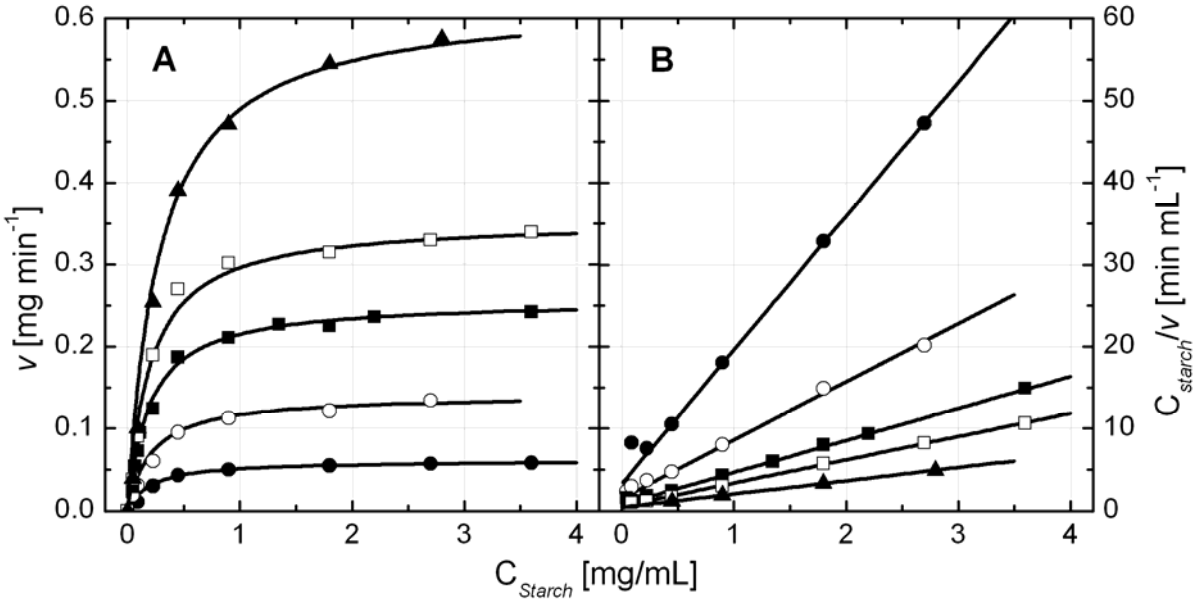

Fig. 4.32: *Michaelis-Menten* plot (A) and corresponding *Hanes* plot (B) of glucoamylase from *A.niger* (50 µg/mL ACES buffer (50 mM; pH4.5)) at ambient pressure and different temperatures using thermally gelatinized maize starch as substrate. The symbols denote the applied temperature as follows: 20°C (●), 30°C (○), 40°C (■), 50°C (□), and 60°C (▲).

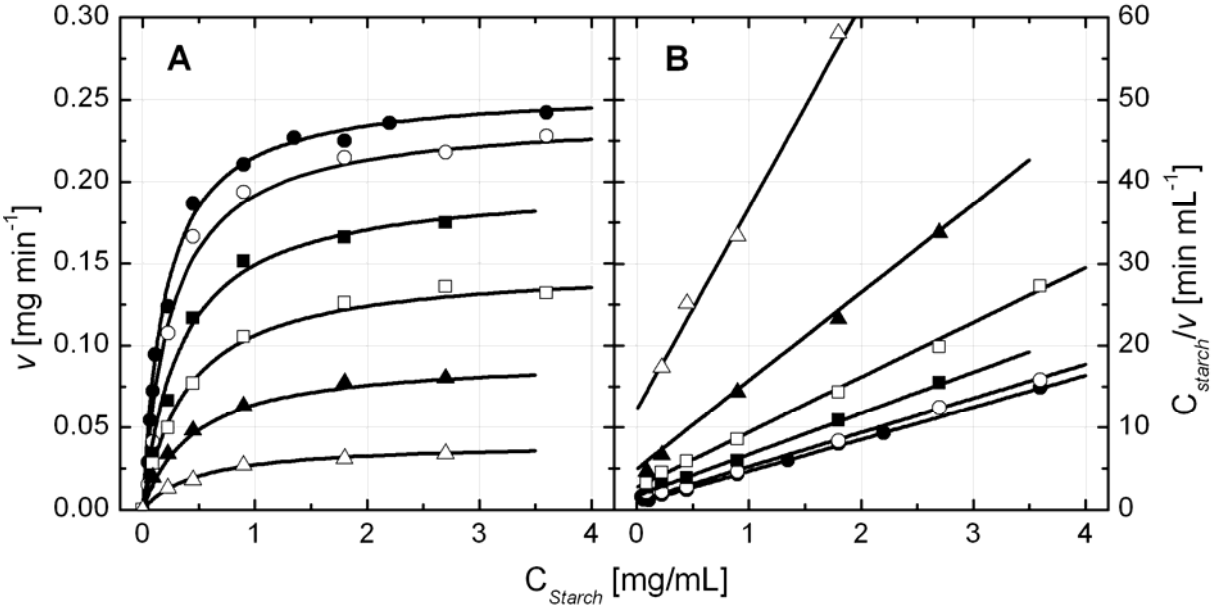

Fig. 4.33: *Michaelis-Menten* plot (A) and corresponding *Hanes* plot (B) of glucoamylase from *A.niger* (50 µg/mL ACES buffer (50 mM; pH 4.5)) at 40°C and different pressures using thermally gelatinized maize starch as substrate. The symbols denote the applied pressure as follows: 0.1 (●), 200 (○), 300 (■), 400 (□), 500 (▲), and 600 (△) MPa.

The dependence of the catalytic activity of an enzyme on the substrate concentration is usually described by the *Michaelis-Menten* constant K_m and, therefore, this constant was

calculated by the Hanes equation (2.14). In the *Hanes* plots shown in Fig. 4.32 B and Fig. 4.33 B the product of inverse initial rate of conversion and starch concentration is plotted versus the concentration of maize starch, which gives a straight line under isobaric/isothermal conditions. The gradient of the straight line is $1/V_{max}$, intersection with the abscissa is $-K_m$ and with the ordinate K_m/V_{max}. Fig. 4.34 shows the calculated *Michaelis-Menten* constant K_m (A) and the corresponding maximal rate of enzyme catalysis V_{max} (B) for the different pressure-temperature combinations investigated. In the pT domains investigated, the K_m of glucoamylase was increased in the same way as the V_{max} is decreased by pressure. This is in accordance with the observations of maltose conversion by glucoamylase described in the previous chapter (4.4.2). Obviously, pressure reversibly changes the structure of glucoamylase leading to a disadvantageous conformation which impairs the enzyme-substrate affinity and stability of the enzyme-substrate complex. This expressed by higher K_m values at increasing pressures. Empirically, the dependence of K_m (50 µg/mL glucoamylase in 50 mM ACES buffer (pH 4.5; containing 1% gelatinized maize starch) on pressure could be described by the following function:

$$K_m = F_0 + F_1 p^{1.5} \qquad \textbf{(4.11)}$$

Regression analysis gave the good fit (r^2 = 0.978) using the following parameter values: F_0: -0.205 ± 0.009; F_1: 2.144*10^{-5} ± 0.142*10^{-5}.

So far it has been shown that the apparent K_m is affected by temperature and pH (Baks et al. 2006; Turner and Pollock 1993), but probably for the first time, this study has shown the effect of high hydrostatic pressures on K_m.

For a better understanding of the real pT effect on V_{max} the even at higher temperatures, the apparent catalytic rate of glucoamylase was corrected using the suggested model for glucoamylase inactivation (see chapter 4.4.1). Since it has been reported that the glucoamylase isoenzyme GA1 cleaves starch about 9 fold faster than GA2 (Svensson et al. 1982) it was assumed that GA2 contributes only by 10% to the total conversion rate detected in conversion kinetics of maize starch in the presence of glucoamylase. On the supposition that there is no effect of the substrate on enzyme stability, and using an excess of substrate the kinetics of the reaction can then be formulated as follows:

$$\begin{aligned} \frac{d[Glucose]}{dt} &= V_{max} \cdot 0.9 \cdot [GA1] + V_{max} \cdot 0.1 \cdot [GA2] \\ \frac{d[GA1 + GA2]}{dt} &= -k1_{inact} \cdot [GA1] - k2_{inact} \cdot [GA2] \end{aligned} \qquad \textbf{(4.12)}$$

Similar to methodology described in the previous chapters, these equations have been solved numerically for the conversion rate constant k_{conv} and fitted to the kinetics of glucose release.

The inactivation rate constants $k1_{inact}$ and $k2_{inact}$ has to be calculated for the particular p-T conditions. In Fig. 4.34 the corrected (B) V_{max} values are shown for all pressure-temperature combinations tested. Similar to the results of maltose conversion (Fig. 4.29) a strong decrease of V_{max} with increasing pressures can be observed throughout the experimental conditions investigated (40-80°C, 0.1-600 MPa). Evidently, the conversion reaction is intensely accelerated with the increase of temperature.

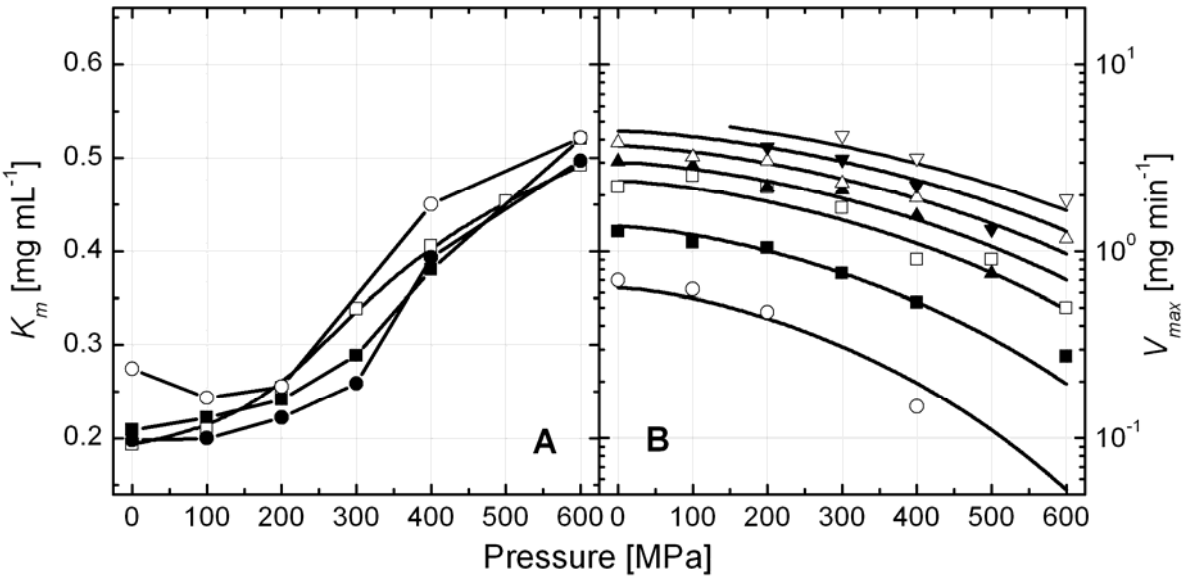

Fig. 4.34: Responds of the Michaelis-Menten constant K_m (A) and maximal rate of enzyme catalysis V_{max} (B) of glucoamylase from *A.niger* (50 µg/mL ACES buffer (50 mM; pH 4.5; containing 10 mg/mL gelatinized maize starch)) to pressure at 30°C (●), 40°C (○), 50°C (■), 60°C (□), 65°C (▲), 70°C (△), 75°C (▼), and 80°C (▽).

The response of the corrected V_{max} values of glucoamylase (with maize starch as substrate) to pressure and temperature can be described empirically by Eqn. 4.13:

$$\ln(V_{max}) = I_0 + I_1 p^{1.5} + I_2 T^{0.5} \qquad \textbf{(4.13)}$$

A good fit was found by regression analysis for the following parameter values: I_0: -6.886 ± 0.3178932; I_1: -0.0001.089*10^{-4} ± 0.072*10^{-4}, I_2: 0.997 ± 0.041.

In Fig. 4.35 the overall reaction of maize starch hydrolysis by glucoamylase in response to combined p-T treatment is presented for a 30 min process. The diagram plot was obtained by integration of the two competing reactions (enzyme inactivation and starch conversion) for a fixed process time, assuming a high excess of starch throughout the whole process. Isolines denote the percentage release of glucose units relative to the maximum (at 270 MPa and 80°C). At ambient pressure, the glucose release due to conversion of maize starch is highest at 60°C after 30 min. However, increasing the pressure the course of isolines is shifted to higher

temperatures resulting in an absolute maximum of starch hydrolysis by glucoamylase in the vicinity of 80°C and 270 MPa. At this optimal condition the yield of glucose is about twice as high compared to optimum at ambient pressure (60°C). However, the optimum of starch conversion is slightly different to the optimal hydrolysis of maltose found at 318 MPa and 84°C. This might be explained by the described differences of glucoamylase activity on different substrates (Christensen et al. 1999; Svensson et al. 1986; Svensson et al. 1982).

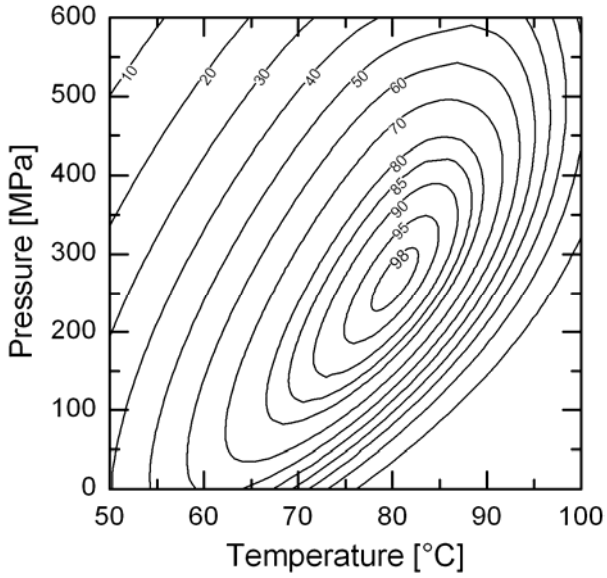

Fig. 4.35: Liberated glucose from hydrolysis of thermally gelatinized maize starch by glucoamylase versus temperature and pressure after 30 minutes exposure time. Experimental conditions: 0.1 M ACES buffer, pH 4.5, containing 10 mg/mL maize starch and 0.25 µg/mL glucoamylase. Isolines denote the percentage relative to the maximum release observed at 270 MPa and 80°C.

4.5 Phase transition kinetics of maize starch in aqueous solution

The complete loss in birefringence of maize starch granules in response to various pressure/temperature conditions has been studied kinetically. The degree of gelatinization continuously increased with exposure time. Examples are shown in Fig. 4.36 for 40°C (A) and 60°C (A), respectively. The kinetics for the other temperatures tested are not shown explicitly. Generally it was found that by increasing the pressure the rate of the starch granule gelatinization could be increased, significantly. In a similar way, the reaction was influenced by the temperature. Here, however, the gelatinization rate is increasing progressively when a certain threshold temperature is exceeded. Fig. 4.37 shows of maize starch granules gelatinization in aqueous solution at 30°C at the different stages of a pressure cycle (650 MPa, 20 min). It is evident that process starch granule swelling is not spontaneous but shows a clear time dependency.

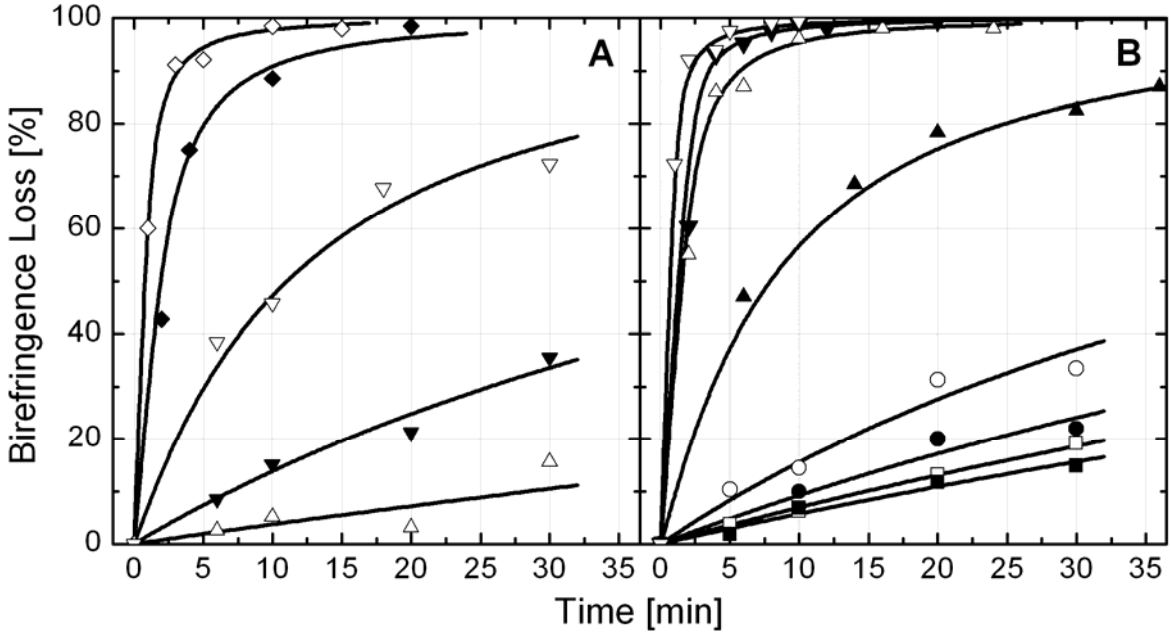

Fig. 4.36: Complete loss in birefringence of maize starch at 40°C (A) and 60°C (B). The symbols denote the applied pressures as follows: 0.1 (■), 100 (□), 200 (●), 300 (○), 400 (▲), 450 (△), 500 (▼), 550 (▽), 600 (◆) and 650 (◇) MPa.

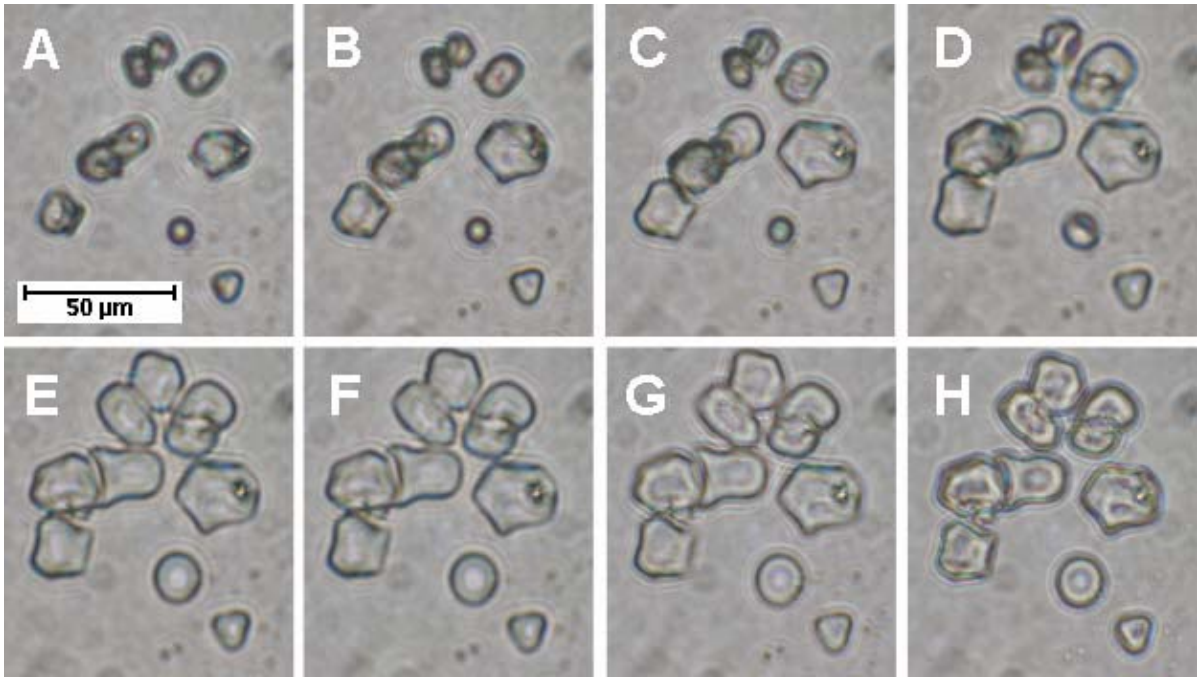

Fig. 4.37: *In-situ* observation of maize starch granules gelatinization in aqueous solution at 30°C and 0.1 MPa (A), pressure increase up to 650 MPa (B), after 1 min at 650 MPa (C), after 2 min at 650 MPa (D), after 5 min at 650 MPa (E), after 10 min at 650 MPa (F), after 20 min at 650 MPa (G), and after pressurization at 650 MPa for 20 min and pressure release to ambient pressure (H). Photographs have been obtained with a high pressure microscope described elsewhere (Urrutia Benet 2005).

The analysis of starch gelatinization kinetics relies on the hydration and melting progress as a function of time under specified conditions. Starch gelatinization has often been described by a first order reaction (Lund 1984; Marcotte et al. 2004; Zanoni et al. 1995). However, this is quite surprising as starch granules of the same origin often show differences in their chemical and physical properties depending e.g. on granule size and granule size distribution (Singh and Kaur 2004; Vasanthan and Bhatty 1996). In the p-T plane the isobaric/isothermal gelatinization curves of maize starch showed clear deviations from first order kinetics. Therefore, the gelatinization process was described as a n^{th}-order reaction, expressing the relative increase of gelatinized starch granules (N/N_0) as a function of time under constant pressure and temperature conditions:

$$1 - \frac{N}{N_0} = (1 + (n-1) \cdot k'_{gel} \cdot t)^{\frac{1}{1-n}} \qquad \textbf{(4.14)}$$

$$\text{with } k'_{gel} = k_{gel} (N_0)^{(n-1)} \qquad \textbf{(4.15)}$$

with n as the reaction order which has to be determined by minimizing the cumulative standard error of fit over a wide range of reaction orders, i.e., averaging the predictive error in all individual kinetics of the complete experimental kinetic data set. k' is the specific gelatinization rate constant (min^{-1}) which is regressively obtained from fitting n-th order kinetics (Eqn. 4.14) to the gelatinization data. This allows an appropriate description of curves which show significant deviations from log-linear behaviour.

Regression analysis yielded, that the accumulated error of fit over all kinetic data sets is minimized by using a homogeneous reaction order of n=1.65 in Eqn. 4.14. Plotting the derived specific gelatinization rate constants k_{gel} [min^{-1}] versus pressure indicates that apart from the highest pressure level tested, the isobaric temperature functions of k'_{gel} show no linearity (Fig. 4.38). The prevailing sigmoidal shape of the curves indicates that the decomposition of the starch granules is governed by at least two mechanisms of action.

Mathematically, the effect of pressure and temperature on k_{gel} can be described by Eqn. 4.16 which holds true for $k'_{gel} > 10^{-3}$ min^{-1} and $k'_{gel} < 5$ min^{-1}:

$$\ln(k_{gel}) = m(p) + a(p) \cdot \frac{T - T_m(p)}{\left|(T - T_m(p))^{b(p)}\right|} \qquad \textbf{(4.16)}$$

T [°C] is the temperature and $T_m(p)$ [°C] denotes the inflection point of the k´ temperature function which is often referred to as the melting temperature of the starch granules. The pressure effect on the parameter m(p), a(p) and b(p) was empirically fitted by the following simple equations:

$$T_m = a_{Tm} + b_{Tm} \cdot \exp\left(\frac{p}{c_{Tm}}\right) \qquad \textbf{(4.17)}$$

a_{Tm} = 67.24 ± 0.61 °C; b_{Tm} = -0.090 ± 0.054 °C; c_{Tm} = 97.11 ± 9.71 MPa

$$m = a_m + b_m \cdot p \quad \textbf{(4.18)}$$

a_m = -1.87 ± 0.23 °C; b_m = 3.125*10^{-4} ± 7.94*10^{-4} MPa^{-1}

$$a = \exp\left(a_a + b_a \cdot p^3\right) \quad \textbf{(4.19)}$$

a_a = 0.468 ± 0.124 [-]; b_a = -8.97*10^{-9} ± 2.56*10^{-9} MPa^{-3}

$$b = a_b + b_b \cdot p^2 \quad \textbf{(4.20)}$$

a_b = 0.633 ± 0.063 [-]; b_b = -8.93*10^{-7}± 5.18*10^{-7} MPa^{-2}

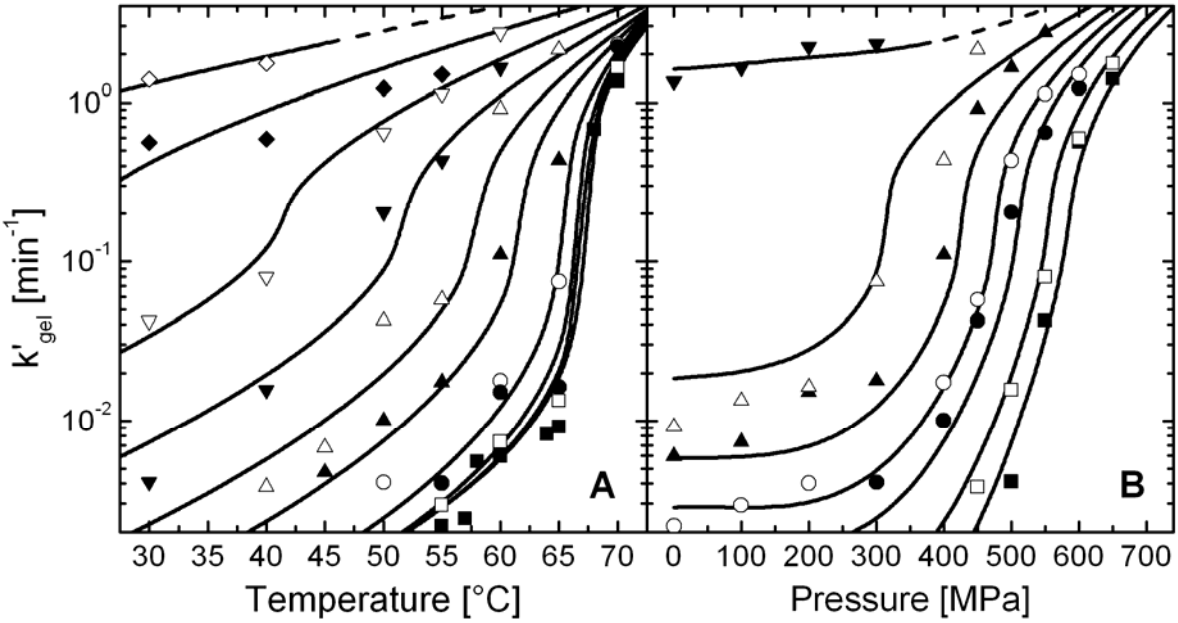

Fig. 4.38: The impact of temperature and pressure on the gelatinization rate constants k´$_{gel}$. A: The dependence of k´$_{gel}$ on temperature at 0.1 (■), 100 (□), 200 (●), 300 (○), 400 (▲), 450 (△), 500 (▼), 550 (▽), 600 (◆) and 650 (◇) MPa. B: The dependence of k´$_{gel}$ on pressure at 30°C (■), 40°C (□), 50°C (●), 300 (○), 400 (▲), 450 (△), 500 (▼), 550 (▽), 600 (◆) and 650 (◇) MPa.

The graphical representation of Eqn. 4.16 (Fig. 4.38) suggests, that the points of inflection of kgel´ as a function of temperature is shifted to lower temperatures when the starch granules are exposed to higher pressures. Accordingly, the related parameter T_m is progressively reduced when the pressure exceeds 300 MPa (Fig. 4.39). This diagram already anticipates the shape of the isorate curves which can be derived by identifying those p/T conditions which solve Eqn. 4.14 for a given degree of gelatinization N/N_0 and a given treatment time t when substituting k´$_{gel}$ by Eqn. 4.16. For a treatment time of 30 min, the required p/T conditions for 10, 50, 90 and 100% gelatinization of maize starch granules were calculated (Fig. 4.40 A). In the pT diagram

the synergistic effect of pressure and temperature is expressed by left shaped isorate lines at pressures higher than 300 MPa. Below, the almost vertical lines indicate pressure invariance and the sole impact of temperature on the gelatinization rate. Fig. 4.40 B shows an isorate diagram of 50 % maize starch gelatinization after different time intervals. The similarity to the phase transition diagrams in Fig. 4.40 B is evident and proves there is an interrelation between thermodynamics and kinetics of starch gelatinization - at least on a phenomenological basis.

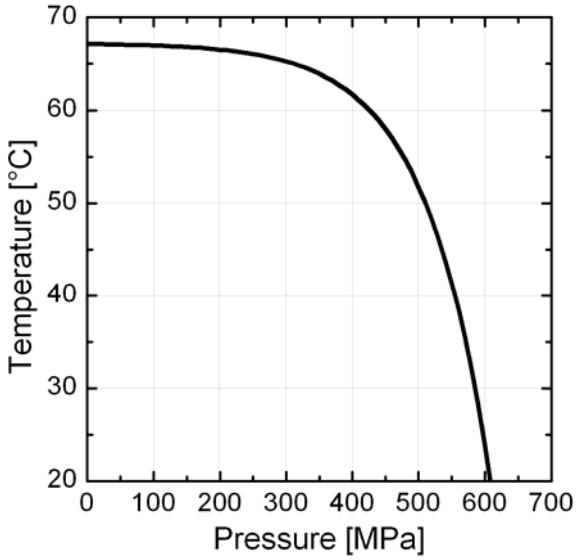

Fig. 4.39: Pressure dependence of the model parameter T_m (melting temperature)

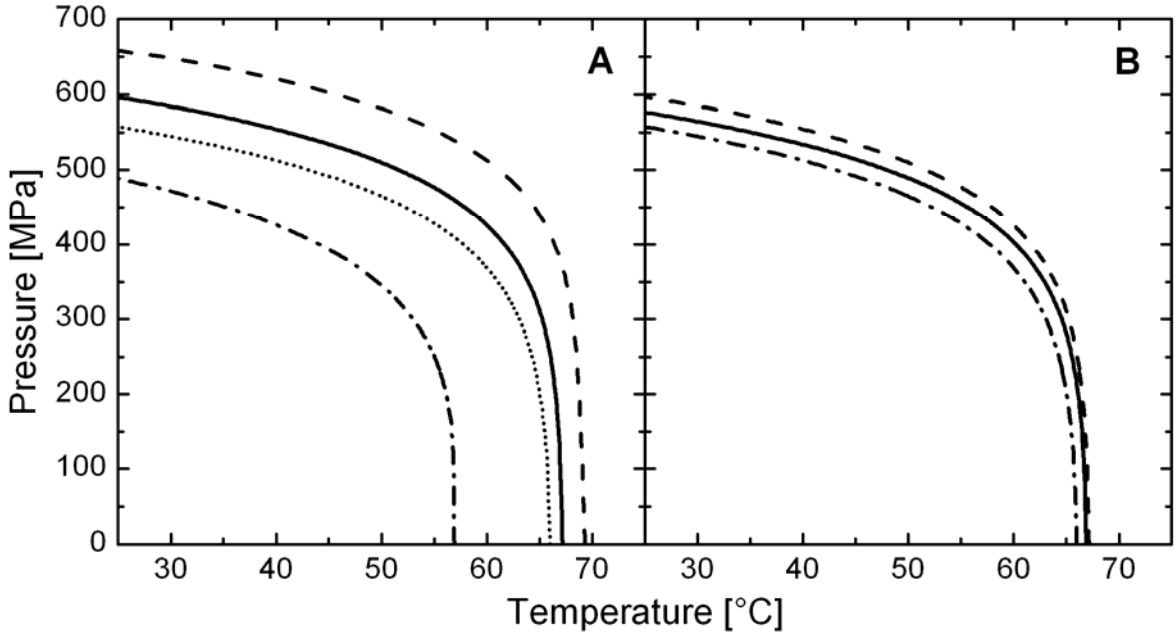

Fig. 4.40: Pressure-temperature isorate diagrams of maize starch gelatinization. A: Isorate lines of 10% (┅), 50% (┅), 90% (—) and 100% (┅) gelatinization of maize starch after 30 min. B: 50% gelatinization of maize after 5 min (┅), 15 min (—) and 30 min (╍) combined pT treatment.

Gelatinization is generally considered to be a multi-stage process. After the swelling of the amorphous domains, the growth ring structure of the granule starts to disintegrate and the crystalline regions undergo melting simultaneously with a progressively increased hydration (Oates 1997). Increasing particle size and re-association of solubilized amylose is supposed to produce an increase in viscosity and gel formation.

In this analysis the gelatinization by a combination of temperature and high pressure is based on the microscopically detected loss in birefringence. Douzals et al. (2001) reported that the birefringence method often slightly overestimates the gelatinized fraction in comparison with DSC measurements. However, the method has been found suitable to detect very low degrees of starch gelatinization and has been used by a number of authors so far (Bauer and Knorr 2005; Douzals et al. 2001; Lelievre 1973; Thevelein et al. 1981). In other studies it was found, that the viscosity of high pressure treated granule suspensions is usually lower than that of heat treated samples (Stolt et al. 2001; Stute et al. 1996). Simultaneously to the change in birefringence other structural changes are differently affected by temperature and pressure, respectively.

Different from heat gelatinization, the pressurized starch granules remain intact or just partly disintegrated and the solubilization of amylose is rather poor. It has been assumed, that the crystalline components are prevented from melting since the amylopectin in the granule is stabilized by the still present amylose (Stolt et al. 2001). This could explain why maize starch is completely decomposed while waxy maize starch (containing almost no amylose) is not. In fact the hydration of the largely amorphous regions of the growth rings is the first step of gelatinization, but surprisingly, at this point there is hardly any water absorbed from the crystalline lamellae (Jacobs et al. 1998). Since it is also know that starch granules can deposit reversibly about 30% of water it is questionable whether the amorphous regions of the granule play an important role in controlling the rate of gelatinization (Parker and Ring 2001). For heat gelatinization it is more likely that the loss of crystallinity is the rate limiting step which is certainly of importance for pressure induced process, too.

For all starches it is evident that the gelatinization temperature is decreasing when the suspension is exposed to higher pressure. This is especially true at lower temperatures. The pressure effect is by far smaller when the treatment temperature is approaching the gelatinization temperature at ambient pressure.

The curves in Fig. 4.40 have been derived from microscopic inspections of the granule's birefringence. Along those lines the viscosity of the gelatinized suspension is increasing with increasing temperature. In other words: the structural network for pressure induced gels is much weaker. Incomplete granule gelatinization with no or only partial melting of the crystalline regions prevents amylose and amylopectin from gel formation as it happens in thermal gelatinization. In

contrast, it can be assumed that the hydration of the amorphous domain either in the growth ring structures or in the lamellar structure of the crystalline regions is improved by pressure. The main contribution to increase the viscosity of high pressure suspension comes from the irreversibly swollen granules which are reducing the liquid's free volume.

Although the gelatinization by high pressure and by high temperature is different in mechanism and in granule degradation, in both situations the reached level of hydration is sufficient to allow enzymatic attack and the continued decomposition of the polysaccharide macromolecules.

4.6 Enzymatic starch conversion in different pressure/temperature domains

4.6.1 Effect of pressure and temperature on maize starch conversion by glucoamylase

In Fig. 4.41 the competing reactions of enzymatic hydrolysis of native starch granules are presented schematically. Typically starch granules first have to degrade before they get accessible for amylolytic break-down. For instantce, it has been reported that the activity of glucoamylase from *A.niger* towards gelatinized starch is around 100- fold higher than on granular starch (Svensson et al. 1982). Since reaction equilibrium and kinetics of the three pathways are affected by temperature and pressure but potentially in a different manner, it is useful to find optimum pressure-temperature (p-T) conditions which maximize the catalytic reaction.

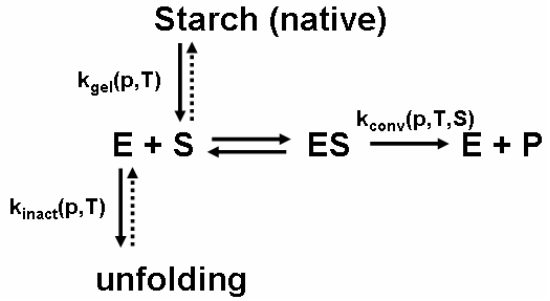

Fig. 4.41: Reaction scheme of enzymatic starch hydrolysis, superimposed by starch gelatinization and enzyme unfolding. E: enzyme; S: substrate; P: product.

In the previous chapters the effect of pressure, temperature and substrate concentration on k_{inact}, k_{conv} and k_{gel} of glucoamylase and maize starch in model systems has been presented.

In order to conclude on the pT effect on the conversion of native maize starch by glucoamylase, the reaction can be written as follows:

$$\frac{d[GA1+GA2]}{dt} = -k1_{inact}\cdot[GA1] - k2_{inact}\cdot[GA2]$$
$$\frac{d[Glu\cos e]}{dt} = \frac{V_{\max}\cdot[S]}{K_m+[S]}\cdot 0.9\cdot[GA1] + \frac{V_{\max}\cdot[S]}{K_m+[S]}\cdot 0.1\cdot[GA2] \qquad \textbf{(4.21)}$$
$$\frac{d[S]}{dt} = 1-(k_{gel}\cdot[S]^{-1.65})$$

[S] is the concentration of degraded starch granules and [GA1] and [GA2] are the enzyme concentration of GA1 and GA2, respectively. Similar to the methodology described in the previously section, these equations have been solved numerically for the maximal rate of starch conversion V_{max} using the functional relations of Eqn. 3.5 with the parameters of Tab. 4.5; Eqn. 4.11; Eqn 4.13 and 4.16.

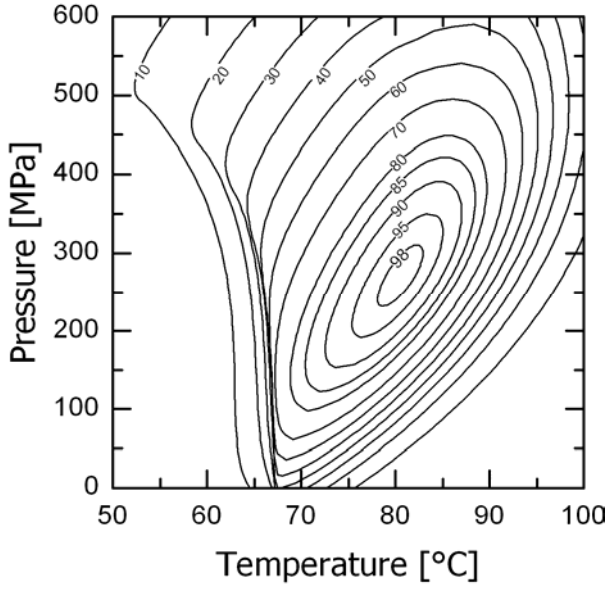

Fig. 4.42: Liberated glucose from hydrolysis of native maize starch by glucoamylase versus temperature and pressure after 30 minutes exposure time. Experimental conditions: 0.1 M ACES buffer, pH 4.5, containing 50 mg/mL maize starch and 0.25 µg/mL glucoamylase. Isolines denote the percentage relative to the maximum release observed at 270 MPa and 80°C.

Fig. 4.42 presents the overall reaction of native maize starch hydrolysis by glucoamylase in different pT domains for a 30 min process. The landscape plot has been obtained by integration of the three competing reactions (starch hydrolysis, enzyme inactivation and substrate conversion) for a fixed process time. Isolines denote the percentage release of glucose relative to the maximum (at 270 MPa and 80°C). In the high temperature domain the lines in Fig. 4.42 are similar to Fig. 4.35 which indicates that here the effect of starch gelatinization on the conversion rate is negligible. However, at lower temperatures (<70°C) a deformation of the isolines is visible and at temperatures below 63°C and pressures below 500 MPa there is hardly any release of glucose from maize starch. In this area, the starch granules stay intact which

impedes enzymatic break-down of the starch. At ambient pressure starch gelatinization takes place at temperatures where glucoamylase already starts to inactivate. Therefore, glucose production after 30 min is relatively low at ambient pressure conditions. An increase of the pressure can stabilizes the enzyme from thermal induced inactivation and hence, it is not surprising that the release of glucose from of maize starch granules due to enzymatic conversion was found to be approximately 150% higher at 270 MPa and 80°C compared to optimal conditions at ambient pressure (68°C).

Due to the high gelatinization temperatures of starches, enzymatic starch saccharification is usually performed in two steps in industry (see chapter 2.2.4). Nevertheless this study shows that due to the opposite effects of pressure on starch gelatinization and enzyme stability it is possible to achieve high saccharification rates by increasing the pressure and temperature. There is no doubt that this shortens the processing time and may reduce the process costs.

4.6.2 Effect of pressure and temperature on the conversion of barley malt starch by combined action of α- and β-amylase.

Thermally gelatinized barley malt starch has been exposed to combined action of α- and β-amylase in different pressure temperature domains. Fig. 4.43 exemplarily shows kinetics of fermentable sugars liberation at 50°C and 70°C for different pressures. At non denaturing temperatures (50°C) the conversion rate is impaired at elevated pressures. Higher temperatures accelerate the starch hydrolysis but it also leads to an inactivation of the enzymes. As already described previously (chapter 4.1 and 4.2), α- and β-amylase from barley malt are stabilized against heat denaturation when subjected to pressures of approximately 200 MPa. Therefore it is not surprising that at 70°C (Fig. 4.43 B) highest production of reducing sugars was detected at 100-200 MPa after 40 minutes. Using the previously proposed inactivation models it was possible to correct the apparent conversion kinetics. However, since at high concentrations of barley malt both amylases showed slightly higher stabilities towards pressure and temperature than in the model system (data not shown) correction factors has been used to compensate the difference in enzyme inactivation rate constants. The model of α-amylase inactivation in responds to pressure and temperature (Eqn. 3.5 using the parameters shown in Tab. 4.1) was corrected by the factor 0.95 and the model describing the pT dependence of the inactivation rate constant $k_{inact,\beta}$ of β-amylase (Eqn. 3.5 using the parameters shown in Tab. 4.2) was corrected by the factor 0.9. Finally the kinetics of sugar formation was formulated as follows:

$$\frac{d[sugar]}{dt} = k_{conv} \cdot [AA + BA]$$
$$\frac{d[AA + BA]}{dt} = -k_{inact,\alpha} \cdot [AA]^{2.1} - k_{inact,\beta} \cdot [BA]^{1.4} \qquad \textbf{(4.22)}$$

Here, the conversion reaction is of order 1.0 (due to the large excess of substrate). The reaction of enzyme inactivation is of order 2.1 and 1.4, respectively. These equations have been solved numerically for the conversion rate constant k_{conv} and fitted to the kinetics of starch hydrolysis (Fig. 4.43). The inactivation rate constants $k_{inact,\alpha}$ (α-amylase) and $k_{inact,\beta}$ (β-amylase) has to be specified for the particular p-T condition. The concentration of α-amylase [AA] and β-amylase [BA] is introduced relative to the initial concentration and has randomly been set to 0.6 and 0.4, respectively.

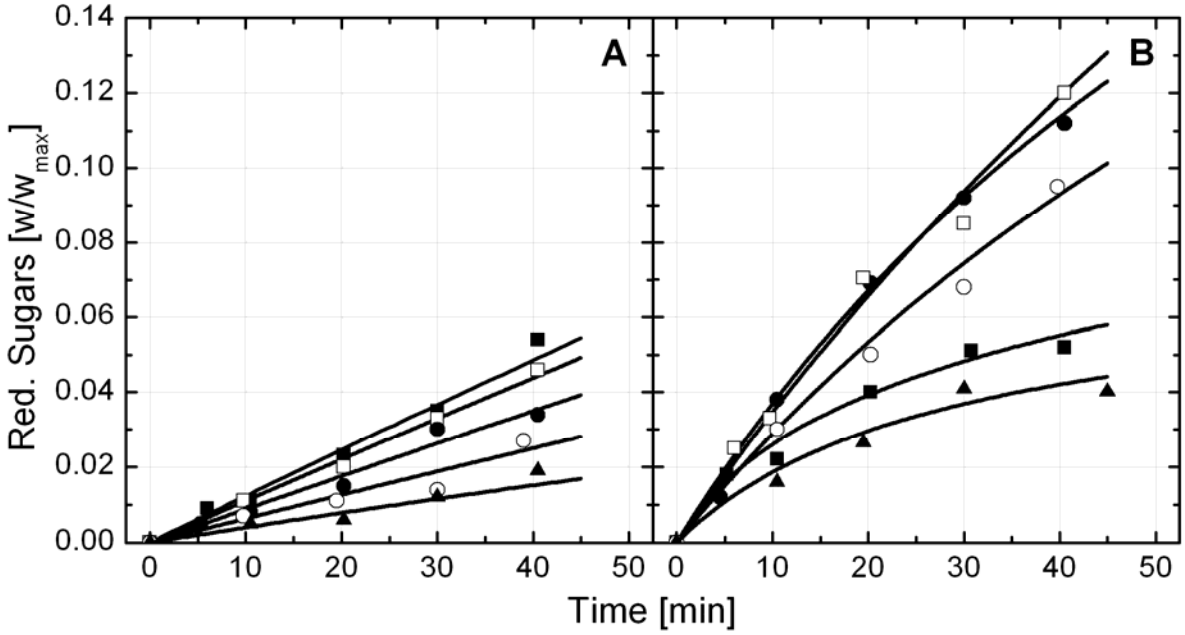

Fig. 4.43: Liberation of reducing sugars from barely malt starch by α- and β-amylase in ACES buffer (0.1 M; pH 5.6; containing 10 mg/mL gelatinized barely malt starch, 90 mM NaCl and 3.8 mM $CaCl_2$) at 50°C (A) and 70°C (B). The symbols denote the applied pressures as follows: 0.1 (■); 100 (□); 200 (●); 300 (○); and 400 (▲) MPa.

In Fig. 4.44 k_{conv} is plotted logarithmically versus pressure indicating a linear decrease of the rate constant with increasing pressure throughout the temperature range investigated (40-80°C). Apparently, the conversion reaction is accelerated at higher temperatures. This behaviour of k_{conv} is in accordance to the results found previously. The response of the conversion rate was then empirically described by Eqn. 4.23:

$$\ln(k_{conv}) = \left(J_0 + J_1 \cdot p^{1.5} + J_2 \cdot T^2\right)^{-1} \qquad \textbf{(4.23)}$$

Regression analysis of the conversion rates yielded the following parameters: J_0 = -0.155 ± 0.098; $J_1 = 5.763*10^{-6} \pm 5.119*10^{-6}$; $J_2 = -4.562*10^{-5} \pm 2.328*10^{-5}$.

After reintegrating the models for enzyme inactivation and substrate conversion the over-all reaction for the liberation of fermentable sugars due to enzymatic starch hydrolysis in response

to different p-T combinations can be calculated for a fixed treatment time. After 30 min mashing malt starch in the presence of malt α- and β-amylase a maximum of liberated fermentable sugars was found at 163 MPa and 71°C (Fig. 4.7). The isolines in Fig. 4.7 denote the percentage of sugar release relative to this maximum. Under optimal conditions (163 MPa and 71°C) the liberation of fermentable sugar is approximately 30% higher than at optimal conditions at ambient pressure (63°C). As already shown also for other enzymes, pressure is shifting the equilibrium of thermal reaction acceleration and simultaneously enzyme inactivation towards higher pressures and temperatures.

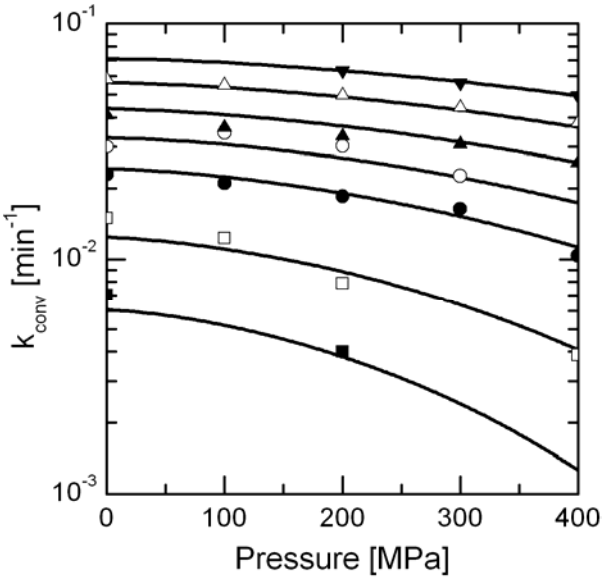

Fig. 4.44: Pressure dependence of the conversion rate constant (k_{conv}) of joint action of α- and β-amylase in ACES buffer (0.1 M; pH 5.6; containing 250 mg/mL gelatinized barely malt starch, 90 mM NaCl and 3.8 mM $CaCl_2$) at 40°C (■); 50°C (□); 60°C (●); 65°C (○); 70°C (▲); 75°C (△) and 80°C (▼).

Nowadays, breweries tend to use “high temperature-short-time” mashing processes applying high mashing-in temperatures of approximately 60°C and short temperature rests (Methner, F-J, personal communication). The total process time averages approximately 90-100 minutes. Based on the found effects of pressure and temperature on the catalytic activity, a temperature-time profile for a mashing process under high pressure conditions was calculated by approximation. For mashing at 100 MPa the following pressure time profile was estimated to give the same conversion rates as the standard profile at ambient pressure: 20 min at 65°C, 20 min at 70°C and 20 min at 75°C. High pressure mashing at 150 MPa yielded: 20 min at 70°C, 20 min at 75°C and 20 min at 80°C. Heating rate was assumed to be 1°C/min.

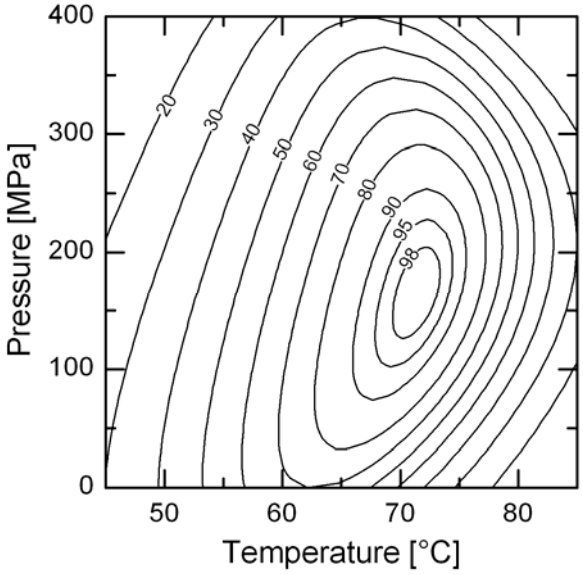

Fig. 4.45: Liberated reducing sugars from barely malt starch by α- and β-amylase in ACES buffer (0.1 M; pH 5.6; containing 10 mg/mL gelatinized barely malt starch, 90 mM NaCl and 3.8 mM $CaCl_2$) at different pressure-temperature conditions after 30 minutes exposure time. Isolines denote the percentage relative to the maximum release observed at 163 MPa and 71°C.

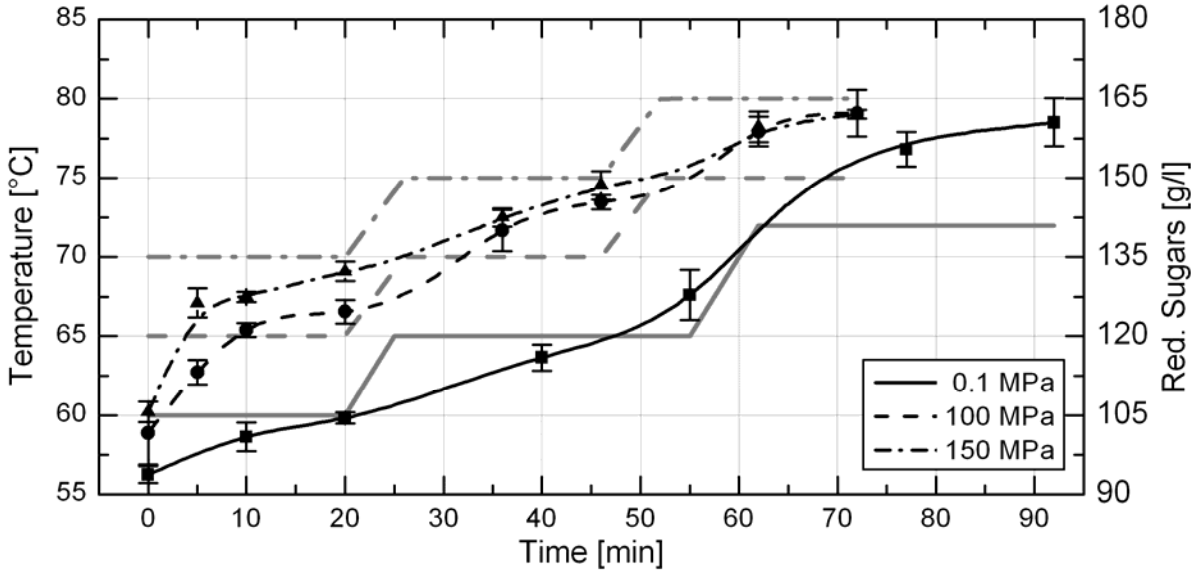

Fig. 4.46: Temperature-time profiles of different mashing programs and the corresponding amounts of liberated reducing sugars. The symbols denote the applied pressures as follows: 0.1 (■); 100 (●); and 150 (▲) MPa.

Fig. 4.46 shows the selected temperature time profiles at 0.1, 100 and 150 MPa and the corresponding amount of reducing sugars at different time intervals. It is evident that the enzymatic hydrolysis of starch and hence, the liberation of sugars can be accelerated by

applying 100 MPa and using an appropriate temperature-time profile. After 72 minutes the sugar concentration in the mash was similar to the concentration of sugars found at the end of the reference mashing program (after 93 min). The increase of pressure up to 150 MPa with the corresponding temperature-time profile did not result in a higher amount of sugars or shorter mashing times. The amount of sugar released in the beginning to the mashing program was significantly higher than in the other mashes presumably due to high gelatinization rates of the starch and high enzymatic starch conversion at 70°C. However, in the course of mashing the release of sugars slowed down and finally equalled to the concentration of reducing sugars found in the mash treated at 100 MPa.

Finally, the three mashes were analysed with regard to fermentable sugars. HPLC analysis of the in the final mashes showed no significant differences in the concentration of fermentable sugars (Fig. 4.47). However, small changes of the composition have been detected which might be explained by a shift in catalytic activity of the numerous enzymes present in barley malt (Stenholm 1997). Whereas the concentration of the most important sugar maltose was slightly increased in the high pressure mashes (0.1 MPa: 105.7 g/L; 100 MPa: 108.1 g/L; 150 MPa: 109.1 g/L) bei., the concentration of maltotriose was found to be reduced (0.1 MPa: 19.0 g/L, 100 MPa: 17.9 g/L, 150 MPa: 15.1 g/L). The concentration of glucose changed from 7.6 g/L (0.1 MPa) to 21.3 g/L (150 MPa). Fructose remained at a concentartion of approximately 3 g/L in all three mashes.

However, it can be concluded that the mashing time (saccharification of barley malt starch) can be reduced by approximately 25% when applying pressures in the range 100-150 MPa and increasing the average temperature by approximately 5°C. This can be explained by 3 factors influencing the rate of starch conversion: 1. The digestability of starch granules is strongly increased after hydration (i.e. gelatinization). Since the rate of starch granule swelling and subsequent gelatinization is increased by temperature the enzymatic action is accelerated aslo. 2. The catalytic rate of the most important enzymes in mashing (α- and β-amylase) is significantly increased by temperature. 3. Pressure up to 200 MPa increases the thermo-stability the activity of α- and β-amylase and hence preserves their activity at higher temperatures.

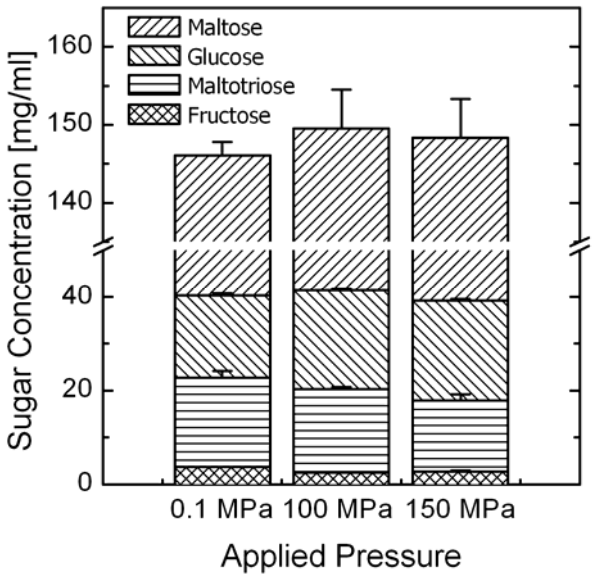

Fig. 4.47: Concentration of fermentable sugars (maltose, glucose, maltotriose, fructose) in the mash at the end of the three different mashing programs at 0.1, 100 and 150 MPa shown in Fig. 4.46.

5. CONCLUSIONS AND PERSPECTIVE

Due to its low production costs amylolytic enzymes are nowadays widely used for the industrial production of fermented foods, alcoholic beverages and glucose syrups from starch and cellulose. Large production scale and low profit margins of those products always results in a demand for an acceleration of the rate of enzymatic cleavage of the starch macromolecule. Usually the increase of the temperature can significantly speed up the catalytic rate of an enzymatic reaction, however, at higher temperatures the effect on enzyme denaturation becomes dominant and the conversion rate is decreasing again.

In this study the applicability of high hydrostatic pressure to accelerate enzymatic conversions of food biopolymers has been investigated for various enzyme-substrate systems.

The effects of high pressure and temperature on the stability and catalytic activity of α-amylase, β-amylase and β-glucanase from barley malt, β-glucanase from *Bacillus subtilis* as well as glucoamylase from *Aspergillus niger* in pressure invariant ACES buffer are presented. Furthermore, gelatinization kinetics of maize starch granules have been investigated in different pressure temperature domains. In the last phase of this study, enzymatic starch conversion was studied in different pressure temperature domains using the example of maize starch saccharification by glucoamylase from *Aspergillus niger* and barley malt conversion by combined action of α-and β-amylase from barley.

Although numerous reports state that thermal and pressure inactivation of enzymes can be described by first order kinetics (Ludikhuyze et al. 2002; Seyderhelm et al. 1996), the isobaric/isothermal kinetics of α- and β-amylase as well as of β-glucanases indicated significant deviations from simple first-order kinetics in the p-T domain investigated (30-75°C; 0.1-1000 MPa). Therefore, the inactivation kinetics were simply described by a n^{th}-order reaction model. Enzyme inactivation of an higher order was related to the existence of several isoenzyme fractions and possible interactions with stabilizing components in their extracts or samples. The reaction order n of the enzyme inactivation has been determined by minimizing the cumulative standard error of the curve fits of the complete experimental kinetic data sets. An order of 1.4 (β-amylase), 1.6 (β-glucanase from barley), 1.8 (β-glucanase from *B.subtilis*), and 2.1 (α-amylase) was found to be the minimum of the error function derived from regression analysis and used for the determination of the rate constants k_{inact} of all p-T conditions tested. The inactivation kinetics of glucoamylase showed a clear biphasic character which was related to the presence of two isoenzyme forms with different p-T stabilites. Hence, the kinetics were sufficiently described by a two-fractional-model using first-order kinetics.

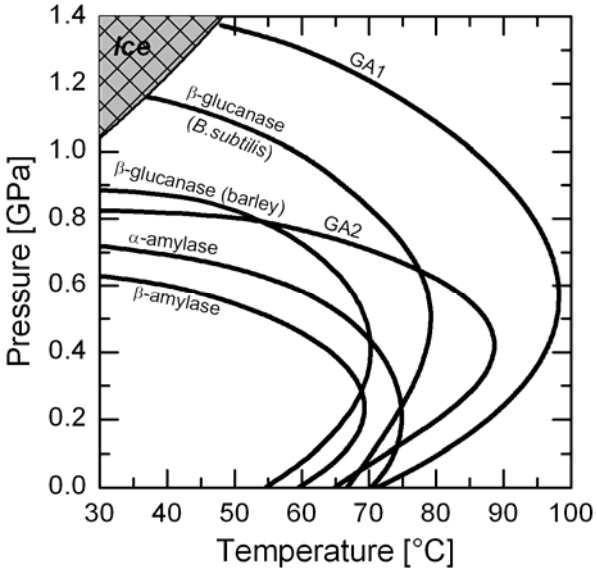

Fig. 5.1: Pressure-temperature isorate diagram for 95% inactivation of β-amylase, β-glucanase (barley malt) and β-glucanase (*B.subtilis*) in ACES buffer (pH 5.6; 0.1 M), α-amylase in ACES buffer (pH 5.6; 0.1 M, containing 90 mM NaCl and 3.8 mM $CaCl_2$), and glucoamylase isoenzymes GA1 and GA2 in ACES buffer (pH 4.5; 0.1 M) after 30 minutes exposure time.

The change of the inactivation rate constant k_{inact} in response to pressure and temperature were mathematically described using third-degree, thermodynamically based polynomial equations. Fig. 5.1 shows the isorate lines of 95% inactivation of enzymes investigated in this study occurring after 30 min treatment time. Elliptical shaped isorate lines were found for all enzymes, indicating specific resistance towards combined pressure-temperature treatment. Glucoamylase isoenzyme GA1 was the most stable enzyme in this collection, preserving most of its activity up to 1200 MPa at temperatures below 60°C. β-amylase showed the lowest pressure resistance and quickly lost its activity at pressures higher 550 MPa and room temperature. In the presence of Ca^{2+} ions α-amylase is inactivated at 720 MPa, GA2 at 810 and β-glucanase at approximately 900 MPa and 30°C after 30 min. Furthermore, the enzymes show a significant stabilization against thermal induced denaturation at approximately 200 (α- and β-amylase), 400 MPa (β-glucanase from barley and GA2), 500 MPa (β-glucanase from *B.subtilis*), and 600 MPa (GA1). At these specific pressures k_{inact} is of approximately 20-200 times slower than at atmospheric pressure and leads to such elliptical shaped isorate-curves. The differences in pressure and temperature stability can be explained by the differences in structure and conformation of the enzymes presented. It has been reported that even minimal variations in the amino acid sequence of an enzyme can cause extreme differences in its physical stability (Christensen et al. 1999; Svensson et al. 1986). However, the effect of enzyme structure on thermal and/or piezo stability is not fully understood yet. It is apparent from Fig. 5.1 that the

thermo-stability of an enzyme cannot be related to its pressure-stability. For instance, β-glucanase from barley showed a high sensitivity to temperature but resisted higher pressures than enzymes with a higher thermo-stability.

In order to estimate the pressure and temperature effects on an enzymatic catalyzed substrate conversion, the reaction has to be corrected from the superimposed effect on enzyme inactivation. By fitting the kinetics of substrate conversion to the kinetic models of enzyme stability it was possible to gain insights into the p-T dependence of the hydrolytic rate of the enzymes investigated. After correction, most enzymes investigated showed a reduction of their catalytic rate under elevated pressure (up to 600 MPa) conditions throughout a wide range of temperature (30-80°C). However, disregarding the overlapping enzyme inactivation, a strong acceleration of the conversion rate by temperature was detected. Fig. 5.2 shows the pressure dependence of the conversion rate constant k_{conv} of the five enzymes investigated at 50°C. For a better comparison, k_{conv} is presented relative to the specific rate constant found at ambient pressure. It is evident, that in case of α-amylase, β-amylase and β-glucanase from barley malt, as well as glucoamylase from *Aspergillus niger* the catalytic rate constant k_{conv} increases with increasing pressure. In contrast, the catalytic activity of β-glucanase from *B.subtilis* was strongly increased at elevated pressures. Compared to ambient pressure a 3.5 fold acceleration of β-glucan hydrolysis by this β-glucanase was detected at 200-300 MPa and 50°C. At higher pressures the catalytic rate decreased again, but still at 600 MPa k_{conv} was higher than at ambient pressure.

The native conformation of enzymes is often reversibly changed even at pressures of a few MPa. It is, therefore, not surprising that such changes of the tertiary and quaternary structure of an enzyme leads to changes in its catalytic activity. A reversible increase or decrease of the catalytic activity of enzymes has been reported by a number of authors (Dallet and Legoy 1996; Duvetter 2006; Masson et al. 2004; Mozhaev et al. 1996b; Verlent et al. 2005) and can be related either to favourable or detrimental changes of the protein structure which improve or impair substrate binding to the active centre. However, enzymatic catalysed reactions that are accompanied by a decrease in volume at constant temperature are favoured under high pressure conditions which might explain the highly accelerated degradation of Azo-barley glucan by β-glucanase from *B.subtilis* under high hydrostatic pressure conditions.

The effect of pressure and temperature on k_{conv} was described using empirical mathematic models which were then combined with the previously formulated models describing the enzyme inactivation in responds to pressure and temperature. With this procedure a specific maximum of product release was identified for the overall reaction of substrate conversion and simultaneously occurring enzyme inactivation. As a result of the thermo-stabilization of the

enzymes these optimums are shifted to higher temperatures and pressures. Highest enzymatic conversion of individual substrates was found at 100 MPa and 60°C (β-amylase), 165 MPa and 66°C (α-amylase), 220 MPa and 55°C (β-glucanase from barley malt), 270 MPa and 80°C (glucoamylase with maize starch), 307 MPa and 63°C (β-glucanase from *B.subtilis*) and 318 MPa and 84°C (glucoamylase with maltose) after 30 min exposure time. These optimal p-T conditions provide an acceleration of enzymatic catalysis of approximately 20-400% after 30 minutes compared to the maximal rate at atmospheric pressure.

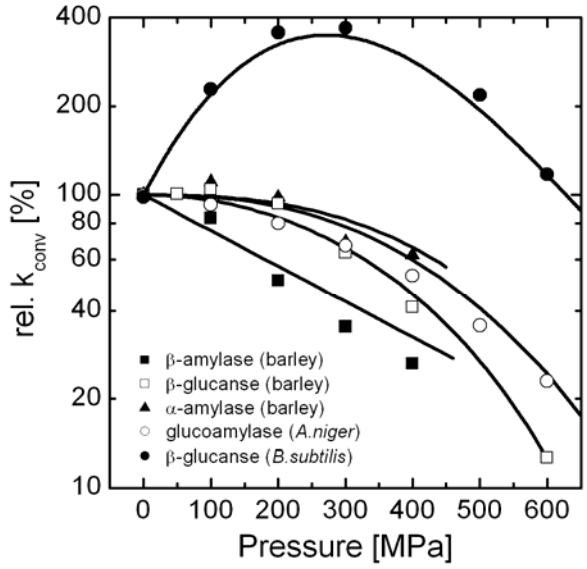

Fig. 5.2: The changes of the conversion rate constants k_{conv} with pressure at 50°C. k_{conv} is presented relative to the specific rate constant at 50°C and ambient pressure.

At present, the knowledge on the mechanistic background of pressure induced starch gelatinization is not complete; p-T diagrams showing the phase transition of starches over a wide range of temperature and pressure are rare. In this study, the loss in birefringence has been used as an indicator of granule gelatinization of maize starch in response to combinations of pressure (<650 MPa) and temperature (<75°C). Starch gelatinization at ambient pressure as well as under high pressure followed a reaction order of 1.65. The often reported difference in high temperature gels and high pressure gels is not reflected by specific gelatinization kinetics.

Using a sigmoidal secondary model with T_m as reference point, the rate constant of starch granule gelatinization was formulated as a function of pressure and temperature. From this model lines of identical effect were calculated and plotted in a pressure temperature diagram. The rate of birefringence loss was found to be temperature dependent, only, unless the pressure is exceeding 300 MPa. At those pressures, the isorate lines are bended to the left, indicating that

the phase transition in birefringence is occurring at lower temperatures. High pressure gels are weaker than thermal induced gels, however it has been found that the reachable degree of hydration is sufficient to convert the almost inert starch granule to a substrate for enzymatic action.

In the final stage of this study it was shown that the enzymatic conversion of native maize starch granules by glucoamylase could be accelerated up to 2.5 fold by increasing the pressure and temperature up to optimal conditions (e.g. 270 MPa and 80°C for a 30 min process). In addition, it was proven that the enzymatic conversion of barley malt starch (the mashing process in breweries and distilleries) into fermentable sugars can be reduced by approximately 25% in time by increasing the pressure to 100 MPa in combination with a suitable temperature-time profile.

The applications of pressure-temperature related changes are numerous. They are ranging from elimination of virus infectivity from food under milder temperature conditions to the unfolding of food proteins for the generation of gels with well defined properties.

This study has shown that high hydrostatic pressure is a powerful tool to affect enzyme stability and catalytic activity. Basic data on the impact of pressure, temperature and treatment time on selected enzymes and maize starch have been acquired at lab scale.

It was shown that by applying high hydrostatic pressures the enzymatic starch saccharification can be accelerated significantly and could be operated in an one step process without previous starch gelatinization. The use of high pressure treatment to initiate subsequent biodegradation either at ambient or at elevated pressure provides interesting options for food and bioprocessing. The combination of polysaccharide stability data and the kinetics of enzyme inactivation is particularly interesting, since a better availability of the substrate and a more stable enzyme with a comparably high turnover rate is extremely promising for large-scale enzymatic in food and biotechnology. The dependence of the catalytic activity of enzymes on pressure and temperature also creates opportunities to manipulate chemical reactions. For example, enzyme-catalyzed transformation of two substrates might be regulated if the catalytic conversion of both substrates differs under pressure.

Increasing prices of fossil fuels and environmental factors have also triggered the demand of fuels and fuel surrogates from renewable resources. For a short time, bioethanol is used as a fuel substitute to reduce greenhouse gas emissions and the dependence from diminishing oil supplies. Bioethanol is mainly produced by fermentation of sugars which are usually recovered by enzymatic hydrolysis of starch or cellulose rich crops. However, this conversion process is very expensive and is still in its early stages of development. The presented data in this study,

(especially that of β-glucanase from *B.subtilis*) has shown the potential of high hydrostatic pressure to accelerate the catalytic reactivity of amylases and cellulases and may contribute to an efficient bioethanol production. Nevertheless, trials using biomaterial with high cellulose content should be performed in a technical scale and there is still a lack of knowledge on how cellulases act on cellulose under high hydrostatic pressure conditions.

In addition, the understanding of the mechanisms of action either for protein unfolding or for starch gelatinization by combined pressure-temperature treatment is still not completely understood. A more profound knowledge of how pressure and temperature act in combination will make high pressure technology to a more and more accepted process in industry.

6. CURRICULUM VITAE & LIST OF PUBLICATIONS

Roman Buckow

Ph.D. Student, M.Eng Food Engineering

Address:

Berlin University of Technology
Department of Food Biotechnology and
Food Process Engineering
Koenigin – Luise – Str. 22
14195 Berlin
Germany

Phone: +49 30 314 71257
Fax: +49 30 832 76 63

email: roman.buckow@tu-berlin.de

Roman Buckow
Fontanepromande 7
10967 Berlin
Germany

Phone: +49 30 6950 8413
Mobile: +49 171 221 2046
Fax: +49 30 691 4985

Email: roman.buckow@web.de

Biography

Since 09/2002	Ph.D. student at Berlin University of Technology, Prof. Dr. D. Knorr, Pressure and temperature effects on the enzymatic conversion of biopolymers
06/2002	M.Eng. (Dipl.-Ing.) Food Technology, Diploma-Thesis: Ultrasonication of mash from barley malt and its effect on the filtration and on the extraction of soluble solids, Prof. Dr. D. Knorr
1993-2002	Studies of Chemistry and Food Technology at Berlin University of Technology
Date of birth	March, 25th, 1973

Eidesstattliche Erklärung

Ich erkläre an Eides statt, dass die vorliegende Dissertation in allen Teilen von mir selbständig angefertigt wurde und die benutzten Hilfsmittel vollständig angegeben worden sind.

Weiter erkläre ich, dass ich nicht schon anderweitig einmal die Promotionsabsicht angemeldet oder ein Promotionseröffnungsverfahren beantragt habe.

Veröffentlichungen von irgendwelchen Teilen der vorliegenden Dissertation sind von mir wie folgt vorgenommen worden.

Berlin, 15.11.2006

Peer-reviewed primary publications:

1. **S. Lori, R. Buckow, D. Knorr, V. Heinz, A. Lehmacher (submitted).** Inactivation of *Campylobacter* spp. by heat and high hydrostatic pressure. Journal of Food Protection.
2. **S. Isbarn, R. Buckow, A. Himmelreich, D. Knorr, A. Lehmacher, V. Heinz (accepted).** Inactivation of avian influenza virus by heat and high hydrostatic pressure. Journal of Food Protection.
3. **R. Buckow, U. Weiss, V. Heinz, D. Knorr (in press).** Stability and catalytic activity of α-amylase from barley malt at different pressure-temperature conditions. Biotechnology & Bioengineering.
4. **R. Buckow, V. Heinz, D. Knorr (accepted).** High pressure phase transition kinetics of maize starch. Journal of Food Engineering.
5. **S. Fischer, W. Ruß, R. Buckow, V. Heinz, H. Ulmer, J. Behr, R. Meyer-Pittroff, D. Knorr, R. Vogel (2006).** Effects of hydrostatic high pressure on microbiological and technological characteristics of beer. Monatsschrift für Brauwissenschaft, 60:
6. **D. Knorr, V. Heinz, R. Buckow (2006).** High pressure application for food biopolymers. Biochimica et Biophysica Acta – Proteins and Proteomics, 1764(3): 619–631.
7. **D. Margosch, M. Ehrmann, R. Buckow, V. Heinz, R. Vogel, M. Gänzle (2006).** High pressure mediated survival of *Clostridium botulinum* and *Bacillus amyloliquifaciens* endospores at high temperature. Applied and Environmental Microbiology, 72(5): 3476-3481.
8. **R. Buckow, V. Heinz, D. Knorr (2005).** Effect of high hydrostatic pressure-temperature combinations on the activity of β-glucanase from barley malt. Journal of the Institute of Brewing, 111(3): 282–289.
9. **R. Buckow, V. Heinz, D. Knorr (2005).** Two fractional model for evaluating the activity of glucoamylase from *Aspergillus niger* under combined pressure and temperature conditions. Trans IChemE, Food and Bioproducts Processing, 83(C3): 220-228.
10. **V. Heinz, R. Buckow, D. Knorr (2005).** Catalytic activity of β-amylase from barley in different pressure-temperature domains. Biotechnology Progress, 21(6): 1632-1638.

Other publications

1. **R. Buckow, V. Heinz, D. Knorr (2006).** Stability of food quality related enzymes in different high pressure-temperature domains. In: Proceedings of 3rd International Meeting on High Pressure Chemical Engineering 2006, VDI Verlag, (*in press*).
2. **M. Gänzle D. Margosch, R. Buckow, M. Ehrmann, V. Heinz, R. Vogel (2006).** Pressure and heat resistance of *Clostridium botulinum* and other endospores. In: High pressure processing of foods (C. J. Dooner, C. P. Dunne, F. E. Feeherry Eds.), IFT Press, Blackwell Publishing, (*in press*)
3. **R. Buckow, V. Heinz, D. Knorr (2006).** Effect of high hydrostatic pressure and temperature on the enzymatic biotransformation of maize starch. In: Proceedings of *GDL Congress "Food Technology 2005*", VDI Verlag, (*in press*).
4. **R. Buckow, V. Heinz, D. Knorr (2005).** Acceleration of the beer mashing process by applying high hydrostatic pressure. In: Proceedings of IntradFood - EFFoST Conference 2005, Elsevier, London. 1359-1362.

Selected oral presentations at scientific meetings

1. **R. Buckow, S. Lori, S. Isbarn, D. Knorr, A. Lehmacher,_V. Heinz (2006).** High pressure temperature isokinetic diagrams of pathogenous microbes and viruses. Oral presentation at *4th* International Conference on High Pressure Bioscience and Biotechnology, 25-29 September 2006, Tsukuba, Japan.

2. **R. Buckow, V. Heinz, D. Knorr (2006).** Optimized high pressure pasteurization of raw meat. Oral presentation at *44th EHPRG International Conference*, 4-8 September 2006, Prague, Czech Republic.

3. **R. Buckow, V. Heinz (2006).** New software tool for predicting pressure/temperature effects on microbes and enzymes. Oral presentation at *AFE-Tech First Workshop - Applied food emerging technologies*, 5-7 July 2006, Barcelona, Spain.

4. **R. Buckow, V. Heinz, D. Knorr (2006).** Evaluation of pressure / temperature effects on food safety and quality. Oral presentation at *1st SAFE Consortium International Congress* "*Nutrition and Food Safety: Evaluation of Benefits and Risks*", 11-14 June 2006, Budapest, Hungary.

5. **R. Buckow, V. Heinz, D. Knorr (2006).** High Pressure Processing: Efficiency Analysis and Optimization of Treatment Conditions. Oral presentation at *International Symposium Food Factory of the Future 3*, 7-9 June 2006, Gothenburg, Sweden.

6. **R. Buckow, V. Heinz, D. Knorr (2006).** Stability of food quality related enzymes in different high pressure-temperature domains. Oral presentation at *3rd International Meeting on High Pressure Chemical Engineering*, 10-12 May 2006, Erlangen, Germany.

7. **R. Buckow, V. Heinz, D. Knorr (2006).** High pressure phase transition kinetics of maize starch in aqueous systems. Oral presentation at *57th Starch Convention,* 26-28 April 2006, Detmold, Germany.

8. **R. Buckow, V. Heinz, D. Knorr (2006).** Stability and activity of enzymes under high pressure. Oral presentation at *The annual meeting of the GVC on food process technology*, 22-24 March 2006, Reinbeck, Germany.

9. **R. Buckow (2006).** What's the feature of high pressure preservation? Oral presentation at *MSTI-Symposium - Preservation without preservatives*, 22-23 February 2006, Munich, Germany.

10. **V. Heinz, R. Buckow (2006).** High pressure food processing as a tool for the elimination of virus. Oral presentation at *The Department of Livestock Development*, 18 February 2006, Bangkok, Thailand.

11. **V. Heinz, R. Buckow (2006).** Non-thermal technologies in food and bioprocessing. Oral presentation at *Washington State University*, 8 February 2006, Pullman (WA), USA.

12. **R. Buckow, V. Heinz, D. Knorr (2005).** Effect of high hydrostatic pressure and temperature on the enzymatic biotransformation of corn starch. Oral presentation at *GDL Congress "Food Technology 2005*", 6-8 October 2005, Dresden, Germany.

13. **R. Buckow, V. Heinz, D. Knorr (2005).** Effect of high hydrostatic pressure and temperature on the enzymatic biotransformation of corn starch. Oral presentation at *4th European Young Cereals Scientists and Technologists Workshop* , 29 June - 01 July 2005, Vienna, Austria.

14. **R. Buckow, A. Ardia, V. Heinz, D. Knorr (2004).** High hydrostatic pressure effects on microbial stability in acidic beverages. Oral presentation at *The Safe Consortium – Novel (mild) preservation technologies in relation to food safety*, 22-23 January 2004, Brussels, Belgium.

15. **R. Buckow, V. Heinz, D. Knorr (2003).** Effects of high pressure and temperature on inactivation, stabilization and conversion rate of hydrolytic enzymes. Oral presentation at *Joint Meeting of the Nonthermal processing division of IFT and EFFoST – Workshop on Nonthermal food preservation*, 7-10 September 2003, Wageningen, The Netherlands.

16. **V. Heinz, A. Ardia, R. Buckow, D. Knorr (2003).** Survival of bacteria under pressures up to 1.5 GPa – new apparatus for experiments under isothermal conditions, Oral presentation at *Joint 19th AIRAPT and 41st EHPRG International Conference*, 7-11 July 2003, Bordeaux, France.

17. **V. Heinz, A. Ardia, R. Buckow, D. Knorr (2003).** Inactivation of spores by pressure assisted heating, Oral presentation at *1st FEMS Congress of European Microbiologists*, 29 June- 3 July 2003, Ljubljana, Slovenia.

Selected poster presentations at scientific meetings

1. **R. Buckow, S. Isbarn, D. Knorr, A. Lehmacher, V. Heinz (2006).** High pressure inactivation of avian influenza virus in poultry meat. Poster presentation at the annual IFT-NPD/EFFoST Workshop *Non Thermal Food 2006*, 11-13 September 2006, Cork, Ireland.
2. **A. Mathys, R. Buckow, V. Heinz, D. Knorr (2006).** Theoretical calculation of the pH-value in buffers under high pressure. Poster presentation at *3rd International Meeting on High Pressure Chemical Engineering*, 10-12 May 2006, Erlangen, Germany.
3. **R. Buckow, V. Heinz, D. Knorr (2005).** Acceleration of the beer mashing process by applying high hydrostatic pressure. Poster presentation at *IntradFood – EFFoST Conference 2005*, 25-28 October 2005, Valencia, Spain.
4. **R. Buckow, V. Heinz, D. Knorr (2005).** Enzymatic conversion reactions under high pressure. Poster presentation at *Nonthermal Processing Division Meeting and Workshop*, 15-16 September 2005, Wyndmoor PA, USA.
5. **R. Buckow, V. Heinz, D. Knorr (2005).** Effect of high hydrostatic pressure and temperature on the enzymatic biotransformation of corn starch. Poster presentation at *ICC Jubilee Conference*, 03-06 July 2005, Vienna, Austria.
6. **R. Buckow, V. Heinz, D. Knorr (2004).** Improvement of the conversion activity of β-amylase and β-glucanase from barley malt by combined high pressure and temperature conditions. Poster presentation at *Annual status seminar: High Pressure Food Technology and Food Process Engineering*, 21-22 September 2004, Freising, Germany.
7. **R. Buckow, V. Heinz, D. Knorr (2004).** Effect of a combined high pressure and temperature treatment on the stability and conversion rate of β–amylase and glucoamylase. Poster presentation at *International Congress on Engineering and Food (ICEF9)*, 7-11 March 2004, Montpellier, France.
8. **R. Buckow, V. Heinz, D. Knorr (2003).** Short time, high pressure treatment of beverages. Poster presentation at *The Safe Consortium – Newly Emerging Pathogens, Including Risk Assessment and Risk Management*, 24-25 April 2003, Brussels, Belgium.
9. **R. Buckow, I. Virkajärvi, V. Heinz, D. Knorr (2001).** Ultrasonication of mash from barley malt and its effect on the filtration and on the extraction of soluble solids. Poster presentation at *EUROCRAFT 2001*, 5-7 December 2001, Berlin, Germany.

7. REFERENCES

Aa KF, R.; Lindahl, V.; Tronsmo, A. 1994. Characterization of production and enzyme properties of an endo-beta-1,4-b-glucanase from *Bacillus subtilis* CK-2 isolated from compost soil. Antonie van Leeuwenhoek 66:319-326.

Ahern TJ, Klibanov AM. 1985. The mechanisms of irreversible enzyme inactivation at 100°C. Science 228:1280-1284.

Ajandouz EH, Abe J, Svensson B, Marchis-Mouren G. 1992. Barley malt-a-amylase. Purification, action pattern, and subsite mapping of isozyme 1 and two members of the isozyme 2 subfamily using p-nitrophenylated maltooligosaccharide substrates. Biochimica et Biophysica Acta 1159:193-202.

Aleshin AE, Hoffman C, Firsov LM, Honzatko RB. 1994. Refined crystal structures of glucoamylase from *Aspergillus awamori* var. X100. Journal of Molecular Biology 238:575-591.

Alvarez-Martinez MA, Torrent J, Lange R, Verdier J-M, Balny C, Liautard J-P. 2003. Optimized overproduction, purification, characterization and high-pressure sensitivity of the prion protein in the native (PrPC-like) or amyloid (PrP(Sc)-like) conformation. Biochimica et Biophysica Acta 1645(2):228-240.

Anderson WA, McClure PJ, Baird-Parker TC, Cole MB. 1998. The application of a log-logistic model to describe the thermal inactivation of *Clostridium botulinum* at 213B at temperatures below 121-1°C. Journal of Applied Bacteriology 80:283-290.

Anonymus. 2006. http://www.goosepoint.com/productsOystersPressure.html.

Arabas J, Szczepek J, Dmowki L, Heinz V, Fonberg-Broczek M. 1999. New technique for kinetic studies of pressure-temperature induced changes of biological materials. In: Ludwig H, editor. Advances in high pressure bioscience and biotechnology. Berlin: Springer. p 537-540.

Ardia A. 2004. Process considerations on the application of high pressure treatment at elevated temperature levels for food preservation (Dissertation). Berlin: Berlin University of Technology. 102 p.

Arica MY, Alaeddinoglu NG, Hasirci V. 1998. Immobilization of glucoamylase onto activated pHEMA/EGDMA microspheres: properties and application to a packed-bed reactor. Enzyme Microb. Technol. 22:152-157.

Au KS, Chan KY. 1987. Purification and properties of the endo-1,4-beta-glucanase from *Bacillus subtilis*. Journal of General Microbiology 133:2155-2162.

Bak SN, Ekengren Ö, Ekstam K, Härnulv G, Pajunen E, Prucha P, Rasi J. 2001. Manual of Good Practice. Convention TaEFotEB, editor. Nürnberg: Hans Carl-Verlag. 129 p.

Baks T, Janssen AEM, Boom RM. 2006. The effect of carbohydrates on a-amylase activity measurements. Enzyme and Microbial Technology 39(1):114-119.

Balny C. 1998. High Pressure Enzyme Kinetics. In: Ludwig H, editor. Advances in High Pressure Bioscience and Biotechnology. Heidelberg: Springer Verlag.

Balny C, Masson P. 1993. Effects of high pressure on proteins. Food Reviews International 9:611-628.

Bamforth CW, Martin HL, Wainwright T. 1979. A role for carboxypeptidase in the solubilization of barley b-glucan. Journal of the Institute of Brewing 85:334-338.

Barbosa-Cánovas GV, Pothakamury UR, Palou E, Swanson BG. 1997. Nonthermal preservation of foods. New York: Marcel Dekker. 276 p.

Baskakov IV, Legname G, Baldwin MA, Prusiner SB, Cohen FE. 2002. Pathway complexity of prion protein assembly into amyloid. The Journal of Biological Chemistry 277(24):21140-21148.

Bauer BA, Knorr D. 2005. The impact of pressure, temperature and treatment time on starches: pressure-induced starch gelatinisation as pressure time temperature indicator for high hydrostatic pressure processing. Journal of Food Engineering 68:329–334.

Belitz H-D, Grosch W, Schieberle P. 2004. Food chemistry. Belitz H-D, Grosch W, Schieberle P, editors. Berlin: Springer Verlag. 1070 p.

Bertroft E, Andtfolk C, Kulp SE. 1984. Effect of pH, temperature, and calcium ions on barley malt a-amylase isozymes. Journal of the Institute of Brewing 90:298-302.

Biochemistry NCotIUo. 1992. Enzyme Nomenclature 1992. San Diego: Academic Press.

Bissinger H. 2002. Enzyme Kinetics. Weinheim: Wiley-VCH Verlag GmbH. 255 p.

Blanshard JMV. 1987. Starch granule structure and function: a physicochemical approach. In: Galliard T, editor. Starch: properties and potential. Chichester, GB: John Wiley and Sons. p 16-54.

Boonyaratanakornkit BB, Park CB, Clark DS. 2002. Pressure effects on intra- and intermolecular interactions within proteins. Biochimica et Biophysica Acta 1595:235-249.

Borda D, Van Loey A, Smout C, Hendrickx M. 2004. Mathematical models for combined high pressure and thermal plasmin inactivation kinetics in two model systems. Journal of Dairy Science 87:4042–4049.

Bozonnet S, Kim T-j, Bønsager BC, Kramhøft B, Nielsen PK, Bak-jensen KS, Svensson B. 2003. Engineering of barley a-amylase. Biocatalysis and Biotransformation 21:209-214.

Brandts JF, Oliveira RJ, Westort C. 1970. Thermodynamics of protein denaturation. Effect of pressure on the denaturation of Ribonuclease A. Biochemistry 9(4):1038-1047.

Bridgman PW. 1912. Water in the liquid and five solid forms under pressure. Proceedings of the American Academy of Arts and Science XLVII(13):441-558.

Bridgman PW. 1914. The Coagulation of albumen by pressure. Journal of Biological Chemistry 19(4):511-512.

Bridgman PW. 1931. The physics of high pressure. London: G. Bells & Sons. XXX p.

Briggs GE, Haldane JBS. 1925. A note on the kinetics of enzyme action. Biochemical Journal 19:338-339.

Brown P, Meyer R, Cardone F, Pocchiari M. 2003. Ultra-high-pressure inactivation of prion infectivity in processed meat: A practical method to prevent human infection. PNAS 100(10):6093-6097.

Buckow R, Heinz V, Knorr D. 2005a. Effect of high hydrostatic pressure-temperature combinations on the activity of b-glucanase from barley malt. Journal of the Institute of Brewing 111(3):282–289.

Buckow R, Heinz V, Knorr D. 2005b. Two fractional model for evaluating the activity of glucoamylase from *Aspergillus niger* under combined pressure and temperature conditions. Trans IChemE, Part C, Food and Bioproducts Processing 83(C3):220-228.

Buleon A, Tran V. 1990. Systematic conformational search for the branching point of amylopectin. International Journal of Biological Macromolecules 12:345–352.

Bush DB, Sticher L, van Huystee R, Wagner D, Jones RL. 1989. The calcium requirement for stability and enzymatic activity of two isoforms of barley aleurone a-amylase. Journal of Biological Chemistry 264:19392-19398.

Calci KR, Meade GK, Tezloff RC, Kingsley DH. 2005. High-pressure inactivation of hepatitis A virus within oysters. Applied and Environmental Microbiology 71(1):339–343.

Castro SM, Van Loey A, Saraiva JA, Smout C, Hendrickx M. 2006a. Identification of pressure/temperature combinations for optimal pepper (*Capsicum annuum*) pectin methylesterase activity. Enzyme and Microbial Technology 38(6):831-838.

Castro SM, Van Loey A, Saraiva JA, Smout C, Hendrickx M. 2006b. Inactivation of pepper (*Capsicum annuum*) pectin methylesterase by combined high-pressure and temperature treatments. Journal of Food Engineering 75:50-58.

Cavaille D, Combes D. 1996. Effect of high hydrostatic pressure and additives on the dynamics of water: a spectroscopic study. Journal of Ramanan Spectroscopy 27:853-857.

Chaplin MF. 2006. Water structure and behaviour.

Cheftel JC. 1992. Effects of high hydrostatic pressure on food constituents: An overview. In: Balny C, Hayashi R, Heremans K, Masson P, editors. High Pressure and Biotechnology. Montrouge: John Libbey Eurotext. p 195-209.

Cheftel JC. 1995. High-pressure, microbial inactivation and food preservation. Food Science and Technology International 1:75-90.

Chen H, Hoover DG, Kingsley DH. 2005. Temperature and treatment time influence high hydrostatic pressure inactivation of feline calicivirus, a norovirus surrogate. Journal of Food Protection 68(11):2389-2394.

Chen H, Joerger RD, Kingsley DH, Hoover DG. 2004. Pressure inactivation kinetics of phage 8 CI 857. Journal of Food Protection 67(3):505-511.

Christensen T, Frandsen TP, Kaarsholm NC, Svensson B, Sigurskjold BW. 2002. Physicochemical characterisation of the two active site mutants Trp52-Phe and Asp55-Val of glucoamylase from Aspergillus niger. Biochimica et Biophysica Acta 1601:163-171.

Christensen T, Svensson B, Sigurskjold BW. 1999. Thermodynamics of reversible and irreversible unfolding and domain interactions of glucoamylase from Aspergillus niger studied by differential scanning and isothermal titration calorimetry. Biochemistry 38:6300-6310.

Christensen U, Olsen K, Stoffer BB, Svensson B. 1996. Substrate binding mechanism of Glu180-Gln, Asp176-Asn, and wild-type glucoamylases from Aspergillus niger. Biochemistry 35:15009-15018.

Cohen FE, Prusiner SB. 1998. Pathologic conformations of prion proteins. Annu. Rev. Biochem. 67:793-819.

Colloc'h N, Girard E, Dhaussy A-C, Kahn R, Ascone I, Mezouar M, Fourme R. 2006. High pressure macromolecular crystallography: The 140-MPa crystal structure at 2.3 A resolution of urate oxidase, a 135-kDa tetrameric assembly. Biochimica et Biophysica Acta 1764(3):391-397.

Comrie AAD. 1967. Brewing liquor - a review. Journal of the Institute of Brewing 73:335-341.

Cooke D, Gidley MJ. 1992. Loss of crystalline and molecular order during starch gelatinisation: origin of the enthalpic transition. Carbohydrate Research 227:103-112.

Crelier S, Robert MC, Claude J, Juillerat MA. 2001. Tomato (Lycopersicon esculentum) Pectin Methylesterase and Polygalacturonase Behaviors Regarding Heat- and Pressure-Induced Inactivation. Journal of Agriculture and Food Chemistry 49:5566-5575.

Dallet S, Legoy M-D. 1996. Hydrostatic pressure induces conformational and catalytic changes on two alcohol dehydrogenases but no oligomeric dissociation. Biochimica et Biophysica Acta 1294:15-24.

Dalmadi I, Rapeanu G, Van Loey A, Smout C, Hendrickx M. 2006. Characterisation and inactivation by thermal and pressure processing of strawberry (*Fragaria Ananassa*) polyphenol oxidase: a kinetic study. Journal of Food Biochemistry 30:56-76.

Debye P, Hueckel E. 1923. Zur Theorie der Elektrolyte I. Physikalische Zeitschrift 24:185-206.

Doan DNP, Fincher GB. 1992. Differences in the thermostabilities of barley (1-3,1-4)-b-glucanases are only partly determined by N-glycosylation. FEBS 309(3):265-271.

Douzals JP, Perrier-Cornet JM, Coquille JC, Gervais P. 2001. Pressure-temperature phase diagram for wheat starch. Journal of Agriculture and Food Chemistry 49:873-876.

Duvetter TF, I.; Sila, D. N.; Verlent, I.; Smout, C.; Clynen, E.; Schoofs, L.; Schols, H.; Hendrickx, M.; Van Loey, A. 2006. Effect of temperature and high pressure on the activity and mode of action of fungal pectin methyl esterase. Biotechnology Progress:Published on Web 08/11/2006.

Eglinton JK, Langridge P, Evans DE. 1998. Thermostability variation in alleles of barley beta-amylase. Journal of Cereal Science 28(3):301-309.

Evans DE, Wallace W, Lance RCM, MacLeod LC. 1997. Measurement of beta-amylase in malting barley (*Hordeum vulgare*L.). II. The effect of germination and kilning. Journal of Cereal Science 26:241-250.

Eyring H. 1935. The activated complex in chemical reactions. Journal of Chemical Physics 3:107-115.

Fabian H, Schultz C, Naumann D, Landt O, Hahn U, Saenger W. 1993. Secondary structure and temperature-induced unfolding and refolding of ribonuclease T1 in aqueous solution : a fourier transform infrared spectroscopic study. Journal of Molecular Biology 232:967-981.

Fannon JE, Hauber RJ, BeMiller JN. 1992. Surface pores of starch granules. Cereal Chemistry 69:284-288.

Farkas DF, Hoover DG. 2001. High pressure processing. Journal of Food Science Supplement:47-64.

Fogarty WM, Benson CP. 1983. Purification and Properties of a Thermophilic Amyloglucosidase from Aspergillus niger. Eur. J. Appl. Micobiol. Biotechnol. 18:271-278.

Frandsen TP, Christensen T, Stoffer B, Lehmbeck J, Dupont C, Honzatko RB, Svenson B. 1995. Mutational analysis of the roles in catalysis and substrate recognition of arginines 54 and 305,

aspatic acid 309, and tryptophan 317 located at subsides 1 and 2 in glucoamylase from Aspergillus niger. Biochemistry 34:10162-10169.

Frandsen TP, Fierobe HP, Svensson B. 2000. Engineering specificity and stability in glucoamylase from Aspergillus niger. In: Alberghina L, editor. Protein Engineering in Industrial Biotechnology. Amsterdam: Harwood Academic. p 189-206.

French DM. 1984. Organization of starch granules. In: Whistler RL, Paschall EF, BeMiller JN, editors. Starch chemistry and technology. New York: Academic Press. p 188-189.

Gallant DJ, Bouchet B, Baldwin PM. 1997. Microscopy of starch: evidence of a new level of granule organization. Carbohydrate Polymers 32:177-191.

Gallant DJ, Bouchet B, Buléon A, Pérez S. 1992. Physical characteristics of starch granueles and susceptibility to enzymatic degradation. European Journal of Clinical Nutrition 46:S3-S16.

Garcia AF, Butz P, Tauscher B. 2002. Mechanism-based irreversible inactivation of horseradish peroxidase at 500 MPa. Biotechnology Progress 18:1076-1081.

Garcia AF, Heindl P, Voigt H, Büttner M, Wienhold D, Butz P, Stärke J, Tauscher B, Pfaff E. 2004. Reduced proteinase K resistance and infectivity of prions after pressure treatment at 60°C. Journal of General Virology 85:261-264.

Gaspari LP, Silva ACB, Gomes AMO, Freitas MS, Ano Bom APW, Schwarcz D, Mestecky J, Novak MJ, Foguel D, Silva JL. 2002. Hydrostatic pressure induces the fusion-active state of enveloped viruses. Journal of Biological Chemistry 277:8433-8439.

Gekko K. 2002. Compressibility gives new insights into protein dynamics and enzyme function. Biochimica et Biophysica Acta 1595:382-386.

Giddings NJ, Allard HA, Hite BH. 1929. Inactivation of the tobacco mosaic virus by high pressure. Phytopathology 19:749-750.

Gidley MJ, Bociek SM. 1985. Molecular organization in starches: a ^{13}C CP/MAS NMR study. Journal of the American Chemical Society 107:7040-7044.

Godet MC, Tran V, Delage MM, Buléon A. 1993. Molecular modelling of the specific interactions involved in the amylose complexation by fatty acids. International Journal of Biological Macromolecules 15:11-16.

Goldberg RN, Kishore N, Lennen RM. 2002. Thermodynamic quantities for the ionization reaction of buffers. Journal of Physical and Chemical Reference Data 31:231-370.

Gomes MRA, Clark R, Ledward DA. 1998. Effects of high pressure on amylases and starch in wheat and barley flours. Food Chemistry 63(3):363-372.

Greenwood CT. 1997. Observation on the structure of the starch granule. In: Blanshard JMV, Mitchell JR, editors. Polysaccharides in Food. London: Butterworths. p 139.

Grime KH, Briggs DE. 1995. Release and activation of barley b-amylase. Journal of the Institute of Brewing 101:337-343.

Gross M, Jaenicke R. 1994. Proteins under pressure: The influence of high hydrostatic pressure on structure, function and assembly of proteins and protein complexes. European Journal of Biochemistry 221:617-630.

Grove SF, Lee A, Lewis T, Stewart CM, Chen H, Hoover DG. 2006. Inactivation of foodborne viruses of significance by high pressure and other processes. Journal of Food Protection 69(4):957–968.

Guerin JR, Lance RCM, Wallace W. 1992. Release and activation of barley beta-amylase by malt endopeptidase. Journal of Cereal Science 15:5-14.

Guiavarc'h Y, Segovia O, Hendrickx M, Van Loey A. 2005. Purification, characterization, thermal and high-pressure inactivation of a pectin methylesterase from white grapefruit (*Citrus paradisi*). Innovative Food Science and Emerging Technologies 6(4):363-371.

Guiavarc'h Y, Sila D, Duvetter T, Van Loey A, Hendrickx M. 2003. Influence of sugars and polyols on the thermal stability of purified tomato and cucumber pectin methylesterases: a basis for TTI development. Enzyme and Microbial Technology 33:544-555.

Guyer RB, Holmquist JW. 1954. Enzyme regeneration in high temperature–short time sterilized canned foods. Food Technology 8:547–550.

Hamann SD. 1982. The influence of pressure on ionization equilibria in aqueous solutions. Journal of Solution Chemistry 11:63-68.

Hashizume C, Kimura K, Hayashi R. 1995. Kinetic analysis of yeast inactivation by high pressure treatment at low temperatures. Bioscience, Biotechnology and Biochemistry 59:1455-1458.

Hawley SA. 1971. Reversible pressure-temperature denaturation of chymotrypsinogen. Biochemistry 10(13):2436-2442.

Hei DJ, Clark DS. 1994. Pressure stabilization of proteins from extreme thermophiles. Applied and Environmental Microbiology 60:932-939.

Heindl P, Garcia AF, Buttner M, Voigt H, Butz P, Tauscher B, Pfaff E. 2005. Some physico-chemical parameters that influence proteinase K resistance and the infectivity of PrPSc after high pressure treatment. Brazilian Journal of Medical and Biological Research 38(8):1223-1231.

Heinz V, Buckow R, Knorr D. 2005. Catalytic activity of b-amylase from barley in different pressure/temperature domains. Biotechnology Progress 21:1632-1638.

Heinz V, Knorr D. 1996. High pressure inactivation kinetics of *Bacillus subtilis* cells by a three-state-model considering distribution resistance mechanisms. Food Biotechnology 10:149-161.

Heinz V, Knorr D. 2002. Effects of high pressure on spores. In: Hendrickx ME, Knorr D, editors. Ultra high pressure treatments of foods. New York: Kluwer Academic/ Plenum Publishers. p 77-114.

Heinz V, Kortschack F; 2002. Method for modifying the protein structure of PrP^{sc} in a targeted manner. Germany patent WO 02/49460.

Hendrickx M, Ludikhuyze L, Van den Broeck I, Weemaes C. 1998. Effects of high pressure on enzymes related to food quality. Trends in Food Science & Technology 9(5):197-203.

Heremans K. 1982. High pressure effects on proteins and other biomolecules. Annual Review of Biophysics and Bioengineering 11:1-21.

Heremans R, Smeller L. 1998. Protein structure and dynamics at high pressure. Biochimica et Biophysica Acta 1386:353-370.

Hernandez A, Cano MP. 1998. High-Pressure and Temperature Effects on Enzyme Inactivation in Tomato Puree. J. Agric. Food Chem. 46:266-270.

Hirata A, Adachi M, Utsumi S, Mikami B. 2004. Engineering of the pH optimum of *Bacillus cereus* b-amylase: Conversion of the pH optimum from a bacterial type to a higher-plant type. Biochemistry 43:12523-12531.

Hiromi K, Hamauzu Z, Takahashi K, Ono S. 1966. Kinetic study on Gluc-amylase: II. Competition between two types of substrate having a-1,4 and a-1,6 glucosidic linkage. The Journal of Biochemistry 59(4):411-418.

Hiromi K, Ohnishi M, Tanaka A. 1983. Subsite structure and ligand binding mechanism of glucoamylase. Molecular and Cellular Biochemistry 51:79-95.

Hite BH. 1899. The effects of pressure in preservation of milk. West Virgina Agricultural Experiment Station Bulletin 58:15-35.

Hizukuri S. 1986. Polymodal distribution of the chain lengths of amylopectins, and its significance. Carbohydrate Research 147:342-347.

Hoj PB, Fincher GB. 1995. Molecular evolution of plant b-glucan endohydrolase. The Plant Journal 7(3):367-379.

Home S, Pietilä K, Sjöholm K. 1993. Control of glucanolysis in mashing. Journal of the American Society of Brewing Chemists 51:108-113.

Home S, Stenholm K, Williamson A, Autio K. Propertiers of starch and cell wall components and their effects on processing; 1999; Melbourne.

Hon CC, Reilly PJ. 1979. Properties of b-amylase immobilized to alkylamine porous silica. Biotechnology and Bioengineering 21:505-512.

Hrmova M, Fincher GB. 1993. Purification and properties of three (1-->3)-b-D-glucanase isoenzymes from young leaves of barley (*Hordeum vulgare*). The Biochemical Journal 289:453-461.

Imberty A, Chanzy H, Pérez S, Bulèon A, Tran V. 1988. The double-helical nature of the crystalline part of A-starch. Journal of Molecular Biology 201:365-378.

Imberty A, Pérez S. 1988. A revisit to three dimensional structure of B-type starch. Biopolymers 27:1205-1221.

Indrawati, Van Loey A, Fachin D, Ly Nguyen B, Verlent I, Hendrickx M. 2002. Overview: Effect of high pressure on enzymes related to food quality - Kinetics as a basic for process engineering. High-Pressure Research 22:613-618.

Isbarn S, Buckow R, Himmelreich A, Lehmacher A, Heinz V. 2007. Inactivation of avian influenza virus by heat and high hydrostatic pressure. Journal of Food Protection:*in press*.

Jacobs H, Mischenko N, Koch MHJ, Eerlingen RC, Delcour JA, Reynaers H. 1998. Evaluation of the impact of annealing on gelatinisation at intermediate water content of wheat and potato starches: A differential scanning calorimetry and small angle X-ray scattering study. Carbohydrate Research 306:1-10.

Jaenicke R. 1981. Enzymes under extremes of physical conditions. Ann. Rev. Biophys. Bioeng. 10:1-67.

Jones RL, Jacobsen JV. 1991. Regulation of synthesis and transport of secreted proteins in cereal aleurone. International Review of Cytology 126:49-88.

Juge N, Andersen JS, Tull D, Roepstorff P, Svensson B. 1996. Overexpression, Purification, and Characterization of Recombinant Barley -Amylases 1 and 2 Secreted by the Methylotrophic YeastPichia pastoris. Protein Expression and Purification 8(2):204–214.

Juge N, Le Gal-Coeffet MF, Furniss CSM, Gunning AP, Kramhoft B, Morris VJ, Williamson G, Svensson B. 2002. The starch binding domain of glucoamylase from Aspergillus niger: overview of its structure, function, and role in raw-starch hydrolysis. Biologia 57(11):239-245.

Kadziola A, Abe J, Svenson B, Haser R. 1994. Crystral and molecular structure of barley a-amylase. Journal of Molecular Biology 239:104-121.

Kadziola A, Søgaard M, Svensson B, Haser R. 1998. Molecular structure of a barley a-amylase-inhibitor complex: implications for starch binding and catalysis. Journal of Molecular Biology 278:205-217.

Katopo H, Song Y, Jane J. 2001. Effect and mechanism of ultrahigh hydrostatic pressure on the structure and properties of starches. Carbohydrate Polymers 47:233-244.

Kaya H, Chan HS. 2002. Towards a consistent modeling of protein thermodynamic and kinetic cooperativity: how applicable is the transition state picture to folding and unfolding? Journal of Molecular Biology 315(4):899-909.

Kessler HG. 1996. Lebensmittel- und Bioverfahrenstechnik - Molkereitechnologie. München: Verlag A. Kessler.

Kettunen A, Hämäläinen JJ, Stenholm K, Pietilä K. 1996. A model for the prediction of b-glucanase activity and b-glucan concentration during mashing. Journal of Food Engineering 29(2):185-200.

Kingsley DH, Chen H, Hoover DG. 2004. Inactivation of selected picornaviruses by high hydrostatic pressure. Virus Research 102(2):221-224.

Kingsley DH, Hoover DG, Papafragkou E, Richards GP. 2002. Inactivation of hepatitis A virus and a calicivirus by high hydrostatic pressure. Journal of Food Protection 65(10):1605-1609.

Kitamura Y, Itoh T. 1987. Reaction volume of protonic ionization for buffering agents. Prediction of pressure dependence of pH and pOH. J. Sol. Chem. 16(9):715-725.

Klibanov AM. 1983. Stabilization of enzymes against thermal inactivation. Advances in Applied Microbiology 29:1-28.

Knorr D, Heinz V. 2001. Development of nonthermal methods for microbial control. In: Block SS, editor. Disinfection, sterilization, and preservation. 5 ed. Philadephia: Lippincott Williams & Wilkins. p 853-877.

Knorr D, Heinz V, Buckow R. 2006. High pressure application for food biopolymers. Biochimica et Biophysica Acta 1764(3):619-631.

Knudsen JC, Lund BM, Bauer R, Quist KB. 2004. Interfacial and molecular properties of high pressure-treated b-lactoglobulin. Langmuir 20:2409-2415.

Kreis M, Williams M, Buxton B, Pywell J, Hejgaard J, Svendsen I. 1987. Primary structure and differential expression of b-amylase in normal and mutant barleys. European Journal of Biochemistry 169:517-525.

Kunugi S, Kitayaki M, Yanagi Y, Tanaka N, Lange R, Balny C. 1997. The effect of high pressure on thermolysin. European Journal of Biochemistry 248(2):567-574.

Kunugi S, Tanaka N. 2002. Cold denaturation of proteins under high pressure. Biochimica et Biophysica Acta 1595:329-344.

Kuwata K, Li H, Yamada H, Legname G, Prusiner SB, Akasaka K, James TL. 2002. Locally disordered conformer of the hamster prion protein: A crucial intermediate to PrPSc. Biochemistry 41:12277-12283.

Ladero M, Ferrero R, Vian A, Santos A, Garcia-Ochoa F. 2005. Kinetic modelling of the thermal and pH inactivation of a thermostable [beta]-galactosidase from Thermus sp. strain T2. Enzyme and Microbial Technology 37(5):505-513.

Lassalle MW, Yamada H, Akasaka K. 2000. The pressure-temperature free energy-landscape of staphylococcal nuclease monitored by 1H NMR. Journal of Molecular Biology 298(2):293-302.

Lelievre J. 1973. Starch gelatinization. Journal of Applied Polymer Science 18:293-296.

Leloup VM, Colonna P, Ring SG, Roberts K, Wells B. 1992. Microstructure of amylose gels. Carbohydrate Polymers 18:189-197.

Lesch H, Stadlbauer H, Friedrich J, Vanderkooi JM. 2002. Stability diagram and unfolding of a modified cytochrome c: what happens in the transformation regime? Biophysical Journal 82:1644-1653.

Li Y, Lu J, Gu G. 2005. Control of arabinoxylan solubilization and hydrolysis in mashing. Food Chemistry 90:101–108.

Ludikhuyze L, De Cordt S, Weemaes C, Hendrickx M, Tobback P. 1996. Kinetics for heat and pressure-temperature inactivation of *Bacillus subtilis* a-amylase. Food Biotechnology 10(2):105-129.

Ludikhuyze L, Van den Broeck I, Weemaes C, Herremans C, Van Impe J, Hendrickx M, Tobback P. 1997. Kinetics for isobaric-isothermal inactivation of bacillus subtilis a-amylase. Biotechnoloy Progress 13:532-538.

Ludikhuyze L, Van Loey A, Indrawati, Denys S, Hendrickx M. 2002. Effects of high pressure on enzymes related to food quality. In: Hendrickx M, Knorr D, editors. Ultra High Pressure Treatments of Foods. New York: Kluwer Academic / Plenum Publisher. p 115-166.

Ludikhuyze L, Van Loey A, Indrawati, Smout C, Hendrickx M. 2003. Effects of combined pressure and temperature on enzymes related to quality of fruits and vegetables: From kinetic information to process engineering aspects. Critical Reviews in Food Science and Nutrition 43(5):527-586.

Ludwig H, Bieler C, Hallbauer K, Scigalla W. 1992. Inactivation of microorganisms by hydrostatic pressure. In: Balny C, Hayashi R, Heremans K, editors. High pressure and biotechnology. London: John Libbey and Co., Ltd. p 25-32.

Lullien-Pellerin V, Balny C. 2002. High pressure as a tool to study some proteins properties: conformational modification, activity and oligomeric dissociation. Innovative Food Science and Emerging Technologies 3:209-221.

Lund D. 1984. Influence of time, moisture, ingredients, and processing conditions on starch gelatinization. Critical Reviews in Food Science and Nutrition 20:249-73.

Ly-Nguyen B, Van Loey AM, Fachin D, Verlent I, Indrawati, Hendrickx M. 2002. Partial purification, characterization, and thermal and high-pressure inactivation of pectin methylesterase from carrots (*Daucus carrota* L.). Journal of Agriculture and Food Chemistry 50:5437-5444.

Ly-Nguyen B, Van Loey AM, Smout C, Verlent I, Duvetter T, Hendrickx ME. 2003. Effect of mild-heat and high-pressure processing on banana pectin methylesterase: A kinetic study. Journal of Agriculture and Food Chemistry 51(27):7974-7979.

Ma Y, Stewart DC, Eglinton JK, Logue SJ, Langridge P, Evans DE. 2000. Comparative enzyme kinetics of two allelic forms of barley (Hordeum vulgare L.) beta-amylase. Journal of Cereal Science 31:335-344.

Ma YF, Evans DE, Logue SJ, Langridge P. 2001. Mutations of barley beta-amylase that improve substrate-binding affinity and thermostability. Molecular Genetics and Genomics 266:345-352.

MacGregor AW. 1978. a-Amylase I from malted barley - physical properties and action pattern on amylase. Cereal Chemistry 55(5):754-765.

MacGregor AW. 1987. a-amylase, limit dextrinase and a-glucosidase enzymes in barley and malt. Critical Reviews in Biotechnology 5:117-128.

MacGregor AW. 1991. Starch degrading enzymes. Ferment 4:178-182.

MacGregor AW, Bazin SL, Izydorczyk MS. 2002. Gelatinisation characteristics and enzyme susceptibility of different types of barley starch in the temperature range 48-72°C. Journal of the Institute of Brewing 108(1):43-47.

MacGregor AW, Bazin SL, Macri LJ, Babb JC. 1999. Modelling the contribution of alpha-amylase, beta-amylase and limit dextrinase to starch degradation during mashing. Journal of Cereal Science 29:161-169.

MacGregor AW, LaBerge DE, Meridith WOS. 1971. Changes in kernels during groth and maturation. Cereal Chemistry 48:255-269.

MacGregor EA. 1988. a-amylase structure and activity. Journal of Protein Chemistry 7(4):399-415.

MacGregor EA, Janecek S, Svensson B. 2001. Relationship of sequence and structure to specificity in the a-amylase family of enzymes. Biochimica et Biophysica Acta 1546:1-20.

Machado MF, Saraiva J. 2002. Inactivation and reactivation kinetics of horseradish peroxidase in phosphate buffer and buffer-dimethylformamide solutions. Journal of Molecular Catalysis B: Enzymatic 19-20:451-457.

Makimoto S, Taniguchi Y. 1988. Pressure effects on substrate activation phenomena in the a-chymotrypsin-catalyzed hydrolysis of p-nitrophenyl acetate. Biochimica et Biophysica Acta 954:343-346.

Marcotte M, Sablani SS, Kasapis S, Baik O-D, Fustier P. 2004. The thermal kinetics of starch gelatinization in the presence of other cake ingredients. International Journal of Food Science & Technology 39.

Margosch D, Ehrmann MA, Buckow R, Heinz V, Vogel RF, Gänzle MG. 2006. High pressure mediated survival of *Clostridium botulinum* and *Bacillus amyloliquifaciens* endospores at high temperature. Applied and Environmental Microbiology 72:3476–3481.

Marshall WL, Franck EU. 1081. Ion product of water substance, 0-1000°C, 1-10,000 bars - new international formulation and its background. Journal of Physical and Chemical Reference Data 10:295-304.

Masson P, Balny C. 2005. Linear and non-linear pressure dependence of enzyme catalytic parameters. Biochimica et Biophysica Acta 1724(3):440-450.

Masson P, Bec N, Frement MT, Nachon F, Balny C, Lockridge O, Schopfer LM. 2004. Rate-determining step of butyrylcholinesterase-catalyzed hydrolysis of benzoylcholine and benzoylthiocholine. European Journal of Biochemistry 271:1980-1990.

Mathys A, Heinz V, Knorr D. Theoretical calculation of the pH-value in buffers under high pressure. In: Fito P, Toldrá F, editors; 2005; Valencia, Spain. Elsevier. p 329-332.

Matsumoto T, Makimoto S, Taniguchi Y. 1997. Effect of pressure on the mechanism of hydrolysis of maltotetraose, maltopentaose, and maltohexose catalyzed by porcine pancreatic a-amylase. Biochimica et Biophysica Acta 1343:243-250.

McCleary BV. 1986. A soluble chromogenic substrate for the assay (1,3)(1,4)-b-d-glucanase (lichenase). Carbohydrate Polymers 6:307-318.

McCleary BV, Bouhet F, Driguez H. 1991. Measurement of amyloglucosidase using p-nitrophenyl a-maltoside as substrate. Biotechnology Techniques 5:255-258.

McCleary BV, Shameer I. 1987. Assay of malt b-glucanase using Azobarley Glucan: an improved precipitant. Journal of the Institute of Brewing 93:87-90.

McCleary BV, Sheehan H. 1987. Measurement of cereal a-amylase: a new assay procedure. Journal of Cereal Science 6:237-251.

Meersman F, Smeller L, Heremans K. 2006. Protein stability and dynamics in the pressure-temperature plane. Biochimica et Biophysica Acta 1764(3):346-354.

Mentré P, Hoa GHB. 2000. Effects of high hydrostatic pressures on living cells: a consequence of the properties of macromolecules and macromolecules-associated water. Int. Rev. Cyt. 201:1-84.

Michaelis L, Menten M. 1913. Die Kinetik der Invertinwirkung. Biochemische Zeitschrift 49:333-369.

Mikami B, Yoon HJ, Yoshigi N. 1999. The crystal structure of the sevenfold mutant of barley b-amylase with increased thermostability at 2.5 A resolution. Journal of Molecular Biology 285:1235-1243.

Morild E. 1981. The theory of pressure effects on enzymes. Advances in Protein Chemistry 34:93-166.

Moscatelli EA, Ham EA, Rickes EL. 1961. Enzymatic properties of a b-glucanase from *Bacillus subtilis*. Journal of Biological Chemistry 236(11):2858-2862.

Moussa M, Perrier-Cornet JM, Gervais P. 2006. Synergistic and antagonistic effects of combined subzero temperature and high pressure on Escherichia coli. Applied Environmental Microbiology 72:150-156.

Mozhaev VV, Berezin IV, Martinek K. 1988. Structure-stability relationships in proteins: fundamental tasks and strategy for the development of stabilized enzyme catalysts for biotechnology. Critical Reviews in Biochemistry 23:235-281.

Mozhaev VV, Heremans K, Frank J, Masson P, Balny C. 1994. Exploring the effects of high hydrostatic pressure in biotechnological applications. Trends in Biotechnology 12:493-501.

Mozhaev VV, Heremans K, Frank J, Masson P, Balny C. 1996a. High pressure effects on protein structure and function. Proteins 24:81-91.

Mozhaev VV, Lange R, Kudryashova EV, Balny C. 1996b. Application of high hydrostatic pressure for increasing activity and stability of enzymes. Biotechnology and Bioengineering 52(2):320-331.

Mozhaev VV, Martinek K. 1982. Inactivation and reactivation of proteins (enzymes). Enzyme and Microbial Technology 4:299-309.

Muhr AH, Wetton RE, Blanshard JMV. 1982. Effect of hydrostatic pressure on starch gelatinisation, as determined by DTA. Carbohydrate Polymers 2:91-102.

Müller JJ, Thomsen KK, Heinemann U. 1998. Crystal structure of barley 1,3-1,4-b-glucanase at 2.0-A resolution and comparison with bacillus 1,3-1,4-b-glucanase. The Journal of Biological Chemistry 273(6):3438-3446.

Nanmori T, Shinke R, Aoki K, Nishira H. 1983. Purification and characterization of beta-amylase from Bacillus cereus BQ10-S1 Spo II. Agricultural and Biological Chemistry 47(5):941-947.

Narziß L. 1985. Das Brauen mit hoher Stammwürze. Die Technologie der Würzebereitung. 6 ed. Stuttgart: Ferdinant Enke Verlag. p 352-354.

Narziss L. 1993. b-glucan and filterability. Brauwelt International 5:435-442.

Nash DP, Jonas J. 1997. Structure of pressure-assisted cold denatured lysozyme and comparison with lysozyme folding intermediates. Biochemistry 36:14375-14383.

Nielsen AD, Pusey ML, Fuglsang CC, Westh P. 2003. A proposed mechanism for the thermal denaturation of a recombinant *Bacillus halmapalus* a-amylase-the effect of calcium ions. Biochimica et Biophysica Acta 1652(1):52-63.

Nielsen JE, Borchert TV. 2000. Protein engineering of bacterial a-amylases. Biochimica et Biophysica Acta 1543:254-274.

Nielsen PK, Bønsager BC, Fukuda K, Svensson B. 2004. Barley a-amylase/subtilisin inhibitor: structure, biophysics and protein engineering. Biochimica et Biophysica Acta 1696:157-164.

Nienhaus GU. 2004. Physik der Proteine. Physik Journal 4:37-43.

Nishida N, Katamine S, Manuelidis L. 2005. Reciprocal interference between specific CJD and scrapie agents in neural cell cultures. Science 310:493-496.

Northrop DB. 2002. Effects of high pressure on enzyme activity. Biochimica et Biophysica Acta 1595:71-79.

Nunes CS, Castro SM, Saraiva JA, Coimbra MA, Hendrickx ME, Van Loey AM. 2006. Thermal and high pressure stability of purified pectin methylesterase from plums (*Prunus Domestica*). Journal of Food Biochemistry 30:138-154.

Oates CG. 1997. Towards an understanding of starch granule structure and hydrolysis. Trends in Food Science & Technology 8:375-382.

Palou E, Hernandez-Salgado C, Lopez-Malo A, Barbosa-Canovas GV, Swanson BG, Welti-Chanes J. 2000. High pressure-processed guacamole. Innovative Food Science and Emerging Technologies 1:69-75.

Parker R, Ring SG. 2001. Aspects of the physical chemistry of starch. Journal of Cereal Science 34:1-17.

Paul PL, Morita RY. 1971. Effects of hydrostatic pressure and temperature on the uptake and respiration of amino acids by a facultatively psychrophilic marine bacterium. Journal of Bacteriology 108:835-843.

Peleg M, Normand MD, Corradini MG. 2005. Generating microbial survival curves during thermal processing in real time. Journal of Applied Microbiology 98:406-417.

Penniston JT. 1971. High hydrostatic pressure and enzymic activity: Inhibition of multimeric enzymes by dissociation. Archives of Biochemistry and Biophysics 142(1):322-332.

Perera C, Hoover R, Martin AM. 1997. The effect of hydroxypropylation on the structure and physicochemical properties of native, defatted and heat-moisture treated potato starches. Food Research International 30:235-247.

Perrier Cornet JM, Tapin S, Serenella G, Gervais P. 2004. High pressure inactivation of *Saccharomyces cerevisiae* and *Lactobacillus plantarum* at subzero temperatures. Journal of Biotechnology 115:405-412.

Polakovic M, Bryjak J. 2002. Modelling of the kinetics of thermal inactivation of glucoamylase from Aspergillus niger. Journal of Molecular Catalysis B: Enzymatic 19-20:443-450.

Priev A, Almagor A, Yedgar S, Gavish B. 1996. Glycerol decreases the volume and compressibility of protein interior. Biochemistry 35:2061-2066.

Prusiner SB. 1991. Molecular biology of prion diseases. Science 252:1515-1522.

Raabe E, Knorr D. 1996. Kinetics of starch hydrolysis with *Bacillus amyloliquefaciens*-a-amylase under high hydrostatic pressure. Starch 48(11/12):409-414.

Rademacher B, Hinrichs J. 2006. Effects of high pressure treatment on indigenous enzymes in bovine milk: Reaction kinetics, inactivation and potential application. International Dairy Journal.

Rapeanu G, Van Loey A, Smout C, Hendrickx M. 2005. Thermal and high-pressure inactivation kinetics of polyphenol oxidase in victoria grape must. Journal of Agriculture and Food Chemistry 53:2988-2994.

Reilly PJ. 1999. Protein engineering of glucoamylase to improve industrial performance - A review. Starch / Stärke 51(8-9):269-274.

Reyns KMFA, Soontjens CCF, Cornelis K, Weemaes CA, Hendrickx ME, Michiels CW. 2000. Kinetic analysis and modelling of combined high-pressure–temperature inactivation of the yeast *Zygosaccharomyces bailii*. International Journal of Food Microbiology 56:199–210.

Riahi E, Ramaswamy HS. 2004. High Pressure inactivation kinetics of amylase in apple juice. Journal of Food Engineering 64:151-160.

Rickes EL, Ham EA, Moscatelli EA, Walther OH. 1962. The isolotion and biological properties of a b-glucanase from *B. subtilis*. Archives of Biochemistry and Biophysics 69:371-375.

Rizvi AF, Tong CH. 1997. Fractional conversion for determing texture degradation kinetics of vegetables. Journal of Food Science 62:1-7.

Robert X, Haser R, Svensson B, Aghajari N. 2002. Comparison of crystal structures of barley a-amylase 1 and 2: implications for isozyme differences in stability and activity. Biologia 57:59-70.

Robson LM, Chambliss GH. 1989. Cellulases of bacterial origin. Enzyme and Microbial Technology 11:626-644.

Rodenburg KW, Juge N, Guo XJ, Sogaard M, Chaix JC, Svensson B. 1994. Domain B protruding at the third beta strand of the alpha/beta barrel in barley alpha-amylase confers distinct isozyme-specific properties. Eur J Biochem 221(1):277-284.

Rodrigo D, Cortés C, Clynen E, Schoofs L, Van Loey A, Hendrickx M. 2006a. Thermal and high-pressure stability of purified polygalacturonase and pectinmethylesterase from four different tomato processing varieties. Food Research International 39(4):440-448.

Rodrigo D, Jolie R, Van Loey A, Hendrickx M. 2006b. Combined thermal and high pressure inactivation kinetics of tomato lipoxygenase. European Food Research and Technology 222:636 - 642.

Rogers JC. 1985. Two barley a-amylase gene families are refulated differently in aleuron cells. The Journal of Biological Chemistry 260(6):3731-3738.

Rubens P, Heremans K. 2000. Pressure-temperature gelatinization phase diagram of starch: An in situ fourier transform infrared study. Biopolymers 54:524-530.

Rumpold BA. 2005. Impact of high hydrostatic pressure on wheat, tapioca, and potato starches. Berlin: Berlin Technical University. 120 p.

Saad-Nehme J, Silva JL, Meyer-Fernandes JR. 2001. Osmolytes protect mitochondrial F_0F_1-ATPase complex against pressure inactivation. Biochimica et Biophysica Acta 1546(1):164-170.

Saboury AA, Karbassi F. 2000. Thermodynamic studies on the interaction of calcium ions with alpha-amylase. Thermochimica Acta 362:121-129.

San Martín MF, Barbosa-Cánovas GV, Swanson BG. 2002. Food processing by high hydrostatic pressure. Critical Reviews in Food Science and Nutrition 42(6):627-645.

Sasvári Z, Asboth B. 1998. Formation of disulfid-bridged dimers during thermoinactivation of glucoamylase from Aspergillus niger. Enzyme Microb. Technol. 22:466-470.

Sauer J, Sigurskjold W, Christensen U, Frandsen TP, Mirgorodskaya E, Harrison M, Roepstorff P, Svensson B. 2000. Glucoamylase: structure/function relationships and protein engineering. Biochimica et Biophysica Acta 1543:275-293.

Scharnagl C, Reif M, Friedrich J. 2005. Stability of proteins: Temperature, pressure and the role of the solvent. Biochimica et Biophysica Acta 1749:187-213.

Scheraga HA, Némethy G, Steinberg IZ. 1962. The contribution of hydrophobic bonds to the thermal stability of protein conformations. Journal of Biological Chemistry 237(2506-2508).

Schlüter O, Benet GU, Heinz V, Knorr D. 2004. Metastable states of water and ice during pressure-supported freezing of potato tissue. Biotechnology Progress 20:799-810.

Selmi B, Marion D, Perrier Cornet JM, Douzal JP, Gervais P. 2000. Amyloglucosidase hydrolysis of high-pressure and thermally gelatinized corn and wheat starches. Journal of Agriculture and Food Chemistry 48(7):2629-2633.

Seyderhelm I, Boguslawski S, Michaelis G, Knorr D. 1996. Pressure induced inactivation of selected food enzymes. Journal of Food Science 61(2):308-310.

Sierks MR, Svensson B. 1996. Catalytic mechanism of glucoamylase probed by mutagenesis in conjunction with hydrolysis of a-D-glucopyranosyl and maltooligosaccharides. Biochemistry 35:1865-1871.

Sila DN, Smout C, Satara Y, Vu ST, Van Loey A, Hendrickx M. 2007. Combined thermal and high pressure effect on carrot pectinmethylesterase stability and catalytic activity. Journal of Food Engineering 78:755-764.

Silva JL, Cordeiro Y, Foguel D. 2006. Protein folding and aggregation: two sides of the same coin in the condensation of proteins revealed by pressure studies. Biochimica et Biophysica Acta 1764(3):443-451.

Silva JL, Weber G. 1993. Pressure stability of proteins. Annual Review of Physical Chemistry 44:89-113.

Singh N, Kaur L. 2004. Morphological, thermal, rheological and retrogradation properties of potato starch fractions varying in granule size. Journal of the Science of Food and Agriculture 84:1241-1252.

Singh N, Singh J, Kaur L, Sodhi NS, Gill BS. 2003. Morphological, thermal and rheological properties of starches from different botanical sources. Food Chemistry 81:219-231.

Slack PT, Wainwright T. 1980. Amylolysis of large starch granules from barleys in relation to their gelatinisation temperatures. Journal of the Institute of Brewing 86:74-77.

Slakeski N, Fincher GB. 1992. Barley (1-3,1-4)-b-glucanase isoenzyme EI gene expression is mediated by auxin and gibberellic acid. FEBS Letters 306(2,3):98-102.

Smeller L. 2002. Pressure-temperature phase diagram of biomolecules. Biochimica et Biophysica Acta 1595:11-29.

Smeller L, Fidy J. 2002. The enzyme horseradish peroxidase is less compressible at higher pressures. Biophysical Journal 82:426–436.

Smeller L, Heremans K. 1997. Some thermodynamic and kinetic consequences of the phase diagram of protein denaturation. In: Heremans K, editor. High Pressure Research in Bioscience and Biotechnology. Louvain: Leuven University Press. p 55-58.

Smelt JP, Hellemons JC, Patterson M. 2002. Effects of high pressure on vegetative microorganisms. In: Hendrickx M, Knorr D, editors. Ultra High Pressure Treatments of Foods. New York: Kluwer Academic / Plenum Publisher. p 55-76.

Smolin N, Winter R. 2004. Molecular dynamics simulations of staphylococcal nuclease: properties of water at the protein surface. Journal of Physical Chemistry B 108:15928–15937.

Smolin N, Winter R. 2006. A molecular dynamics simulation of SNase and its hydration shell at high temperature and high pressure. Biochimica et Biophysica Acta - Proteins & Proteomics 1764:522-534.

Søgaard M, Abe J, Martin-Eauclaire M-F, Svensson B. 1993. a-amylases: structure and function. Carbohydrate Polymers 21:137-146.

Solomon EB, Hoover DG. 2004. Inactivation of *Campylobacter jejuni* by high hydrostatic pressure. Letters in Applied Microbiology 38:505-509.

Sonoike K, Setoyama T, Kuma Y, Kobayashi S. 1992. Effect of pressure and temperature on the death rates of *Lactobacillus casei* and *Escherichia coli*. In: Balny C, Hayashi R, Heremans K, Masson P, editors. High Pressure and Biotechnology. Montrouge: John Libbey Eurotext. p 297-301.

Sopanen T, Laurière C. 1989. Release and activity of bound b-amylase in germinating barley grains. Plant Physiology 89:244-249.

Sorimachi K, Le Gal-Coeffet MF, Williamson G, Archer DB, Williamson MP. 1997. Solution structure of the granular starch binding domain of *Aspergillus niger* glucoamylase bound to beta-cyclodextrin. Structure 5:647-661.

Southall SM, Simpson PJ, Gilbert HJ, Williamson G, Williamsom MP. 1999. The starch-binding domain from glucoamylase disrupts the structure of starch. FEBS Letters 447:58-60.

Stellmach B. 1986. Bestimmungsmethoden Enzyme. Darmstadt: Steinkopff Verlag.

Stenholm K. 1997. Malt limit dextrinase and its importance in brewing. Espoo: VTT Publications. 117 + 28 p.

Stewart DC, Hawthorne D, Evans DE. 1998. Cold sterile filtration: A small scale filtration test and investigation of membrane plugging. Journal of the Institute of Brewing 104:321-326.

Stewart GG, Russell I. 1985. Modern Brewing Biotechnology. In: Moo-Young M, editor. Comprehensive Biotechnology. 1 ed. Frankfurt: Pergamon Press. p 335-383.

Stoforos NG, Crelier S, Robert MC, Taoukis PS. 2002. Kinetics of tomato pectinmethylesterase inactivation by temperature and high pressure. Journal of Food Science 56:1404-1407.

Stolt M, Oinonen S, Autio K. 2001. Effect of high pressure on the pysical properties of barley starch. Innovative Food Science and Emerging Technologies 1:167-175.

Stute R, Kingler RW, Boguslawski S, Eshtiaghi MN, Knorr D. 1996. Effects of high pressure treatment on starches. Starch 48(11/12):399-408.

Sun Z, Henson CA. 1991. A quantitative assessment of the imporatance of barley seed a-amylase, b-amylase, debranching enzyme, and a-glucosidase in starch degradation. Archives of Biochemistry and Biophysics 284(2):298-305.

Svensson B. 1988. Regional distant sequence homology between amylases, a-glucosidase and transglucanosylase. FEBS Letters 230:72-76.

Svensson B. 1994. Protein engineering in the a-amylase family: catalytic mechanism, substrate specifity, and stability. Plant Molecular Biology 25:141-157.

Svensson B, Bak-Jensen KS, Jensen MT, Sauer J, Gottschalk TE, Rodenburg KW. 1999. Studies on structure, function, and protein engineering of starch-degrading enzymes. Journal of Applied Glucoscience 46(1):49-63.

Svensson B, Gibson RM, Haser R, Astier JP. 1987. Crystallization of barley malt a-amylases and preliminary x-ray diffraction studies of the high pI isozyme, a-amylase 2. Journal of Biological Chemistry 262(28):13682-13684.

Svensson B, Jespersen H, Sierks MR, MacGregor EA. 1989. Sequence homology between putative raw-starch binding domains from different starch-degrading enzymes. Biochemical Journal 264:309-311.

Svensson B, Larsen K, Gunnarsson A. 1986. Characterization of a glucoamylase G2 from Aspergillus niger. European Journal of Biochemistry 154:497-502.

Svensson B, Larsen K, Svendsen I, Boel E. 1983. The complete amino acid sequence of the glycoprotein, glucoamylase G1 from Aspergillus niger. Carlsberg Research Communications 48:517-527.

Svensson B, Pedersen TG, Svendsen I, Sakai T, Ottesen M. 1982. Characterization of two forms of glucoamylase from Aspergillus niger. Carlsberg Research Communications 47:55-69.

Svensson E, Eliasson AC. 1995. Crystalline changes in native wheat and potato starches at intermediate water levels during gelatinization. Carbohydrate Polymers 26:171-176.

Takahashi T, Kawauchi S, Suzuki K, Nakao E. 1994. Bindability and Digestibility of High Pressure-Treated Starch with Glucoamylase from Rhizopus sp. Journal of Biochemistry 116:1251-1256.

Tako M, Hizukuri S. 2002. Gelatinization mechanism of potato starch. Carbohydrate Polymers 48(4):397-401.

Tanaka A, Hoshino E. 2003. Secondary calcium-binding parameter of *Bacillus amyloliquefaciens* a-amylase obtained from inhibition kinetics. Journal of Bioscience and Bioengineering 96(3):262-267.

Tanaka N, Ikeda C, Kanaori K, Hiraga K, Konno T, Kunugi S. 2000. Pressure effect on the conformational fluctuation of apomyoglobin in the native state. Biochemistry 39:12063-12068.

Tanaka N, Mitani D, Kunugi S. 2001. Pressure-induced perturbation on the active site of beta-amylase monitored from the sulfhydryl reaction. Biochemistry 40:5914-5920.

Tang H, Mitsunaga T, Kawamura Y. 2006. Molecular arrangement in blocklets and starch granule architecture. Carbohydrate Polymers 63:555-560.

Tauscher B. 1995. Pasteurization of food by hydrostatic high pressure: chemical aspects. Zeitschrift für Lebensmittel-Untersuchung und -Forschung 200(1):3-13.

Teeter MM. 1991. Water–protein interactions: theory and experiment. Annual Review of Biophysics and Biophysical Chemistry 20(^):577-600.

Tegge G. 2004. Stärke und Stärkederivate. Tegge G, editor. Hamburg: Behr's Verlag. 305 p.

Thevelein JM, Van Assche JA, Heremans K, Gerlsma SY. 1981. Gelatinisation temperature of starch, as influenced by high pressure. Carbohydrate Research 93:304-307.

Tian S-M, Ruan K-C, Qian J-F, Shao G-Q, Balny C. 2000. Effects of hydrostatic pressure on the structure and biological activity of infectious bursal disease virus. Eur. J. Biochem. 267:4486-4494.

Tibbot BK, Wong DWS, Robertson GH. 2002. Studies on the C-terminal region of barley a-amylase 1 with emphasis on raw starch-binding. Biologia 57(11):229-238.

Tomazic SJ, Klibanov AM. 1988. Mechanisms of irreversible thermal inactivation of Bacillus a-amylases. Journal of Biological Chemistry 263:3086-3091.

Torrent J, Alvarez-Martinez MT, Harricane MC, Heitz F, Liautard JP, Balny C, Lange R. 2004. High pressure induces scrapie-like prion protein misfolding and amyloid fibril formation. Biochemistry 43:7162-7170.

Torrent J, Alvarez-Martinez MT, Heitz F, Liautard JP, Balny C, Lange R. 2003. Alternative prion structural changes revealed by high pressue. Biochemistry 42:1318-1325.

Torres JA, Velazquez G. 2005. Commercial opportunities and research challenges in the high pressure processing of foods. Journal of Food Engineering 67:95-112.

Tsou C-L. 1986. Location of the active sites of some enzymes in limited and flexible molecular regions. Trends in Biochemical Sciences 11(10):427-429.

Tucker GA. 1995. Fundamentals of enzyme activity. In: Tucker GA, Woods LFJ, editors. Enzymes in Food Processing. London: Blackie Academic & Professional. p 1-21.

Turner LB, Pollock CJ. 1993. The effect of temperature and pH on the apparent Michaelis constant of glutathione reductase from maize (Zea mays L.). Plant Cell and Environment 16:289-295.

Urrutia Benet G. 2005. High-pressure low-temperature processing of foods: impact of metastable phases on process and quality parameters. Berlin: Berlin Technical University. 196 p.

Vallee BL, Stein EA, Sumerwell WN, Fischer EH. 1959. Metal content of a-amylases of various origins. Journal of Biological Chemistry 234:2901-2905.

Vallee F, Kadziola A, Bourne Y, Juy M, Rodenburg KW, Svensson B, Haser R. 1998. Barley a-amylase bound to its endogenous protein inhibitor BASI: crystal structure of the complex at 1.9 å resolution. Structure 6:649-659.

Van den Broeck I, Ludikhuyze LR, Van Loey AM, Hendrickx ME. 2000a. Inactivation of orange pectinesterase by combined high-pressure and temperature treatments: A kinetic study. Journal of Agriculture and Food Chemistry 48:1960-1970.

Van den Broeck I, Ludikhuyze LR, Weemaes CA, Van Loey A. 2000b. Effect of temperature and/or pressure on tomato pectinesterase activity. Journal of Agriculture and Food Chemistry 48:551-558.

Van der Maarel MJ, van der Veen B, Uitdehaag JCM, Leemhuis H, Dijkhuizen L. 2002. Properties and applications of starch-converting enzymes of the a-amylase family. Journal of Biotechnology 94:137-155.

Van Eldik R, Asano T, Le Noble WJ. 1989. Activation and reaction volumes in solution. 2. Chemical Reviews 89:549-688.

Várallyay E, Sasvári Z, Hoschke A, Asbóth B. 1994. A potential protein engineering side in Aspergillus niger glucoamylase: Vicinity of disulphide bridge 449-222. Acta Alimentaria 23:93-103.

Vasanthan T, Bhatty RS. 1996. Physicochemical properties of small- and large-granule starches of waxy, regular, and high-amylose barleys. Cereal Chemistry 73:199-207.

Verghese JN, Garrett TP, Colman PM, Chen L, Hoj PB, Fincher GB. 1994. Three-dimensional structures of two plant beta-glucan endohydrolases with distinct substrate specificities. Proc Natl Acad Sci USA 91(7):2785-2789.

Verlent I, Smout C, Duvetter T, Hendrickx ME, Van Loey A. 2005. Effect of temperature and pressure on the activity of purified tomato polygalacturonase in the presence of pectins with different patterns of methyl esterification. Innovative Food Science and Emerging Technologies 6:293-303.

Verlent I, Van Loey A, Smout C, Duvetter T, Hendrickx ME. 2004a. Purified tomato polygalacturonase activity during thermal and high-pressure treatment. Biotechnology and Bioengineering 86(1):63-71.

Verlent I, Van Loey A, Smout C, Duvetter T, Ly Nguyen B, Hendrickx ME. 2004b. Changes in purified tomato pectinmethylesterase activity during thermal and high pressure treatment. Journal of the Science of Food and Agriculture 84:1839-1847.

Violet M, Meunier JC. 1989. Kinetic study of the irreversible thermal denaturation of Bacillus licheniformis alpha-amylase. Biochemical Journal 263:665–670.

Waigh TA, Donald AM, Heidelbach F, Riekel C, Gidley MJ. 1999. Analysis of the native structure of starch granules with small angle x-ray microfocus scattering. Biopolymers 49:91-105.

Waigh TA, Gidley MJ, Komanshek BU, Donald AM. 2000. The phase transformations in starch during gelatinisation: a liquid crystalline approach. Carbohydrate Research 328:165-176.

Waigh TA, Hopkinson I, Donald AM, Butler MF, Heidelbach F, Riekel C. 1997. Analysis of the native structure of starch granules with X-ray microfocus diffraction. Macromolecules 30:3813-3820.

Waigh TAP, P.; Riekel, C.; Gidley, M. J.; Donald, A. M. 1998. Chiral side-chain liquid-crystalline polymeric properties of starch. Macromolecules 31:7980-7984.

Weemaes C, De Cordt S, Goossens K, Ludikhuyze L, Hendrickx M, Heremans K, Tobback P. 1996. High pressure, thermal, and combined pressure-temperature stabilities of a-amylases from *Bacillus* Species. Biotechnology and Bioengineering 50:49-56.

Weemaes CA, De Cordt SV, Ludikhuyze LR, Van den Broeck I, Hendrickx ME, Tobback P. 1997. Influence of pH, benzoic acid, EDTA, and glutathione on the pressure and/or temperature inactivation kinetics of mushroom polyphenoloxidase. Biotechnology Progress 13:25-32.

Wilkinson N, Kurdzeil AS, Langton S, Needs E, Cook N. 2001. Resistance of poliovirus to inactivation by high hydrostatic pressures. Innovative Food Science and Emerging Technologies 2:95-98.

Woodward JR, Fincher GB. 1982a. Purification and chemical properties of two 1,3;1,4-b-glucan endohydrolases from germinating barley. European Journal of Biochemistry 121:663-669.

Woodward JR, Fincher GB. 1982b. Substrate specificies and kinetic properties of two (1,3;1-4)-b-glucan endo-hydrolases from germinating barley (*Hordeum vulgare*). Carbohydrate Research 106:111-122.

Xiong R, Xie G, Edmondson AS, Linton RH, Sheard MA. 1999. Comperison of the Baranyi model with the modified Gompertz equation for modelling thermal inactivation of *Listeria monocytogenes* Scott A. Food Microbiology 16:269-279.

Yamaguchi A, Yamada TH, Akasaka K. 1995. Thermodynamics of unfolding of ribonuclease A under high pressure. A study by proton NMR. Journal of Molecular Biology 250:689-694.

Yamashita H, Hayase F, Kato H. 1985. b-Glucanases in malt that form insoluble material. Agricultural and Biological Chemistry 49:1313-1320.

Yoshigi N, Okada Y, Maeba H, Sahara H, Tamaki T. 1995. Construction of a plasmid used for the expression of a seven-mutant barley b-amylase with increased thermostability in Escherichia coli and properties of the sevenfold-mutant b-amylase. Journal of Biochemistry 118:562-567.

Yoshigi N, Okada Y, Sahara H, Koshino S. 1994. Expression in Escherichia coli of cDNA encoding barley beta-amylase and properties of recombinant beta-amylase. Bioscience, Biotechnology and Biochemistry 58:1080-1086.

Zanoni B, Schiraldi A, Simonetta R. 1995. A naive model of starch gelatinization kinetics. Journal of Food Engineering 24(1):25-33.

Zech R, Domagk GF. 1986. Enzyme: Biochemie, Pathobiochemie, Klinik, Therapie. Zech R, Domagk GF, editors. Weinheim: VCH Verlagsgesellschaft mbH. 184 p.

Zhang J, Peng X, Jonas A, Jonas J. 1995. NMR study of the cold, heat, and pressure unfolding of ribonuclease A. Biochemistry 34(27):8631-8641.

Zhou J-M, Zhu L, Balny C, Perrett S. 2001. Pressure denaturation of the yeast prion protein Ure 2. Biochemical and Biophysical Research Communications 287:147-152.

Zimm BH, Bragg JK. 1959. Theory of the phase transition between helix and random coil in polypeptide chains. The Journal of Chemical Physics 31:526-535.

Zipp A, Kauzmann W. 1973. Pressure denaturation of metmyoglobin. Biochemistry 12(21):4217-4228.

Zobel HF. 1988. Starch crystal transformations and their industrial importance. Starch 40:44-50.

Zook CD, Parish ME, Braddock RJ, Balaban MO. 1999. High pressure inactivation kinetics of *Saccharomyces cerevisiae* ascospores in orange and apple juice. Journal of Food Science 64:533-535.